ISTANBUL TECHNICAL UNIVERSITY ★ GRADUATE SCHOOL OF SCIENCE ENGINEERING AND TECHNOLOGY

ROBUST DOMINANT POLE PLACEMENT WITH LOW ORDER CONTROLLERS

Ph.D. THESIS

Emre DİNCEL

Department of Control and Automation Engineering

Control and Automation Engineering Programme

MARCH 2019

ISTANBUL TECHNICAL UNIVERSITY ★ GRADUATE SCHOOL OF SCIENCE ENGINEERING AND TECHNOLOGY

ROBUST DOMINANT POLE PLACEMENT WITH LOW ORDER CONTROLLERS

Ph.D. THESIS

Emre DİNCEL
(504122106)

Department of Control and Automation Engineering

Control and Automation Engineering Programme

Thesis Advisor: Prof. Dr. Mehmet Turan SÖYLEMEZ

MARCH 2019

İSTANBUL TEKNİK ÜNİVERSİTESİ ★ FEN BİLİMLERİ ENSTİTÜSÜ

**DÜŞÜK MERTEBELİ KONTROLÖRLER İLE DAYANIKLI
BASKIN KUTUP ATAMA**

DOKTORA TEZİ

Emre DİNCEL
(504122106)

Kontrol ve Otomasyon Mühendisliği Anabilim Dalı

Kontrol ve Otomasyon Mühendisliği Programı

Tez Danışmanı: Prof. Dr. Mehmet Turan SÖYLEMEZ

MART 2019

Emre DİNCEL, a Ph.D. student of ITU Graduate School of Science Engineering and Technology 504122106 successfully defended the thesis entitled "ROBUST DOMINANT POLE PLACEMENT WITH LOW ORDER CONTROLLERS", which he prepared after fulfilling the requirements specified in the associated legislations, before the jury whose signatures are below.

Thesis Advisor :   **Prof. Dr. Mehmet Turan SÖYLEMEZ**   ....
                      Istanbul Technical University

Jury Members :   **Prof. Dr. Leyla GÖREN SÜMER**   ....
                      Istanbul Technical University

                      Prof. Dr. İbrahim Beklan KÜÇÜKDEMİRAL   ....
                      Glasgow Caledonian University

                      Asst. Prof. Dr. Ali Fuat ERGENÇ   ....
                      Istanbul Technical University

                      Asst. Prof. Dr. Nevra BAYHAN   ....
                      Istanbul University-Cerrahpasa

Date of Submission :   **10 January 2019**
Date of Defense :   **8 March 2019**

To my family...

FOREWORD

First of all, I would like to thank Prof. Dr. Mehmet Turan Söylemez, my advisor, for his assistance, support and understanding in each phase. This challenging thesis progress has been successful thanks to his guidance and valuable advices. His support to me and my family was priceless not only during the PhD process but also during my double lung transplant process.

I would also like to thank Prof. Dr. Leyla Gören for being a member of the steering committee. She was always ready to help whenever I need. Her bright ideas and valuable contributions helped much to improve the thesis.

I would like to acknowledge the support of Prof. Dr. İbrahim Beklan Küçükdemiral, the last member of the steering committee, for his time and advices during the thesis progress.

Furthermore, I would like to thank all of the colleagues, whom I have been together in ITU Department of Control and Automation Engineering since 2011, for their unconditional help. In particular, I would like to thank İlhan Mutlu, Oytun Eriş, Sabri Yılmaz and Uğur Yıldırım very much.

I am also grateful to Asst. Prof. Dr. Barış Nesimioğlu for his true friendship and all his support. He was always there when I needed help on any issue.

This thesis was a challenge for me not only because of the difficulty of the PhD process but also due to my health problems. Hereby, I would like to thank all my doctors, especially Assoc. Prof. MD. Erdal Yekeler, head of the lung transplantation team in the Department of Thoracic Surgery&Lung Transplantation in Turkiye Yuksek Ihtisas Training and Research Hospital, to perform my double lung transplantation successfully. Thus, I had an occasion to complete my thesis.

In addition, I owe many thanks to Elif Baltacıoğlu, who has a very special place in my heart, due to her priceless support during the thesis writing period. Whenever I lost my motivation, she always convinced me to keep going on and so I finished this thesis in time.

Lastly, I would like to thank my family who has always been with me not only during this thesis progress but also during whole my life. The unlimited support, confidence, and love of my mother Çiğdem Dincel, my father Fikret Dincel and my dear brother Efe Dincel for me made this long journey to end with a success. It is really hard to express my feelings and appreciations for them with the words.

March 2019   Emre DİNCEL

TABLE OF CONTENTS

ABBREVIATIONS

2D	**:**	Two-Dimensional
3D	**:**	Three-Dimensional
CRB	**:**	Complex Root Boundary
DOF	**:**	Degree of Freedom
DPP	**:**	Dominant Pole Placement
DPRA	**:**	Dominant Pole Region Assignment
FOPDT	**:**	First Order Plus Dead-Time
IMC	**:**	Internal Model Control
IRB	**:**	Infinite Root Boundary
ISE	**:**	Integral-Square-Error
LHP	**:**	Left Half Plane
LTI	**:**	Linear Time Invariant
MIMO	**:**	Multi Input Multi Output
P	**:**	Proportional
PD	**:**	Proportional Derivative
PI	**:**	Proportional Integral
PID	**:**	Proportional Integral Derivative
PLC	**:**	Programmable Logic Controllers
RDPP	**:**	Robust Dominant Pole Placement
RHP	**:**	Right Half Plane
RRB	**:**	Real Root Boundary
SISO	**:**	Single Input Single Output
SOPDT	**:**	Second Order Plus Dead-Time
TITO	**:**	Two Input Two Output
Z-N	**:**	Ziegler-Nichols

SYMBOLS

$\mathbb{C}$	: Set of complex numbers.
$\mathbb{C}^-$	: Open left half plane.
$\mathbb{R}$	: Set of real numbers.
$\mathbb{R}^+$	: Set of positive real numbers.
δ	: Number of the unstable roots in parameter space.
Γ_F	: Nyquist path in s-domain.
$\Gamma_{\tilde{G}}$	: Nyquist contour in $\tilde{G}$-plane.
Ω	: Frequency variable.
∂D	: Boundary of the D-region.
σ	: Real part of dominant poles in continuous-time domain.
ω	: Imaginary part of dominant poles in continuous-time domain.
σ_z	: Real part of dominant poles in discrete-time domain.
ω_z	: Imaginary part of dominant poles discrete-time domain.
ζ	: Damping ratio.
ω_n	: Natural frequency.
Re	: Real part of the expression.
Im	: Imaginary part the expression.
j	: Imaginary unit.
$\boldsymbol{H}_m$	: m^{th} Hurwitz matrix.
L	: Time delay in seconds.
$G(s)$	: Continuous transfer function of the plant.
$F(s)$	: Continuous transfer function of the controller.
$G(z)$	: Discrete transfer function of the plant.
$C(z)$	: Discrete transfer function of the controller.
$N_G(s)$	: Numerator part of transfer function G(s).
$D_G(s)$	: Denominator part of transfer function G(s).
$N_F(s)$	: Numerator part of controller F(s).
$D_F(s)$	: Denominator part of controller F(s).
$N_G(z)$	: Numerator part of transfer function G(z).
$D_G(z)$	: Denominator part of transfer function G(z).
$N_C(z)$	: Numerator part of controller C(z).
$D_C(z)$	: Denominator part of controller C(z).
$G_0(s)$	: Nominal transfer function of the uncertain system G(s,q).
$\tilde{G}(s)$	: Modified transfer function of G(s).
$\tilde{G}(z)$	: Modified transfer function of G(z).
$G(s,q)$	: Uncertain plant transfer function.
$P_c(s)$	: Closed-loop system characteristic polynomial in continuous-time domain.
$P_c(z)$	: Closed-loop system characteristic polynomial in discrete-time domain.
$P_r(s)$	: Residue polynomial in continuous-time domain.
$P_r(z)$	: Residue polynomial in discrete-time domain.

$\widetilde{P_r}(s)$	: Modified residue polynomial in continuous-time domain.
P_{V_i}	: Vertex polynomials.
P_{E_i}	: Edge polynomials.
$P_c(s, Q)$	: An uncertain polynomial family.
$p(s, q)$	: Polynomial with parametric uncertainties.
$P_c(t)$	: The Chebyshev representation of the polynomial $P_c(z)$.
K_{pi}	: Proportional gain of PI controller in PI-PD controller.
K_{pd}	: Proportional gain of PD controller in PI-PD controller.
$c_k(t)$	: First kind of Chebyshev polynomials.
$s_k(t)$	: Second kind of Chebyshev polynomials.
$f_i(\omega), f_i(\gamma)$	: Boundary functions.
x_i	: Intersection points of Nyquist curve and real axis.
$\mathscr{K}$	: Gain intervals in which the root count does not change.
$\overline{K}_j$	: The feasible gain intervals.
m	: Dominance factor.
m_{max}	: Maximum achievable dominance factor.
K_d	: Derivative gain for PID controller.
K_i	: Integral gain for PID controller.
K_p	: Proportional gain for PID controller.
s	: Complex argument for the Laplace transform.
$r(t)$	: Reference input.
$u(t)$	: Control sign.
$y(t)$	: System output.
q_i	: Uncertain parameters.

LIST OF TABLES

LIST OF FIGURES

ROBUST DOMINANT POLE PLACEMENT WITH LOW ORDER CONTROLLERS

SUMMARY

It is clear that the first necessary condition is to provide the stability of a closed-loop control system. If the closed-loop system is not stable, the frequency or time domain specifications do not have any meaning. Therefore, there are many studies in the literature on the calculation of stabilizing controllers both in continuous and discrete time domain. Computation of all stabilizing controller parameters is an advantage due to the fact that the controller parameters, which satisfy some closed-loop performance criteria, are actually a subset of the stabilizing parameter set.

On the other hand, the stabilization of closed-loop system alone is not enough in many cases. For this reason, the calculation of the controller parameters such that the closed-loop system satisfies desired performance specifications has an important place.

In the control system design, the pole placement approach is a widely used and popular technique to obtain the desired closed-loop performance. Therefore, there are several controller design studies based on the dominant pole placement approach in the literature. In order to provide the desired time domain characteristics such as settling time and overshoot, a pair of dominant poles is assigned to the corresponding locations. The adopted assumption here is that the remaining poles are located m times away (m is chosen as 3-5 in general) from this dominant pole pair. Even though the dominant pole placement is an effective design method, if this assumption is violated (i.e. the remaining poles are not located far enough from the dominant poles), it leads to another problem that is the desired performance specifications in the closed-loop are not guaranteed to be met.

The first main problem studied in this thesis is the design of low order controllers (such as PI, PID, PI-PD) in continuous-time domain via dominant pole placement approach to satisfy desired performance criteria in the closed-loop. The mentioned problem is already solved in the literature and presented in the second chapter. Apart from the presentation of existing results, for the systems without time-delay, an easier approach which is based on well-known Routh-Hurwitz method, is also proposed. For the time-delay systems, dominant pole placement problem is very challenging; therefore, it is better to use the discrete-time domain representation for such systems.

During the thesis, P, PI, PID and PI-PD type controllers are considered as low order controllers. However, P controllers are not usually preferred due to steady-state error in the closed-loop. On the other hand, in case of PI controller usage, it is possible to assign the dominant pole pair to the desired locations; however, there is not any parameter left to assign the remaining poles. It may cause the dominant pole placement approach to fail since the non-dominant poles can be located in the dominant region. As a result, PID controllers are the mostly considered in the thesis both in continuous-time domain and discrete-time domain.

The controller zeros may also be problem if their location is close to the dominant pole pair. If the conventional PID controller structure is used, there is always a chance that the controller zeros are located in the dominant region or even in the right half plane (or outside of the unit circle in z-domain) due to the fact that the dominant pole placement method considers only poles of the closed-loop system. However, the PI-PD structure has a significant advantage that the controller zero can be placed arbitrarily; thus, it helps the transient response of the closed-loop system to be obtained as desired.

In continuous time domain, especially when a higher order system is considered, it becomes a difficult task to provide dominant pole placement due to the fact that the remaining poles cannot be always placed far away for chosen performance criteria and dominance factor (m). Therefore, it is important to know the maximum achievable dominance factor for a considered system, hence, another problem which is defined as the calculation of maximum dominance factor with a PID controller shows up. In the thesis two different approach is proposed to calculate the maximum value of the dominance factor for all-pole systems and for the systems with open-loop zeros, respectively.

On the other hand, the dominant pole region in which the dominant poles can be assigned to satisfy a desired dominance factor can be obtained. It means that the limitations on dominant pole pair selection such that the dominant pole placement approach works well can be found. Therefore, a method is proposed to find the dominant poles region in s-plane to guarantee dominant pole placement with continuous PI and PID controllers.

In the dominant pole placement approach, it may be a challenge to keep the remaining poles away from the dominant pole pair with limited parameters. Nevertheless it is possible to widen the closed-loop performance criteria instead of choosing strict specifications. This results the dominant pole pair to be located in a specified region instead of a point, hence, the dominant pole region assignment problem shows up. In this thesis, solution to the dominant pole region assignment problem is given with the help of parameter space approach and generalized Nyquist theorem for continuous P, PI and PID controllers.

It should be noted that most of the installed control systems around the world use older technology where it is not possible to reduce the sampling time below a certain limit without making considerable expenses. In addition to this, in some of the new systems reducing the sampling time comes with a cost, which might not be required due to marketing reasons. In such situations, direct digital design is required to ensure the performance of the controller when applied in the digital world.

Even if the controller design can be performed in continuous-time domain and then discretized by taking sampling time as small as desired, the design in continuous-time domain is not always straightforward. Especially for the time-delay systems, the design via dominant pole placement is a challenge due to the fact that there are infinitely many poles in the closed-loop system. Since the remaining poles can be located in the dominant pole region, the design process should be carried out carefully if the considered system has time-delay. Nevertheless, it is possible to take advantage of the control system design in discrete-time domain so that the number of closed-loop system poles caused by the time-delay becomes finite when the time delay is a multiple of the sampling time. It leads the direct digital controller design to be an important aspect in dominant pole placement method.

The same problems defined in the continuous-time domain are also considered in discrete-time domain and solved in the thesis. First of all, the parametrization of the discrete PI and PID controllers which assign dominant pole pair is completed and after that in order to assign the remaining poles, two different approaches based on modified Nyquist theorem and Chebyshev polynomials are proposed. The maximum dominance factor, in other words, the disc of minimum possible radius in which the non-dominant poles can be placed in z-plane for a chosen performance criteria is calculated via Routh-Hurwitz based method with bilinear transformation. Limitation on dominant pole pair selection in z-plane is also found.

It is also aimed to perform the dominant pole region assignment with discrete P/PI/PID controllers. The methodology is very similar to the pole region assignment in continuous-time domain. However, here, it is much easier to design such controllers for time-delay systems by taking advantage of discrete-time domain. First of all, the proposed method is explained through P controller again with the help of generalized Nyquist theorem, then it is extended to design of digital PI and PID controllers via parameter space approach.

In the control systems, two types of uncertainties can be defined called as unstructured and structured (or parametric) uncertainties. If the system parameters are not known exactly but their intervals are known then it is defined as a parametric uncertainty. In order to analyse the stability of systems with parametric uncertainties, several methods have already been proposed such as the Kharitonov Theorem, the Edge Theorem, the Mapping Theorem and the Tsypkin-Polyak loci. In case of a parametric uncertainty, it is not possible to place closed-loop system poles to the exact locations, but instead it is expected two of the closed-loop poles to be in desired region such as a disc, a rectangle etc. and other poles to be far away from the dominant pole region. A robust PID controller design to provide dominant pole placement in the closed-loop for parametric uncertain systems is studied for the systems with interval type and affine-linear type closed-loop characteristic polynomials, respectively.

Due to the natural structure of the considered problem, different stability regions (D-stability) are required to be considered; therefore, even if the characteristic polynomial is an interval polynomial, the Kharitonov theorem can not be sufficient to calculate the desired gain intervals. Instead of using edge polynomials whose stability or D-stability check requires complex calculations, it is shown that the vertex polynomials are sufficient to be checked if the considered D-stability region satisfies a property (decreasing phase property). It is also shown that for most of the important regions in control engineering, the decreasing phase property is satisfied.

Finally, for the affine-linear type characteristic polynomials, a new method is proposed which is based on finding the invariant gain intervals which is a lot easier than using Edge theorem. Thus, it becomes possible to assign the dominant poles to the desired region in s-plane whereas the remaining poles are also located away from the dominant pole region under all possible perturbations.

As a conclusion, the main problems related with the dominant pole placement is solved for low order controllers and both in continuous-time and discrete-time domains. Derived results are then used to design a robust low order controller via robust dominant pole placement for the systems with parametric uncertainties.

DÜŞÜK MERTEBELİ KONTROLÖRLER İLE DAYANIKLI BASKIN KUTUP ATAMA

ÖZET

Bir kapalı çevrim kontrol sisteminde kararlılığın sağlanmasının ilk gerekli koşul olduğu açıktır. Eğer kapalı çevrim sistem kararlı değilse frekans ya da zaman tanım bölgesi kriterlerinin de bir önemi kalmayacaktır. Bu nedenle, literatürde kararlı kılan kontrolörlerin hesabına ilişkin hem sürekli zaman hem de ayrık zaman domeninde pek çok çalışma yapılmıştır. Kararlı kılan kontrolörlerin hesabı, kapalı çevrimde belirli performans ölçütlerini sağlayan kontrolör kümesinin aslında kararlı kılan parametre kümesinin içinde yer alması nedeniyle bir avantajdır.

Diğer taraftan, kapalı çevrimin kararlı kılınması pek çok durumda tek başına yeterli değildir. Bu nedenle kapalı çevrimde istenilen performans ölçütlerini sağlayacak olan kontrolör kümesinin hesabı önemli bir yere sahiptir.

Kontrol sistem tasarımında, kutup atama yöntemi sıklıkla kullanılan ve popüler olan tekniklerden birisidir. Bu nedenle baskın kutup atama yaklaşımını temel alan çeşitli kontrolör tasarım yöntemleri literatürde önerilmiştir. Amaçlanan aşım, yerleşme zamanı gibi zaman domeni karakteristiklerini sağlamak amacıyla baskın kutup çifti s-tanım bölgesinde ilgili yerlere atanır. Buradaki varsayım diğer tüm kutupların baskın kutuplardan m kat (m genellikle 3-5 arası seçilir) uzakta olduğudur. Baskın kutup atama yöntemi etkili bir yöntem olmasına karşın eğer bu varsayım geçerli olmaz ise (yani diğer kutuplar baskın kutup çiftinden yeterki kadar uzakta bulunmazsa) kapalı çevrimde amaçlanan performans ölçütlerinin garanti edilememesi gibi bir problem ortaya çıkacaktır.

Bu tezde üzerinde çalışılan ilk ana problem düşük mertebeden (PI, PID, PI-PD gibi) kontrolörlerin sürekli zaman domeninde baskın kutup atama yaklaşımı ile tasarımıdır. Bahsi geçen problem literatürde hali hazırda çözülmüş ve tezin ikinci bölümünde sunulmuştur. Var olan yöntemlerin sunumunun dışında, zaman gecikmesi olmayan sistemler için Routh-Hurwitz tabanlı daha kolay bir yaklaşım da önerilmiştir. Zaman gecikmesine sahip sistemler için ise sürekli zamanda baskın kutup atama problemi oldukça zor olacağından, bu tarz sistemler için ayrık zaman yaklaşımının kullanılması daha uygundur.

Düşük mertebeden kontrolörler olarak tez süresince P, PI, PID ve PI-PD tipi kontrolörler ele alınmıştır. Ancak, P tipi kontrolörler genellikle kapalı çevrimde sürekli hal hatasına neden olduklarından pek tercih edilmemektedir. Diğer yandan, PI kontrolör kullanımı durumunda ise kapalı çevrimde baskın kutup çiftini atamak mümkün iken, geriye kalan kutupları konumlandıracak bir serbest parametre kalmamaktadır. Bu da baskın olmayan kutupların baskın bölgede konumlanmasına ve baskın kutup atama yönteminin başarısız olmasına neden olabilir. Sonuç olarak bu tezde hem sürekli zamanda hem de ayrık zamanda çoğunlukla PID tipi kontrolörler ele alınmıştır.

Tasarım sonucunda kontrolör sıfırları da eğer baskın bölge civarında konumlanmış ise problem olabilir. Klasik PID kontrolör yapısı kullanılması durumunda kontrolör sıfırlarının baskın bölge içerisinde ve hatta sağ yarı s-düzleminde (ya da z-düzleminde birim çemberin dışında) konumlanma şansı her zaman bulunmaktadır. Bunun nedeni de baskın kutup atama yaklaşımının yalnızca kapalı çevrim kutuplarını dikkate almasıdır. Ancak PI-PD yapısının, kontrolör sıfırının istenilen şekilde konumlanmasını sağladığından, önemli bir avantajı bulunmaktadır. Bu da kapalı çevrim geçici hal yanıtının arzulandığı şekilde elde edilmesine yardımcı olmaktadır.

Sürekli zaman domeninde, özellikle yüksek mertebeden bir sistem ele alındığında baskın kutup atamanın sağlanması, geriye kalan kutupların belirlenen performans ölçütleri ve baskınlık faktörü (m) için her zaman yeteri kadar uzağa atılamaması nedeniyle zor olabilmektedir. Bu nedenle ele alınan sistem için elde edilebilecek olası maksimum baskınlık faktörünün bilinmesi önemlidir. Bu da PID kontrolörler ile maksimum baskınlık faktörünün hesabı problemini gündeme getirmektedir. Bu tezde maksimum baskınlık faktörü hesabı, sırasıyla açık çevrim transfer fonksiyonu yalnızca kutuplardan oluşan sistemler için ve açık çevrimde sıfırı da olan sistemler için iki farklı yaklaşım üzerinden yapılmıştır.

Diğer yandan, amaçlanan sabit bir baskınlık faktörünü sağlayacak olan ve kapalı çevrim baskın kutuplarının atanacağı bölgenin bulunması da mümkündür. Bunun anlamı, baskın kutup atama yaklaşımının düzgün çalışması için kapalı çevrimde baskın kutup çiftinin seçimindeki kısıtlamaların bulunmasıdır. Böylece, s-tanım bölgesinde baskınlığı garantileyecek olan baskın kutup bölgesinin sürekli PI ve PID kontrolörler için elde edilmesi amacıyla bir yöntem önerilmiştir.

Baskın kutup atama yaklaşımında, geriye kalan kutupların baskın kutup çiftinden uzakta konumlanması eldeki kısıtlı parametre sayısı ile oldukça zor olabilmektedir. Buna rağmen kapalı çevrim performans ölçütlerini kesin sabit değerler seçmek yerine genişletmek yani belirli değerler arasına almak mümkündür. Bu da baskın kutupların bir noktada değil de belirli bir bölgenin içerisinde yer alması anlamına gelmektedir. Sonuç olarak bu kez de baskın kutup bölgesi atama problemi ortaya çıkmaktadır. Bu tezde baskın kutup bölgesi atama problemine çözüm genelleştirilmiş Nyquist teoremi ve parametre uzayı yaklaşımları üzerinden sürekli P, PI ve PID tipi kontrolörler için verilmiştir.

Dünyadaki kontrol sistemlerin çoğunluğunda örnekleme zamanının önemli ek harcamalar yapılmadan belirli limitler altına çekilemeyeceği eski teknolojiler kullanmaktadır. Bununla birlikte bir takım yeni sistemlerde de örnekleme zamanının olabildiğince küçük yapılmak istenmesi beraberinde maliyeti de getirmektedir. Bu gibi durumlarda, dijital dünyada gerçeklenen kontrolörün performansını garanti altına almak için doğrudan ayrık kontrolör tasarımı gerekli olmaktadır.

Kontrolör tasarımı sürekli zamanda yapılıp daha sonra olabildiğince küçük bir örnekleme zamanı seçilerek ayrıklaştırılabilse de, sürekli zaman domeninde tasarım her durumda kolay değildir. Özellikle zaman gecikmesine sahip sistemlerde kapalı çevrimdeki sonsuz sayıda kutup nedeniyle baskın kutup atama yaklaşımı ile tasarım oldukça zor olmaktadır. Baskın kutup çifti dışında kalan kutupların baskın bölgede konumlanma riski yüksek olduğundan, zaman gecikmeli sistemlerde tasarım dikkatli bir biçimde yürütülmelidir. Ancak, kontrolör tasarımında ayrık zaman domeninin avantajını kullanmak mümkündür. Böylece kapalı çevrimde ölü zamandan kaynaklı kutuplar, zaman gecikmesinin katı olacak şekilde bir örnekleme zamanı seçilmesi ile

sınırlı sayıda olacaktır. Bu da doğrudan dijital kontrolör tasarımını baskın kutup atama problemi içerisinde önemli bir başlık haline getirmektedir.

Sürekli zaman domeninde tanımlanan problemlerin aynısı bu tez kapsamında ayrık zaman domeninde de ele alınmış ve çözülmüştür. İlk olarak, baskın kutup çiftini atayacak olan ayrık PI ve PID kontrolörlerin parametrizasyonu yapılmış, sonrasında geriye kalan kutupların atanması amacıyla, modifiye edilmiş Nyquist yaklaşımı ve Chebyshev polinomları yaklaşımları önerilmiştir. Maksimum baskınlık faktörünün, diğer bir deyişle seçilen performans ölçütleri için z-düzleminde baskın olmayan kutupların konumlandırılabileceği olası en küçük yarıçaplı diskin bulunması için bilineer dönüşüm yardımıyla Routh-Hurwitz tabanlı bir yöntem sunulmuştur. Z-düzleminde baskın kutup çiftinin seçimindeki kısıtlamalar da benzer şekilde bulunmuştur.

Ayrık P/PI/PID tipi kontrolörler ile baskın kutup bölgesi atama problemi de ele alınmıştır. Kullanılan yöntem sürekli zaman domenindeki yöntem ile benzerdir. Ancak burada, ayrık zaman domeninin avantajını kullanarak zaman gecikmeli sistemler için tasarımın yapılması daha kolay olmaktadır. İlk olarak genelleştirilmiş Nyquist teoremi yardımıyla P tipi kontrolörler için daha sonra parametre uzayı yaklaşımı ile PI ve PID tipi kontrolörler için önerilen yöntem açıklanmıştır.

Kontrol sistemlerinde yapısal olmayan ve yapısal (parametrik) belirsizlik olmak üzere iki çeşit belirsizlikten söz etmek mümkündür. Eğer sistem parametrelerinin değerleri tam olarak bilinemiyor ancak değiştiği aralık biliniyor ise bu parametrik belirsizlik olarak tanımlanır. Parametrik belirsiz sistemlerin kararlılık analizi için literatürde Kharitonov teoremi, kenar teoremi, haritalama teoremi ve Tsypkin-Polyak eğrisi gibi yöntemler bulunmaktadır. Parametrik belirsizlik olması durumunda, kapalı çevrim kutuplarını belirli noktalara atamak mümkün olmamaktadır. Bunun yerine kapalı çevrim baskın kutuplarının disk, dikdörtgen vs. gibi bir bölgenin içerisinde tutulması, diğer kutuplarında olabildiğince uzakta konumlanması amaçlanmaktadır. Sırasıyla aralık ve kaymış doğrusal biçimde kapalı çevrim karakteristik polinomuna sahip sistemler için baskın kutup atamayı sağlayacak olan dayanıklı PID kontrolör tasarımı üzerinde çalışılmıştır.

Ele alınan problemin yapısı gereği, farklı kararlılık bölgelerinin (D-kararlılık) ele alınması gerekmektedir. Bu nedenle, kapalı çevrim karakteristik polinomu aralık tipi bile olsa, Kharitonov teoremi amaçlanan kazanç aralıklarının hesabı için yeterli olmamaktadır. Ancak, kararlılık ya da D-kararlılığın test edilmesi kompleks hesaplamalar gerektiren kenar polinomlarının kullanımı yerine, eğer ele alınan D-kararlılık bölgesi belli bir özelliği (azalan faz özelliği) sağlıyor ise köşe polinomlarının kullanımının yeterli olacağı gösterilmiştir. Buna ek olarak, kontrol mühendisliğinde ele alınan önemli bölgelerin büyük çoğunluğunun da azalan faz özelliğini sağladığı belirtilmiştir.

Son olarak, kaymış doğrusal tip kapalı çevrim karakteristik polinoma sahip olan sistemler için de değişmez kazanç aralıklarının hesabına dayanan yeni bir yöntem önerilmiştir. Önerilen bu yöntem kenar teoreminin kullanımından çok daha kolaydır. Böylelikle olası tüm belirsizlikler altında dahi baskın kutupların s-düzleminde amaçlanan bölgede tutulurken, diğer kalan kutupların da baskın kutup bölgesinde uzakta konumlanması mümkün hale gelmektedir.

Özetle, bu tezde düşük mertebeden kontrolörler kullanılarak baskın kutup atama ile ilgili temel problemler ele alınmış ve hem sürekli zaman hem de ayrık zaman domenlerinde çözümler verilmiştir. Elde edilen sonuçlar daha sonrasında parametrik belirsiz sistemler için dayanıklı baskın kutup atama yaklaşımı ile dayanıklı düşük mertebeden kontrolör tasarımı için kullanılmıştır.

1. INTRODUCTION

1.1 Motivation

Dominant pole placement (DPP) is an important problem in the linear control system design. Since the performance criteria of a closed-loop system are determined by the dominant poles strongly, the non-dominant poles are desired to be placed far away from the dominant poles so that the closed-loop system transient response is obtained as desired.

Even if the arbitrary pole placement can be done with an output feedback controller with order of at least plant order minus one [1] or using a full state feedback controller if the system is controllable [2], these approaches have problems in the practical applications. Using full state feedback controller is not always possible, because of several physical constraints (e.g. due to states that cannot be measured) and costs more than the output feedback in general because of the number of measurement elements used in the system. Moreover, in the industrial applications, low order controllers that can be implemented via standard technologies are preferred. It is said that, in the industrial applications, PID type controllers are the most well-known and commonly used controllers [3]. Therefore, providing guaranteed dominant pole placement using such controllers became an important subject to examine.

Nowadays, most of the industrial systems are controlled by digital control devices. However, most of the installed control systems around the world use older technology where it is not possible to reduce the sampling time below a certain limit without making considerable expenses. In addition to this, in some of the new systems reducing the sampling time comes with a cost, which might not be required due to marketing reasons. In such situations, direct digital design is required to ensure the performance of the controller when applied in the digital world. Therefore, it is also important to study on discrete-time low order controllers to perform dominant pole placement; however, academic studies are limited in this area.

1

On the other hand, in most of the practical applications, it is not possible to obtain the perfect model of the system, thus, the model contains uncertain parameters. If the system parameters are not known exactly but their intervals are known then it is defined as a parametric uncertainty. It is clear that the consideration of systems with parametric uncertainty is very important in terms of the dominant pole placement. Although there exists several methods to deal with the parametric uncertain systems, studies about the robust dominant pole placement (RDPP) are also limited. Therefore, it is also aimed to apply existing methods in order to guarantee robust dominant pole placement under parametric uncertainties.

1.2 Literature Survey

Pole placement approach in control system design is one of the most popular and very effective design approaches to design feedback controllers for the linear time invariant (LTI) systems because its design procedure is not complex and closed-loop system performance is predictable and can be changed easily as desired [4, 5]. Moreover, this approach can be well applied to both continuous and discrete time systems [6].

The performance specifications of a closed-loop system such as settling time, overshoot, and rise time are determined by the dominant pole locations strongly. In addition, as it is known from the control theory, for the LTI systems, there are several formulas proposed to calculate transient response characteristics of a system. In general, these formulas are based on the second order system approximation; therefore, more reliable results are obtained if the system satisfies this approximation as much as possible. For this reason, it is expected for two of the closed-loop system poles to be in the dominant region and the other poles to be outside of the dominant region. If the non-dominant poles are not placed far enough from the dominant poles, predicting the closed-loop system transient response is difficult and satisfying the performance criteria becomes very challenging in such cases.

For the reasons explained above, dominant pole placement is an important subject to examine in control theory. In the literature, DPP approach was introduced by Persson and Åström [7] and was further explained in [8]. For the systems of first or second order with short dead time, the presented methods work well. However, if the higher-order systems are considered, the chosen closed-loop poles may not be

2

dominant in reality and usually performance specifications are not met in such cases since their design method uses simplified models.

For the single input-single output (SISO) linear time invariant systems, all of the closed-loop system poles can be placed using a full state feedback controller in complex plane arbitrarily if the system is controllable [2]. If an output feedback controller is desired to be used, in order to be able to place all of the system poles arbitrarily, order of the output feedback controller should be at least plant order minus one [1]. However, using full state feedback controller is not always possible, because of some physical constraints (e.g. due to states that cannot be measured) and costs more than the output feedback in general because of the number of measurement elements used in the system. Moreover, in the industrial applications, controllers that can be implemented via standard technologies and are of low order are preferred. Consider the fact that majority of the processes in industry are controlled by PID type controllers due to their simple structure and acceptable robustness [9, 10]. Because of its importance in the practical applications and the possibility for improvement, PID type controller design is still one of the most active research areas in control theory. Therefore, it is important to provide DPP using low order controllers and especially PI and PID controllers from the practical point of view.

It is possible to place all of the closed-loop system poles to the desired location with PID controllers if the system is first or second order due to the degree of freedom (DOF) of the PID controller [11]. However, if PID controller is used to control higher order systems, only three of the closed-loop poles can be placed to the desired locations to satisfy desired performance criteria [12]. The remaining poles can affect the transient response adversely depending on their locations. For this reason, guaranteeing the DPP with low order controllers is a difficult task.

Although there are several techniques have already been proposed about the dominant pole placement with low order controllers [13–15], one of the most recent and important attempt to design low order controllers to provide DPP for SISO systems is proposed in 2009 [1]. In that publication, for the systems that are higher-order or have time delay, dominant pole placement procedure with PID controllers via modified Nyquist plot and root-locus method has been proposed. The aim was to place dominant pole pair to the desired locations and to provide the remaining poles to be placed

3

"m" times away from these dominant poles. Especially for the systems with time delay, the pole placement technique includes a risk on dominant poles because of the possibility for closed-loop dominant poles to lose their meaning caused by the infinite spectrum of poles [16]. Due to the fact that the conventional pole placement methods are not generally appropriate for the time delay systems, modified Nyquist plot design approach works well to guarantee dominance of the closed-loop system poles using PID controllers. After that Yinya and others contributed to this study by considering the locations of the closed-loop zeros and by defining another interesting dominant pole region [17]. The same DPP approach is also applied to place non-dominant poles "m" times away from the dominant poles for SISO systems by using the first order compensator [18].

In the above dominant pole placement studies, systems are modeled in continuous time domain and designed controllers are also expressed in continuous time. Even if the modified Nyquist plot design is successfully applied and can be used for time-delay systems, the determination of the number of encirclements is not always straightforward. Thus, it is possible to take advantage of discrete-time domain representation during the pole placement procedure. On the other hand, in the industrial automation systems, processes are usually controlled by computer based systems such as industrial PCs or PLCs. Since discrete-time control systems become an important subject to examine as a result of the advancing technology, it also provides a significant advantage to be able to find the discrete-PID controller parameters which guarantee DPP. Dincel and Söylemez studied dominant pole placement problem in discrete time domain and applied the modified Nyquist plot approach to discrete-time control systems [19]. It is shown that modified Nyquist plot method is still valid in discrete-time domain and it is possible to find relevant discrete-PID controller parameters.

Another important problem in dominant pole placement is to find the farthest location where all of the non-dominant poles can be placed using a low order controller. In the methods mentioned above, the non-dominant poles are expected to be placed "m" times away from the dominant poles but the value of the "m" should be specified. Therefore, the only way to find the maximum value of "m" is to use trial and error approach. However, Söylemez solved the problem which is estimate of the smallest stabilizable

4

left-half-plane for all pole plants [20]. After that, with the help of the theorem given in this publication, Üstoğlu and Söylemez proposed a calculation method to find the most distant location where the non-dominant poles can be placed with a continuous PID controller at least for all pole systems [11]. In addition to that study, Dincel and Söylemez solved the same mentioned problem using a different approach [21]. If the systems consists of open-loop zeroes or in case of a system with parametric uncertainty, there is not any proposed method yet to this problem in the literature. Furthermore, to the best of our knowledge, there is not any solution to the same problem for the systems represented in discrete time domain.

The similar problem can also be stated as to find dominant pole region in order to guarantee the dominance in the closed-loop with low order controllers (In other words, the limitations on the dominant pole pair selection if non-dominant poles are desired to be placed on the left side of a particular line certainly). In this case, the value of "m" is fixed; however, the dominant pole locations in complex s-plane is to be determined. Dincel and Söylemez proposed a method based on the well-known Routh table to find the limitations on dominant pole pair selection so that DPP approach works well and desired performance specifications are met as accurate as possible in the closed-loop [22].

In the industrial applications, multiple input–multiple output (MIMO) systems are encountered especially in the process control applications. In particular, two input–two output (TITO) processes are frequently encountered multi-variable processes. Furthermore, it is possible to treat many of the multi-variable processes which have more than two inputs/outputs as several two by two subsystems [23–25]. Therefore, designing low order controllers for these kinds of systems has also an important place. In order to control a TITO control system, a decoupler plus a decentralized PID controller approach are used to design mostly [26–28]. Therefore, even if the controlled process is not higher order, the resulting model of the process with decoupler becomes higher order. As a result, the mentioned problems are still valid during the DPP if low order controllers are used. The proposed design approach in [1] is also found to be eligible to design low order controllers for TITO systems. Maghade and Patre applied the guaranteed dominant pole placement approach to control TITO systems [29]. In their study, the higher-order decoupled subsystems

are reduced into simple dynamics such as first-order plus dead-time or second-order plus dead-time and the dominant poles are placed at desired locations. As a result, it can be said that the derived results for SISO systems can also be used for most of the TITO systems with the help of decoupling approach.

In the control systems, two types of uncertainties can be defined called as unstructured and structured (or parametric) uncertainties. If the system parameters are not known exactly but their intervals are known then it is defined as a parametric uncertainty. In order to analyze the stability of systems with parametric uncertainties, several methods have already been proposed such as the Kharitonov Theorem, the edge theorem, the mapping theorem, the Tsypkin-Polyak loci [6, 30, 31] and root locus approach [32, 33]. Although many researchers have been studied and still continue to study on stabilization of the entire plant using robust low order (especially PID type) controllers via different techniques [34–39], the robust performance is also important. However, in most of the robust PID controller design studies and mentioned references, only the robust stabilization case is considered. For the robust performance, in some of the studies, the PID controller parameters which satisfy some performance criteria is obtained from the resulting stabilizing set by using an optimization or just trial-error approach. There also exists few studies in which the robust performance is satisfied through the gain and phase margins.

In order to deal with robust performance problem in a systematic way, the existing robust controller design methods can be combined with the dominant pole placement approach. If the considered system contains uncertain parameters, it is not possible to place closed-loop system poles to the desired points. In this case, it is expected two of the closed-loop poles to be in desired region such as a disc, a rectangle etc. and other poles to be far away from the dominant pole region.

1.3 Goal and Unique Aspect of the Thesis

Guaranteeing the dominant pole placement is a challenge if low order controllers are desired to be used. In some of the recent studies, low order controller design methods are proposed (please note that P, PI, PID and PI-PD type controllers are considered as low order controllers in this thesis) such that all of the closed-loop non-dominant poles

are located away from the dominant pole pair for SISO systems. However, there still exists some problems that should be solved.

One of the problems can be stated as to find low order discrete controller sets which provide dominant pole placement in discrete-time domain, since processes in industry are usually controlled by computer based systems such as industrial computers or programmable logic controllers (PLC). Here, it is aimed to propose systematic DPP methods that can be used especially for time-delay systems. Derived results are also used for the solution of the problems defined below.

Finding the maximum "m" value which means to calculate the farthest location where all of the non-dominant poles can be placed in case of a continuous low order controller usage is also a problem to be solved. Studies in that area are very limited in the literature and does not cover the systems which have open-loop zeros or parametric uncertainty. To the best of our knowledge, there is not any solution to the mentioned problem for the systems represented in discrete time domain. Therefore, in the context of this thesis, solution to the mentioned problems is given.

Another problem is stated as to find dominant pole region in order to guarantee the dominance in the closed-loop with low order controllers. In other words, to find limitations on the dominant pole pair choice if non-dominant poles are desired to be placed on the left side of a particular line certainly. Obviously, this problem is directly related with the calculation of farthest location of non-dominant poles, thus, the similar approach is used for this problem.

In the dominant pole placement approach, it is a challenge to keep the unassigned poles away from the dominant poles with limited parameters. Sometimes it is required to widen the closed-loop performance specifications instead of choosing strict criteria. It is already meaningful for most of the systems to have time domain characteristics between the minimum and maximum desired values. This results the dominant pole pair to be located in a specified region instead of a point, hence, the dominant pole region assignment (DPRA) problem shows up. In this thesis, DPRA problem is also solved both for continuous and discrete time systems.

For the systems with parametric uncertainty, the closed-loop poles are desired to be in a region instead of a point; therefore, the selection of robust controller parameters

should be done such that the dominant poles are located in a desired region whereas the remaining poles are located away from the dominant pole pair even in the worst case. In the context of this thesis, it is finally aimed to develop a systematic low order robust controller design method to be able to deal with uncertain parameters.

1.4 Structure of the Thesis

First of all, the motivation, goal of the thesis, unique aspects of the thesis and the detailed literature survey are given in Chapter 1.

The second chapter, titled as dominant pole placement in continuous-time SISO systems, starts with the calculation of PI/PID controller set which assigns the dominant poles to desired locations in complex s-plane. The calculation of controller subset, which guarantees the non-dominant poles to be away from the dominant pole pair, is then presented with the help of existing methods from literature. After that the calculation of the maximum dominance factor with PID controllers is given in Section 2.4. A method is presented for all-pole systems and then a generalized approach is given for the systems with open-loop zeros. The reverse problem, which is stated as the finding of dominant pole region in order to guarantee the dominance in the closed-loop, is then given in Section 2.5 both for PI and PID controllers. Lastly, the dominant pole region assignment problem is presented and solution to this problem is given for P, PI and PID controller cases (two different approach is used for PI and PID controllers).

In the third chapter, the similar dominant pole placement problems are solved in discrete time domain. Here, the calculation of controller subset, which assign non-dominant poles, is performed via two different approach named as modified Nyquist curve and Chebyshev polynomials. The rest of Chapter 3 is organized same as the previous one. However, only one method is proposed for maximum dominance factor and dominant pole region assignment in z-plane.

The fourth chapter contains the results for robust PID controller design via dominant pole placement. Firstly, the preliminaries about well-known robust control theorems are given in Section 4.1. The types of parametric uncertainties are presented and the stability tests are given both for interval and affine-linear polynomials. The robust

dominant pole placement (RDPP) problem with PID controllers is then solved both for interval type characteristic polynomials and affine linear characteristic polynomials, respectively.

All derived results in this thesis about the (robust) dominant pole placement are summarized in Chapter 5. Finally, the conclusive remarks and possible future studies are also given.

2. DOMINANT POLE PLACEMENT IN CONTINUOUS-TIME SISO SYSTEMS

It is known that the closed-loop poles are strongly responsible for the transient response of system. Therefore, a pair of dominant poles is assigned to the corresponding locations in order to provide the desired time domain characteristics such as settling time and overshoot [31]. Thus, the desired behavior in the closed-loop is obtained by only assigning two closed-loop poles. However, the adopted assumption here is that the remaining poles are located far away (3-5 times in general) from the dominant pole pair. Although the dominant pole placement is an effective design method, if the assumption is violated (i.e. the remaining poles are not located far enough from the dominant poles), the desired performance specifications in the closed-loop are not guaranteed to be met [40].

In this chapter, it is desired to perform dominant pole placement for continuous single input-single output systems. First of all, the mentioned methods in literature survey is presented and after that several dominant pole placement approaches for the systems without time-delay are proposed. Maximum dominance factor calculation and the limitations of dominant pole pair selection problems are also considered and solved. Furthermore, the dominant pole region assignment problem with P, PI and PID controllers is also covered in this section.

2.1 Parametrization of Controller Set Assigns Dominant Poles

Since there are two of the closed-loop poles to be assigned as dominant poles, the DOF of controller should be greater than or equal to 2. It means that at least 2 parameters are required to be tuned; therefore, it is possible to consider PI and PID controllers. For PID controller case, one more parameter remains to change the locations of non-dominant poles, whereas, there is not any parameter left to deal with non-dominant poles if PI controller is used. For this reason, the designer should be careful about the locations of the remaining closed-loop poles after PI controller design.

2.1.1 Parametrization of PI controllers

Let $G(s)$ and $F(s)$ be the open-loop transfer function of a system and the transfer function of a controller, respectively.

$$G(s) = \frac{N_G(s)}{D_G(s)} \tag{2.1}$$

$$F(s) = \frac{N_F(s)}{D_F(s)} \tag{2.2}$$

In order to perform the dominant pole placement, firstly, two of the closed-loop poles should be placed to the locations of $s_{1,2} = \sigma \pm j\omega$ in complex s-plane where $\sigma < 0$. Here, σ and ω are determined from the desired performance criteria such as settling time and overshoot.

Consider a closed-loop system with unit feedback illustrated in Figure 2.1. The closed-loop system characteristic polynomial can then be obtained as:

$$P_c(s) = D_F(s)D_G(s) + N_F(s)N_G(s) \tag{2.3}$$
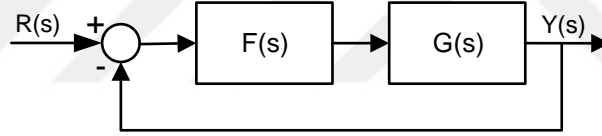
Figure 2.1 : A closed-loop system with unit feedback.

It is clear that the desired dominant poles are expected to be the roots of the characteristic polynomial; therefore, they should satisfy the equation given above. One of the dominant poles can be substituted into (2.3) as follows.

$$P_c(\sigma + j\omega) = D_F(\sigma + j\omega)D_G(\sigma + j\omega) + N_F(\sigma + j\omega)N_G(\sigma + j\omega) = 0 \tag{2.4}$$

The complex equation given above can be solved by decomposing it into its real and imaginary parts,

$$(D_{F_{Im}}D_{G_{Im}} - D_{F_{Re}}D_{G_{Re}}) + (N_{F_{Im}}N_{G_{Im}} - N_{F_{Re}}N_{G_{Re}}) = 0 \tag{2.5}$$

$$(D_{F_{Re}}D_{G_{Im}} + D_{F_{Im}}D_{G_{Re}}) + (N_{F_{Re}}N_{G_{Im}} + N_{F_{Im}}N_{G_{Re}}) = 0 \tag{2.6}$$

where

$$N_{F_{Im}} = Im\left\{N_F(\sigma + j\omega)\right\}, \ N_{F_{Re}} = Re\left\{N_F(\sigma + j\omega)\right\}$$

$$N_{G_{Im}} = Im\{N_G(\sigma + j\omega)\}, \ N_{G_{Re}} = Re\{N_G(\sigma + j\omega)\}$$

$$D_{F_{Im}} = Im\{D_F(\sigma + j\omega)\}, \ D_{F_{Re}} = Re\{D_F(\sigma + j\omega)\}$$

$$D_{G_{Im}} = Im\{D_G(\sigma + j\omega)\}, \ D_{G_{Re}} = Re\{D_G(\sigma + j\omega)\}$$

It is clear that the transfer function of the system is known; therefore, the real and imaginary parts of the numerator ($N_{G_{Re}}, N_{G_{Im}}$) and denominator ($D_{G_{Re}}, D_{G_{Im}}$) are known. On the other hand, the real and imaginary parts of the denominator of PI controller transfer function ($D_{F_{Re}}, D_{F_{Im}}$) are also known. The only unknown parameters are included by the numerator of PI controller. Thus, it is possible to find the unknown parameters by solving ($N_{F_{Re}}, N_{F_{Im}}$) with the help of (2.5) and (2.6) as follows.

$$N_{F_{Re}} = -\frac{N_{G_{Im}}Y - N_{G_{Re}}X}{Z} \tag{2.7}$$

$$N_{F_{Im}} = -\frac{N_{G_{Im}}X + N_{G_{Re}}Y}{Z} \tag{2.8}$$

Here, the auxiliary polynomials X, Y and Z are defined as below.

$$X = D_{F_{Im}}D_{G_{Im}} - D_{F_{Re}}D_{G_{Re}} \tag{2.9}$$

$$Y = D_{F_{Re}}D_{G_{Im}} + D_{F_{Im}}D_{G_{Re}} \tag{2.10}$$

$$Z = N_{G_{Im}}^2 + N_{G_{Re}}^2 \tag{2.11}$$

In addition to this, it is possible to obtain $N_{F_{Re}}$ and $N_{F_{Im}}$ for the PI controller as follows.

$$N_{F_{Re}} = K_i - \sigma K_p \tag{2.12}$$

$$N_{F_{Im}} = \omega K_p \tag{2.13}$$

Finally, with the help of above expressions, the PI controller parameters K_p and K_i are obtained in terms of the parameters σ and ω as follows.

$$K_p = -\frac{N_{G_{Im}}X + N_{G_{Re}}Y}{\omega Z} \tag{2.14}$$

$$K_i = -\frac{N_{G_{Im}}Y - N_{G_{Re}}X}{Z} - K_p\sigma \tag{2.15}$$

The parametrization of all PI controllers set, which assigns the dominant pole pair to the desired locations ($s_{1,2} = \sigma \pm j\omega$), is completed. However, the remaining closed-loop poles may be located anywhere (including unstable region) in complex s-plane as mentioned earlier.

Example 2.1:

Consider the system with following open-loop transfer function,

$$G(s) = \frac{N_G(s)}{D_G(s)} = \frac{1}{(s+2)^2}$$

to be controller with a PI controller given below.

$$F(s) = \frac{N_F(s)}{D_F(s)} = \frac{K_p s + K_i}{s}$$

Let us find the PI controller parameters which assign the dominant poles to the points of $s_{1,2} = -1 \pm 1.049$ in s-plane.

If the required calculations are done,

$$X = 2.1, \ Y = -2.2, \ Z = 1$$

are found. Finally, the PI controller parameters are found via (2.14) and (2.15) as follows.

$$K_p = 2.1, \ K_i = 4.2$$

The closed-loop system characteristic polynomial with the designed PI controller is given as follows.

$$Pc(s) = s^3 + 4s^2 + 6.1s + 4.2$$

The roots of the above polynomial is then calculated as follows.

$$s_{1,2} = -1 \pm 1.049 j, \ s_3 = -2$$

It is seen that the desired dominant poles in s-plane can be assigned using a PI controller and the parameters of PI controller can easily be calculated via the given formula.

2.1.2 Parametrization of PID controllers

The parametrization of PID controllers is done in a similar way. However, the expressions of $N_{F_{Re}}$ and $N_{F_{Im}}$ should be obtained for PID controller case as follows.

$$N_{F_{Re}} = K_i + \sigma K_p + (\sigma^2 - \omega^2) K_d \tag{2.16}$$

$$N_{F_{Im}} = \omega K_p + 2\sigma \omega K_d \tag{2.17}$$

The PID controller parameters K_i and K_d are then obtained in terms of the parameter K_p and the location of dominant poles with the help of given expressions in the previous subsection as follows [40]:

$$\begin{pmatrix} K_d \\ K_i \end{pmatrix} = \begin{pmatrix} -\frac{1}{2\sigma} & 0 \\ \frac{\sigma^2 - \omega^2}{2\sigma} & 1 \end{pmatrix} \begin{pmatrix} \frac{N_{G_{Im}}X + N_{G_{Re}}Y}{\omega Z} \\ \frac{-N_{G_{Im}}Y + N_{G_{Re}}X}{Z} \end{pmatrix} - \begin{pmatrix} \frac{1}{2\sigma} \\ \frac{\sigma^2 + \omega^2}{2\sigma} \end{pmatrix} K_p \qquad (2.18)$$

Two of the closed-loop poles are located in the desired locations in complex s-plane for $\forall K_p \in \mathbb{R}$; however, as in PI controller case, the remaining poles can be located anywhere. It is required to find the feasible K_p interval in order to assign the unassigned poles to the non-dominant pole region. Here, due to the PID controller, one more parameter exists to perform this task.

Please note that for the time-delay systems, parametrization process is the same; however, since the open-loop transfer function $(G(s))$ consists of time-delay term (e^{-sL}), the expressions are found as follows.

$$N_{F_{Re}} = \frac{(N_{G_{Re}}\sin(L\omega) - N_{G_{Im}}\cos(L\omega))Y + (N_{G_{Re}}\cos(L\omega) + N_{G_{Im}}\sin(L\omega))X}{Z} \qquad (2.19)$$

$$N_{F_{Im}} = \frac{(N_{G_{Re}}\sin(L\omega) - N_{G_{Im}}\cos(L\omega))X - (N_{G_{Re}}\cos(L\omega) + N_{G_{Im}}\sin(L\omega))Y}{Z} \qquad (2.20)$$

After that the PI or PID controller parameters, which assign the dominant poles to the desired locations, can be found in a similar way.

Example 2.2:

Consider the fourth order system with following open-loop transfer function,

$$G(s) = \frac{N_G(s)}{D_G(s)} = \frac{1}{(s+1)^2(s+3)^2}$$

to be controller with a PID controller given below.

$$F(s) = \frac{N_F(s)}{D_F(s)} = \frac{K_d s^2 + K_p s + K_i}{s}$$

Let us find the PID controller parameter set which assign the dominant poles to the points of $s_{1,2} = -0.5 \pm 0.5243 j$ in s-plane.

If the required calculations are done,

$$X = 0.8466, \ Y = -2.3328, \ Z = 1$$

are found. The PID controller parameters (K_d and K_i) are then found in terms of the parameter K_p via (2.18) as below.

$$K_d = -4.4489 + K_p, \quad K_i = 0.7357 + 0.5249K_p$$

The closed-loop system characteristic polynomial with the designed PID controller is given as follows.

$$P_c(s) = s^5 + 8s^4 + 22s^3 + (19.55 + K_p)s^2 + (9 + K_p)s + (0.7357 + 0.5249K_p)$$

The roots of the above polynomial can be given as follows for various K_p values.

$$s_{1,2} = -0.5 \pm 0.5243j, \quad s_{3,4} = -3.409 \pm 1.271j, \quad s_5 = -0.1814 \quad (K_p = 1)$$

$$s_{1,2} = -0.5 \pm 0.5243j, \quad s_{3,4} = -3.199 \pm 0.6226j, \quad s_5 = -0.6029 \quad (K_p = 5)$$

$$s_{1,2} = -0.5 \pm 0.5243j, \quad s_{3,4} = -1.4 \pm 0.8686j, \quad s_5 = -4.2 \quad (K_p = 10)$$

It is seen that the location of dominant pole pair in s-plane does not depend on the parameter K_p. It only affects the location of the remaining (non-dominant) closed-loop pole(s) in s-plane.

2.2 Calculation of PID Controller Subset Assigns Non-Dominant Poles

In this section, it is aimed to give the main results of dominant pole placement with PID controllers which is presented in [1]. In the presented study, the non-dominant poles are placed away from the dominant pole pair via root-locus method (for the systems without time-delay) and modified Nyquist curve method (for time-delay systems).

Besides the presentation of existing results, for the systems without time-delay, an easier method which is based on well-known Routh-Hurwitz stability criterion, is also given. For the time-delay systems, dominant pole placement problem is very challenging; therefore, the discrete-time domain representation is used for such systems and presented in the next part of the thesis.

2.2.1 Design via root-locus method

Root-locus plot shows the variation of the roots of closed-loop system characteristic polynomial as a system parameter changes. Since only the K_p parameter of the PID controller remains in the characteristic polynomial, it is possible to plot the root-locus

as the parameter K_p varies. Thus, it is possible to find the critical value of K_p such that the non-dominant poles are located away from the dominant poles.

Consider the closed-loop system characteristic polynomial in terms of the parameter K_p. The characteristic polynomial can be rewritten as follows

$$P_c(s, K_p) = 1 + K_p \tilde{G}(s) = 0 \tag{2.21}$$

where $\tilde{G}(s)$ is an auxiliary open-loop transfer function to plot the root-locus. It is now possible to determine the critical K_p value by inspecting the root-locus plot. After that K_d and K_i parameters can be calculated and PID controller design is completed.

Example 2.3:

Consider the fourth order system given in the previous example. The closed-loop system characteristic polynomial is found as follows.

$$P_c(s, K_p) = s^5 + 8s^4 + 22s^3 + (19.55 + K_p)s^2 + (9 + K_p)s + (0.7357 + 0.5249K_p)$$

It is possible to re-write the polynomial as below.

$$P_c(s, K_p) = 1 + K_p \frac{s^2 + s + 0.5249}{s^5 + 8s^4 + 22s^3 + 19.55s^2 + 9s + 0.7357} = 0$$

The root-locus plot is drawn for

$$\tilde{G}(s) = \frac{s^2 + s + 0.5249}{s^5 + 8s^4 + 22s^3 + 19.55s^2 + 9s + 0.7357}$$

for the positive values of K_p and illustrated in Figure 2.2.

Let us desire the dominance factor $m = 2$ which means that non-dominant poles are desired to be 2 times away from the dominant pole pair. In this case, the feasible gain interval is found as follow via root-locus plot.

$$K_p \in (7.0735, 20.9738)$$

If the K_p parameter of the PID controller is chosen from the feasible interval, the remaining poles are located on the left side of the line $s = -1$ as desired. Let us choose $K_p = 10$ then the closed-loop poles are calculated as follows.

$$s_{1,2} = -0.5 \pm 0.5243j$$

$$s_{3,4} = -1.4 \pm 0.8686j$$

$$s_5 = -4.2$$

17
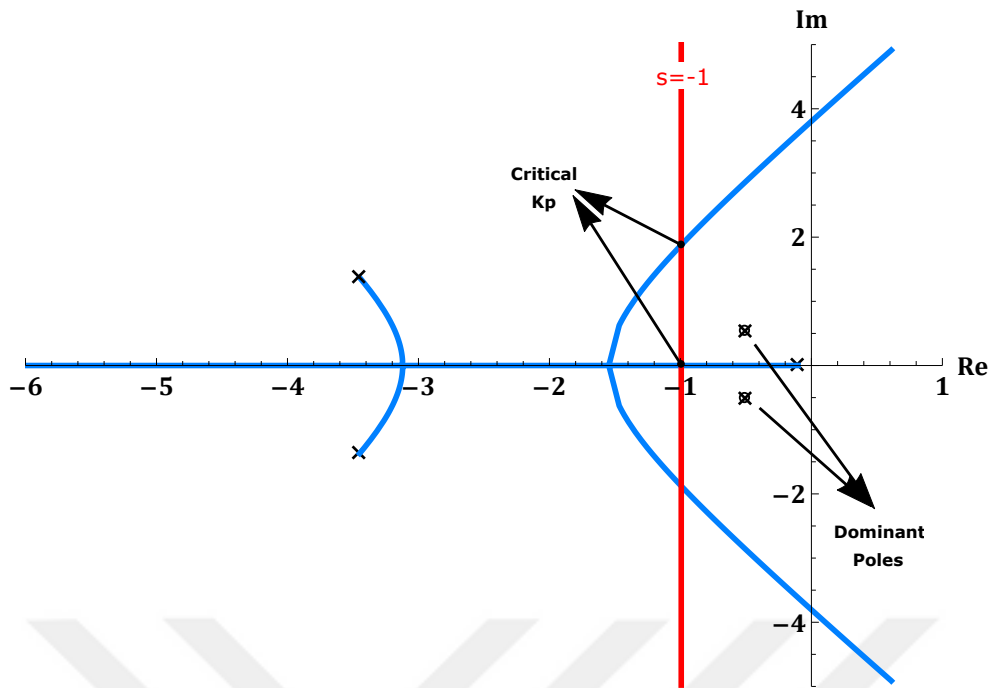
Figure 2.2 : Root locus plot of the auxiliary transfer function (Example 2.3).

Closed-loop pole distribution is shown in Figure 2.3. It can be seen that the remaining poles are located in the non-dominant pole region whereas the dominant poles are assigned to the desired locations in s-plane.
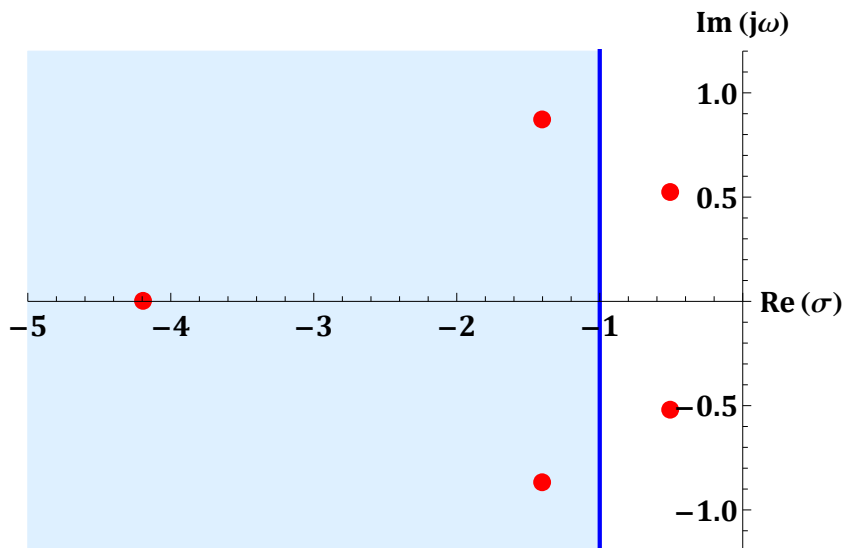
Figure 2.3 : Closed-loop poles with designed PID controller (Example 2.3).

The designed PID controller for this example is given as follows.

$$F(s) = \frac{5.985s^2 + 10s + 5.551}{s}$$

Finally, closed-loop transient response is illustrated in Figure 2.4.
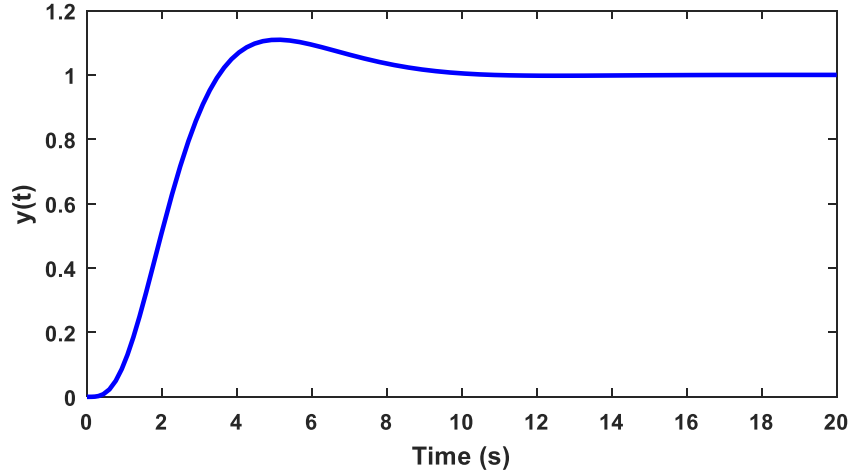
Figure 2.4 : Unit step response of the system with PID controller (Example 2.3).

2.2.2 Design via Routh-Hurwitz method

Even if the root-locus plot shows many useful information graphically, in most cases, calculation of the critical gain values via root-locus (magnitude condition) is not straightforward. However, the feasible gain interval can also be calculated via Routh-Hurwitz method for the polynomial which is constructed by the remaining poles.

Let the closed-loop characteristic polynomial be divided into its dominant and non-dominant part as follows.

$$P_c(s, K_p) = (s^2 + 2\zeta\omega_n s + \omega_n^2)P_r(s, K_p) \tag{2.22}$$

Here $P_r(s, K_p)$ is called as a residue polynomial and its roots are desired to be inside the non-dominant region. It is now possible to find the feasible K_p interval in which the roots of the polynomial $P_r(s, K_p)$ are located on the left side of the $s = m\sigma$ line. In order to check the relative stability, a minor modification over the residue polynomial is required and it can be done by transformation given below.

$$\mathcal{T} : s \mapsto (s + m\sigma) \tag{2.23}$$

Thus, the feasible gain interval can be found via Routh table over the modified reside polynomial $P_r(s + m\sigma, K_p)$.

19

Example 2.4:

Consider again the same example in which the controller is designed via root-locus plot.

$$G(s) = \frac{N_G(s)}{D_G(s)} = \frac{1}{(s+1)^2(s+3)^2}$$

Here, it is aimed to find the same feasible interval via Routh-Hurwitz method.

The closed-loop system characteristic polynomial was found as follows.

$$P_c(s, K_p) = s^5 + 8s^4 + 22s^3 + (19.55 + K_p)s^2 + (9 + K_p)s + (0.7357 + 0.5249K_p)$$

It is possible to re-write the polynomial as below. The first part is constructed by the dominant pole pair and the second part is constructed by the unassigned (remaining) poles.

$$P_c(s, K_p) = (s^2 + s + 0.5249)(s^3 + 7s^2 + 14.475s + K_p + 1.4015)$$

If the transformation given by (2.23) is used over the residue polynomial,

$$P_r(s - 1, K_p) = s^3 + 4s^2 + 3.475s + K_p - 7.0735$$

is obtained. The Routh table can now be created using the modified polynomial above and it is possible to find the same result as

$$K_p \in (7.0735, 20.9738)$$

from the first column of the Routh table.

$$
\begin{array}{c|cc}
s^3 & 1 & 3.475 \\[1em]
s^2 & 4 & K_p - 7.0735 \\[1em]
s^1 & 5.24345 - 0.25K_p & \\[1em]
s^0 & K_p - 7.0735 &
\end{array}
$$

It is seen that the Routh-Hurwitz method is simpler when compared to the root-locus approach and works well even for the higher order characteristic polynomials. However, it is worth to mention that this method is not also able to cover the systems with time-delay.

2.2.3 Design via modified Nyquist plot method

In the reference [1], the modified Nyquist plot method is also proposed since the root-locus method does not work for time-delay systems. Here, it is aimed to use the Nyquist stability criterion in order to find the feasible gain intervals.

Consider the equation (2.21) which is rewritten form of the closed-loop system characteristic polynomial. Suppose that $\tilde{G}(s)$ is a single-valued function with finite number of poles in s-plane. If an arbitrary Nyquist path (Γ_F), which does not cross over the poles or zeros of $\tilde{G}(s)$, is chosen in s-plane then the Nyquist stability criterion says that the $\Gamma_{\tilde{G}}$ contour in $\tilde{G}(s)$-plane encircle the origin $N = Z - P$ times where Z is the number of zeros and P is the number of poles of $\tilde{G}(s)$ inside the Nyquist path Γ_F in s-plane.

If the open-loop system has time-delay term e^{-sL} then the auxiliary transfer function is given in the following form.

$$\tilde{G}(s) = \frac{P_N(s, K_p)}{P_D(s, K_p, e^{sL})} \tag{2.24}$$

Therefore, it becomes impossible to apply Nyquist method directly since the denominator of $\tilde{G}(s)$ becomes a quasi-polynomial. However, it is possible to re-arrange the auxiliary transfer function as follows.

$$\tilde{G}(s) = 1 + G_0(s) = 1 + \tilde{G}_0(s)e^{-sL} = 0 \tag{2.25}$$

Here, it becomes possible to find the number of poles of $\tilde{G}(s)$ through the transfer function of $G_0(s)$ via another Nyquist plot with the help of following equality.

$$P_{\tilde{G}} = Z_{G_0} = N_{G_0} + P_{G_0} \tag{2.26}$$

Thus by applying Nyquist theorem twice, the stabilizing K_p intervals can be calculated. However, instead of stabilizing gain interval, the feasible gain interval is searched. It requires Nyquist path to be modified in order to solve the dominant pole placement problem.

Let us modify the Nyquist path in s-plane as illustrated in Figure 2.5. In this case, it is desired dominant poles to be inside Γ_F whereas the remaining poles are located on the left side of the line $s = m\sigma$. It means that the gain interval, which causes the number of encirclements to be

$$N_{\tilde{G}} = 2 - P_{\tilde{G}} \tag{2.27}$$

21

becomes a feasible interval for the mentioned problem.
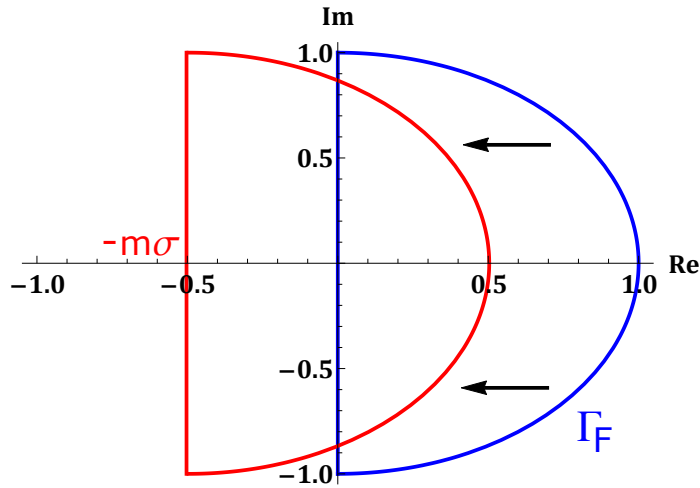
Figure 2.5 : Modification of the Nyquist path in s-plane.

Example 2.5:

Consider the following time-delay system given in [1].

$$G(s) = \frac{1}{s^2 + s + 5} e^{-0.1s}$$

It is desired closed-loop transient response to have maximum of 10% overshoot with 15 seconds of settling time. On the other hand, the remaining poles are desired to be $m = 3$ times away from the dominant poles. The corresponding dominant pole pair is then given as $s_{1,2} = -0.275 \pm 0.375j$. It is possible to find the parametrization of PID controller using the previously presented method as follows.

$$K_d = 7.776 + 1.817K_p, \quad K_i = 1.877 + 0.3937K_p$$

If the obtained parameters are substituted into characteristic equation, the following can be found.

$$1 + K_p \tilde{G}(s) = 1 + K_p \frac{1.817s^2 + s + 0.3937}{e^{0.1s}s^3 + (e^{0.1s} + 7.776)s^2 + e^{0.1s}5s + 1.877} = 0$$

It is required to re-construct the expression of $\tilde{G}(s)$ as given in (2.25). In this case, we have

$$1 + G_0(s) = 1 + \frac{7.776s^2 + 1.877}{s(s^2 + s + 5)} e^{-0.1s} = 0$$

The number of poles of $\tilde{G}(s)$, which is outside of the desired region, can now be found via the transfer function of $G_0(s)$ with the help of (2.26). The modified Nyquist

plot of $G_0(s)$ is illustrated in Figure 2.6. It is seen that there is one anti-clockwise encirclement, on the other hand, the number of poles outside of the desired region is found to be 3 by inspecting the denominator.
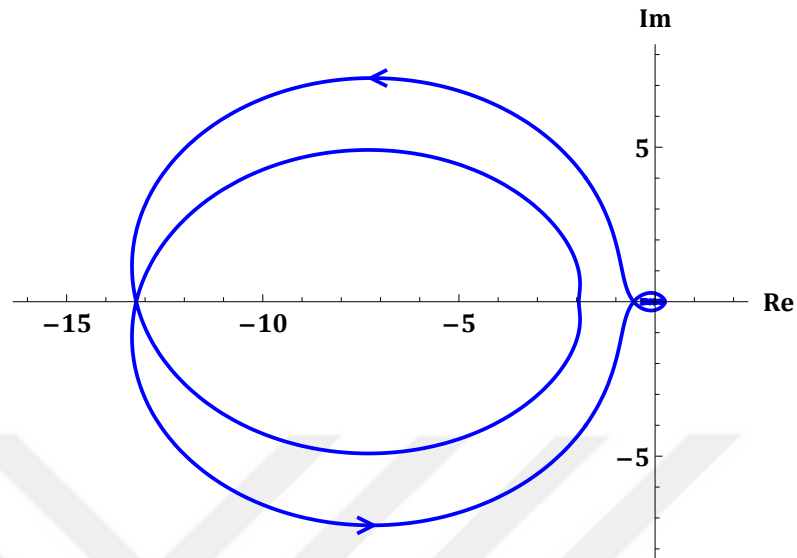
Figure 2.6 : Modified Nyquist plot of the $G_0(s)$ (Example 2.5).

As a result,

$$P_{\tilde{G}} = N_{G_0} + P_{G_0} = -1 + 3 = 2$$

In this case, the modified Nyquist plot of $\tilde{G}(s)$ should have zero encirclements according to (2.27). Let us draw the modified Nyquist plot of $\tilde{G}(s)$ as follows.
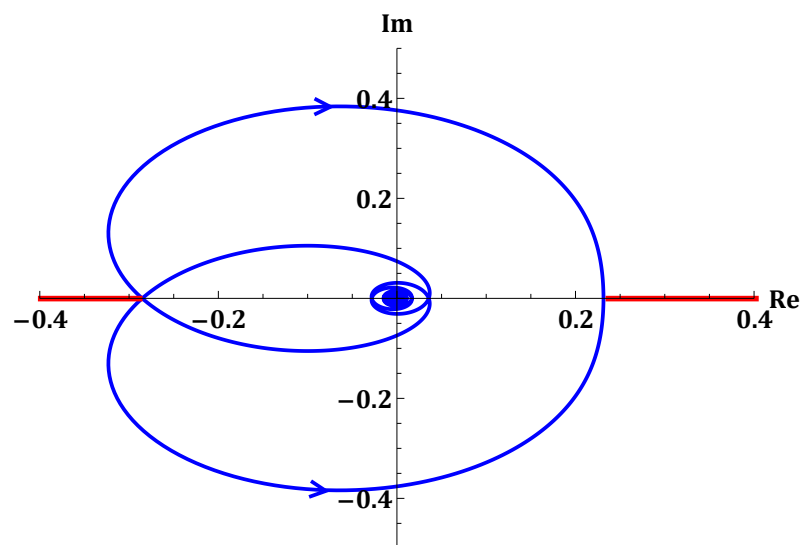
Figure 2.7 : Modified Nyquist plot of the $\tilde{G}(s)$ (Example 2.5).

The critical K_p limits can be seen from the figure and found as follows.

$$K_p \in (-4.322, 3.505)$$

If $K_p = 1$ is chosen from the obtained feasible interval, the designed PID controller is given as

$$F(s) = \frac{9.593s^2 + s + 2.271}{s}$$

and the closed-loop transient response is depicted in Figure 2.8.
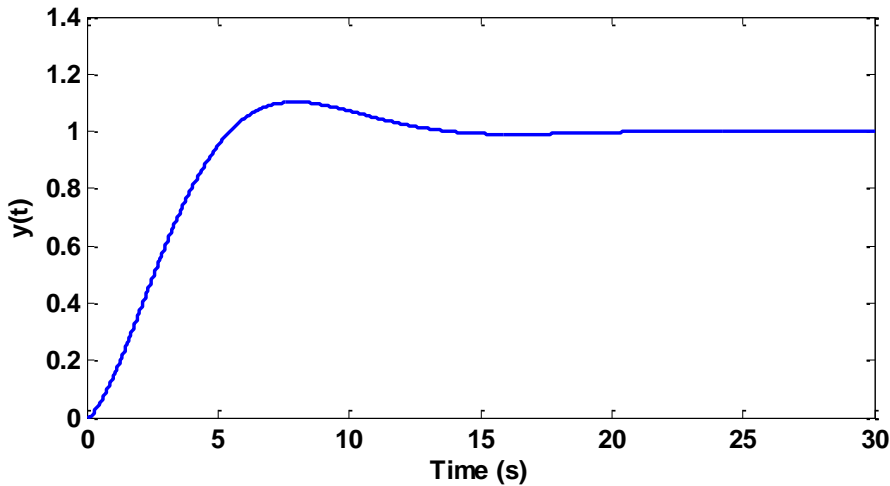
Figure 2.8 : Closed-loop transient response with designed PID controller (Example 2.5).

In this section, the guaranteed dominant pole placement method with PID controllers studied in [1] is presented. It is possible to say that the proposed method works well even for time-delay systems. However, it is seen that dealing with time-delay systems in terms of dominant pole placement is a challenging task. Even if the proposed method provides dominant pole placement, the calculation of feasible gain intervals can be difficult via Nyquist plot. Especially, calculation of the $P_{\tilde{G}}$ through (2.26) may not be straightforward for all systems.

In the presented PID controller design, only the closed-loop system poles are considered; however, PID controller zeros also affects the transient response. If the zeros are ignored during or after design process, the closed-loop response can be obtained much more different than expected.

For the reasons mentioned above, for the time-delay systems, another effective PID controller design method based on dominant pole placement in discrete-time domain

is presented in the next chapter of the thesis. In addition, in order to be able to consider the adverse effects of PID controller zeros, a simple solution (PI-PD controller structure) is proposed in the next section.

2.3 Continuous PI-PD Controller Design In Dominant Pole Placement

As mentioned earlier, providing the dominant pole configuration itself is not enough due to the fact that the closed-loop transient response is also affected by zeros. It is highly possible that at least one of the PID controller zeros can be located in the dominant region or even in the right half s-plane. In this case, the desired closed-loop performance specifications are not met, thus, the dominant pole placement approach loses its advantage.
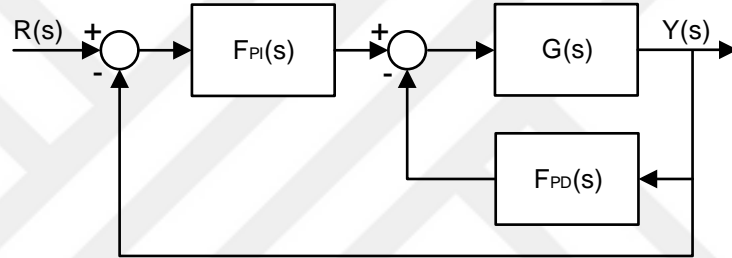
Figure 2.9 : The structure of continuous PI-PD controller.

A solution to the mention problem is the implementation of designed PID controller in PI-PD structure which is given in Figure 2.9. In this configuration, PI controller is located on the forward path (outer loop) and PD controller is located on the feedback path (inner loop).

$$F_{PI}(s) = \frac{K_{pi}s + K_i}{s} \tag{2.28}$$

$$F_{PD}(s) = K_{pd} + K_d s \tag{2.29}$$

If the closed-loop system characteristic polynomials with PID and PI-PD controllers are examined with the same K_i and K_d parameters, it is seen that as long as the equality

$$K_p = K_{pi} + K_{pd} \tag{2.30}$$

is satisfied, the characteristic polynomials have the same roots. It means that if the designed PID controller is implemented in PI-PD form, the closed-loop system pole configuration remains the same. However, the PI-PD structure brings only

25

one real zero in the closed-loop which is two zeros in classical PID controller case. Furthermore, it is possible to place this zero arbitrarily in complex s-plane as follows by just adjusting the K_{pi} parameter. The advantages of PI-PD controller is studied and presented in literature [41–44].

$$s = -\frac{K_i}{K_{pi}} \tag{2.31}$$

Since the PI-PD block diagram is simple to construct, such implementation is not a challenge from the practical point of view. Thus, it can easily be used in the practical applications. Therefore, the designed PID controllers can be implemented as PI-PD controller during simulation studies.

2.4 Calculation of the Maximum Dominance Factor with PID Controller

It is known that in the dominant pole placement approach, if the non-dominant poles are not placed far enough from the dominant pole pair, predicting the closed-loop system transient response is difficult and satisfying the performance criteria becomes very challenging. Therefore, finding the maximum "m" value which means to calculate the farthest location in s-plane, where all of the unassigned poles can be placed, is an important problem to be solved.

In this section, the calculation of maximum dominance factor (m) with PID Controllers is investigated. The mentioned problem is firstly solved for all pole systems (i.e. systems without any zeros) after that a solution to the systems with open-loop zeros is proposed.

2.4.1 Estimate of the maximum dominance factor for all-pole systems

Consider a SISO LTI system which is expressed by the following transfer function.

$$G(s) = \frac{K}{s^n + a_{n-1}s^{n-1} + \cdots + a_1 s + a_0} \tag{2.32}$$

If the PID controller is written depending on the parameter K_p as proposed earlier, then the closed-loop system characteristic polynomial becomes

$$P_c(s) = s^{n+1} + a_{n-1}s^n + \cdots + a_2 s^3 + f_2(K_p)s^2 + f_1(K_p)s + f_0(K_p) \tag{2.33}$$

However, it is known that the obtained characteristic polynomial consists of the dominant poles which are determined using the performance criteria of the closed-loop

response.

$$P_c(s, K_p) = (s^2 + 2\zeta\omega_n s + \omega_n^2)P_r(s, K_p) \tag{2.34}$$

Therefore, it can easily be shown that the expression (2.34) can be reduced to the polynomial of order $n-1$ which is constructed by the non-dominant closed-loop poles as below.

$$P_r(s, K_p) = s^{n-1} + \delta_{n-2}s^{n-2} + \cdots + \delta_1 s + \delta_0(K_p) \tag{2.35}$$

Our main problem, which is stated as how far non-dominant poles can be located away from the dominant poles, is now converted to another problem. This new problem is to find the smallest value of σ such that the polynomial $P_r(s+\sigma, Kp)$ is stabilizable with the parameter K_p. In other words, the left most possible location where all poles of the (2.35) can be placed in s-domain using the K_p parameter.

Here, it has a significant importance that the PID controller parameter K_p appears only in the s^0 coefficient of the obtained polynomial $P_r(s)$. Hence, it is possible to use the solution given in [20] for the problem mentioned above. Summary of the preliminaries and the theorem is given as follows.

Preliminaries: Consider the following characteristic polynomial,

$$P(s) = s^n + a_{n-1}s^{n-1} + \cdots + a_1 s + k \tag{2.36}$$

Let us define the polynomials $P_m(s) \triangleq P_c^m(s)/m!$ (for $m = 1, 2, \ldots, n-1$) where $P_c^m(s)$ denotes the mth derivative of the polynomial $P_c(s)$. Define $\lambda_{rmax} \triangleq \max_{i,m}(\lambda_{r(i,m)})$ such that $\lambda_{r(i,m)}$ are the real roots of the polynomials $P_m(s)$.

Let us define also the polynomials $P_{hm}(s)$ (for $m = 1, 2, \ldots, n-1$) as below,

$$P_{h1}(s) = P_{n-1}(s) \tag{2.37}$$

$$P_{h2}(s) = \begin{vmatrix} P_{n-1}(s) & P_{n-3}(s) \\ 1 & P_{n-2}(s) \end{vmatrix} \tag{2.38}$$

$$P_{h3}(s) = \begin{vmatrix} P_{n-1}(s) & P_{n-3}(s) & P_{n-5}(s) \\ 1 & P_{n-2}(s) & P_{n-4}(s) \\ 0 & P_{n-1}(s) & P_{n-3}(s) \end{vmatrix} \tag{2.39}$$

In more general form,

$$P_{hm}(s) = |\boldsymbol{H}_m| \tag{2.40}$$

Here, $\boldsymbol{H}_m$ is the mth Hurwitz matrix for the polynomial $P(s)$ with coefficients a_i replaced by the polynomials $P_i(s)$ and $k = 0$. Lastly, define the maximum of the real roots of polynomials $P_{hm}(s)$ as λ_{hmax}.

Theorem (Söylemez, 2006): For such polynomial given in (2.36) it is shown that the inequality $\lambda_{rmax} \le \sigma \le \lambda_{hmax}$ holds [20].

It is now possible to find the left most possible non-dominant pole locations. Even if the theorem gives an interval, actually as stated in remarks section of the theorem, exact results can be found if the order of the polynomial $P(s)$ is lower than 5. If the polynomial is second or third order polynomial then $\sigma = \lambda_{rmax} = \lambda_{hmax}$ and if the polynomial is fourth order polynomial then $\sigma = \lambda_{hmax}$.

For our defined problem, it corresponds the order of the polynomial given in (2.34) to be lower than 7. Therefore, we are able to find the exact σ value for the systems with the order up to 5 by using the given theorem. Another important observation is also stated that the interval provided by the theorem is usually a tight interval and λ_{hmax} is often equal to σ.

Example 2.6:

Consider a fourth order process with the transfer function,

$$G(s) = \frac{1}{(s+1)^2(s+5)^2}$$

In the closed-loop, it is expected the system to have maximum 8% overshoot and less than 3s rise time. The related closed-loop dominant poles are $s_{1,2} = -0.4849 \pm j0.6031$. Since the dominant poles are known, it is possible to obtain the PID controller parameters depending on the parameter K_p using (2.18) as follows [45].

$$K_i = 2.604 + 0.6175K_p, \ K_d = -15.39 + 1.031K_p$$

After the necessary calculations, the residue polynomial $P_r(s, K_p)$ is found as below,

$$P_r(s) = s^3 + 11.03s^2 + 34.704s + (4.3485 + 1.031K_p)$$

In order to find the smallest value of σ such that the polynomial $P_r(s+\sigma)$ is stabilizable with the parameter K_p, the theorem given above is used. The polynomials $P_m(s)$ are calculated as follows.

$$P_1(s) = 3s^2 + 22.06s + 34.704$$

$$P_2(s) = 3s + 11.03$$

The maximum real root is found to be $\lambda_{rmax} = -2.2802$. After that the polynomials $P_{hm}(s)$ are found as follows

$$P_{h1}(s) = P_2(s) = 3s + 11.03$$

28

$$P_{h2}(s) = \begin{vmatrix} P_2(s) & 0 \\ 1 & P_1(s) \end{vmatrix} = 9s^3 + 99.2718s^2 + 347.443s + 382.793$$

with the maximum real root of $\lambda_{hmax} = -2.2802$. Since the order of the polynomial $P_r(s)$ is found to be 3, λ_{rmax} is found to be equal to the λ_{hmax} as expected (from the given theorem).

Finally, it is possible to claim that for this system, it is possible to place non-dominant poles with the PID controller

$$m_{max} = \frac{-2.28018}{\sigma} = \frac{-2.2802}{-0.4849} \cong 4.7024$$

times away from the dominant poles for the chosen performance criteria in the closed-loop.

Using a numerical approach and by investigating the variation curve of the unassigned poles with the parameter K_p in the closed-loop, which is given in Figure 2.10, it can be concluded that the obtained σ value is correct.
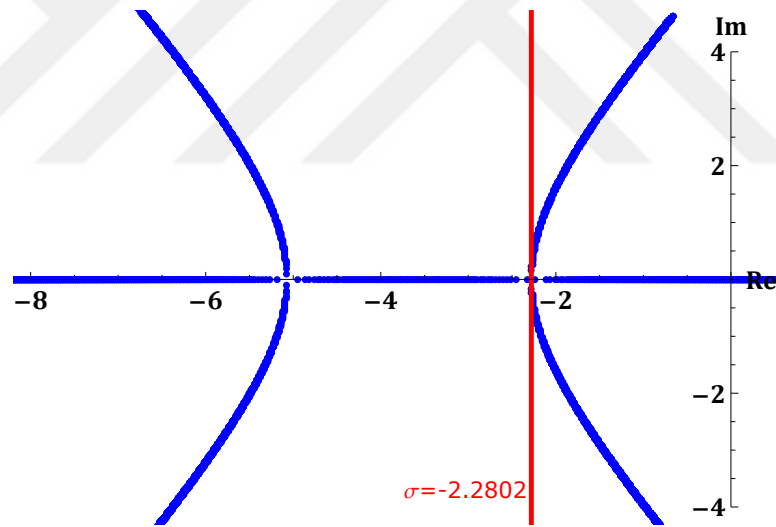
Figure 2.10 : Variation curve of the unassigned closed-loop poles (Example 2.6).

Let us calculate the K_p parameter of the PID controller for the maximum dominance factor.

$$P_r(s = -2.2802) = 0 \longrightarrow K_p = 28.405$$

In this case, the designed PID controller is given as follows.

$$F(s) = 28.405 + \frac{20.145}{s} + 13.9s$$

29

The closed-loop poles are calculated as follows with designed PID controller and are also illustrated in Figure 2.11.

$$s_{1,2} = -0.4849 \pm 0.6031\,j$$

$$s_3 = -2.2802$$

$$s_4 = -6.4698$$
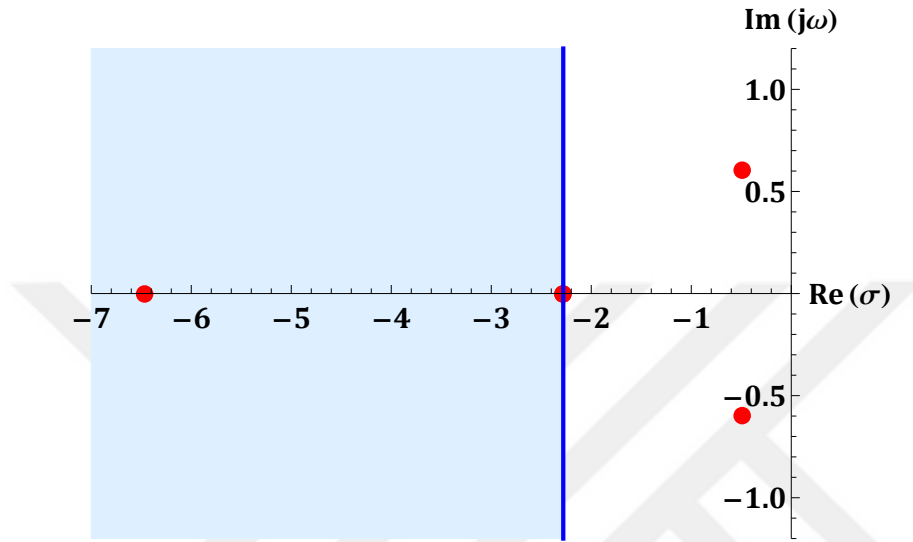
Figure 2.11 : The closed-loop poles with designed PID controller (Example 2.6).

If the designed PID controller is implemented in PI-PD structure with the following PI and PD controllers,

$$F_{PI}(s) = 2.518 + \frac{20.145}{s}$$

$$F_{PD}(s) = 25.887 + 13.9s$$

which assign the controller zero to the point of $s = -8$ in s-plane, the closed-loop system transient response is obtained as in Figure 2.12. It is seen that the rise time of system is around 2.85 seconds with 7% overshoot due to the fact that the dominant poles are assigned to the desired locations in s-plane and the closed-loop system has high enough dominance factor ($m = 4.7$). The control signal for the closed-loop is also depicted in Figure 2.13. It can be said that the control signal is smooth and in limits for the considered system.

Example 2.7:

Consider a higher order system with the following open-loop transfer function.

$$G(s) = \frac{10}{(s^2 + 2s + 4)(s^2 + 8s + 20)(s+4)^2(s+6)}$$
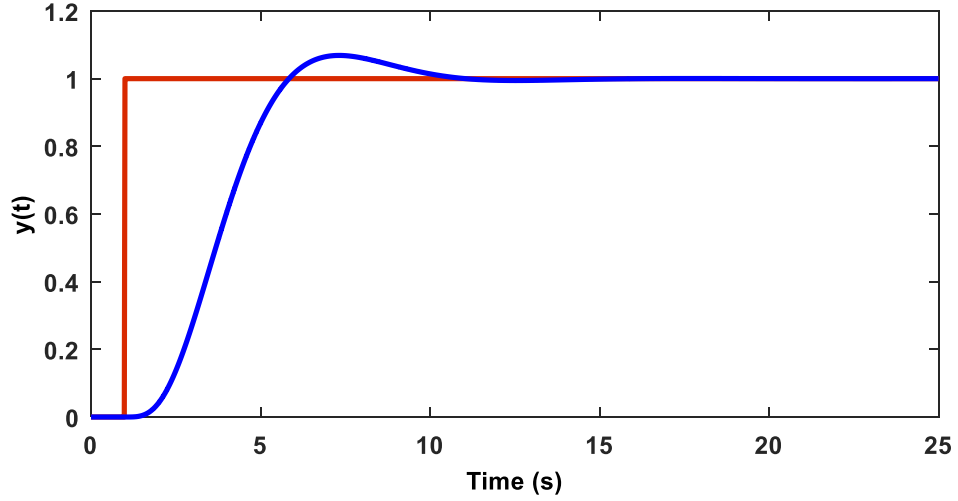
Figure 2.12 : The transient response of the system (Example 2.6).
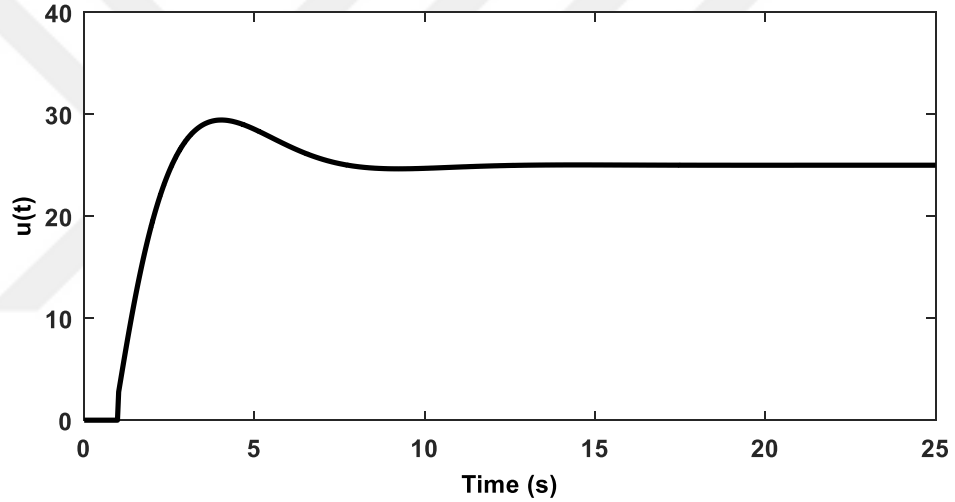
Figure 2.13 : The control signal for designed PI-PD controller (Example 2.6).

Closed-loop performance criteria are chosen as 5% overshoot and 6 seconds settling time. In this case, closed-loop dominant poles are found to be $s_{1,2} = -0.6667 \pm j0.699$. PID controller parameters depending on the parameter K_p are given as below [21].

$$K_i = 237.944 + 0.7K_p$$

$$K_d = -57.437 + 0.75K_p$$

The closed-loop system characteristic polynomial, in terms of the parameter K_p, is then given as follows.

$$P_c(s, K_p) = s^8 + 24s^7 + 244s^6 + 1368s^5 + 4608s^4 + 9568s^3$$
$$+ (11457.6 + 7.5K_p)s^2 + (7680 + 10K_p)s + (2379.44 + 7K_p)$$

31

The residue polynomial can be given as below if polynomial long division is performed.

$$P_r(s, K_p) = s^6 + 22.6666s^5 + 212.843s^4 + 1063.04s^3 + 2991.93s^2$$

$$+ 4586.64s + (2550.06 + 7.5K_p)$$

The polynomials $P_m(s)$ are then calculated through the above polynomial as follows.

$$P_1(s) = 6s^5 + 113.33s^4 + 851.37s^3 + 3189.13s^2 + 5983.87s + 4586.64$$

$$P_2(s) = 15s^4 + 226.67s^3 + 1277.06s^2 + 3189.13s + 2991.93$$

$$P_3(s) = 20s^3 + 226.67s^2 + 851.37s + 1063.04$$

$$P_4(s) = 15s^2 + 113.33s + 212.84$$

$$P_5(s) = 6s + 22.667$$

The maximum real root of the above polynomials is calculated as $\lambda_{rmax} = -3.4915$. After that the polynomials $P_{hm}(s)$ are calculated via the expressions given below.

$$P_{h1}(s) = P_4(s)$$

$$P_{h2}(s) = \begin{vmatrix} P_4(s) & P_2(s) \\ 1 & P_3(s) \end{vmatrix}$$

$$P_{h3}(s) = \begin{vmatrix} P_4(s) & P_2(s) & 0 \\ 1 & P_3(s) & P_1(s) \\ 0 & P_4(s) & P_2(s) \end{vmatrix}$$

$$P_{h4}(s) = \begin{vmatrix} P_4(s) & P_2(s) & 0 & 0 \\ 1 & P_3(s) & P_1(s) & 0 \\ 0 & P_4(s) & P_2(s) & 0 \\ 0 & 1 & P_3(s) & P_1(s) \end{vmatrix}$$

$$P_{h5}(s) = \begin{vmatrix} P_5(s) & P_3(s) & P_1(s) & 0 & 0 \\ 1 & P_4(s) & P_2(s) & 0 & 0 \\ 0 & P_5(s) & P_3(s) & P_1(s) & 0 \\ 0 & 1 & P_4(s) & P_2(s) & 0 \\ 0 & 0 & P_5(s) & P_3(s) & P_1(s) \end{vmatrix}$$

The maximum real root of the polynomials $P_{hm}(s)$ is found to be $\lambda_{hmax} = -2.185$. Therefore it is possible to conclude that non-dominant poles can be placed with the PID controller

$$m_{max} = \frac{(-2.185 \sim -3.4915)}{-0.6667} \cong 3.277 \sim 5.237$$

32

times away from the dominant pole pair. It means that there exists a PID controller that assigns the remaining poles 3.277 times away from the dominant pole pair; however, it is not possible to place them more than 5.237 times away from the dominant poles.

For this example, it is possible to show that $\lambda_{hmax} = -2.185$ is actually equal to σ as stated in the theorem via numerical approach as in Figure 2.14.
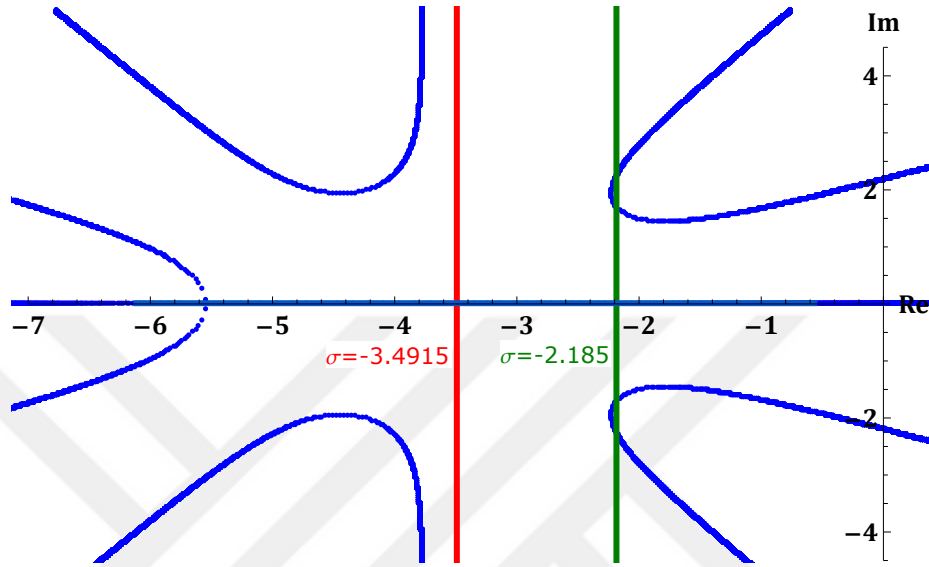
Figure 2.14 : Variation curve of the non-dominant poles (Example 2.7).

The K_p parameter of the PID controller is found as $K_p = 59.42$ for $\lambda_{hmax} = -2.185$. The designed PID controller is then obtained as below.

$$F(s) = 59.42 + \frac{279.52}{s} - 12.877s$$

The closed-loop poles are calculated as

$$s_{1,2} = -0.6667 \pm 0.699j$$

$$s_{3,4} = -2.185 \pm 1.7j$$

$$s_{5,6} = -4.815 \pm 2.102j$$

$$s_7 = -2.185$$

$$s_8 = -6.482$$

with the designed PID controller and are illustrated in the Figure 2.15. As it is seen, the maximum dominance factor is satisfied and the non-dominant poles are located on the left side of the line $s = -2.185$.

Similar to the previous example, if the designed PID controller is implemented in PI-PD structure such that the controller zero is assigned to the point of $s = -6$ in
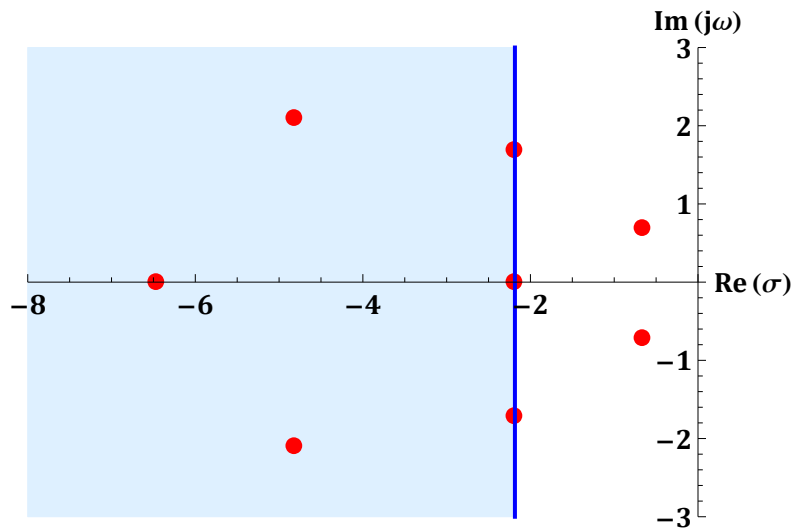
Figure 2.15 : The closed-loop poles with designed PID controller (Example 2.7).

s-plane, we have following PI and PD controllers.

$$F_{PI}(s) = 46.586 + \frac{279.52}{s}$$

$$F_{PD}(s) = 12.834 - 12.877s$$

In this case, the closed-loop system transient response is obtained as in Figure 2.16. It is again seen that the system settles to its final value in around 7.5 seconds with 4.3% overshoot which are very close to the desired performance specifications in the closed-loop.
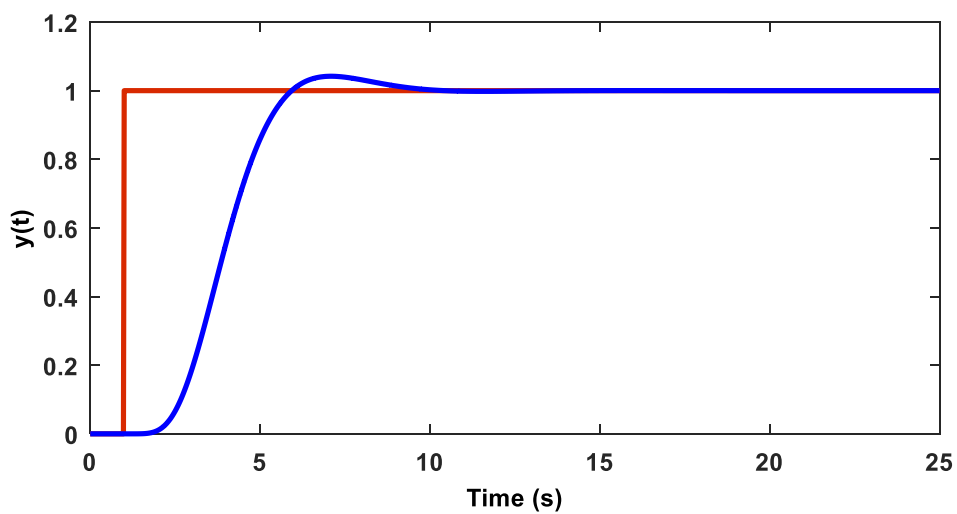
Figure 2.16 : The transient response of the system (Example 2.7).

34

The control signal is given in Figure 2.17 for the designed PI-PD controller. It can be said that the control signal is low (according to the open-loop gain) and smooth which is important during the real-time implementation.
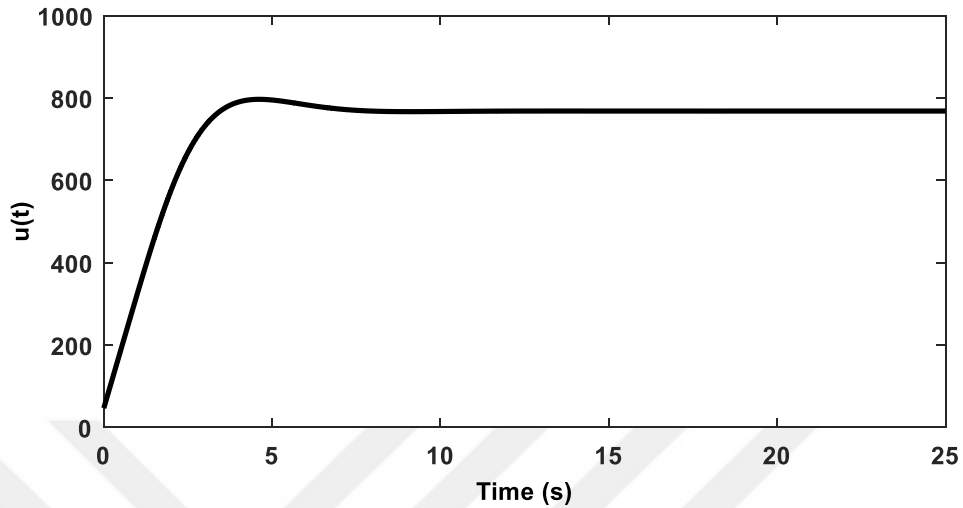
Figure 2.17 : The control signal for designed PI-PD controller (Example 2.7).

2.4.2 Solution to maximum dominance factor problem for the systems with open-loop zeros

In this section, the problem of how far unassigned poles can be located away from the dominant poles with continuous PID controllers is solved. Hence, the previous study is extended to the systems with open-loop zeros.

The first part, which is stated as to express PID controller parameters in terms of the dominant pole locations in s-plane, is the same as previous section. Main problem is stated in the previous part as finding the smallest value of σ such that the polynomial $P_r(s+\sigma)$ is stabilizable. Since it is desired unassigned poles to be located "m" times away from the dominant pole pair, it also means that the polynomial $P_r(s+\sigma)$ should be Hurwitz. It is known that Routh-Hurwitz stability criterion is a frequently used method to check the stability of polynomials. Therefore, Routh-Hurwitz method can be used to check the stability of this polynomial. If the inequalities are written from the first column of Routh table and are then simplified, the region in $K_p - m$ plane which satisfies all of these conditions can be found. Thus, it is possible to find the maximum value of the dominance factor, graphically.

As Routh-Hurwitz stability criterion is used to find the maximum value, the proposed method is valid for all transfer functions even for the ones consist of open-loop zeros. Here, the only possible problem may be the order of the system since it directly affects the complexity of the set of nonlinear equations which are written from the Routh table. However, if the order of system is high enough, it is also possible to use the griding approach over the parameter σ or K_p in order to find the maximum dominance factor (m_{max}).

Example 2.8:

First of all, let us consider the same transfer function given in Example 2.6 with the open-loop transfer function of

$$G(s) = \frac{1}{(s+1)^2(s+5)^2}$$

Here it is aimed to show that the method works both for the systems with or without open-loop zeros.

The residue polynomial constructed by the unassigned poles are given as follows.

$$P_r(s) = s^3 + 11.03s^2 + 34.704s + (4.3485 + 1.031K_p)$$

If the polynomial $P_r(s + m\sigma)$ is created, we have,

$$P_r(s - 0.4849m, K_p) = -4.217 - K_p + 16.32m - 2.5152m^2 + 0.1106m^3$$
$$+ (-33.656 + 10.374m - 0.684m^2)s + (-10.6971 + 1.41077m)s^2 - 0.9698s^3$$

It is now possible to use the Routh-Hurwitz stability criterion and find the inequalities from the first column of Routh table. If the conditions are written and the region in $K_p - m$ plane which satisfies all of these conditions are found, results are obtained as in Figure 2.18.

$$-10.697 + 1.4108m < 0$$
$$\frac{-0.6081(-414.912 + 1.1305K_p + 166.26m - 22.747m^2 + m^3)}{-7.58245 + m} < 0$$
$$(-4.2172 - K_p + 16.3198m - 2.5152m^2 + 0.11057m^3) < 0$$

It is clear from the figure that maximum dominance factor is $m = 4.7$ as found earlier, if the dominant poles are desired to be chosen as $s_{1,2} = -0.4849 \pm 0.6031j$.

As long as the value of the controller parameter K_p is chosen from the obtained feasible interval for a desired dominance factor (m), dominant pole placement works
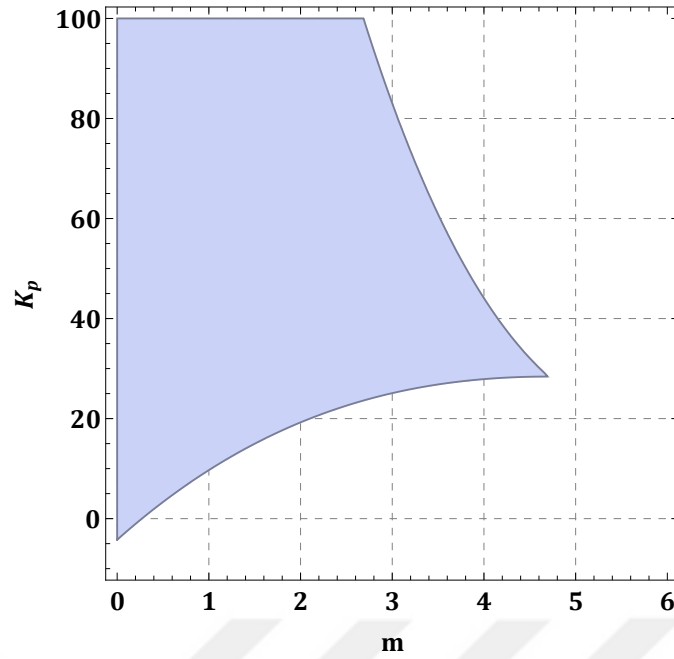
Figure 2.18 : Possible m values and corresponding K_p values (Example 2.8).

well. Therefore, the choice of K_p parameter can be done by considering the additional requirements such as the locations of closed-loop zeros or the magnitude of the control signal.

Example 2.9:

Suppose that the following transfer function to be controlled by a PID controller is given.

$$G(s) = \frac{(s^2 + 8s + 17)}{(s+2)^3(s+4)}$$

It is aimed to find the maximum dominance factor when the dominant poles are calculated as

$$s_{1,2} = -0.8 \pm 0.1j$$

from the requirements on transient response. The modified residue polynomial $P_r(s + m\sigma)$ is found as follows.

$$P_r(s - 0.8m, K_p) = -2939.6 - 2150.88K_p + 3290.78m + 809.74K_pm - 1056.1m^2$$
$$- 80.974K_pm^2 + 103.64m^3 + (-4113.47 - 1012.18K_p + 2640.27m$$
$$+ 202.43K_pm - 388.67m^2)s + (-1650.16 - 126.523K_p + 485.84m)s^2 - 202.43s^3$$

In a similar way, if the conditions from the first column of Routh table are written and simplified, the following figure is obtained in $K_p - m$ plane.

37
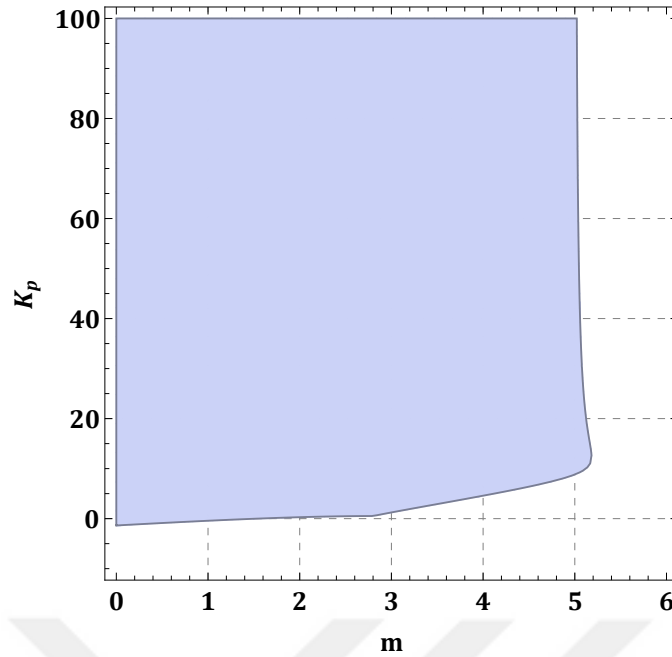
Figure 2.19 : Possible m values and corresponding K_p values (Example 2.9).

The maximum dominance factor can be found as $m_{max} = 5.182$ for the desired dominant pole pair. Let us choose the $K_p = 12.4$ which satisfies the maximum dominance factor, then the closed-loop poles are calculated as below.

$$s_{1,2} = -0.8 \pm 0.1j$$

$$s_{3,4} = -4.146 \pm 1.426j$$

$$s_5 = -7.609$$

It is also possible to illustrate the dominant and non-dominant closed-loop poles as in Figure 2.20.

2.5 Limitations on the Dominant Pole Pair Selection

In this section, it is aimed to find the limitations on the selection of dominant pole pair with the help of the method used in the previous section (Routh-Hurwitz method) so that dominant pole placement approach works well and desired performance criteria are met as accurately as possible in the closed-loop. In other words, it is desired to find the dominant poles region in s-plane to guarantee dominant pole placement with continuous PI and PID controllers. First of all, the region determination method is explained through the PI controller and then it is extended to the PID controller case in a similar way.
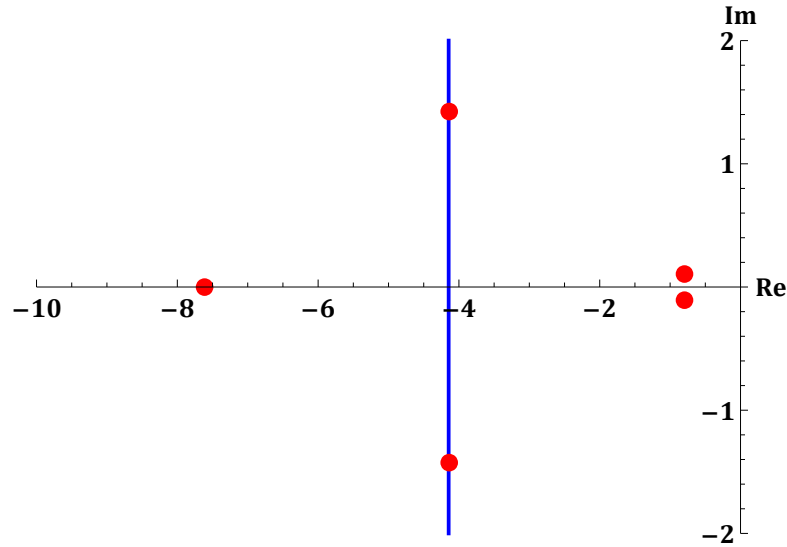
Figure 2.20 : Closed-loop poles in s-plane for $K_p = 12.4$ (Example 2.9).

2.5.1 PI controller case

In order to find the limitations of dominant pole pair selection, PI controller parameters are required to be expressed in terms of the dominant pole locations which is already done and given with (2.14) and (2.15). After that it is expected to find (σ, ω) region in complex s-plane in which the guaranteed dominant pole placement can successfully be done for a specified dominance factor (m).

It is already mentioned in previous section that it is desired unassigned poles to be located "m" times away from the dominant pole pair and hence the polynomial $P_r(s + m\sigma)$ should be Hurwitz. Therefore, all of the (σ, ω) pairs which stabilizes the polynomial $P_r(s + m\sigma)$ constitute a solution to the considered problem [22]. Note that the dominance factor is known and constant here.

Here, it is again possible to use Routh-Hurwitz stability criterion to find the dominant pole region. In order to solve this problem, the polynomial $P_r(s)$ is used again; however, this time the parameters σ and ω are unknown but the dominance factor (m) is known. For that reason, the polynomial consists of the parameters σ and ω as given in (2.41).

$$P_r(s, \sigma, \omega) = \delta_{n-1}(\sigma, \omega)s^{n-1} + \cdots + \delta_1(\sigma, \omega)s + \delta_0(\sigma, \omega) \qquad (2.41)$$

Therefore, the inequalities, which are written from the first column of Routh table, define regions in (σ, ω) plane (actually in complex s-plane). Intersections of all these

39

regions (if it is not an empty set) give the dominant pole region in which dominant pole placement is guaranteed for the desired "m" value.

Example 2.10:

Consider a fourth order system with one left half plane zero which is expressed by the following transfer function [22].

$$G(s) = \frac{4(s+4)}{(s^2+2s+2)(s+1)^2}$$

In the closed-loop, it is expected non-dominant poles to be "m" times away from the dominant pole pair with PI controller. First of all, parameters of the PI controller should be found as below.

$$K_i = \frac{(\sigma^2+\omega^2)(22+56\sigma+55\sigma^2+24\sigma^3+3\sigma^4-(-2\sigma^2+8\sigma+9)\omega^2-\omega^4)}{4(16+8\sigma+\sigma^2+\omega^2)}$$

$$K_p = \frac{-4-24\sigma-45\sigma^2-39\sigma^3-16\sigma^4-2\sigma^5+(16\sigma^2+25\sigma+11)\omega^2+2\sigma\omega^4}{2(16+8\sigma+\sigma^2+\omega^2)}$$

It is now possible construct the polynomial $P_r(s,\sigma,\omega)$ as follows,

$$P_r(s,\sigma,\omega) = \gamma_3 s^3 + \gamma_2 s^2 + \gamma_1 s + \gamma_0$$

where

$$\gamma_3 = (16+8\sigma+\sigma^2+\omega^2)$$

$$\gamma_2 = (64+64\sigma+20\sigma^2+2\sigma^3+4\omega^2+2\sigma\omega^2)$$

$$\gamma_1 = (112+184\sigma+119\sigma^2+32\sigma^3+3\sigma^4-9\omega^2+2\sigma^2\omega^2-\omega^4)$$

$$\gamma_0 = (88+224\sigma+220\sigma^2+96\sigma^3+12\sigma^4-36\omega^2-32\sigma\omega^2+8\sigma^2\omega^2-4\omega^4)$$

The polynomial $P_r(s+m\sigma)$ can be calculated for the different values of "m" and the conditions on σ and ω can be determined with the help of the first column of Routh table. After that the region in s-domain, which is intersection of all these conditions, can be drawn with the help of any software that provides symbolic calculations such as Mathematica.

The dominant poles regions with PI controller are found for $m = 3,\ldots,8$ and are illustrated in Figure 2.21.

It can easily be seen from the figure that if non-dominant (unassigned) poles are desired to be placed further away from the dominant poles, the region in which dominant

40
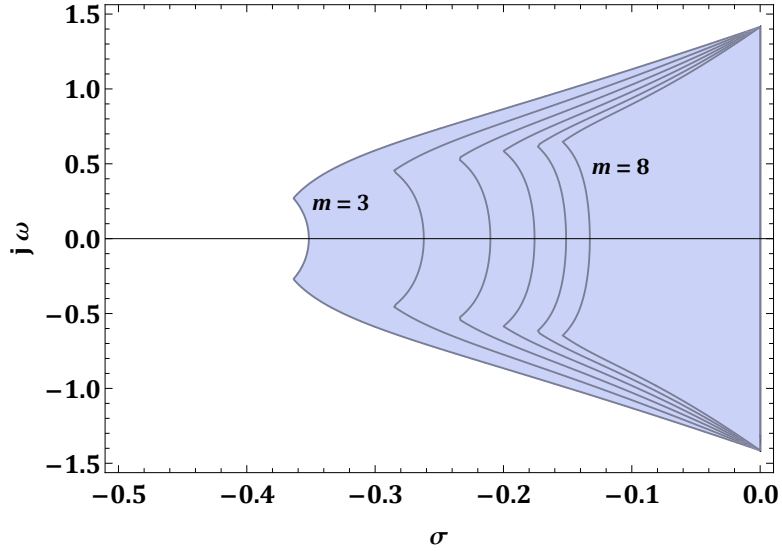
Figure 2.21 : Dominant poles region with PI controller for different m values (Example 2.10).

poles can be assigned shrinks. It actually shows us the limitations on the closed-loop performance specifications for a desired dominance factor when a PI controller is used to control the system.

For instance, if the desired dominance factor is given as $m = 4$ and the dominant pole pair is chosen as $s_{1,2} = -0.26 \pm 0.26j$ (one of the limit value in the region) then the PI controller is found as follows.

$$F(s) = \frac{0.00668(s + 3.705)}{s}$$

The closed-loop poles of the system with the designed PI controller is illustrated in Figure 2.22.

2.5.2 PID controller case

Calculation of the limitation on dominant poles selection is similar for PID controller case. After the parameters of PID controller are obtained in terms of the location of dominant pole pair, it is possible to find (σ, ω) region in s-plane where dominant pole placement for a specified "m" value is provided. However, in this case, the polynomial constructed by the unassigned closed-loop poles also depends on the parameter K_p in addition to the parameters σ and ω. Thus, the residue polynomial is given in the following form.

$$P_r(s, \sigma, \omega, K_p) = \delta_{n-1}(\sigma, \omega, K_p)s^{n-1} + \cdots + \delta_1(\sigma, \omega, K_p)s + \delta_0(\sigma, \omega, K_p) \quad (2.42)$$

41
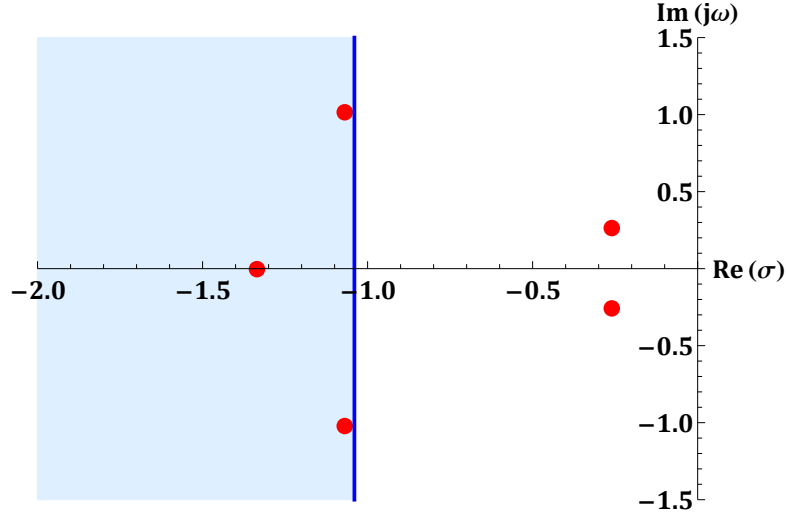
Figure 2.22 : Closed-loop poles with PI controller for $m = 4$ (Example 2.10).

It is again possible to use Routh-Hurwitz criterion to find the conditions on (σ, ω) pair. Here, the intersection of resulting inequalities, which are written from the Routh table for the polynomial of unassigned poles $P_r(s + m\sigma)$, define a region in 3 dimensional $\sigma - \omega - K_p$ plane. Thus, it is possible to see the region in which dominant poles are placed for a desired "m" value, graphically. The corresponding K_p interval can also be found for a chosen (σ, ω) pair.

Example 2.11:

Consider a sixth order process given below [22].

$$G(s) = \frac{1}{(s+1)^2(s+3)^2(s+5)^2}$$

Parameters of the PID controller are found as below,

$$K_i = \frac{(\sigma^2 + \omega^2)}{2\sigma}(-K_p - 225 + 799\sigma^2 + 888\sigma^3 + 381\sigma^4 + 72\sigma^5 + 5\sigma^6 + 799\omega^2 \\ + 888\sigma\omega^2 + 254\sigma^2\omega^2 - 5\sigma^4\omega^2 - 127\omega^4 - 72\sigma\omega^4 - 9\sigma^2\omega^4 + \omega^6)$$

$$K_d = -\frac{1}{2\sigma}(K_p + 225 + 1380\sigma + 2397\sigma^2 + 1776\sigma^3 + 635\sigma^4 + 108\sigma^5 + 7\sigma^6) \\ - \frac{1}{2\sigma}(-799\omega^2 - 1776\sigma\omega^2 - 1270\sigma^2\omega^2 - 360\sigma^3\omega^2 - 35\sigma^4\omega^2 - \omega^6 \\ - 127\omega^4 - 108\sigma\omega^4 - 21\sigma^2\omega^4)$$

After that the polynomial $P_r(s, \sigma, \omega, K_p)$ which is constructed by the unassigned closed-loop poles is found as follows,

$$P_r(s, \sigma, \omega, K_p) = \gamma_5 s^5 + \gamma_4 s^4 + \gamma_3 s^3 + \gamma_2 s^2 + \gamma_1 s + \gamma_0$$

42

where

$$\gamma_5 = 2\sigma$$

$$\gamma_4 = 36\sigma + 4\sigma^2$$

$$\gamma_3 = (254\sigma + 72\sigma^2 + 6\sigma^3 - 2\sigma\omega^2)$$

$$\gamma_2 = (888\sigma + 508\sigma^2 + 108\sigma^3 + 8\sigma^4 - 36\sigma\omega^2 - 8\sigma^2\omega^2)$$

$$\gamma_1 = (1598\sigma + 1776\sigma^2 + 762\sigma^3 + 144\sigma^4 + 10\sigma^5 - 254\sigma\omega^2$$
$$- 144\sigma^2\omega^2 - 20\sigma^3\omega^2 + 2\sigma\omega^4)$$

$$\gamma_0 = (-225 - Kp + 799\sigma^2 + 888\sigma^3 + 381\sigma^4 + 72\sigma^5 + 5\sigma^6 + 799\omega^2$$
$$+ 888\sigma\omega^2 + 254\sigma^2\omega^2 - 5\sigma^4\omega^2 - 127\omega^4 - 72\sigma\omega^4 - 9\sigma^2\omega^4 + \omega^6)$$

As performed in the PI controller design, the polynomial $P_r(s + m\sigma)$ can be calculated for any selected m value and the conditions on σ and ω can be determined using the Routh table. Since the resulting conditions are also depends on the parameter K_p, a region in 3 dimensional σ-ω-K_p space will be obtained for $K_p \in (-\infty, +\infty)$. For instance, if $m = 3$ is chosen then the dominant pole region is shown in Figure 2.23. It is also possible to find this region for different m values.
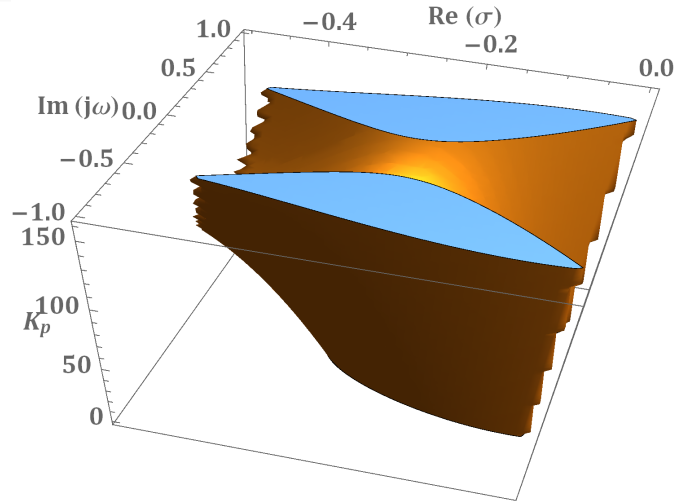
Figure 2.23 : Dominant poles region for PID controller case (Example 2.11).

For instance, if $K_p = 140$ is chosen by inspecting the above figure then the limitations on the dominant pole pair is illustrated in Figure 2.24. As long as the (σ, ω) pair is taken from this obtained region, the dominance factor $m = 3$ is guaranteed for the chosen K_p value.
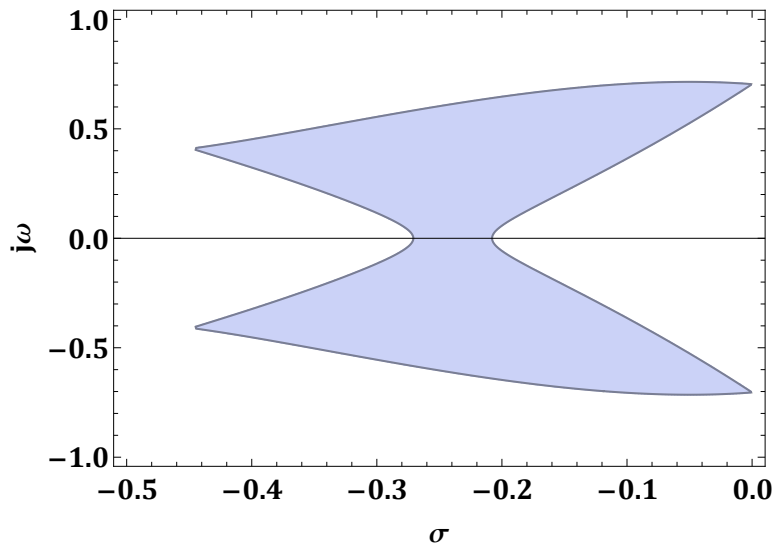
Figure 2.24 : Dominant poles region in s-plane for $K_p = 140$ (Example 2.11).

Let us choose the dominant pole pair as $s_{1,2} = -0.4 \pm 0.33j$ which is one of the limit values in the above figure. In this case, the PID controller is found as follows.

$$F(s) = 140 + \frac{78.45}{s} + 87.13s$$

On the other hand, the closed-loop poles with the designed PID controller are given in Figure 2.25.
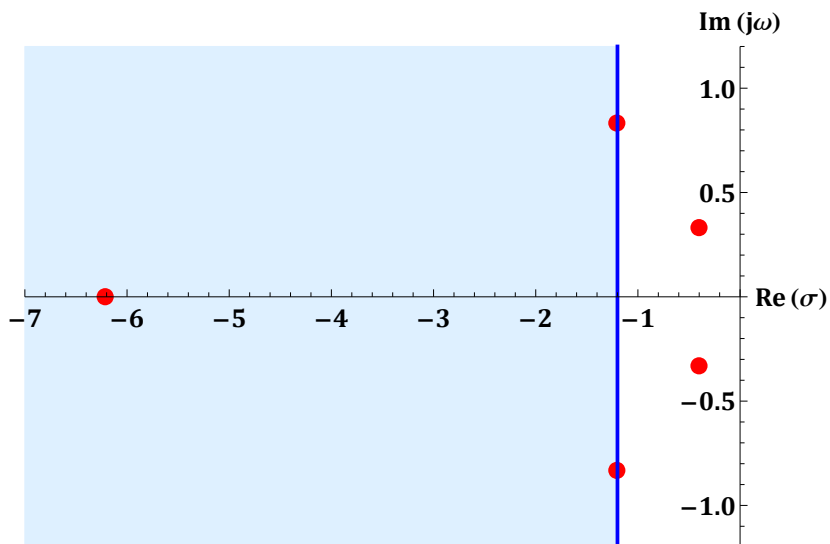
Figure 2.25 : The closed-loop poles in s-plane for $K_p = 140$ (Example 2.11).

It is seen that the limitations on dominant pole placement are found successfully when the dominance factor is predetermined.

Note that it is not always possible to place non-dominant poles "*m*" times away from the dominant pole pair using a lower order controller especially higher order systems are considered. For this reason, (σ, ω) pair which satisfies the inequalities written from the first column of Routh table might be an empty set for a selected "m" value. In this case, sometimes changing the desired dominance factor may work to obtain a solution.

2.6 Dominant Pole Region Assignment in Continuous-Time Domain

In the dominant pole placement approach, the degree of freedom for the PID controllers is enough to assign dominant poles; however, it may be a challenge to keep the remaining poles away from the dominant pole pair with only one remaining parameter (e.g. K_p). Furthermore, there is no parameter left to assign the remaining poles in case of the PI controller. Nevertheless it is possible to widen the closed-loop performance criteria instead of choosing strict specifications. Thus, it may become possible to find the controller parameters and the dominant pole placement is performed. It is already meaningful for most of the systems to have time domain characteristics between the minimum and maximum desired values. This results the dominant pole pair to be located in a specified region instead of a point, hence, the dominant pole region assignment (DPRA) problem shows up.

2.6.1 P controller case

If P controller is used to control a system, it is better to desire only one performance criterion. One of the proper choices can be settling time criterion to be satisfied in the closed-loop with a P type controller. In this case, the closed-loop dominant pole pair should be located in a region bounded by the lines $s_1 = \sigma_{min}$ and $s_2 = \sigma_{max}$ in the s-plane and remaining poles should be located on the left side of a particular line $s_3 = \sigma_a$. The desired pole configuration in the closed-loop is illustrated in Figure 2.26.

The characteristic polynomial of a closed-loop control system with unity feedback is given as follows.

$$P_c(s) = 1 + F(s)G(s) = 0 \tag{2.43}$$
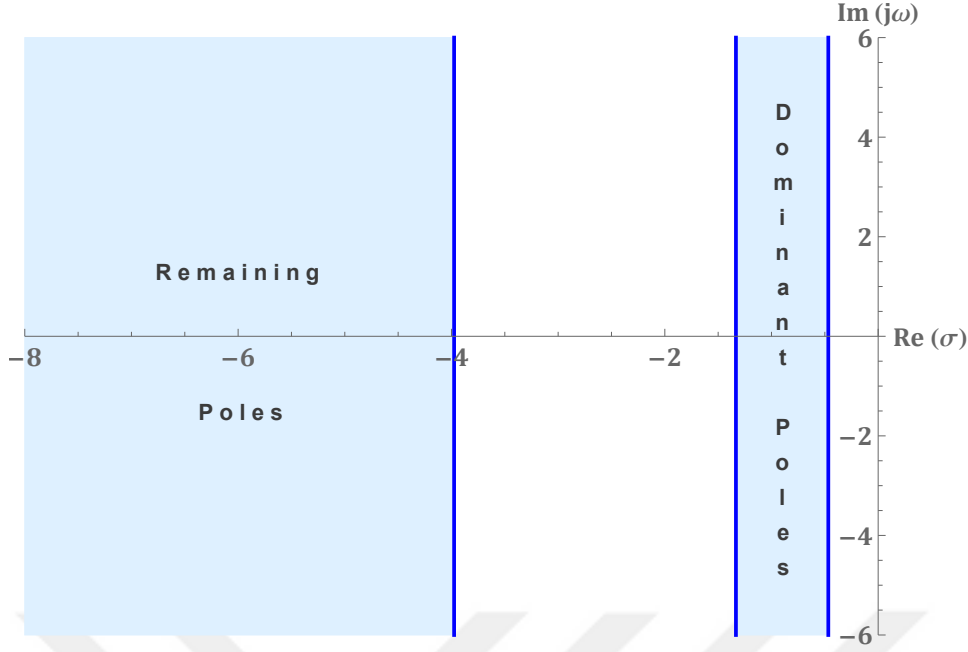
Figure 2.26 : The desired pole configuration with P controller.

If P controller is used,

$$P_c(s) = 1 + K_p \frac{N(s)}{D(s)} = 0 \tag{2.44}$$

can be written. Let dominant poles be $s_{1,2} = \sigma \pm j\omega$ where $\sigma \in [\sigma_{min}, \sigma_{max}]$ and $\omega \in \mathbb{R}$. It is clear that equation (2.44) should be satisfied by the dominant pole pair. For the open-loop transfer function $G(s)$, let s be replaced by $\sigma + j\omega$,

$$G(\sigma + j\omega) = \frac{N_{Re} + jN_{Im}}{D_{Re} + jD_{Im}} \tag{2.45}$$

where

$$D_{Im} = Im[D(\sigma + j\omega)], D_{Re} = Re[D(\sigma + j\omega)]$$

$$N_{Im} = Im[N(\sigma + j\omega)], N_{Re} = Re[N(\sigma + j\omega)]$$

If (2.45) is re-arranged,

$$G(\sigma + j\omega) = \frac{(N_{Re}D_{Re} + N_{Im}D_{Im}) + j(N_{Im}D_{Re} - N_{Re}D_{Im})}{D_{Re}^2 + D_{Im}^2} \tag{2.46}$$

and by defining

$$X(\omega) = N_{Re}D_{Re} + N_{Im}D_{Im}$$

$$Y(\omega) = N_{Im}D_{Re} - N_{Re}D_{Im}$$

$$Z(\omega) = D_{Re}^2 + D_{Im}^2$$

46

it is possible to write the following equality.

$$G(\sigma + j\omega) = \frac{X(\omega)}{Z(\omega)} + j\frac{Y(\omega)}{Z(\omega)} \tag{2.47}$$

Here, the critical frequencies (ω_i^*), which cause roots to cross $s = \sigma$ line in complex s-plane, can be calculated using (2.48).

$$Im[G(\sigma + j\omega)] = \frac{Y(\omega)}{Z(\omega)} = 0 \tag{2.48}$$

After that the intersection points (x_i) of Nyquist curve and real axis can be found with the help of following expression ($\omega^* = 0$ and $\omega^* = \infty$ are also added to the critical frequencies as necessary).

$$x_i = \frac{X(\omega_i^*)}{Z(\omega_i^*)} \tag{2.49}$$

It is now possible to calculate the gain intervals with the help of Nyquist theorem. These intervals can be found by $\mathcal{K}_i \in \left(-\frac{1}{x_i}, -\frac{1}{x_{i+1}}\right)$ such that $x_i < x_{i+1}$ for $i = 1, 2, \ldots$ and the union of these intervals, in which number of the closed-loop system poles (u) located on the right side of the line $s = \sigma$ are found to be as desired, gives the feasible interval. The final gain interval is calculated as below.

$$\overline{K} \in \bigcup_{j=1}^{n} \mathcal{K}_j \tag{2.50}$$

Here, it is expected dominant poles to be located between the lines $s_1 = \sigma_{min}$ and $s_2 = \sigma_{max}$ in the s-plane and remaining poles to be located on the left side of the $s_3 = \sigma_a$. Therefore, the proposed calculation method should be applied three times for $G_1 = G(\sigma_{min} + j\omega)$ such that $u = 0$, $G_2 = G(\sigma_{max} + j\omega)$ and $G_3 = G(\sigma_a + j\omega)$ such that $u = 2$. As a result, the feasible interval of controller parameter K_p to provide dominant pole placement is found as follows.

$$K_p \in \bigcap_{j=1}^{3} \overline{K}_j \tag{2.51}$$

If the resulting set is found to be an empty set ($K_p = \emptyset$), it means that there is not any P controller which satisfies the configuration given in Figure 2.26 for the desired values of $\sigma_{min}, \sigma_{max}$ and σ_a.

Example 2.12:

For the system whose transfer function is given as,

$$G(s) = \frac{(s^2 + 4s + 16)(s + 8)}{(s + 0.9)(s + 2)(s + 3)(s + 4)(s + 6)}$$

it is desired to find the P controller set such that $\sigma_{min} = 0.8$, $\sigma_{max} = 1.333$ and $\sigma_a = 3.1$ so the dominance factor is $m = 3.1/1.333 \cong 2.33$ in the worst case.

For $G_1(\omega) = G(-0.8 + j\omega)$ we have,

$$X(\omega) = 2549.11 - 9275.42\omega^2 + 392.07\omega^4 - 37.72\omega^6 - \omega^8$$

$$Y(\omega) = 2.8(3436.34\omega - 1078.07\omega^3 + 51.82\omega^5 + \omega^7)$$

$$Z(\omega) = (0.16 + \omega^2)(1.96 + \omega^2)(5.76 + \omega^2)(11.56 + \omega^2)(29.16 + \omega^2)$$

The critical frequencies (ω_i^*), intersection points (x_i), number of the poles (u_i), which are located on the right side of the line $s = -0.8$ and corresponding gain intervals are given in Table 2.1. Resulting gain interval is found as follows.

$$\overline{K}_1 \in (-0.0454, 1.4922) \bigcup (30.1678, \infty)$$

If the same procedure is applied for $G_2(\omega)$ and $G_3(\omega)$, we obtain the gain intervals as below and the important values (ω_i^*, x_i, u_i) are given in Table 2.2 and Table 2.3, respectively.

$$\overline{K}_2 \in (0.0722, 42.1)$$

$$\overline{K}_3 \in (0.009758, 37.623)$$

Table 2.1 : Calculated gain intervals for $G_1(\omega)$

ω_i^*	x_i	u_i	$\mathcal{K}_i$
0	22.028	1	$-0.0454 > \mathcal{K}_1 > -\infty$
1.419	−0.67	**0**	$1.4922 > \mathcal{K}_2 > -0.0454$
3.914	−0.0331	2	$30.1678 > \mathcal{K}_3 > 1.4922$
∞	0	**0**	$\infty > \mathcal{K}_4 > 30.1678$

Finally, the P controller set, which satisfies the desired pole configuration in the closed-loop, is given as follows.

$$K_p \in \bigcap_{j=1}^{3} \overline{K}_j \in (0.0722, 1.4922) \bigcup (30.1678, 37.623)$$

For instance, if $K_p = 35$ is chosen to control the given system, the closed-loop poles in s-plane is given in Figure 2.27.

Table 2.2 : Calculated gain intervals for $G_2(\omega)$

ω_i^*	x_i	u_i	$\mathcal{K}_i$
0	-13.846	1	$0.0722 > \mathcal{K}_1 > -\infty$
4.19	-0.02375	**2**	$42.1 > \mathcal{K}_2 > 0.0722$
∞	0	0	$\infty > \mathcal{K}_3 > 42.1$

Table 2.3 : Calculated gain intervals for $G_3(\omega)$

ω_i^*	x_i	u_i	$\mathcal{K}_i$
0	-102.48	3	$0.00976 > \mathcal{K}_1 > -\infty$
5.134	-0.0266	**2**	$37.623 > \mathcal{K}_2 > 0.00976$
∞	0	4	$\infty > \mathcal{K}_3 > 37.623$

Please, however, note that it is not always possible to satisfy such configuration with a P controller for all systems. In most cases, the intersection of the gain intervals may be an empty set so it may be required to change desired pole regions both for the dominant and non-dominant poles. A pre-made root-locus analysis can help to the determination of the limits.
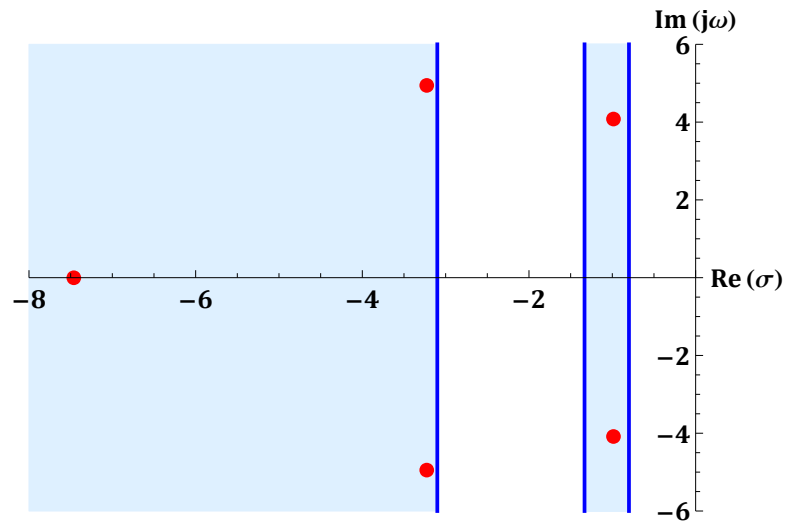
Figure 2.27 : The closed-loop poles with designed P controller (Example 2.12).

On the other hand, the variation of dominance factor is also illustrated in Figure 2.28 when K_p parameter takes value from the obtained feasible interval.
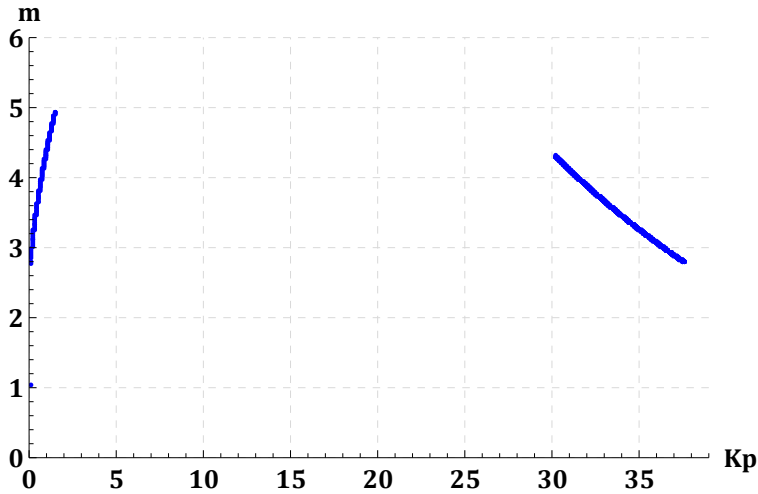
Figure 2.28 : Variation of the dominance factor by K_p (Example 2.12).

2.6.2 PI and PID controller cases

If the system is controlled by a PI or PID controller, it is possible to assign two of the closed-loop poles to the desired locations of $s_{1,2} = \sigma \pm j\omega$ in s-plane. However, it is useful to desire the closed-loop poles to be assigned in a specific region instead of a single point. It may also increase the chance of obtaining higher dominance factor in terms of the dominant pole placement.

Dominant pole region assignment problem is solved via parameter space approach and 2 different method is proposed to assign non-dominant poles. In the first method, the remaining poles are desired to be "m" times away from the dominant poles in the closed-loop. It means that the location of non-dominant poles are written in terms of the dominant poles such as $\sigma_{non} = m\sigma$ so the desired dominance factor is guaranteed. However, in the second method, the non-dominant poles are desired to be located on the left side of a constant line such as $\sigma_{non} = a$. It is worth to note that the computational complexity of the first proposed method is higher than the second one.

Since the proposed approach is similar for both PI and PID controllers, they are given together in this section. For PI controller case, the desired dominant pole region in s-plane is transferred to the $K_p - K_i$ parameter space and after that the border in s-plane for non-dominant poles is transferred. For PID controller case, the same procedure is done for $K_d - K_i$ parameter space and then it is repeated for different values of K_p with the help of griding approach.

50

2.6.2.1 Method 1: Constant Dominance Factor

For a PI controller, it is given that the K_p and K_i parameters are calculated in terms of the parameters σ and ω as follows.

$$K_p(\sigma, \omega) = -\frac{N_{G_{Im}}X + N_{G_{Re}}Y}{\omega Z} \tag{2.52}$$

$$K_i(\sigma, \omega) = -\frac{N_{G_{Im}}Y - N_{G_{Re}}X}{Z} - K_p(\sigma, \omega)\sigma \tag{2.53}$$

Consider the following region, in which the dominant pole pair is desired to be placed,

$$\mathscr{D}_1 = \left\{ \begin{array}{c} s = \sigma \pm j\omega \mid \sigma \in \mathbb{R}^-, \omega \in \mathbb{R}^+ \\ \sigma_{min} \leq \sigma \leq \sigma_{max}, \ \omega_{min} \leq \omega \leq \omega_{max} \end{array} \right\} \tag{2.54}$$

It is possible to map the $\mathscr{D}$ region to the PI controller parameter space by plotting the functions $K_p(\sigma, \omega)$ and $K_i(\sigma, \omega)$ for the given intervals of σ and ω.

It is worth to note that the dominant pole region can also be bounded by the different performance specifications such as settling time, damping ratio (ζ) or natural frequency (ω_n). Therefore, the parametrization given by (2.52) and (2.53) can also be obtained in terms of the other parameters, for instance, by substituting $s_{1,2} = -\zeta\omega_n \pm j\omega_n\sqrt{1-\zeta^2}$ in the characteristic polynomial for the following region,

$$\mathscr{D}_2 = \left\{ \begin{array}{c} s = -\zeta\omega_n \pm j\omega_n\sqrt{1-\zeta^2} \mid \zeta, \omega_n \in \mathbb{R}^+ \\ \zeta_{min} \leq \zeta \leq \zeta_{max}, \ \omega_{nmin} \leq \omega_n \leq \omega_{nmax} \end{array} \right\} \tag{2.55}$$

or $s_{1,2} = \sigma \pm j\frac{\sigma}{\zeta}\sqrt{1-\zeta^2}$ for the region given below.

$$\mathscr{D}_3 = \left\{ \begin{array}{c} s = \sigma \pm j\frac{\sigma}{\zeta}\sqrt{1-\zeta^2} \mid \sigma \in \mathbb{R}^-, \zeta \in \mathbb{R}^+ \\ \zeta_{min} \leq \zeta \leq \zeta_{max}, \ \sigma_{min} \leq \sigma \leq \sigma_{max} \end{array} \right\} \tag{2.56}$$

It is clear that two of the closed-loop poles are located in the desired region as long as (K_p, K_i) pair is chosen from the obtained controller parameter space; however, it is required to find the sub-region in which the remaining closed-loop poles are also located "m" times away from the dominant pole pair.

$$\widetilde{\mathscr{D}} = \left\{ s \in \mathbb{C} \mid Re(s) \leq m\sigma, \ \sigma \in \mathbb{R}^-, m \in \mathbb{R}^+ \right\} \tag{2.57}$$

Here, the subset of PI controller parameters such that the remaining poles are located on the left side of a line $s = m\sigma$ can be found through the residue polynomial. It leads to the relative stabilization problem for the polynomial $P_r(s, \sigma, \omega)$; however, it is easily converted to the stability problem over the polynomial $P_r(s + m\sigma, \sigma, \omega)$.

In order to solve the mentioned stability problem above, the polynomial $P_r(j\Omega + m\sigma, \sigma, \omega)$ can be decomposed into its real and imaginary parts and then solved for (Ω, σ) by equating both parts to zero for $\forall \omega^* \in [\omega_{min}, \omega_{max}]$. Since solving these equations for every ω^* in the interval is not practical, it is possible to use gridding approach over the parameter ω in order to obtain the solution. After that for the resulting values of $\sigma^* \in [\sigma_{min}, \sigma_{max}]$, it is possible to map the achieved (σ^*, ω^*) pairs into the parameter space of PI controller with the help of (2.52) and (2.53). Thus, the root boundaries in $K_p - K_i$ plane are found. As a final step, number of the roots, which are located on the right side of the line $s = m\sigma$ in the resulting regions, can be calculated and the desired parameter region is obtained [40].

Example 2.13 (PI Controller):

Consider a fourth order system with the following transfer function.

$$G(s) = \frac{s-2}{s^4 + 8s^3 + 27.5s^2 + 30s + 28}$$

It is desired to control the given system with a PI controller such that the closed-loop system has damping ratio of $0.6266 \leq \zeta \leq 0.826$ and the natural frequency of $0.484 \leq \omega_n \leq 0.798$. For the desired performance specifications, the dominant pole region in s-plane is illustrated in Figure 2.29.
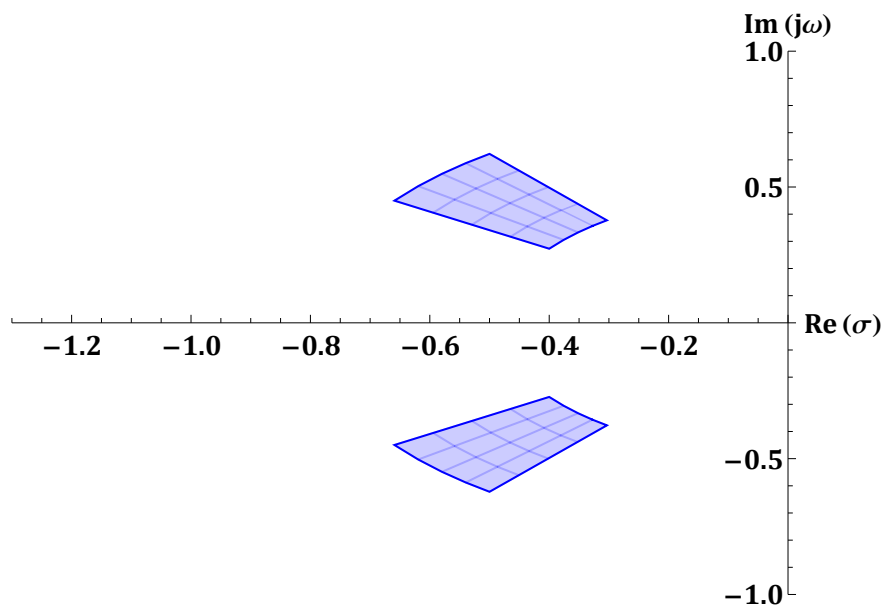
Figure 2.29 : The desired dominant pole region in s-plane (Example 2.13).

First of all, the PI controller parameters (K_p, K_i) are expressed in terms of the parameters ζ and ω_n as follows.

$$K_p(\zeta, \omega_n) = -125 + \frac{139}{1 + \zeta \omega_n + 0.25 \omega_n^2} + 95\zeta \omega_n + (10 - 40\zeta^2)\omega_n^2 + (-4\zeta + 8\zeta^3)\omega_n^3$$

$$K_i(\zeta, \omega_n) = -278 + \frac{1112(1 + \zeta \omega_n)}{4 + 4\zeta \omega_n + \omega_n^2} + 47.5\omega_n^2 - 20\zeta \omega_n^3 + (-1 + 4\zeta^2)\omega_n^4$$

It is now possible to map the desired region into parameters space for $\omega_n \in [\omega_{nmin}, \omega_{nmax}]$ and $\zeta \in [\zeta_{min}, \zeta_{max}]$. If the parametric plot is drawn in the $K_p - K_i$ plane, Figure 2.30 is obtained.
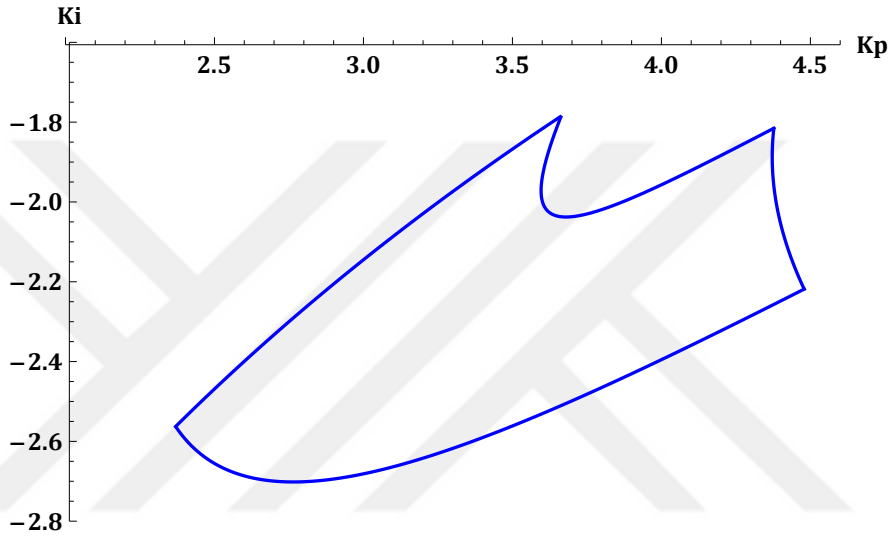
Figure 2.30 : The corresponding region in parameter space (Example 2.13).

As long as the PI controller parameters are chosen inside the obtained region, it is guaranteed that dominant poles are assigned to the desired region in s-plane. However, it is also expected the remaining poles to be located away from the dominant pole pair if possible.

Let the remaining poles to be located on the left side of $s = -3\zeta \omega_n$ line that means the dominance factor to be $m = 3$ for the closed-loop system. Here, the polynomial $P_r(s, \zeta, \omega_n)$ should be obtained through the closed-loop characteristic polynomial as follows.

$$P_c(s, \zeta, \omega_n) = (s^2 + 2\zeta \omega_n s + \omega_n^2)P_r(s, \zeta, \omega_n)$$

The polynomial $\widetilde{P}_r(s, \zeta, \omega_n) = P_r(s - 3\zeta \omega_n, \zeta, \omega_n)$ should then be found in order to convert the relative stabilization problem to the stability problem as below.

$$\widetilde{P}_r(s, \zeta, \omega_n) = s^3 + \beta_2 s^2 + \beta_1 s + \beta_0$$

53

where

$$\beta_0 = -95 + \frac{556}{4 + 4\zeta\omega_n + \omega_n^2} - 42.5\zeta\omega_n + (2 + 112\zeta^2)\omega_n^2 + \zeta(3 - 57\zeta^2)\omega_n^3$$

$$\beta_1 = 27.5 - 64\zeta\omega_n + (-1 + 43\zeta^2)\omega_n^2$$

$$\beta_2 = 8 - 11\zeta\omega_n$$

Let us substitute $s = j\Omega$ and decompose the polynomial $\widetilde{P}_r(s, \zeta, \omega_n)$ into the real and imaginary parts. The root boundaries are found by solving

$$\begin{aligned} Re\left(\widetilde{P}_r(j\Omega, \zeta^*, \omega_n)\right) &= 0 \\ Im\left(\widetilde{P}_r(j\Omega, \zeta^*, \omega_n)\right) &= 0 \end{aligned} \implies \omega_n^* \in [\omega_{nmin}, \omega_{nmax}]$$

for a fixed $\zeta^* \in [\zeta_{min}, \zeta_{max}]$ using the gridding approach. Finally, the achieved (ζ^*, ω_n^*) pairs are mapped into the PI controller parameter space. Figure 2.31 shows the sub-regions and the number of poles (δ) located on the right side of the line $s = -3\zeta\omega_n$ in those regions. PI controller design process is completed by choosing a (K_p, K_i) pair from the sub-region where $\delta = 0$. Note that only a real root boundary (RRB) exists in this example [40].
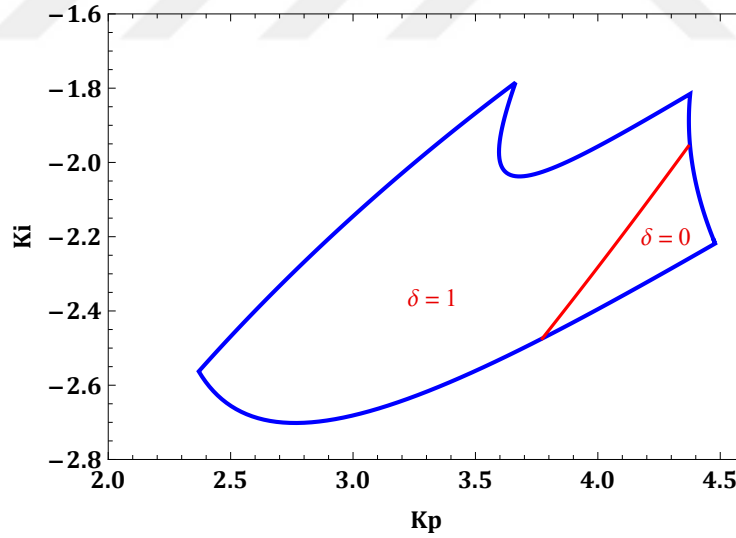
Figure 2.31 : The resulting sub-regions to ensure dominant pole placement (Example 2.13).

Let us choose the PI controller parameters as $K_p = 4.1$ and $K_i = -2.2$ from the feasible region where $\delta = 0$. In this case, the closed-loop poles are given in Figure 2.32. It is seen that dominant poles are assigned in the desired pole region and the remaining poles are located 3 times away from the dominant pole pair.

54
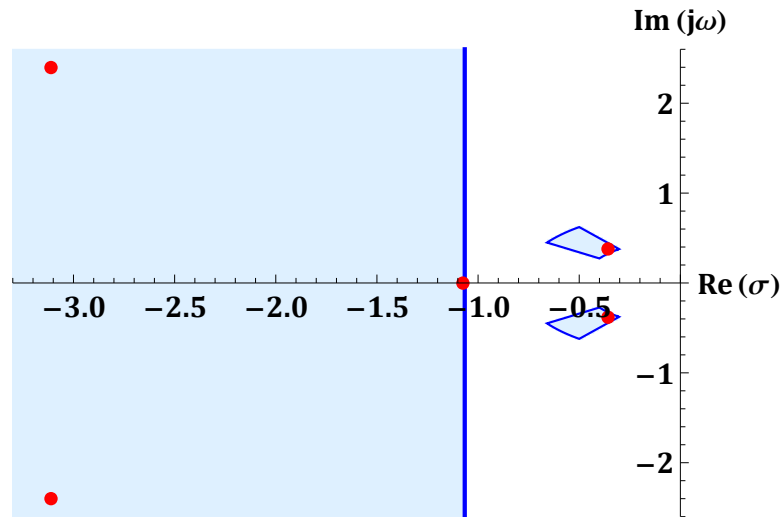
Figure 2.32 : The closed-loop poles with designed PI controller (Example 2.13).

Example 2.14 (PID Controller):

Consider the high order system with the following open-loop transfer function.

$$G(s) = \frac{10}{(s^2 + 2s + 4)(s^2 + 8s + 20)(s+4)^2(s+6)}$$

The closed-loop dominant pole region, which is illustrated in Figure 2.33, is bounded by $\zeta \in [0.69, 0.826]$ and $\sigma \in [0.6, 0.9]$
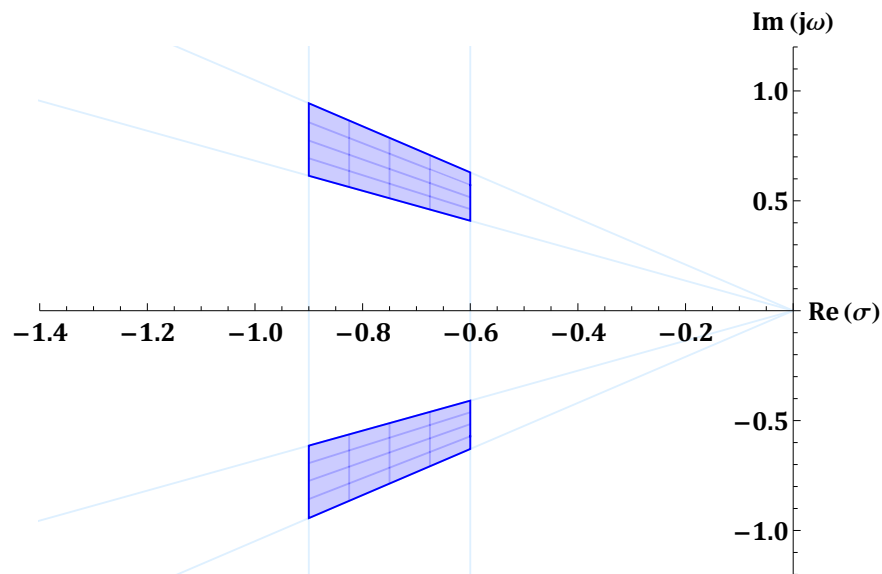
Figure 2.33 : The desired dominant pole region in s-plane (Example 2.14).

Here, the same procedure is used as in the previous example; however, since the controller to be designed is a PID controller, the desired region is mapped into 2D

parameters space (K_i, K_d) for a fixed $K_p = k_p^*$. The final region in 3D space can then be obtained by gridding the K_p parameter.

For instance, Figure 2.34 shows the regions which are mapped from the s-plane for different values of the K_p parameter to the $K_i - K_d$ parameter space. It is also possible to illustrate these regions as a 3D graphic (Figure 2.35).
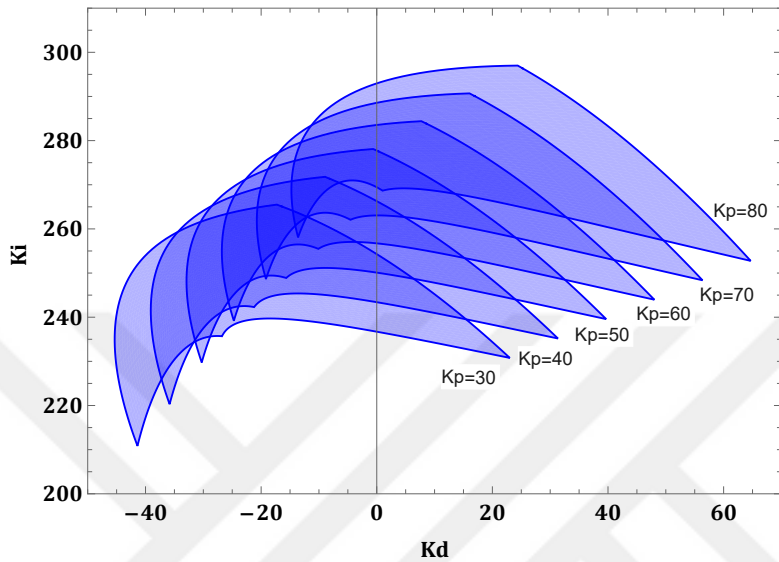
Figure 2.34 : The corresponding regions in $K_d - K_i$ plane (Example 2.14).
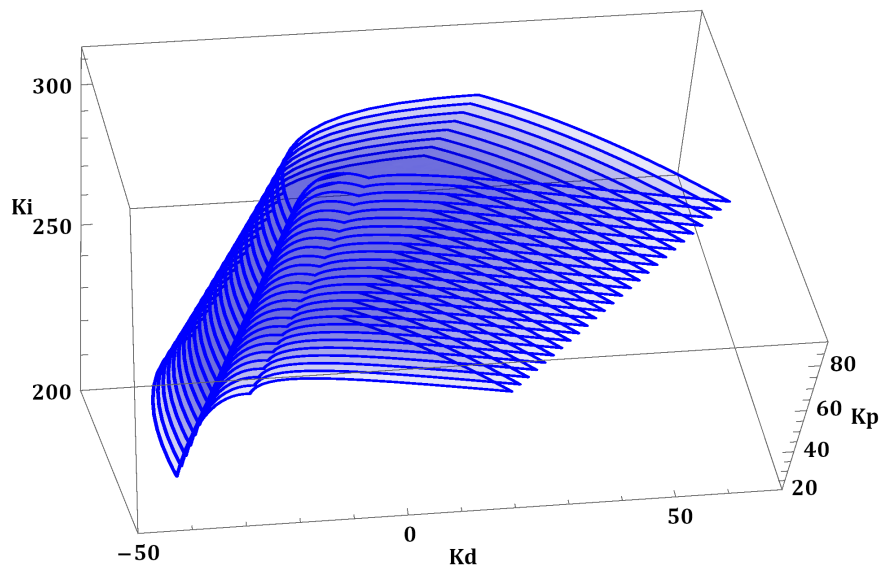
Figure 2.35 : The corresponding regions in 3D parameter space (Example 2.14).

Let the remaining poles to be located on the left side of the line $s = 3\sigma$ that means the dominance factor to be $m = 3$ again for the closed-loop system. After the polynomial

$\widetilde{P}_r(s, \zeta, \sigma, k_p^*) = P_r(s + 3\sigma, \zeta, \sigma, k_p^*)$ is obtained, the root boundaries can be found by equating the real and imaginary parts of the polynomial $\widetilde{P}_r(j\Omega, \zeta, \sigma, k_p^*)$ to zero. The next step is to map the achieved (ζ^*, σ^*) pairs into the $K_i - K_d$ plane. Figure 2.36 shows the sub-regions in parameter plane for $K_p = 50$.
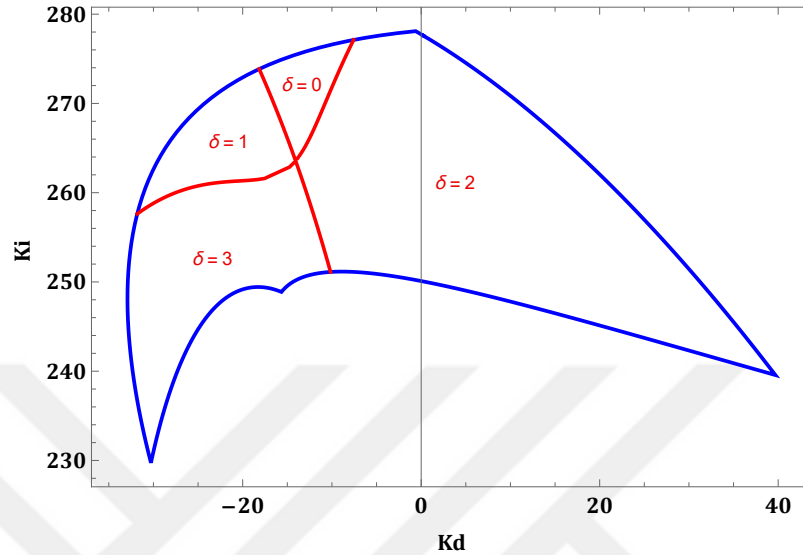
Figure 2.36 : Sub-regions divided by the root boundaries (Example 2.14).

It is seen from the figure that two root boundaries (a real root boundary and a complex root boundary) divide the parameter space into 4 sub-regions. The sub-region where $\delta = 0$ constitutes a solution to our problem. The same calculations are done for $K_p \in [30, 80]$ and the regions are obtained as a 3D figure as follows.
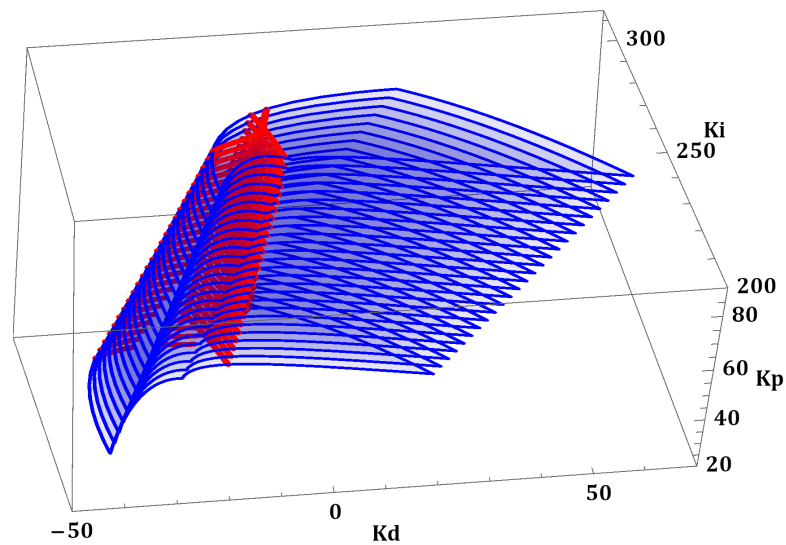
Figure 2.37 : PID controller parameter space and sub-regions (Example 2.14).

The closed-loop pole spread of the system with designed PID controller is given in Figure 2.38. It is seen that the dominant pole region assignment is performed successfully through the proposed method [40].
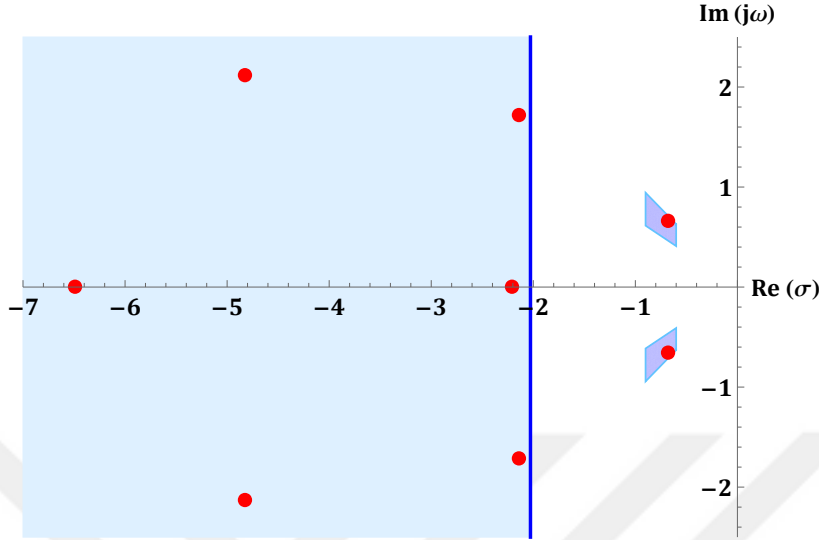
Figure 2.38 : The closed-loop poles with designed PID controller (Example 2.14).

2.6.2.2 Method 2: Constant Relative Stability Border

It is mentioned that the previously proposed method guarantees the desired dominance factor; however, it may bring computational complexity if the system order is high. In such cases, the non-dominant poles can be placed on the left side of a constant line $s = a$ instead of a varying line $s = m\sigma$.

First of all, the desired dominant pole region is mapped into the $K_p - K_i$ (for PI controller) or $K_d - K_i$ (for PID controller) plane via the presented method in previous sub-section. After that the real and complex root boundaries should be calculated, respectively. Let the closed-loop system characteristic polynomial be donated as $P_c(s)$. For the real root boundary,

$$P_{c_{PI}}(s = a, K_p, K_i) = 0 \tag{2.58}$$

$$P_{c_{PID}}(s = a, K_p = k_p^*, K_i, K_d) = 0 \tag{2.59}$$

should be found for PI and PID controller, respectively, and the corresponding line in parameter space ($K_p - K_i$ or $K_d - K_i$ for a fixed K_p) should be drawn. For the complex root boundary, this time the following equations should be solved for (K_p, K_i)

or (K_d, K_i) for a fixed K_p and then should be drawn in parameter space for $\Omega \in \mathbb{R}$.

$$Re\left[P_{c_{PI}}(s = j\Omega + a, K_p, K_i)\right] = 0$$

$$Im\left[P_{c_{PI}}(s = j\Omega + a, K_p, K_i)\right] = 0$$

(2.60)

$$Re\left[P_{c_{PID}}(s = j\Omega + a, K_p = k_p^*, K_i, K_d)\right] = 0$$

$$Im\left[P_{c_{PID}}(s = j\Omega + a, K_p = k_p^*, K_i, K_d)\right] = 0$$

(2.61)

For a PI controller, the procedure is completed by choosing (K_p, K_i) pair from the obtained feasible interval where $\delta = 0$. For a PID controller these regions are drawn as 3D plot for different values of the parameter K_p and the feasible (K_p, K_i, K_d) values are chosen to finalize the design.

Example 2.15:

Let us explain the design procedure through the same transfer function with the previous example.

$$G(s) = \frac{s - 2}{s^4 + 8s^3 + 27.5s^2 + 30s + 28}$$

The same dominant pole region is desired ($\zeta \in [0.69, 0.826]$ and $\sigma \in [0.6, 0.9]$) for the dominant pole pair; however, it is desired the non-dominant poles to be on the left side of the line $s = -2$ with a PID controller.

The characteristic polynomial with PID controller can be calculated and the real and complex root boundaries can be found. If the K_d and K_i parameters are calculated via (2.61) for $K_p = 50$, we have the following expressions.

$$K_d = \frac{-134 - 16\Omega^2 + 4\Omega^4 - 4\Omega^6}{20}$$

$$K_i = \frac{4584 - 70\Omega^2 + 32\Omega^4 + 60\Omega^6 - 6\Omega^8}{20}$$

For the real root boundary, the equation given below is obtained.

$$P_c(s = -2, K_p = 50, K_i, K_d) = 0 \implies 5K_i + 20K_d - 1012 = 0$$

If these boundaries are drawn, it is possible to obtain the regions and the number of poles (δ) located on the right side of the line $s = -2$ as in Figure 2.39.

It is seen from the figure that a different region is obtained since the non-dominant poles are desired to be on the left side of a line $s = -2$. Here, the constant dominance factor is not guaranteed and depends on the selection of (K_d, K_i) pair. If the plots are drawn for different values of the parameter K_p the following figure is obtained.
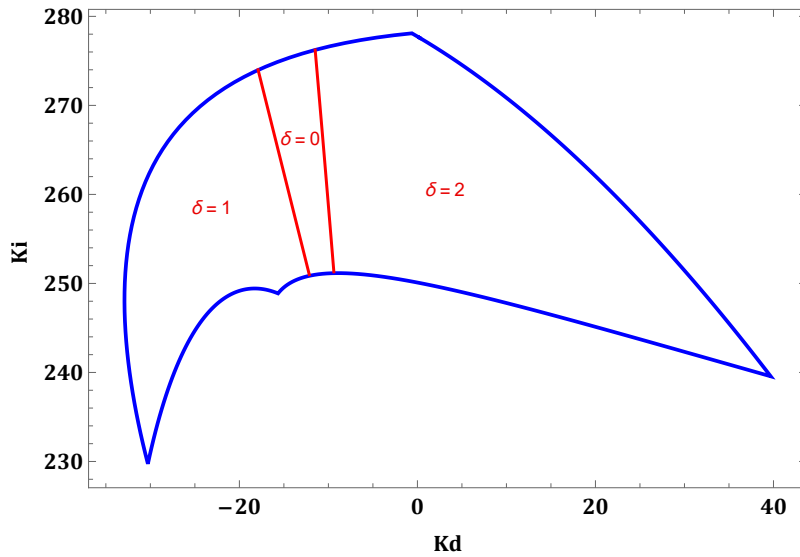
Figure 2.39 : Obtained regions divided by the root boundaries (Example 2.15)
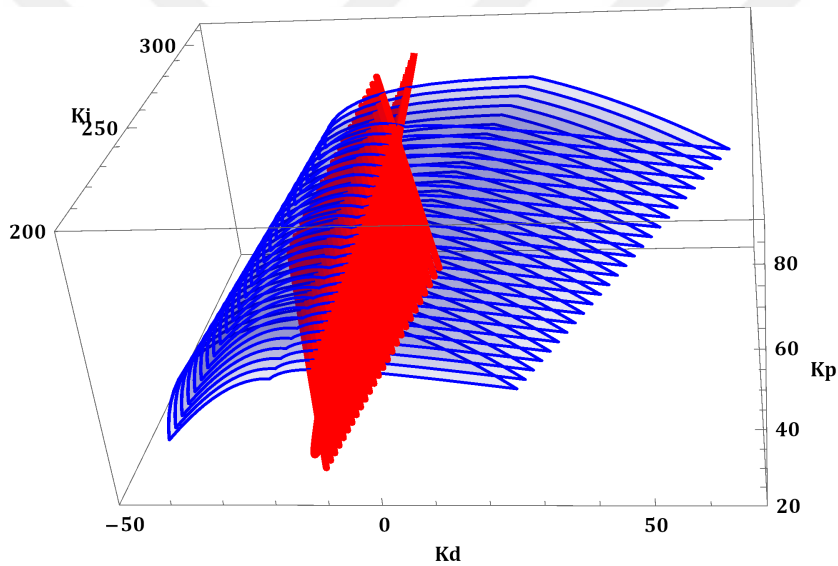
Figure 2.40 : 3D parameter space and the obtained sub-regions (Example 2.15)

Let us choose the controller parameters as $K_p = 50, K_d = -10, K_i = 257$ from the feasible region. The closed-loop poles are illustrated in Figure 2.41 with designed PID controller. Here, the dominance factor is found to be $m = 2.667$ which is lower than the previously obtained value.

In this sub-section, PI and PID controller design method via the dominant pole region assignment approach is proposed in order to assign two of the closed-loop poles in a desired region. Furthermore, the remaining poles are located away from the assigned dominant pole pair. First of all, parametrization of the PI/PID controllers is done and
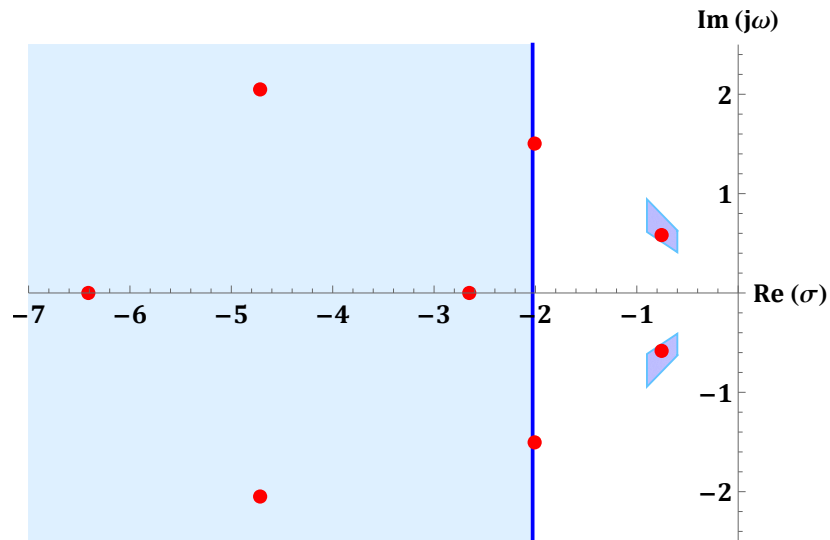
Figure 2.41 : The closed-loop poles with designed PID controller (Example 2.15).

desired dominant pole region is mapped into the controller parameter space. After that the sub-region in which the unassigned poles are located away from the dominant poles is found by calculating the root boundaries.

Note that it is not always possible to place remaining poles away from the dominant pole region especially the order of considered system is too high due to the fact that PI/PID controllers can assign only limited number of poles in the closed-loop. Therefore, if the resulting parameter space does not contain a sub-region where $\delta = 0$, the design process should be repeated by changing the performance specifications and/or the dominance factor.

3. DOMINANT POLE PLACEMENT IN DISCRETE-TIME SISO SYSTEMS

In this chapter, it is aimed to perform dominant pole placement for discrete-time single input-single output systems. It is known that, the pole placement approach is a widely used and popular technique to obtain the desired closed-loop performance [46]. Although the dominant pole placement approach is presented for continuous-time systems, this chapter mainly focuses on time-delay systems to solve the dominant pole placement problem. In the literature, guaranteed dominant pole placement is already proposed [1] for the systems with or without time-delay and also presented in the second section of this thesis. However, with the proposed method (based on modified Nyquist curve), it can be seen that the calculation of feasible gain intervals is difficult due to infinite number of poles caused by time-delay.

On the other hand, as a result of the advancing technology, discrete-time control systems become an important subject to examine. Especially in the industrial automation systems, processes are usually controlled by digital control systems such as industrial PCs or PLCs. Therefore, it provides significant advantage to find the discrete-PID controller parameters which guarantee dominant pole placement.

Even if the controller design can be performed in continuous-time domain and then discretized by taking sampling time as small as desired, most of the installed control systems around the world use older technology where it is not possible to reduce the sampling time below a certain limit without making considerable expenses. In addition to this, in some of the new systems reducing the sampling time comes with a cost, which might not be required due to marketing reasons. In such situations, direct digital design is required to ensure the performance of the controller when applied in the digital world.

First of all, the parametrization of PI and PID controllers are given similar to the continuous-time case. After that the controller subset which guarantees the dominant pole placement is found via two different approach based on modified Nyquist curve in z-plane and Chebyshev polynomials, respectively. The similar problems such as

calculation of maximum dominance factor, performance limitations in the closed-loop and dominant pole region assignment in z-plane are also solved and presented in the following sub-sections.

3.1 Parametrization of Digital PI and PID Controllers To Assign Dominant Poles

Consider the closed-loop control system with arbitrary order discrete transfer function $G(z)$ given with (3.1)

$$G(z) = \frac{N_G(z)}{D_G(z)} = \frac{\beta_m z^m + \beta_{m-1} z^{m-1} + \cdots + \beta_1 z + \beta_0}{z^n + \alpha_{n-1} z^{n-1} + \cdots + \alpha_1 z + \alpha_0}, \; m \leq n \qquad (3.1)$$

and a digital PI or PID controllers whose transfer functions are given in (3.2) and (3.3), respectively.

$$C(z) = \frac{N_C(z)}{D_C(z)} = \frac{(K_p + K_i)z - K_p}{z - 1} \qquad (3.2)$$

$$C(z) = \frac{N_C(z)}{D_C(z)} = \frac{(K_p + K_i + K_d)z^2 - (K_p + 2K_d)z + K_d}{z(z - 1)} \qquad (3.3)$$

For this control system, the closed-loop system characteristic polynomial is given as follows.

$$P_c(z) = D_C(z)D_G(z) + N_C(z)N_G(z) \qquad (3.4)$$

Performance specifications in the closed-loop are strongly determined by the dominant pole locations if the remaining poles are assumed to be located far away from the dominant pole pair. Let dominant poles to be $z_{1,2} = \sigma_z \pm j\omega_z$ for a chosen performance criteria. If the dominant pole locations are substituted into (3.4), the following equality is obtained.

$$P_c(z) = D_C(\sigma_z + j\omega_z)D_G(\sigma_z + j\omega_z) + N_C(\sigma_z + j\omega_z)N_G(\sigma_z + j\omega_z) = 0 \qquad (3.5)$$

The complex equation given above can be solved by decomposing it into its real and imaginary parts,

$$(D_{C_{Im}}D_{G_{Im}} - D_{C_{Re}}D_{G_{Re}}) + (N_{C_{Im}}N_{G_{Im}} - N_{C_{Re}}N_{G_{Re}}) = 0 \qquad (3.6)$$

$$(D_{C_{Re}}D_{G_{Im}} + D_{C_{Im}}D_{G_{Re}}) + (N_{C_{Re}}N_{G_{Im}} + N_{C_{Im}}N_{G_{Re}}) = 0 \qquad (3.7)$$

where

$$N_{C_{Im}} = Im[N_C(\sigma_z + j\omega_z)], \; N_{C_{Re}} = Re[N_C(\sigma_z + j\omega_z)]$$

$$N_{G_{Im}} = Im[N_G(\sigma_z + j\omega_z)], \; N_{G_{Re}} = Re[N_G(\sigma_z + j\omega_z)]$$

$$D_{C_{Im}} = Im\left[D_C(\sigma_z + j\omega_z)\right], \ D_{C_{Re}} = Re\left[D_C(\sigma_z + j\omega_z)\right]$$

$$D_{G_{Im}} = Im\left[D_G(\sigma_z + j\omega_z)\right], \ D_{G_{Re}} = Re\left[D_G(\sigma_z + j\omega_z)\right]$$

It is assumed that the discrete transfer function of the system is known; therefore, the real and imaginary parts of the numerator $(N_{G_{Re}}, N_{G_{Im}})$ and denominator $(D_{G_{Re}}, D_{G_{Im}})$ are known. On the other hand, the real and imaginary parts of the denominator of discrete PI/PID controller transfer function $(D_{C_{Re}}, D_{C_{Im}})$ are also known. The only unknown parameters are included by the numerator of discrete PI/PID controller. It is possible to find those unknown parameters by solving $(N_{C_{Re}}, N_{C_{Im}})$ with the help of (3.6) and (3.7) as follows.

$$N_{C_{Re}} = -\frac{N_{G_{Im}}Y - N_{G_{Re}}X}{Z} \tag{3.8}$$

$$N_{C_{Im}} = -\frac{N_{G_{Im}}X + N_{G_{Re}}Y}{Z} \tag{3.9}$$

Here, X, Y and Z are defined as below.

$$X = D_{C_{Im}}D_{G_{Im}} - D_{C_{Re}}D_{G_{Re}} \tag{3.10}$$

$$Y = D_{C_{Re}}D_{G_{Im}} + D_{C_{Im}}D_{G_{Re}} \tag{3.11}$$

$$Z = N_{G_{Im}}^2 + N_{G_{Re}}^2 \tag{3.12}$$

For a digital PI controller given in (3.2), it can be shown that,

$$\begin{aligned}
N_{C_{Re}} &= Re\left[((K_p + K_i)z - K_p)|_{z=\sigma_z+j\omega_z}\right] \\
&= K_p(-1 + \sigma_z) + K_i\sigma_z
\end{aligned} \tag{3.13}$$

$$\begin{aligned}
N_{C_{Im}} &= Re\left[((K_p + K_i)z - K_p)|_{z=\sigma_z+j\omega_z}\right] \\
&= (K_p + K_i)\omega_z
\end{aligned} \tag{3.14}$$

Thus, the PI controller parameters are obtained as follows.

$$\begin{pmatrix} K_p \\ K_i \end{pmatrix} = \begin{pmatrix} 1 & \frac{\sigma_z}{\omega_z} \\ -1 & \frac{1-\sigma_z}{\omega_z} \end{pmatrix} \begin{pmatrix} -\frac{N_{G_{Re}}X - N_{G_{Im}}Y}{Z} \\ -\frac{N_{G_{Im}}X + N_{G_{Re}}Y}{Z} \end{pmatrix} \tag{3.15}$$

For the digital PID controller given in (3.3), it is possible to write,

$$\begin{aligned}
N_{C_{Re}} &= Re\left[((K_p + K_i + K_d)z^2 - (K_p + 2K_d)z + K_d)|_{z=\sigma_z+j\omega_z}\right] \\
&= K_d((-1 + \sigma_z)^2 - \omega_z^2) + K_p(-\sigma_z + \sigma_z^2 - \omega_z^2) + K_i(\sigma_z^2 - \omega_z^2)
\end{aligned} \tag{3.16}$$

$$\begin{aligned}
N_{C_{Im}} &= Im\left[((K_p + K_i + K_d)z^2 - (K_p + 2K_d)z + K_d)|_{z=\sigma_z+j\omega_z}\right] \\
&= K_d(2\sigma_z - 2)\omega_z + K_p(2\sigma_z - 1)\omega_z + K_i(2\sigma_z\omega_z)
\end{aligned} \tag{3.17}$$

65

Finally, PID controller parameters K_i and K_d can be obtained in terms of the parameter K_p by solving (3.8) and (3.9) with the help of (3.16) and (3.17) as follows.

$$
\begin{pmatrix} K_d \\ K_i \end{pmatrix} = \begin{pmatrix} \frac{(-1+\sigma_z)^2-\omega_z^2}{\Delta} & \frac{(2-2\sigma_z)\omega_z}{\Delta} \\ \frac{-\sigma_z^2+\omega_z^2}{\Delta} & \frac{2\sigma_z\omega_z}{\Delta} \end{pmatrix} \begin{pmatrix} -\frac{N_{G_{Im}}X+N_{G_{Re}}Y}{Z} \\ -\frac{N_{G_{Im}}Y-N_{G_{Re}}X}{Z} \end{pmatrix}
$$
$$
- \begin{pmatrix} 1+\frac{1-\sigma_z}{-\sigma_z+\sigma_z^2+\omega_z^2} \\ 1+\frac{\sigma_z}{-\sigma_z+\sigma_z^2+\omega_z^2} \end{pmatrix} \frac{K_p}{2}
\tag{3.18}
$$

where

$$
\Delta = -2\omega_z(\sigma_z^2+\omega_z^2-\sigma_z)
\tag{3.19}
$$

It is clear that the obtained controller parameter set, which defines a line in 3-dimensional parameter space (K_p, K_i, K_d), places the two of the closed-loop system poles (i.e. dominant poles) to the points of $z = \sigma_z \pm j\omega_z$ in z-plane.

$$
\mathscr{P} := \left\{ \begin{array}{l} (K_p, K_i, K_d) \in \mathbb{R}^3 \mid z_{1,2} = \sigma_z \pm j\omega_z, \ z_k \in \mathbb{C} \\ k = 3, \ldots, n+2, \ \forall K_p \in \mathbb{R} \end{array} \right\}
\tag{3.20}
$$

Thus, the parametrization of the PI and PID controllers that assign the dominant poles is completed. It is also important to note that the given formula is valid for all linear time invariant systems with or without a time delay that is a multiple of the sampling time.

However, it is also desired to find the subset of the controller parameters which place the remaining poles in a disc with specified radius so that dominant pole placement can be done successfully. Hence, the desired performance criteria in the closed-loop are achieved as accurately as possible.

3.2 Calculation of Digital PID Controller Subset Assigns Non-Dominant Poles

In this section, similar to the continuous PID controller case, it is aimed to find the digital PID controller subset which assigns the non-dominant poles inside a disc of radius r^m centered at the origin in z-plane where $r = \sqrt{\sigma_z^2 + \omega_z^2}$ and m is the dominance factor (it is usually enough to choose m around 3-5) so that the dominant pole placement in discrete-time domain is performed.

$$
\widetilde{\mathscr{P}} := \left\{ \begin{array}{l} (K_p, K_i, K_d) \in \mathbb{R}^3 \mid z_{1,2} = \sigma_z \pm j\omega_z, \ |z_k| \leq |z_{1,2}|^m \\ m \in \mathbb{R}^+, \ k = 3, \ldots, n+2 \ , \ \forall K_p \in [K_{p_{min}}, K_{p_{max}}] \subset \mathbb{R} \end{array} \right\}
\tag{3.21}
$$

There are two different approaches proposed in this thesis to calculate the K_p parameter of PID controller. First design method is based on the modified discrete Nyquist plot

as proposed for continuous time case and the second design method is based on the Chebyshev polynomials.

3.2.1 Design via modified discrete Nyquist plot

After the PID controller is written depending on the parameter K_p it is possible to apply the well-known Nyquist plot method. It is also important to remark that the this procedure is valid for all $G(z)$ systems regardless of the time delay.

In order to use the Nyquist method, the controller parameter K_p must be separated from the equation. For this purpose, the closed-loop system characteristic polynomial can be written in following form.

$$P_c(z) = 1 + K_p \tilde{G}(z) = 0 \tag{3.22}$$

After that the modified Nyquist plot through the expression $\tilde{G}(r^m e^{j\gamma})$ can be drawn and with the help of Nyquist stability criterion, the feasible gain intervals can be calculated.

The Nyquist path, which covers the whole z-plane outside of the unit circle (i.e. instability region), is given as in Figure 3.1. In Nyquist stability analysis, it is expected
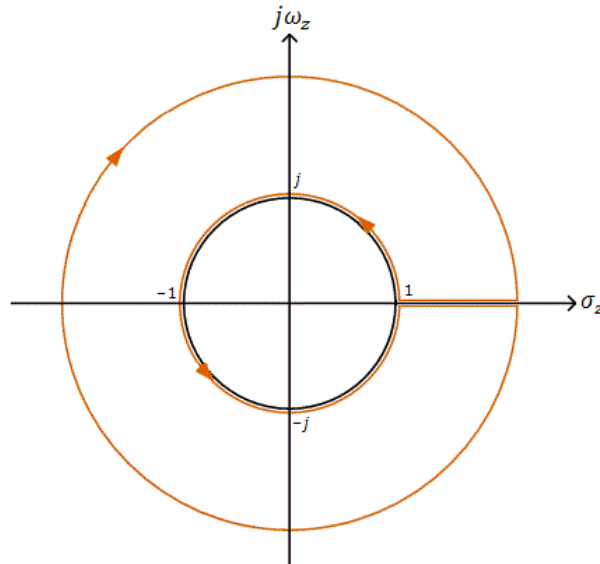
Figure 3.1 : Nyquist path in z-plane.

to find the number of the unstable closed-loop system poles by just checking the number of unstable open-loop system poles and the number of the encirclements of the Nyquist plot around a critical point. However, here it is aimed to design a controller

to guarantee the dominant pole placement. For this reason, it is required to modify the Nyquist plot so that the Nyquist path encloses the circle which is located away from the dominant poles instead of the unit circle. If the distance between the determined closed-loop dominant poles and the origin is r then the Nyquist path should enclose the circle whose radius is r^m (m is usually 3-5) as given in Figure 3.2. Since two of the
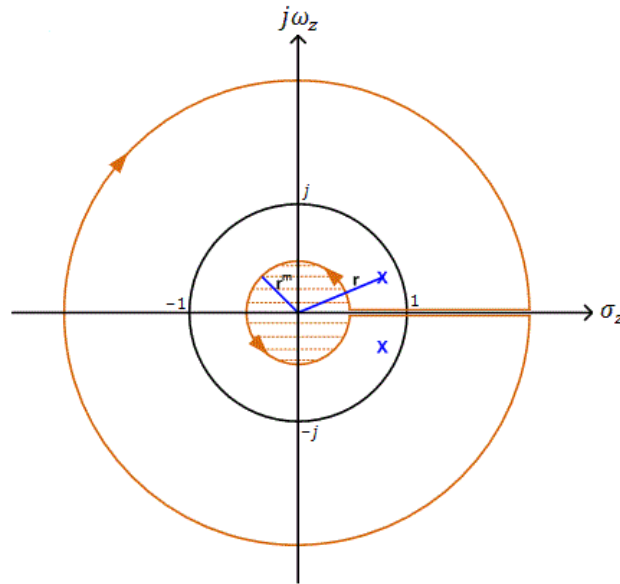
Figure 3.2 : Modified nyquist path in z-plane.

closed-loop system poles should be in the dominant region, the value of Z should be two. In addition, from the open-loop system transfer function, the number of open-loop poles which are outside of the circle of radius r^m (P) is also known. Therefore, if the formula

$$N = 2 - P \tag{3.23}$$

is used, it is possible to find the number of encirclements to guarantee dominant pole placement.

Example 3.1:

Consider the following first order process with time delay.

$$G(s) = \frac{1}{s+1}e^{-0.3s}$$

The corresponding discrete-time transfer function with zero order hold can be obtained by taking the sampling time as 0.1 seconds as below.

$$G(z) = \frac{0.09516}{z^3(z-0.9048)}$$

68

In the closed-loop, it is desired to control the given process with 5% overshoot and 6 seconds settling time. Corresponding closed-loop poles in z-domain are given as follows.

$$z_{1,2} = 0.9332 \pm 0.0654j = 0.9355e^{\pm 0.07j}$$

The PID controller parameters K_i and K_d can be calculated in terms of the parameter K_p as given below.

$$K_d = -3.103 + 7.5383K_p$$

$$K_i = 0.0493 + 0.0752K_p$$

After that it is possible to find the closed-loop system characteristic polynomial and to obtain the new transfer function by separating the parameter K_p as mentioned in (3.22).

$$\tilde{G}(z) = \frac{0.8195(z^2 - 1.8664z + 0.87514)}{z^6 - 1.90484z^5 + 0.90484z^4 - 0.291z^2 + 0.59132z - 0.2957}$$

The magnitude of the dominants poles is $r = 0.9355$ and if m is chosen as 5, non-dominant poles should be inside the circle of radius $r^m = (0.9355)^5 = 0.7165$. In order to find the required encirclements using (3.23), number of the poles of $\tilde{G}(z)$, which are located in the dominant region, have to be found. If required calculations are done, all poles of $\tilde{G}(z)$ are found to be in the dominant region so $P = 6$ and the required number of the encirclements is found as $N = -4$.
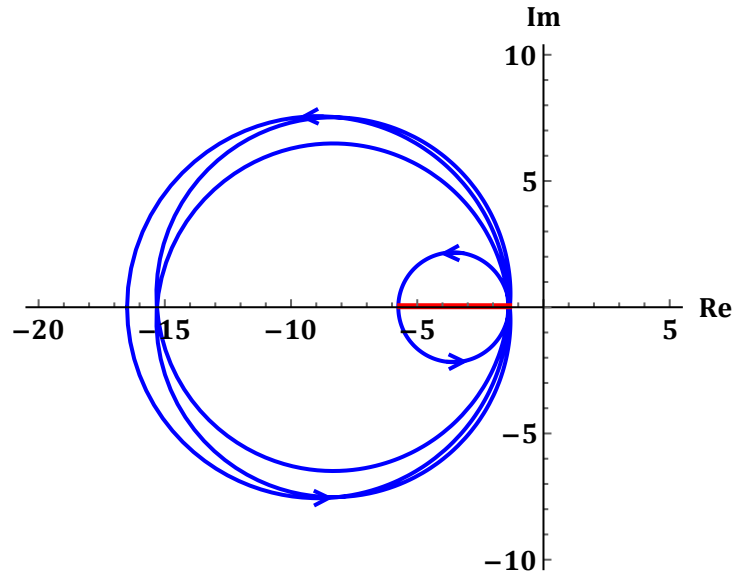
Figure 3.3 : Modified Nyquist plot of the given system (Example 3.1).

The Nyquist plot of $\tilde{G}(r^m e^{j\gamma})$ is drawn and the interval in real axis which satisfies $N = -4$ is found. Figure 3.3 shows the modified Nyquist plot of the considered system.

In the above figure, the red line represents the interval in which the number of the encirclements is found to be $N = -4$. After that it is easy to find the feasible K_p value range since the intersection points of the real axis and Nyquist plot is found. Therefore,

$$K_p \in (\frac{-1}{-5.7937}, \frac{-1}{-1.3937}) = (0.1726, 0.7175)$$

is obtained. If the K_p parameter of the digital PID controller is chosen from the obtained interval, the closed-loop dominant poles are assigned to the dominant region and the remaining poles are located in the non-dominant region. Figure 3.4 shows the variation of non-dominant poles in the closed-loop.
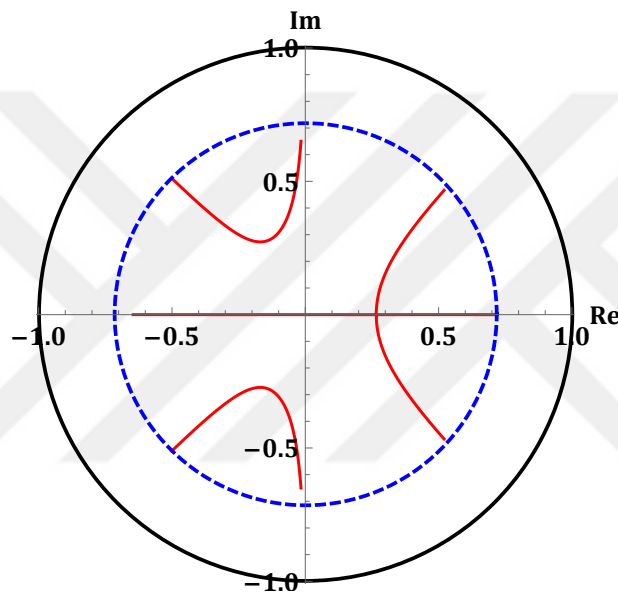
Figure 3.4 : Variation of the non-dominant poles in z-plane (Example 3.1).

If the parameter $K_p = 0.55$ is chosen, the designed discrete PID controller is given as follows.

$$C(z) = \frac{1.6787z^2 - 2.626z + 1.038}{z(z-1)}$$

Figure 3.5 shows the closed-loop pole configuration in z-plane with the designed controller. The closed-loop transient response is illustrated in Figure 3.6 and the control signal is given in Figure 3.7.

It is seen from the figures that the closed-loop system settles to its final value in 5.8 seconds with 5.6% overshoot. The obtained performance criteria in the closed-loop are found to be very close to the desired ones. The small difference between the expected and obtained performance specifications is caused by the controller zeros. On the other
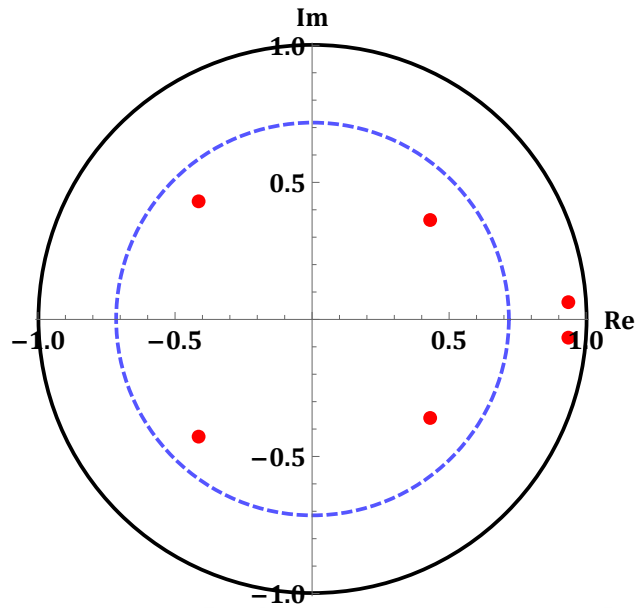
Figure 3.5 : Closed-loop poles with designed controller in z-plane (Example 3.1).

hand, the control signal is found to be smooth and in the proper limits; however, the derivative kick phenomenon is observed at the beginning.

Due to the reasons given above, in order to eliminate the adverse effect of the closed-loop (controller) zeros and the derivative kick phenomenon, the designed discrete PID controller should be implemented in PI-PD structure as mentioned in the previous part of the thesis. Thus, the dominant pole placement in z-plane is successfully performed.
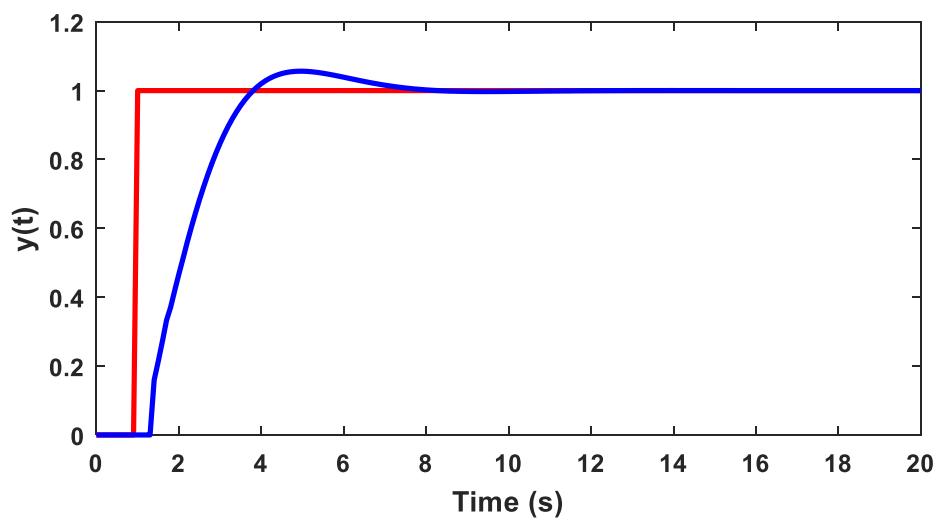
Figure 3.6 : Transient response of the closed-loop system (Example 3.1).
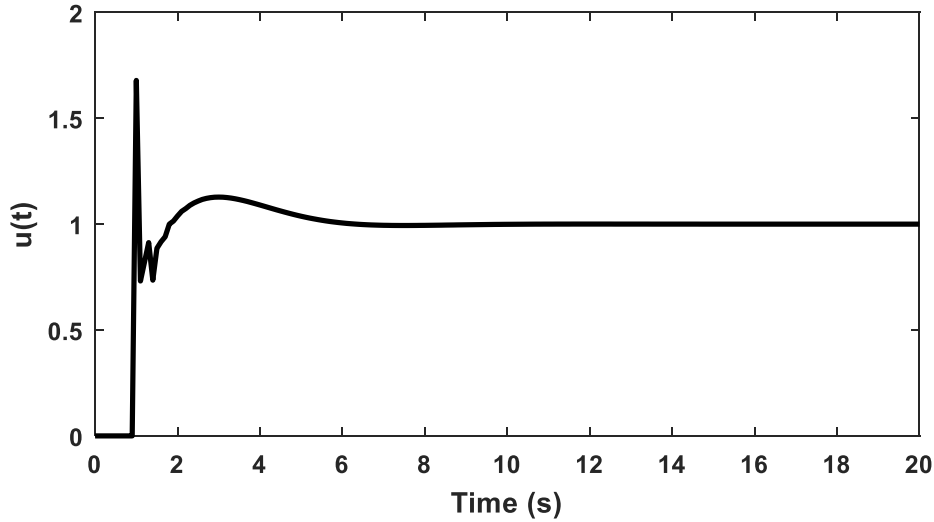
Figure 3.7 : The control signal in the closed-loop (Example 3.1).

Example 3.2:

Consider a high order system with time-delay and one left half plane zero which is given with the following open-loop transfer function.

$$G(s) = \frac{s+3}{(s+1)^2(s+4)^2}e^{-2s}$$

The corresponding discrete transfer function is obtained as follows by taking sampling time as 0.4 seconds.

$$G(z) = \frac{0.00556z^3 + 0.009967z^2 - 0.00213z - 0.000415}{z^5(z^4 - 1.744z^3 + 1.031z^2 - 0.2361z + 0.01832)}$$

It is desired to control the given system in the closed-loop with 5% overshoot and 14 seconds settling time. Corresponding closed-loop poles in z-domain are then calculated as below.

$$z_{1,2} = 0.8856 \pm 0.1067j = 0.892e^{\pm 0.12j}$$

The K_i and K_d parameters of the PID controller is found as follows in terms of the parameter K_p.

$$K_d = -5.61 + 4.424K_p$$

$$K_i = 0.2 + 0.1361K_p$$

The closed-loop system characteristic polynomial can be found and the parameter K_p is separated from the equation as in (3.22). Using the same procedure in previous

72

example, 5 poles of $\tilde{G}(z)$ are found to be in the dominant region ($P = 5$) and the required number of the encirclements is then found as $N = -3$ for the dominance factor $m = 3$.

If the modified Nyquist plot of $\tilde{G}(r^m e^{j\gamma})$ is drawn as in Figure 3.8, the intersection points of real axis and Nyquist curve is calculated and the gain interval which satisfies $N = -3$ is found.
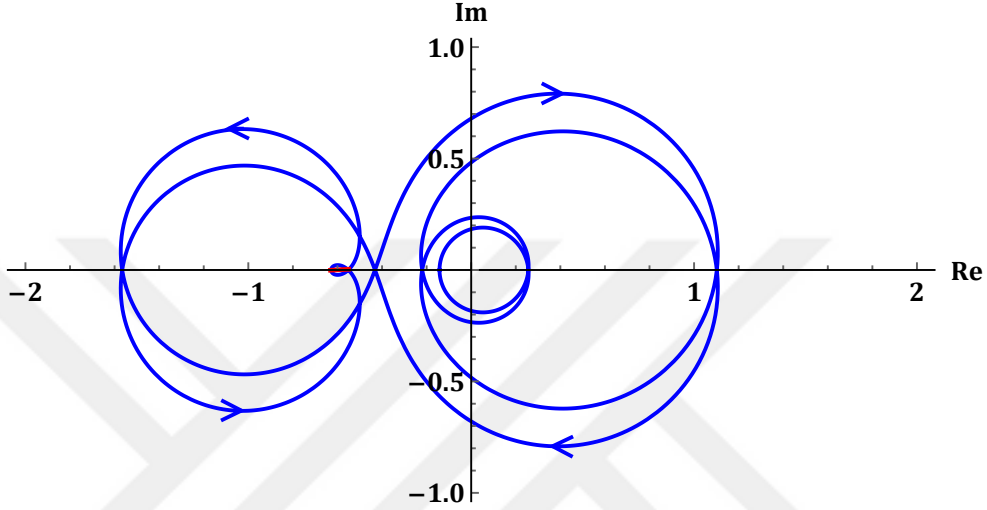
Figure 3.8 : Modified Nyquist plot of the given system (Example 3.2).

The resulting feasible gain interval is calculated as follows.

$$K_p \in (\frac{-1}{-0.62854}, \frac{-1}{-0.55133}) = (1.591, 1.8138)$$

As it is seen the obtained interval is a tight one; therefore, note that it is not always possible to find such a K_p range depending on the determined performance criteria and dominance factor. In some cases, in order to guarantee dominant pole placement for desired m value, it may be required to change the performance criteria.

If $K_p = 1.6$ is selected, the discrete PID controller is given as below.

$$C(z) = \frac{3.486z^2 - 4.5363z + 1.4682}{z(z-1)}$$

The locations of closed-loop dominant and non-dominant poles are illustrated in Figure 3.9. It can easily be seen that the dominant pole pair is assigned to the desired location, whereas, the remaining poles are located inside the disc of radius $r^m = 0.892^3 = 0.7097$.
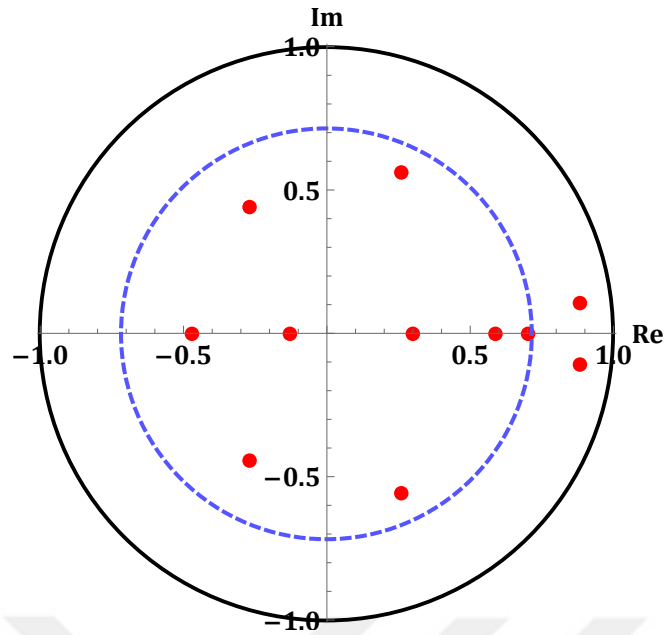
Figure 3.9 : Poles of the given system in the closed-loop (Example 3.2).

Figure 3.10 shows the closed-loop transient response of the system with the designed PID controller. The closed-loop control signal is also illustrated in Figure 3.11.
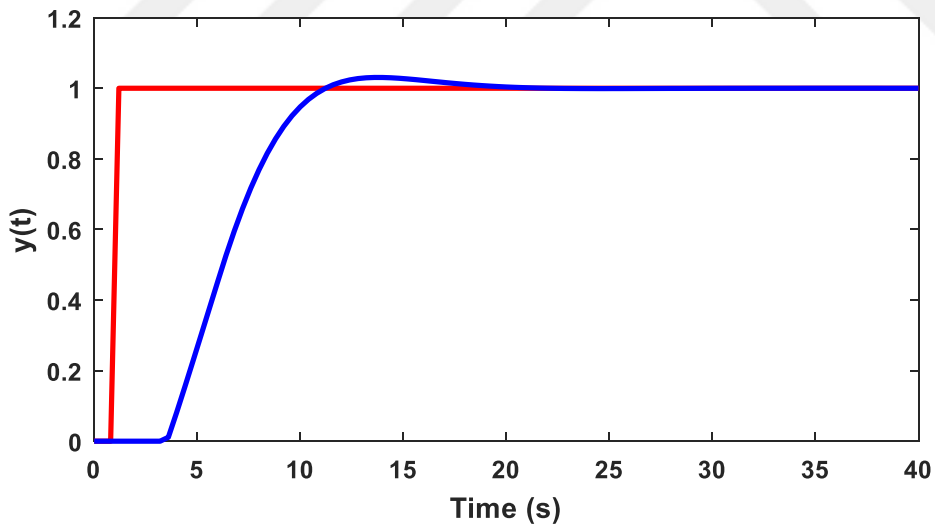
Figure 3.10 : Transient response of the closed-loop system (Example 3.2).

The closed-loop system settles to its final value in 15.7 seconds with 5.2% overshoot. Although there is a slight difference, the closed-loop performance criteria are again close to the desired ones. If the PI-PD structure is used, in this case zeros of the

74
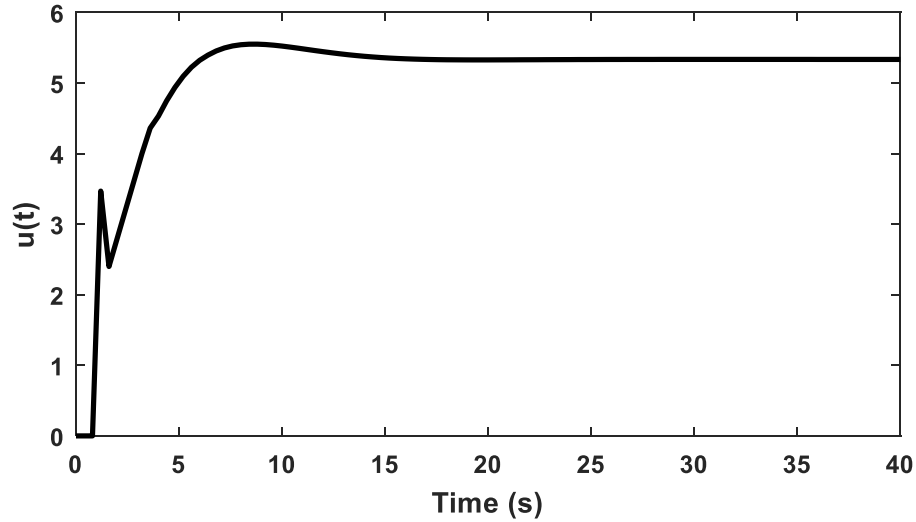
Figure 3.11 : The control signal in the closed-loop (Example 3.2).

controller do not have any adverse effects on transient response, thus, the performance specifications are obtained as expected.

3.2.2 Design via Chebyshev polynomials approach

It is possible to obtain the Chebyshev representation of a discrete-time control system with the help of first and second kinds of Chebyshev polynomials. Thus, the stabilizing gains can be found by just solving sets of linear inequalities. The parametrization of the stabilizing gains, which is based on a generalization of Hermite-Biehler theorem, has already been given in [47]. However, the proposed method requires sign analysis which is exponentially increasing as the order of the system increase. Therefore, in this thesis, the Schur stabilization problem is solved through the Chebyshev polynomials with the help of an easier procedure based on the well-known Nyquist stability criterion as studied in [48].

Consider the closed-loop system characteristic polynomial with a discrete PID controller given with (3.4). This polynomial can be separated into two polynomials, which are constructed by dominant poles and the remaining poles, as follows.

$$P_c(z, K_p) = (z^2 - 2\sigma_z z + (\sigma_z^2 + \omega_z^2))P_r(z, K_p) \tag{3.24}$$

$P_r(z, K_p)$ is a residue polynomial whose roots are desired to be placed in a disc of radius r^m as mentioned earlier. Here, it is possible to use the Chebyshev polynomials in order to calculate the stabilizing gains for the polynomial $P_r(r^m z, K_p)$.

Consider the closed-loop control system with a constant gain $(C(z) = K_p)$. The characteristic polynomial of the closed-loop system is given as follows.

$$P_c(z) = 1 + K_p G(z) = a_n z^n + a_{n-1} z^{n-1} + \cdots + a_1 z + a_0 \qquad (3.25)$$

In order to find the interval of K_p in which all roots of the polynomial $P_c(z)$ are located inside the unit circle, it is required to determine the unit circle image of the polynomial $P_c(z)$.

$$\left\{ P_c(z) : z = e^{j\theta}, \ 0 \le \theta \le 2\pi \right\} \qquad (3.26)$$

However, it is sufficient to determine the image of upper half of the unit circle since the coefficients (a_i) of the polynomial $P_c(z)$ are real, $P_c(e^{j\theta})$ and $P_c(e^{-j\theta})$ are complex conjugate numbers. Therefore, it is possible to write,

$$\left\{ P_c(z) : z = e^{j\theta}, \ 0 \le \theta \le \pi \right\} \qquad (3.27)$$

Since

$$z^k|_{z=e^{j\theta}} = \cos(k\theta) + j\sin(k\theta) \qquad (3.28)$$

the following can be written

$$
\begin{aligned}
P_c\left(e^{j\theta}\right) &= a_n e^{jn\theta} + a_{n-1} e^{j(n-1)\theta} + \cdots + a_1 e^{j\theta} + a_0 \\
&= \underbrace{(a_n\cos(n\theta) + \cdots + a_0)}_{\bar{R}(\theta)} + j \underbrace{(a_n\sin(n\theta) + \cdots + a_1\sin(\theta))}_{\bar{I}(\theta)} \\
&= \bar{R}(\theta) + j\bar{I}(\theta)
\end{aligned}
\qquad (3.29)
$$

It is possible to write $\cos(k\theta)$ and $\frac{\sin(k\theta)}{\sin(\theta)}$ as polynomials in $\cos(\theta)$ with the help of Chebyshev polynomials. Let $t = -\cos(\theta)$. Then, it is clear that t varies from -1 to $+1$ as θ varies from 0 to π. We have,

$$z \triangleq e^{j\theta} = \cos(\theta) + j\sin(\theta) = -t + j\sqrt{1 - t^2} \qquad (3.30)$$

since

$$\sin(\theta) = \sqrt{1 - \cos^2(\theta)} \qquad (3.31)$$

The first kind of Chebyshev polynomials is defined as below for $t \in [-1, +1]$.

$$c_k(t) = \cos(k\theta), \quad k = 1, 2, 3, \ldots \qquad (3.32)$$

76

The second kind of Chebyshev polynomials is also defined as follows for $t \in [-1, +1]$.

$$s_k(t) = \frac{\sin(k\theta)}{\sin(\theta)}, \quad k = 1, 2, 3, \ldots \quad (3.33)$$

It can be shown that

$$s_k(t) = -\frac{1}{k} \frac{dc_k(t)}{dt} \quad (3.34)$$

and the Chebyshev polynomials satisfy the recursive relation given below [49].

$$c_{k+1}(t) = -tc_k(t) - \left(1 - t^2\right) s_k(t) \quad (3.35)$$

Table 3.1 : The first and second kind of Chebyshev polynomials.

k	$c_k(t)$	$s_k(t)$
1	$-t$	1
2	$2t^2 - 1$	$-2t$
3	$-4t^3 + 3t$	$4t^2 - 1$
4	$8t^4 - 8t^2 + 1$	$-8t^3 + 4t$
5	$-16t^5 + 20t^3 - 5t$	$16t^4 - 12t^2 + 1$

Table 3.1 shows the first five of the first and second kind of Chebyshev polynomials obtained with the help of (3.32) and (3.33). If the equations (3.32) and (3.33) are substituted into (3.29) then

$$P_c\left(e^{j\theta}\right)|_{t=-\cos(\theta)} = \underbrace{[a_n c_n(t) + \cdots + a_1 c_1(t) + a_0]}_{R(t)}$$
$$+ j\sqrt{1-t^2} \underbrace{[a_n s_n(t) + \cdots + a_1 s_1(t)]}_{T(t)} \quad (3.36)$$

$$P_c(t) = R(t) + j\sqrt{1-t^2} \, T(t) \quad (3.37)$$

Here, $P_c(t)$ is called the Chebyshev representation of the polynomial $P_c(z)$.

It is now possible to find all stabilizing gains for $P_c(z)$ via Chebyshev polynomials. The characteristic polynomial can also be written as follows.

$$P_c(z) = D(z) + K_p N(z) \quad (3.38)$$

The Chebyshev representations of the polynomials $N(z)$ and $D(z)$ are respectively given as follows.

$$N\left(e^{j\theta}\right)|_{t=-\cos(\theta)} = R_N(t) + j\sqrt{1-t^2} \, T_N(t) \quad (3.39)$$

77

$$D\left(e^{j\theta}\right)\big|_{t=-\cos(\theta)} = R_D(t) + j\sqrt{1-t^2}\,T_D(t) \tag{3.40}$$

If those equations are substituted into the numerator and denominator of $G(z)$ then

$$G(t) = \frac{N(t)}{D(t)} = \frac{R_N(t) + j\sqrt{1-t^2}\,T_N(t)}{R_D(t) + j\sqrt{1-t^2}\,T_D(t)} \tag{3.41}$$

When the numerator and denominator of the above equation is multiplied by the complex conjugate of the denominator, we have

$$\begin{aligned}
G(t) =&\, \frac{R_N(t)\,R_D(t) + \left(1-t^2\right)T_N(t)\,T_D(t)}{R_D^2(t) + (1-t^2)\,T_D^2(t)} \\
&+ j\sqrt{1-t^2}\,\frac{R_D(t)\,T_N(t) - R_N(t)\,T_D(t)}{R_D^2(t) + (1-t^2)\,T_D^2(t)}
\end{aligned} \tag{3.42}$$

$$G(t) = Re\{G(t)\} + jIm\{G(t)\} \tag{3.43}$$

The Nyquist criterion can now be applied to the obtained system. For this purpose,

$$Im\{G(t)\} = 0 \tag{3.44}$$

should be solved. After that if the real roots of the above equation $t^* \in [-1,+1]$ are substituted into the real part of the $G(t)$, this gives the intersections of the Nyquist plot with the real axis. Hence, the gain intervals, in which the number of unstable poles is the same, can be obtained as follows.

$$\mathscr{K}_i = -\frac{1}{Re\{G(t_i^*)\}}, \quad i = 1,2,\dots \tag{3.45}$$

The set of stabilizing gains (K_p) can finally be found as the union of the gain intervals ($\mathscr{K}_i$ where $i = 1,\dots,q$) in which the number of unstable poles is zero.

$$K_p \in \bigcup_{i=1}^{q} \mathscr{K}_i \tag{3.46}$$

Example 3.3:

Consider the same system in Example 3.1 whose discrete-time transfer function is given as follows.

$$G(z) = \frac{0.09516}{z^3(z - 0.9048)}$$

If the closed-loop system characteristic polynomial is found and divided into its dominant and non-dominant parts, we have,

$$P_r(z, K_p) = z^4 - 0.038357z^3 - 0.041964z^2 - 0.044755z - 0.337374 + 0.819662K_p$$

78

It is desired the roots of the above polynomial be inside the disc of radius $r^m = (0.9355)^5 = 0.7165$. Hence the stabilizing gains can be calculated via Chebyshev polynomials through the polynomial

$$P_r(r^m z, K_p) = 0.263597z^4 - 0.0141106z^3 - 0.021545z^2 - 0.032068z$$
$$+ (-0.337374 + 0.819662K_p)$$

The Chebyshev representations of the $N(z)$ and $D(z)$ are obtained using the corresponding first and second kinds of the Chebyshev polynomials as below.

$$R_D(t) = 2.10878t^4 + 0.056443t^3 - 2.15187t^2 - 0.010264t - 0.052232$$

$$T_D(t) = -2.10878t^3 - 0.0564426t^2 + 1.09748t - 0.0179574$$

$$R_N(t) = 0.81966$$

$$T_N(t) = 0$$

The Chebyshev representation $G(t)$ can be constructed by substituting the above expressions into (3.42). After separating the real and imaginary parts of the obtained expression, the real roots (t^*) of (3.44) such that $t^* \in [-1, +1]$ is calculated as follows.

$$t_i^* = [-1, -0.74282, 0.69967, 0.016385, 1]$$

The gain intervals $\mathcal{K}_i$ are then found with the help of (3.45). As a final step, the stabilizing gain interval is found by checking the number of unstable poles (u_i) in these intervals and given in Table 3.2.

Table 3.2 : Gain intervals and corresponding unstable root counts.

u_i	$\mathcal{K}_i$
4	$0.059956 > \mathcal{K}_1 > -\infty$
3	$0.064633 > \mathcal{K}_2 > 0.059956$
1	$0.172633 > \mathcal{K}_3 > 0.064633$
0	$0.717538 > \mathcal{K}_4 > 0.17263$
2	$0.74794 > \mathcal{K}_5 > 0.7175$
4	$\infty > \mathcal{K}_6 > 0.74794$

It is seen from the table that the stabilizing gain interval is found to be

$$K_p \in (0.17263, 0.717538)$$

which is the same result obtained via modified Nyquist method in the previous subsection.

In the modified Nyquist method, calculation of the intersection points of Nyquist curve and real axis may be challenging as the order of the system increases. However, it can be said that the calculation of gain intervals with the help of the Chebyshev polynomials approach is more straightforward process and can easily be handled with a computer software such as Mathematica.

3.3 Digital PI-PD Controller Design In Dominant Pole Placement

3.3.1 PI-PD controller structure in discrete-time domain

In this section, it is aimed to explain the necessity and advantages of the PI-PD controller structure in discrete-time domain. The block diagram related to PI-PD controller is given in Figure 3.12. Here, PD controller is placed on the feedback path in the inner loop and PI controller is placed on the forward path in the outer loop.
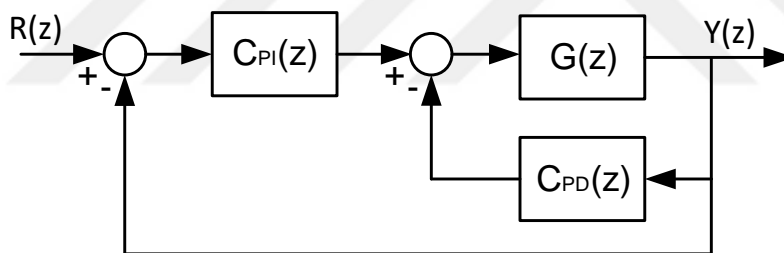
Figure 3.12 : The structure of PI-PD controller.

In comparison to classical PID controller structure, the given 2-DOF controller structure has some important advantages. One of the advantages is that it is possible to locate the PI-PD controller zero anywhere in z-plane as desired. Thus, the adverse effect of the controller zeros in the closed-loop (especially appearing in the PID controller case) is eliminated by the PI-PD controller structure. On the other hand, it is also possible to use this zero to eliminate one of the closed-loop real pole (undesirably) located the in dominant region. Another advantage is that the transient response of the closed-loop system does not have derivative kick phenomenon due to the fact that PD controller is placed on the feedback path.

80

Although the PI-PD controller has advantages over classical PID controller, the controller design for 2-DOF structure may not be a straightforward process. Nevertheless, it can be shown that there is a relation between the classical PID controller structure and PI-PD controller structure. Thus, it is possible to carry out the design process through PID controller structure and then to convert the obtained controller parameters to the PI-PD controller parameters.

Let

$$G(z) = \frac{N_G(z)}{D_G(z)} = \frac{\beta_m z^m + \beta_{m-1} z^{m-1} + \cdots + \beta_1 z + \beta_0}{z^n + \alpha_{n-1} z^{n-1} + \cdots + \alpha_1 z + \alpha_0}, \ m \leq n \quad (3.47)$$

be an arbitrary order discrete-time transfer function of the system to be controlled. If the considered system has time-delay, denominator of the transfer function will consist of the corresponding poles located at $z = 0$ in z-domain.

Let us consider the closed-loop control scheme for PI-PD controller given in Figure 3.12 where the digital PD controller is given as

$$C_{PD}(z) = K_{pd} + K_d \frac{z-1}{z} \quad (3.48)$$

and the digital PI controller is given as

$$C_{PI}(z) = K_{pi} + K_i \frac{z}{z-1} \quad (3.49)$$

The closed-loop system characteristic polynomial for this control scheme can be expressed as below.

$$P_c(z) = K_d N_G(z) - \left(D_G(z) + \left(2K_d + K_{pd} + K_{pi}\right) N_G(z)\right) z \\ + \left(D_G(z) + \left(K_{pd} + K_{pi} + K_i + K_d\right) N_G(z)\right) z^2 \quad (3.50)$$

Let us also consider the closed-loop control scheme for classical PID controller with unit feedback, where the digital PID controller is expressed as follows.

$$C(z) = \frac{N_C(z)}{D_C(z)} = \frac{(K_p + K_i + K_d) z^2 - (K_p + 2K_d) z + K_d}{z(z-1)} \quad (3.51)$$

The closed-loop system characteristic equation for the given block diagram is then expressed as follows.

$$P_c(z) = K_d N_G(z) - (D_G(z) + (2K_d + K_p) N_G(z)) z \\ + (D_G(z) + (K_p + K_i + K_d) N_G(z)) z^2 \quad (3.52)$$

Comparing (3.50) and (3.52), it is clear that as long as the equality

$$K_{pd} + K_{pi} = K_p \quad (3.53)$$

81

is satisfied, the location of the closed-loop system poles are the same; therefore, the transformation between the PID and PI-PD controllers can easily be done. Furthermore, in the classical PID controller structure, it is generally not possible to place the controller zeros as desired and this can cause undesired behaviour in the closed-loop transient response if the controller zeros are located in the dominant region or even outside of the unit circle in z-plane. However, if the PI-PD controller is used, the controller places two zeros, one zero to the point of $z = 0$ and the other zero to the point of

$$z = \frac{K_{pi}}{K_i + K_{pi}} \tag{3.54}$$

in z-plane and it is possible to choose its location arbitrarily as mentioned earlier by adjusting the K_{pi} parameter.

For the reasons mentioned above, the digital PI-PD controller design problem is solved by converting it to the digital PID controller design problem in this thesis.

3.3.2 Procedures of the discrete PI-PD controller design

In this section, it is aimed to present the summary of the algorithm to design a discrete PI-PD controller using the given information in the previous sections. In order to design a discrete PI-PD controller using the proposed method, the following steps are followed.

Step 1: Determine the dominant pole pair ($z_{1,2} = \sigma_z \pm j\omega_z$) in z-domain with the help of desired closed-loop performance criteria.

Step 2: Obtain the digital PID controller parameters K_i and K_d in terms of the parameter K_p using (3.18).

Step 3: Write the closed-loop system characteristic polynomial in terms of the parameter K_p by substituting the digital PID controller parameters found in the previous step.

Step 4: Obtain the residue polynomial $P_r(z, K_p)$, which is constructed by the unassigned closed-loop system poles, as in (3.24).

Step 5: Determine the dominance factor (m) and calculate the radius of the disc (r^m) in which the remaining poles are desired to be assigned.

Step 6: Obtain the polynomial $P_r(r^m z, K_p)$ so that the relative stabilization problem can be converted to the stability problem.

Step 7: Collect the terms multiplied by K_p together and obtain the $N(z)$ and $D(z)$ as in (3.38).

Step 8: Find the Chebyshev representations of the polynomials $N(z)$ and $D(z)$ using the corresponding first and second kinds of the Chebyshev polynomials.

Step 9: Construct $G(t)$ with the help of (3.42).

Step 10: Find the real roots (t^*) of (3.44) such that $t^* \in [-1, +1]$ and calculate the gain intervals $\mathscr{K}_i$ using (3.45).

Step 11: The set of stabilizing gains (K_p) is found as the union of the gain intervals $(\mathscr{K}_i)$, in which the number of poles located outside of the desired disc, is zero $(u = 0)$.

Step 12: Choose any K_p^* from the stabilizing gain interval and find the PID controller by calculating K_i and K_d parameters using (3.18).

Step 13: Finalize the PI-PD controller design by choosing a proper K_{pi} value such that the controller zero is located inside the disc of radius r^m.

Step 14: If the K_p interval is empty for $u = 0$ but a solution exists for $u = 1$, then choose a proper K_{pi} value such that the real pole located outside of the disc of radius r^m is cancelled by the controller zero and finalize the PI-PD controller design. However, this approach can be considered if and only if the real pole is located in stable region and not very close to the unit disc.

Step 15: If the solution set is found to be empty for both cases mentioned above, repeat the design procedure for different m value and/or performance specifications.

Example 3.4 (Simulation Study For PI-PD Design):

In order to demonstrate the proposed design method through a simulation study, the temperature control of crude oil in a fluidized catalytic cracking unit, which is studied by Zou and Lie [43], is considered. Moreover, the proposed method is compared

with the existing PID controller design methods in literature such as Ziegler-Nichols, Internal Model Control (IMC) and H_∞ control as also performed in [43].

Consider the following first order plus dead time (FOPDT) model of the process.

$$G(s) = \frac{K}{\tau s + 1} e^{-Ls} = \frac{1}{(4s+1)} e^{-2.5s}$$

Discrete transfer function of the system by taking the sample time as $t_s = 0.25$ seconds is given as follows.

$$G(z) = \frac{0.060587}{z - 0.939413} z^{-10}$$

Let the closed-loop system time domain characteristics be desired as 11 seconds of settling time with 0.5% overshoot. Corresponding dominant pole pair in z-plane is calculated as below.

$$z_{1,2} = \sigma_z + j\omega_z = 0.91177 \pm j0.0492$$

Parametrization of the discrete PID controllers which assign dominant poles are done as follows.

$$K_i = 0.06539K_p - 0.001963$$

$$K_d = 5.3431K_p - 3.31962$$

The closed-loop system characteristic polynomial with PID controller with the above parameters is given as follows.

$$P_c(z, K_p) = \left(z^2 - 1.82355 + 0.83375\right) P_r(z, K_p)$$

where $P_r(z, K_p)$ is the 11th order polynomial constructed by the remaining poles. The unassigned poles are desired to be assigned in a disc of radius $r = 0.7613$ that means the dominance factor to be $m = 3$. In this case, the polynomial $P_r(0.7613z, K_p)$ is constructed and the relative stability problem is converted to the stability problem. In order to solve this problem, Chebyshev polynomials approach is used as proposed earlier.

The Chebyshev representations of the $N(z)$ and $D(z)$ are obtained using the corresponding first and second kinds of the Chebyshev polynomials as below.

$$R_D(t) = -50.928t^{11} - 3.87953t^{10} + 142.523t^9 + 8.31218t^8$$
$$- 144.6t^7 - 6.203t^6 + 64.1027t^5 + 1.86138t^4 - 11.5815t^3$$
$$- 0.195673t^2 + 0.588615t - 0.2211$$

$$T_D(t) = 50.982t^{10} + 3.87953t^9 - 117.032t^8 - 6.37241t^7$$
$$+ 92.4579t^6 + 3.5017t^5 - 29.3164t^4 - 0.664596t^3$$
$$+ 3.15751t^2 + 0.054359t - 0.073327$$

$$R_N(t) = 0.388271$$

$$T_N(t) = 0$$

It is now possible to construct the Chebyshev representation $G(t)$ by substituting the above expressions into (3.42). After separating the real and imaginary parts of the obtained expression, the real roots (t^*) of (3.44) such that $t^* \in [-1, +1]$ can be calculated, thus, the gain intervals $\mathscr{K}_i$ can be found. As a final step, the stabilizing gain interval is found by checking the number of unstable poles (u_i) in these intervals and given in Table 3.3.

Table 3.3 : Obtained Gain intervals and unstable root counts.

u_i	$\mathscr{K}_i$	u_i	$\mathscr{K}_i$
11	$0.43679 > \mathscr{K}_1 > -\infty$	3	$0.70328 > \mathscr{K}_7 > 0.66397$
9	$0.43906 > \mathscr{K}_2 > 0.43679$	5	$0.70862 > \mathscr{K}_8 > 0.70328$
7	$0.44552 > \mathscr{K}_3 > 0.43906$	7	$0.71031 > \mathscr{K}_9 > 0.70862$
5	$0.4649 > \mathscr{K}_4 > 0.44552$	9	$0.71075 > \mathscr{K}_{10} > 0.71031$
3	$0.56825 > \mathscr{K}_5 > 0.4649$	10	$0.96719 > \mathscr{K}_{11} > 0.71075$
1	$0.66397 > \mathscr{K}_6 > 0.56825$	11	$\infty > \mathscr{K}_{12} > 0.96719$

It is seen from the table that there is not any solution for $u = 0$ which means that for the chosen performance criteria and m value, it is not possible to place all the remaining poles inside the disc of radius $r = 0.7613$. However, there exists a solution for $u = 1$, thus, 10 of 11 closed-loop poles can be assigned away from the dominant region and the remaining real pole can be cancelled using the PI-PD controller zero. For this case

study, it can be shown that the remaining real pole is located in the stable region and not very close to the unit circle.

The parameter K_p is chosen from the interval of $K_p \in (0.56825, 0.66397)$ and the PID controller design is completed. For $K_p = 0.65$, the parameters of PID controller are found as $K_i = 0.0405$ and $K_d = 0.1534$. The digital PI and PD controllers are then given as follows.

$$C_{PI}(z) = K_{pi} + 0.0405 \frac{z}{z-1}$$

$$C_{PD}(z) = (0.65 - K_{pi}) + 0.1534 \frac{z-1}{z}$$

The proper choice of the parameter K_{pi} is made as $K_{pi} = 0.6835$ by adjusting the location of controller zero as mentioned above. The closed-loop pole zero map in z-plane with digital PI-PD controller is depicted in Figure 3.13.
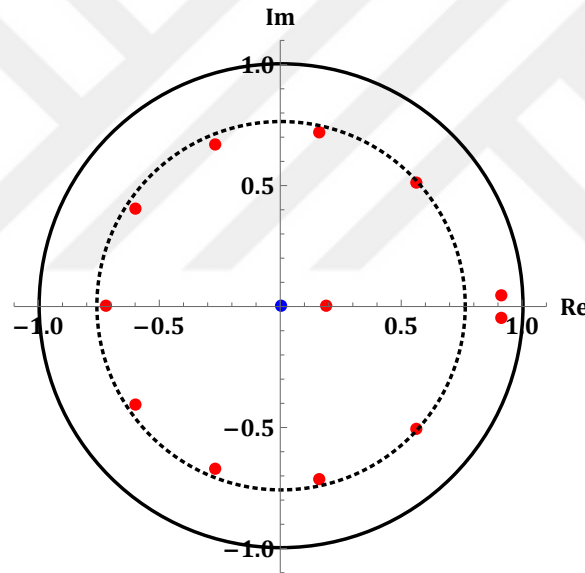
Figure 3.13 : Pole-zero map of the closed-loop system with PI-PD controller.

As mentioned earlier, it is also aimed to show the performance of the proposed controller over the controllers tuned by Ziegler-Nichols method, IMC method and H_∞ method.

$$C(s) = K_c \left(1 + \frac{1}{T_i s + 1} + T_d s \right) \frac{1}{T_f s + 1} \qquad (3.55)$$

For the PID controller structure given by (3.55), the controller parameters are given as follows for the Ziegler-Nichols method.

$$K_c = \frac{1.2\tau}{KL}, T_i = 2L, T_d = \frac{L}{2}, T_f = 0 \qquad (3.56)$$

86

The formula for the IMC method for the same controller structure is also given below.

$$K_c = \frac{\tau + 0.5L}{K(\lambda + 0.5L)}, T_i = \tau + 0.5L, T_d = \frac{\tau L}{2\tau + L}, T_f = 0 \tag{3.57}$$

For the H_∞ method, the PID tuning formula is given by (3.58).

$$K_c = \frac{T_i}{K(2\lambda + 0.5L)}, T_i = \tau + 0.5L, T_d = \frac{\tau L}{2T_i}, T_f = \frac{\lambda^2}{2\lambda + 0.5L} \tag{3.58}$$

Table 3.4 shows the calculated controller parameters for the considered system.

Table 3.4 : Controller parameters.

Parameters	Z-N Method	IMC Method	H_∞ Method
K_c	1.92	1.3125	1.3698
T_i	5	5.25	5.25
T_d	1.25	0.9524	0.9524
T_f	0	0	0.435
λ	−	2.75	1.2912

The simulation studies show that the closed-loop system has 0.5% overshoot and settles to its final value in 11.85 seconds with proposed PI-PD controller. The closed-loop transient response of the system is shown in Figure 3.14 with the proposed PI-PD, Z-N PID, IMC PID and H_∞ PID controllers. In addition, the disturbance rejection performances are also shown in the simulation studies by adding an input disturbance with amplitude of -0.5 at the time $t = 100$ seconds. The control signals of the considered controllers are also depicted in Figure 3.15. Finally, some of the closed-loop performance criteria and the control signal norms are given in Table 3.5.

It is obvious from the figures that the PID controller tuned by Z-N method causes high overshoot and very oscillatory closed-loop response. The control signal has high initial value and also undesired oscillations which is not acceptable for most of the systems. On the other hand, the performance of IMC and H_∞ PID controllers are better than the Z-N PID; however, the oscillatory response still exists and H_∞ PID has around 5.3% overshoot which may not be suitable for many systems. The initial values of control signals are also high (especially for IMC) as said for the Z-N PID controller.

Compared with the other methods, the transient response of the proposed method is very smooth and has nearly zero overshoot with acceptable settling time. Moreover, the
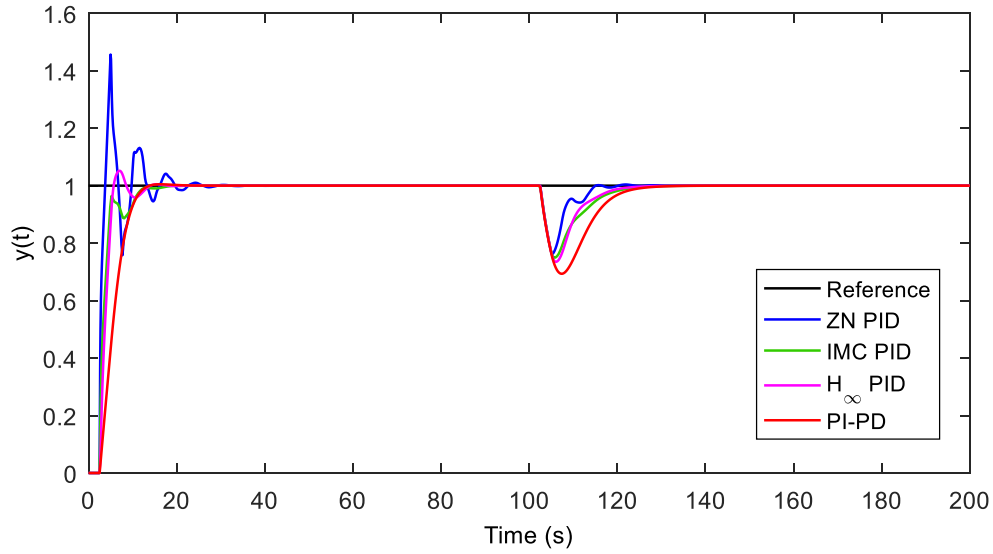
Figure 3.14 : Closed-loop responses of the compared controllers.
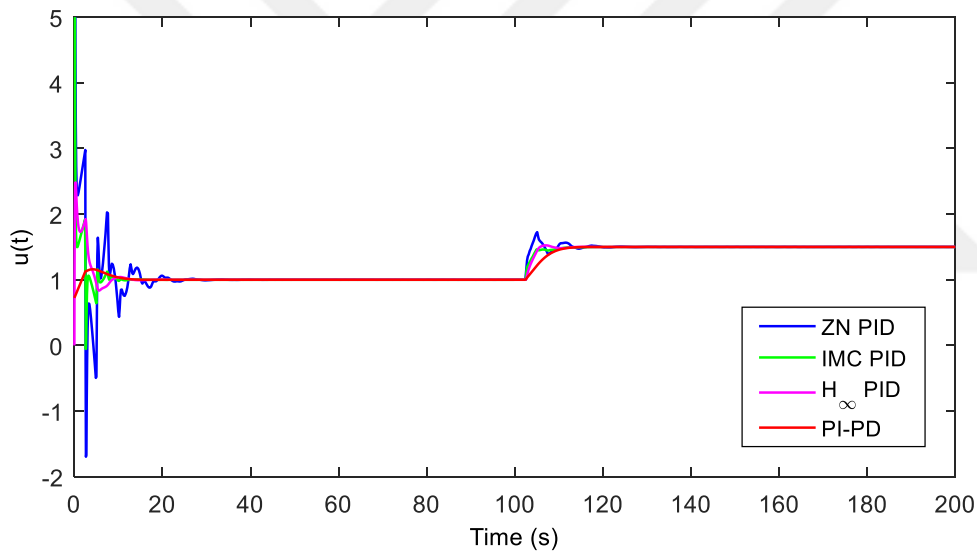
Figure 3.15 : Control signals of the compared controllers.

control signal is also low and very smooth which has a significant importance during the implementation in a real environment. It is worth to note that the performance specifications are very close to the desired ones, and the controller found by the proposed method forms a better alternative especially when overshoot is not required and/or there exist restrictions on the control signal. A possible disadvantage of the proposed method is having a slower initial response (rise time) in comparison to the other methods. This results in poorer ISE performance as can be observed in Table 3.5.

Table 3.5 : Closed-loop performance criteria and control signal norms for nominal system.

	t_s [s]	os [%]	$\|u\|_2$	$\|u\|_\infty$	ISE
Z-N Method	18.92	45.6	19.07	19.2	3.104
IMC Method	11.6	0	18.34	13.81	3.318
H_∞ Method	12.45	5.3	18.11	2.485	3.626
PI-PD Method	11.85	0.5	17.85	1.5	5.183

The robustness of the designed controller is also an important aspect due to the fact that it is not possible to obtain the perfect mathematical model of a system. In case of parametric uncertainties, it is important for a controller to perform an acceptable closed-loop performance. For this reason, the considered controllers are also compared by taking parametric uncertainties into account. All the parameters of the FOPDT system (K, τ and L) are changed $\pm 20\%$ in magnitude simultaneously and the closed-loop system responses are given in the Figure 3.16-Figure 3.19. In addition, the worst values of settling time, overshoot and control signal norms under parametric uncertainties are given in Table 3.6 (Z-N PID is not included due to the unstable response in the worst case).
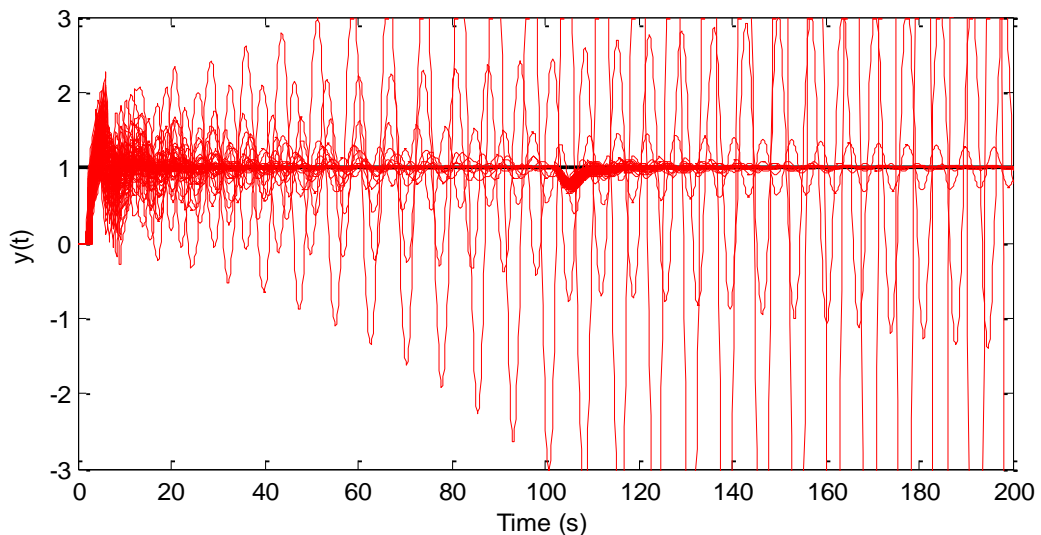
Figure 3.16 : Z-N PID controller under parametric uncertainties.
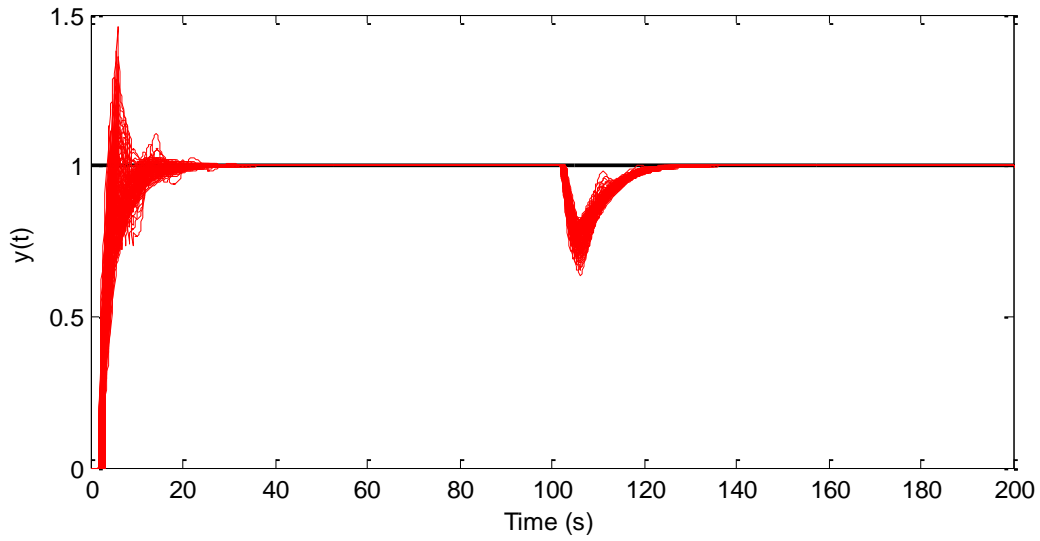
Figure 3.17 : IMC PID controller under parametric uncertainties.
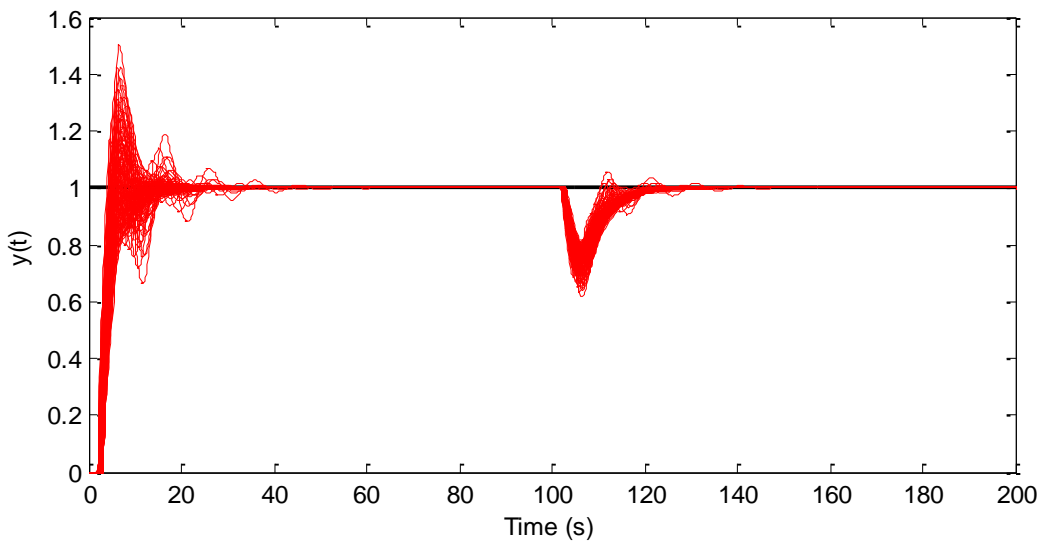
Figure 3.18 : H_∞ PID controller under parametric uncertainties.

Table 3.6 : Settling time, overshoot and control signal norms in the worst case.

	t_s [s]	os [%]	$\|u\|_2$	$\|u\|_\infty$	ISE
IMC Method	23.37	45.8	21.74	13.81	4.295
H_∞ Method	36.75	50.36	21.61	2.485	4.914
PI-PD Method	26.91	14.82	21.26	1.763	6.485
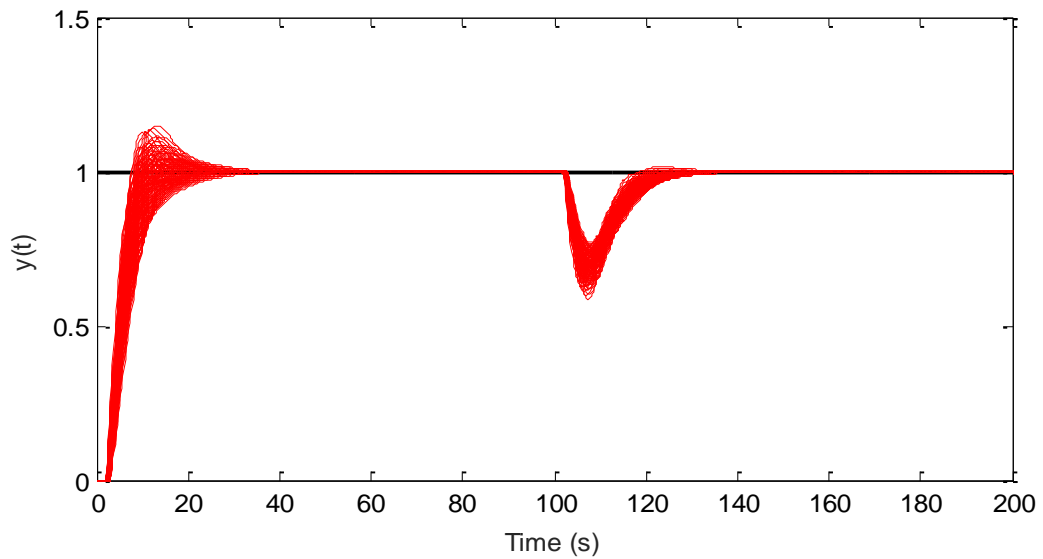
Figure 3.19 : Proposed PI-PD controller under parametric uncertainties.

It is seen that the PID controller tuned via Z-N method could not tolerate the parametric uncertainties and became unstable for some values of the system parameters. Thus, it is not possible to use this controller if there is a chance that the parameters of system changes ±20% in magnitude. The performance of IMC and H_∞ PID controllers under parametric uncertainties is certainly better than Z-N method; however, the closed-loop responses have very high overshoot values (around 50% in the worst case). The closed-loop transient response with proposed controller is still smooth, has always less than 15% overshoot even in the worst case and the disturbance rejection is also acceptable. Therefore, it is clear that the performance of proposed PI-PD controller is the best in terms of robustness.

Example 3.5 (Real-Time Implementation For PI-PD Design):

In this example, it is aimed to show the applicability of proposed PI-PD controller design in a real environment. For this purpose, a fan and plate laboratory system, which is illustrated in Figure 3.20, is considered. In this laboratory set, it is desired to control the position of metal plate, which hangs in the air, in a specific reference position. The movement of plate is provided by the air stream which is produced by a fan controlled via an asynchronous motor. The asynchronous motor is driven by SINAMICS G110 industrial driver and Beckhoff CX9000 PLC is used as a main controller unit. The output of the system (plate angle) is measured by a potentiometer element.
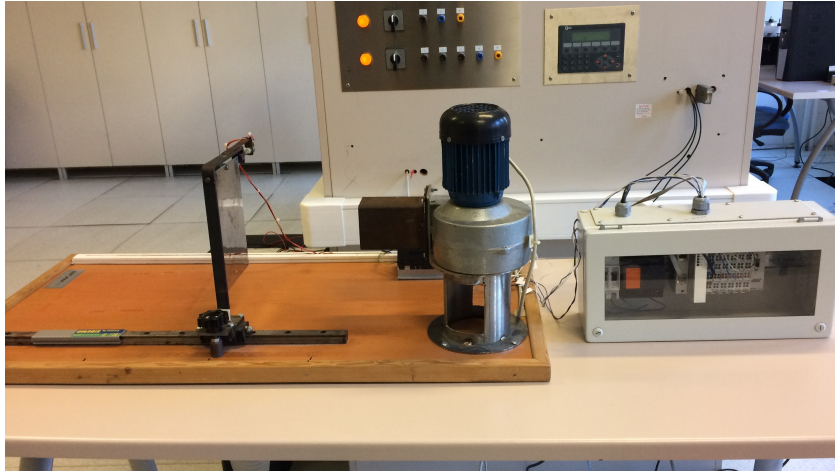
Figure 3.20 : Fan & plate laboratory system.

Linear model of the system is obtained as a second order plus time delay (SOPTD) via system identification as below.

$$G(s) = \frac{14.877}{s^2 + 3.202s + 51.3} e^{-0.25s}$$

The open-loop step response of the system is given in Figure 3.21. The discrete transfer function of the system is obtained by taking sampling time as $t_s = 0.05$ seconds as follows.

$$G(z) = \frac{0.016546 + 0.017457z}{0.85206 - 1.7348z + z^2} z^{-5}$$
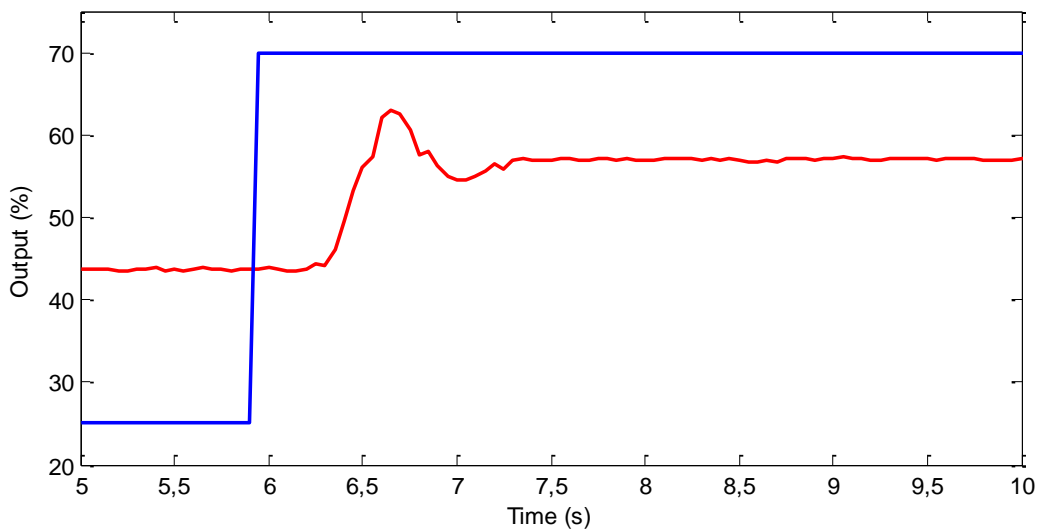
Figure 3.21 : Open-loop response of the fan and plate laboratory system.

It is desired to place the dominant poles to the points of

$$z_{1,2} = \sigma_z + j\omega_z = 0.9 \pm j0.0947$$

which means that 5% overshoot and 2 seconds of settling time in the closed-loop. It is now possible to find the PID controller parameter set (K_p, K_i, K_d) which assigns the dominant poles as follows.

$$K_i = 0.26248 + 0.11707K_p$$

$$K_d = 3.63563 + 5.04544K_p$$

The next step is to find the interval of K_p such that the remaining poles are located inside a disc of radius $r = 0.7788$ in z-plane. The closed-loop system characteristic polynomial and the residue polynomial are found as below.

$$P_c(z, K_p) = \left(z^2 - 1.8 + 0.819\right) P_r(z, K_p)$$

$$P_r(z, K_p) = z^7 - 0.935z^6 + 0.0853z^5 + 0.067z^4 + 0.0507z^3 + 0.0364z^2$$
$$+ (0.0921 + 0.1076K_p)z + 0.07347 + 0.102K_p$$

Here, the Chebyshev polynomials approach can be used after the polynomial $P_r(r^m z, K_p)$ is obtained so that the pole assignment problem is converted to the stability problem. After that if the polynomial $P_r(r^m z, K_p)$ is re-arranged as given in (3.38), the Chevbyshev representation of the $N(z)$ and $D(z)$ can be obtained using the first and second kind of Chebyshev polynomials as follows.

$$R_D(t) = 0.2846 + 1.095t - 3.907t^2 - 9.34t^3 + 10.21t^4 + 19.075t^5 - 6.675t^6 - 11.12t^7$$

$$T_D(t) = -0.108 + 1.306t + 3.974t^2 - 6.872t^3 - 13.514t^4 + 6.675t^5 + 11.12t^6$$

$$R_N(t) = 0.102 - 0.0838t$$

$$T_N(t) = 0.0838$$

The next step is to construct $G(t)$ with the help of (3.42) and to calculate its real and imaginary parts. After that it is possible to find the real roots (t^*) of (3.44) such that $t^* \in [-1, +1]$ and to calculate the gain intervals $\mathcal{K}_i$ using (3.45) as below.

$$t_i^* = \{-1, -0.914, -0.808, -0.297, 0.217, 0.673, 0.939, 1\}$$

$$\mathcal{K}_i = \{-11.154, -3.262, -1.191, -1.106, -0.812, 0.849, 4.01, 21.08\}$$

Table 3.7 : Gain intervals and corresponding unstable root counts.

u_i	$\mathcal{K}_i$	u_i	$\mathcal{K}_i$
7	$-11.154 > \mathcal{K}_1 > -\infty$	2	$0.849 > \mathcal{K}_6 > -0.812$
5	$-3.262 > \mathcal{K}_2 > -11.154$	4	$4.01 > \mathcal{K}_7 > 0.849$
3	$-1.191 > \mathcal{K}_3 > -3.262$	6	$21.08 > \mathcal{K}_8 > 4.01$
1	$-1.106 > \mathcal{K}_4 > -1.191$	7	$\infty > \mathcal{K}_9 > 21.08$
0	$-0.812 > \mathcal{K}_5 > -1.106$		

The stabilizing K_p range is then found by calculating the unstable root count (u_i) in the obtained gain intervals. The resulting gain interval is found as follows.

$$K_p \in (-1.106, -0.812)$$

As long as the K_p parameter is selected in the obtained interval, non-dominant poles are assigned in a disc with radius $r = 0.7788$. Therefore, the proper choice can be done by observing the control signal or the location of the zeros. If $K_p = -0.82$ is chosen, the PID controller parameters are given as $K_i = 0.1665$ and $K_d = -0.5016$. The resulting discrete-PID controller is expressed as below.

$$C(z) = -0.82 + 0.1665\frac{z}{z-1} - 0.5016\frac{z-1}{z}$$

Firstly, the designed digital PID controller is analyzed before the calculation of corresponding digital PI-PD controller. The pole-zero map of the closed-loop control system with the designed PID controller in z-domain is given in Figure 3.22. As it is seen from the figure, the dominant poles are assigned to the desired locations as the remaining poles are located inside the disc with the radius of $r = 0.7788$ in z-plane. However, the closed-loop system has one zero outside of the unit circle; therefore, an inverse response is expected to be observed in the step response of closed-loop system.

The closed-loop system transient response with the designed discrete PID controller is illustrated in Figure 3.23. In the figure, both simulation (carried out through Simulink) and real-time data for fan and plate system are shown. The real-time data shows that the system settles to its final value in around 2.5 seconds with 7% overshoot. The obtained closed-loop system performance criteria are close to the desired ones; however, the inverse response is an undesired phenomenon.
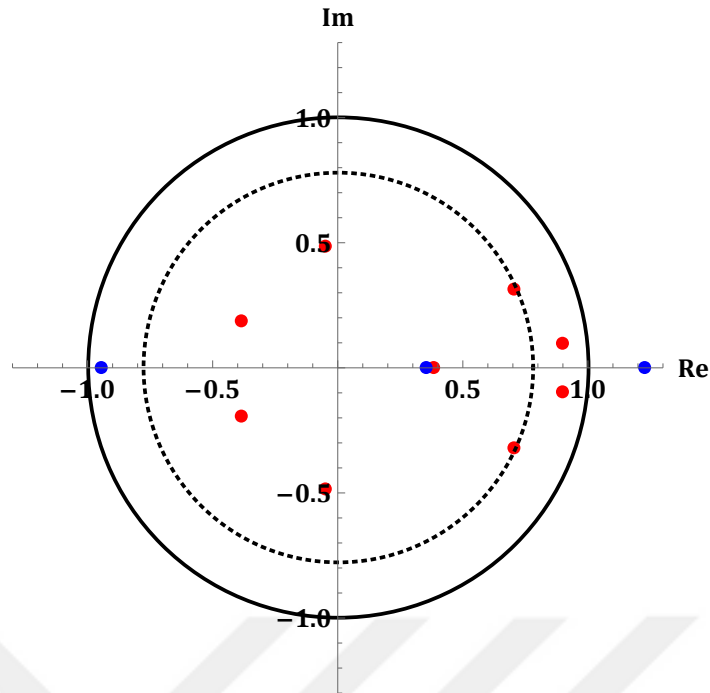
Figure 3.22 : Pole-zero map of the closed-loop system with PID controller in z-domain.
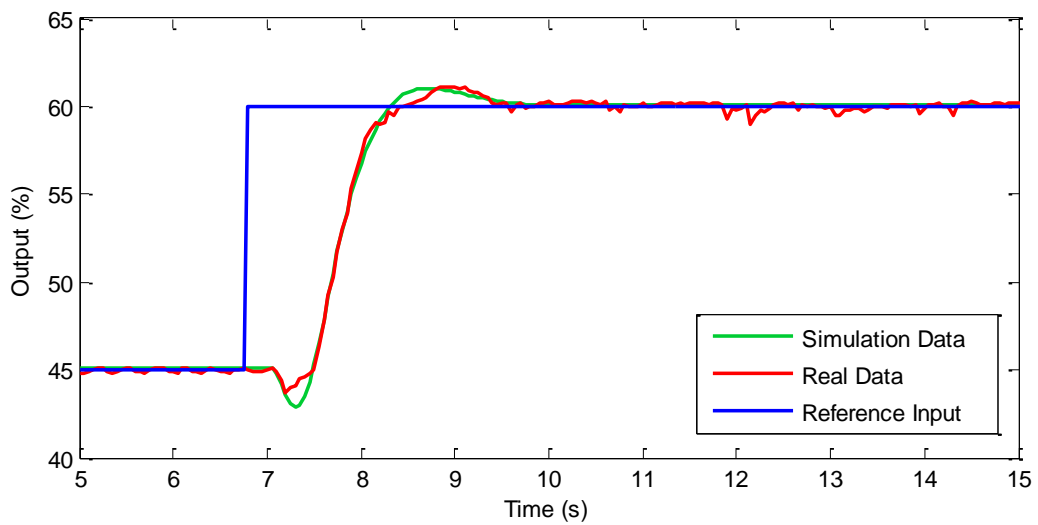
Figure 3.23 : Step response of the closed-loop system with the digital PID controller.

Now, the digital PI-PD controller structure is constructed with the help of designed digital PID controller parameters. In this example, a solution exists for $u = 0$; therefore, the controller design can be finalized by choosing the K_{pi} parameter such that the closed-loop system zero is assigned away from the dominant pole region. Thus, the inverse response caused by the PID controller zero is also eliminated.

For instance, the location of zero is calculated as $z = 0.231$ for $K_{pi} = 0.05$. In this case, the PI and PD controllers are given as follows.

$$C_{PI}(z) = 0.05 + 0.1665\frac{z}{z-1}$$

$$C_{PD}(z) = -0.87 - 0.5016\frac{z-1}{z}$$

such that

$$K_p = K_{pi} + K_{pd} = -0.82$$
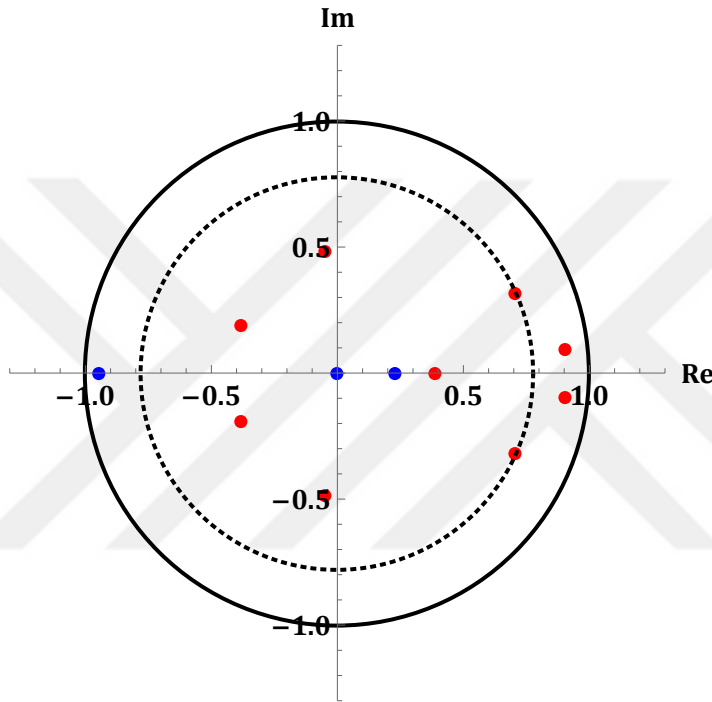
Figure 3.24 : Pole-zero map of the closed-loop system with PI-PD controller in z-domain.

The pole-zero map of the closed-loop control system with the proposed digital PI-PD controller in z-plane is given in Figure 3.24. The locations of closed-loop system poles are the same as expected; however, the controller zeros located inside the unit circle and away from the dominant region.

The step response of closed-loop system is also depicted in Figure 3.25. Here, both simulation and real-time data for the fan and plate system are given again. It is seen from the figure that the system settles to its final value in around 2.3 seconds with 5% overshoot. Moreover, in this case, the inverse response phenomenon does not occur as expected from the proposed digital PI-PD controller.
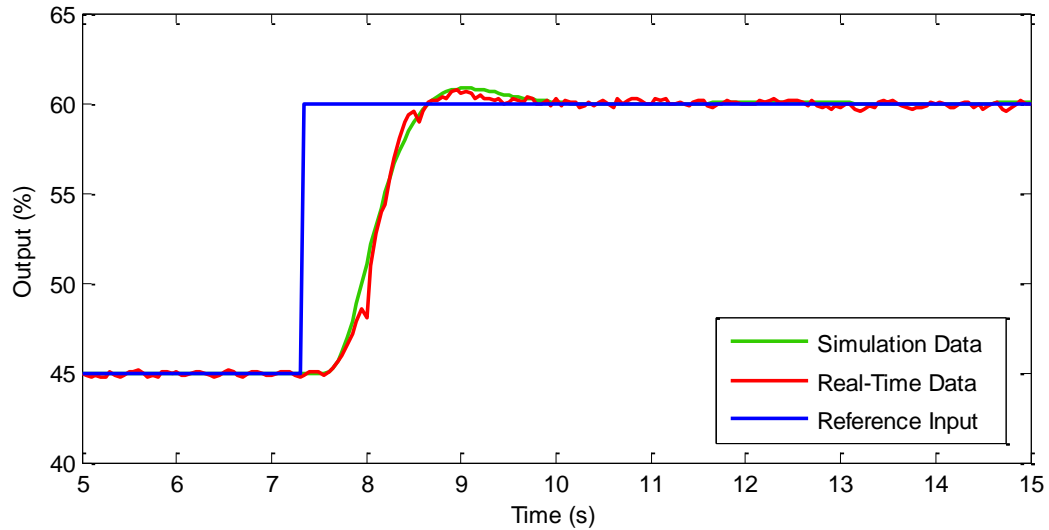
Figure 3.25 : Step response of the closed-loop system with the proposed PI-PD controller.

Note that the proposed design method relies on the placement of dominant pole pair to the desired points and the remaining poles *m* times away from the dominant poles. However, it is not always possible to place the non-dominant poles as desired for the chosen performance specifications and m value. Therefore, if the resulting controller set is found to be empty then the given design process should be repeated for different m value and/or performance criteria until obtaining a non-empty controller parameter set. This can be stated as a drawback of proposed design method.

In many real world applications, overshoot is not required or only a very small overshoot is allowed. It is shown through examples that the proposed method can be used for such applications by choosing the dominant pole locations to provide a critically damped response.

3.4 Calculation of the Maximum Dominance Factor with Digital PID Controller

It is clear that the dominance factor (*m*) has an important place on transient response of the system. In general, it is possible to say that the closed-loop system acts closer to the desired behaviour as the dominance factor increases due to the fact that the effect of the remaining poles on system response becomes negligible. However, it is obvious that it is very hard task to place all the remaining poles inside a disc with a very small radius just using a gain (K_p). Consequently, during the controller design, it

can cause the resulting controller set to become an empty set, if the dominance factor is chosen too high. For this reason, here, it is aimed to find the maximum achievable dominance factor, in other words, the disc with smallest possible radius in z-plane for which dominant pole assignment is possible.

Consider the polynomial $P_r(z, \tilde{r}, K_p)$ which is constructed by unassigned closed-loop poles where the parameter $\tilde{r}$ is given as $\tilde{r} = (\sqrt{\sigma_z^2 + \omega_z^2})^m$. In order to find the minimum value of the $\tilde{r}$, it is possible to use different approaches. Routh-Hurwitz method is the first method to be used with the help of bilinear transformation given as follows.

$$\mathscr{T} : z \mapsto \frac{w+1}{w-1} \tag{3.59}$$

If the Routh table is created from the polynomial given in (3.60),

$$P_r(w, \tilde{r}, K_p) = \alpha_k(\tilde{r}, K_p) w^k + \alpha_{k-1}(\tilde{r}, K_p) w^{k-1} + \cdots + \alpha_0(\tilde{r}, K_p) \tag{3.60}$$

it is possible to say that the inequalities

$$\begin{aligned} &\alpha_k(\tilde{r}, K_p) > 0, \ \alpha_{k-1}(\tilde{r}, K_p) > 0, \\ &\frac{-\alpha_k(\tilde{r}, K_p) \alpha_{k-3}(\tilde{r}, K_p) + \alpha_{k-1}(\tilde{r}, K_p) \alpha_{k-2}(\tilde{r}, K_p)}{\alpha_{k-1}(\tilde{r}, K_p)} > 0, \ \ldots \end{aligned} \tag{3.61}$$

or

$$\begin{aligned} &\alpha_k(\tilde{r}, K_p) < 0, \ \alpha_{k-1}(\tilde{r}, K_p) < 0, \\ &\frac{-\alpha_k(\tilde{r}, K_p) \alpha_{k-3}(\tilde{r}, K_p) + \alpha_{k-1}(\tilde{r}, K_p) \alpha_{k-2}(\tilde{r}, K_p)}{\alpha_{k-1}(\tilde{r}, K_p)} < 0, \ \ldots \end{aligned} \tag{3.62}$$

define a region in two dimensional $\tilde{r} - K_p$ plane. The stabilizing region is then obtained as an intersection of all these inequalities. Thus, the minimum value of the radius can be obtained, or for a chosen $\tilde{r}$ value, the interval of the parameter K_p can be found graphically.

If the inequalities from the Routh table are found to be too complex (i.e. the order of the system is too high) then the gridding approach may be used over the parameter $\tilde{r}$. After that either Routh-Hurwitz method or Chebyshev polynomials approach can be used to find the stabilizing K_p range.

Example 3.6:

Consider again the same system presented in Example 3.1 which has the following open-loop discrete-time transfer function.

$$G(z) = \frac{0.09516}{z^3(z - 0.9048)}$$

If the closed-loop system characteristic polynomial is found in terms of the parameter K_p for the same desired performance criteria, and the residue polynomial is calculated we have,

$$P_r(z, K_p) = z^4 - 0.038357z^3 - 0.041964z^2 - 0.044755z - 0.337374 + 0.819662K_p$$

It is desired to place the roots of the above polynomial inside the disc of minimum possible radius $\tilde{r}$. The modified polynomial is then obtained as below.

$$P_r(z, \tilde{r}, K_p) = \tilde{r}^4 z^4 - 0.038357\tilde{r}^3 z^3 - 0.041964\tilde{r}^2 z^2 - 0.044755\tilde{r}z$$
$$+ (-0.337374 + 0.819662K_p)$$

Here, the above polynomial can be transformed into continuous-time stability plane using (3.59) and Routh table can be created. Finally the inequalities written from the first column of the table define a region which is illustrated in Figure 3.26 in $\tilde{r} - K_p$ plane.
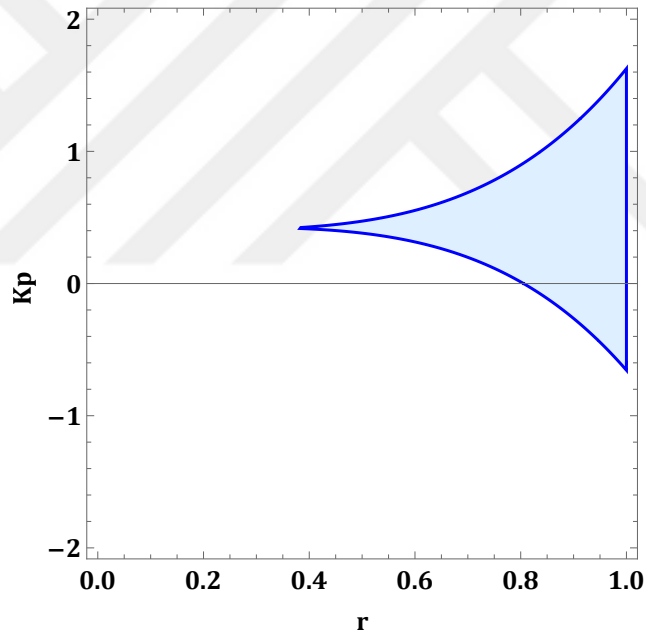
Figure 3.26 : The obtained region in $\tilde{r} - K_p$ plane (Example 3.6).

After the calculations, the minimum value of the radius is found as $\tilde{r} = 0.365$ which means that the maximum value of the dominance factor be

$$r^m = (0.9355)^m = 0.365 \longrightarrow m = 15.11$$

The value of the parameter K_p for the maximum dominance factor can be found via Routh table or from the obtained figure graphically as below.

$$K_p = 0.4189$$

99

The designed digital PID controller is then given as follows.

$$C(z) = 0.4189 + 0.0808\frac{z}{z-1} + 0.055\frac{z-1}{z}$$

Figure 3.27 shows the closed-loop poles of the considered system with the designed controller. It is seen that all of the non-dominant poles are located inside the disc of radius $\tilde{r} = 0.365$ as expected.
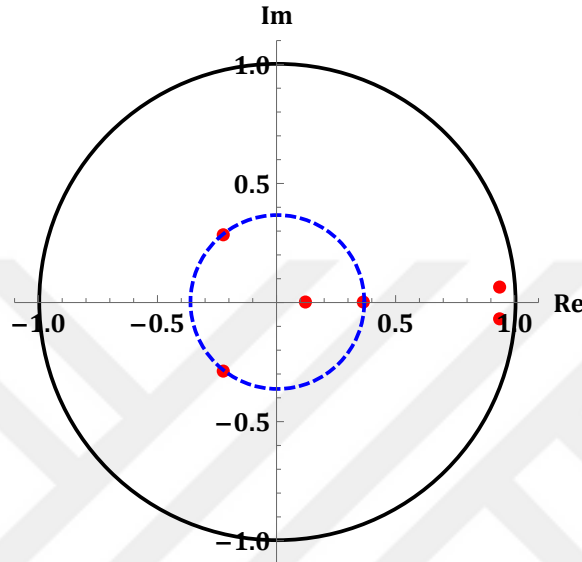
Figure 3.27 : The poles of the system in the closed-loop (Example 3.6).

Example 3.7:

Consider the discrete transfer function of the fan and plate laboratory system.

$$G(z) = \frac{0.016546 + 0.017457z}{z^5(z^2 - 1.7348z + 0.85206)}$$

The closed-loop system characteristic polynomial can then be found in terms of the parameter K_p for the desired performance criteria (2 seconds of settling time, 5% overshoot), and the residue polynomial can be calculated as follows.

$$P_r(z, K_p) = z^7 - 0.93507z^6 + 0.08526z^5 + 0.06695z^4 + 0.05069z^3$$
$$+ 0.036413z^2 + (0.092082 + 0.10758K_p)z + 0.073474 + 0.101965K_p$$

It is again desired to place the roots of the above polynomial inside the disc of minimum possible radius $\tilde{r}$. The modified polynomial can be obtained and transformed into continuous-time stability plane using bilinear transformation. As a final step, the inequalities written from the first column of the Routh table define a region in $\tilde{r} - K_p$ plane. Figure 3.28 shows the obtained region via Mathematica.

100
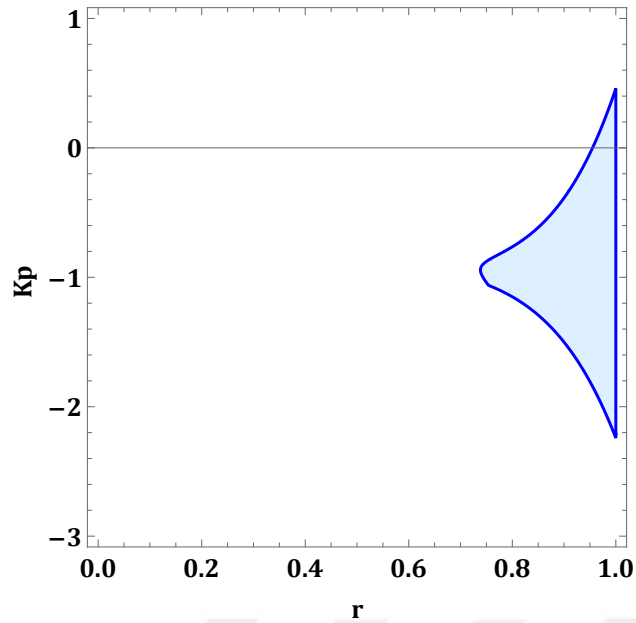
Figure 3.28 : The obtained region in $\tilde{r} - K_p$ plane (Example 3.7).

If the required calculations are done, the minimum value of the radius is found as $\tilde{r} = 0.7385$ which means that the maximum value of the dominance factor be $m = 3.03$. The value of the controller parameter K_p for this dominance factor can be found via Routh table or from the above figure graphically as follows.

$$K_p = -0.948$$

The designed digital PID controller is given as follows.

$$C(z) = \frac{-1.94395z^2 + 3.24288z - 1.14744}{z(z-1)}$$

Figure 3.29 shows the closed-loop poles of the considered system with the designed PID controller. It is seen that the non-dominant poles are located inside the disc of radius $\tilde{r} = 0.7385$ as desired.

3.5 Limitations on the Dominant Poles Selection in Z-Plane

In the previous section, it is aimed to find the controller parameters such that two of the closed-loop system poles are assigned to desired locations and rest of the poles are located inside a disc with smallest possible radius in z-domain. It means that the performance specifications in the closed-loop poles are known; however, the maximum dominance factor (m_{max}) is desired to be found.
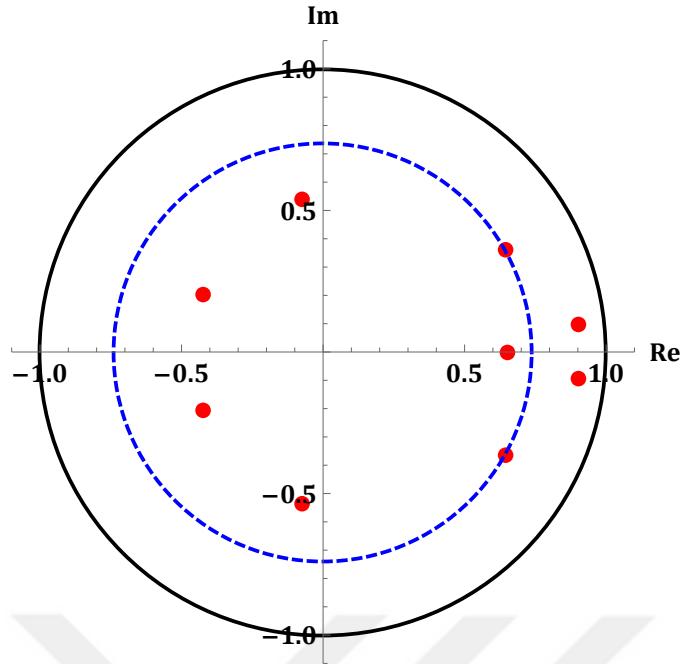
Figure 3.29 : The poles of the system in the closed-loop (Example 3.7).

In this part of thesis, the inverse problem is expected to be solved. If the dominance factor or the radius of disc in which non-dominant poles are assigned is predetermined, the question "What is the limitations on closed-loop performance criteria with discrete PI or PID controllers designed via dominant pole placement?" becomes an important subject to examine. This problem is more meaningful since it is generally enough for the dominance factor to be between 3 and 5 (i.e. predetermined). In order to satisfy this dominance factor, the closed-loop dominant poles should be located in a particular region in z-domain, otherwise, it may not be possible to assign the remaining pole inside the disc with desired radius.

3.5.1 PI controller case

Consider the open-loop discrete transfer function given with (3.1) and a discrete PI controller given with (3.2). The parametrization of the discrete PI controller is already given in (3.15). If those parameters are substituted into the characteristic equation, it is again possible to obtain the polynomial which is constructed by unassigned poles in terms of the σ_z and ω_z as below.

$$P_c(z, \sigma_z, \omega_z) = \left(z^2 - 2\sigma_z z + (\sigma_z^2 + \omega_z^2)\right) P_r(z, \sigma_z, \omega_z) \tag{3.63}$$

After the polynomial $P_r(r^m z, \sigma_z, \omega_z)$ is found for a desired dominance factor, as in the previous section, Routh-Hurwitz method can be used with the help of bilinear transformation in order to find the dominant pole region in $\sigma_z - \omega_z$ plane (actually in z-plane). This region is obtained by drawing the intersection of the regions defined by the inequalities written from the first column of the Routh table. Thus, closed-loop performance limitations with discrete PI controller is found.

Example 3.8:

Consider the following system which is desired to be controlled with a digital PI controller.

$$G(z) = \frac{0.001769 + 0.0491z}{z^3(z - 0.94908)}$$

It is desired to assign non-dominant poles $m = 5$ times away from the dominant pole pair. In this case, the closed-loop performance limitations can be found using the proposed method.

Let dominant pole pair be $z_{1,2} = \sigma_z + j\omega_z$ then for $m = 5$ the discrete PI controller parameters $(K_p(\sigma_z, \omega_z), K_i(\sigma_z, \omega_z))$ can be obtained in terms of the location of dominant pole pair by solving (3.15). After that the polynomial $P_r(z, \sigma_z, \omega_z)$ can be constructed as below.

$$P_r(z, \sigma_z, \omega_z) = \delta_3 z^3 + \delta_2 z^2 + \delta_1 z + \delta_0$$

where

$$\delta_0 = -0.13525\sigma_z^3 + 0.1081\sigma_z^4 + 0.03672\omega_z - 0.036\omega_z^4 + (0.00246 - 0.14564\omega_z^2)\sigma_z$$
$$+ (0.0266 + 0.07206\omega_z^2)\sigma_z^2$$

$$\delta_1 = 0.00123 - 3.682\sigma_z^3 + 3\sigma_z^4 + 0.94778\omega_z^2 - \omega_z^4 + (0.06333 - 3.97\omega z^2)\sigma_z$$
$$+ (0.6721 + 2\omega_z^2)\sigma_z^2$$

$$\delta_2 = -0.00253 - 1.9491\omega_z^2 + (-0.13785 - 1.80496\sigma_z + 2\sigma_z^2 + 2\omega_z^2)\sigma_z$$

$$\delta_3 = 0.0013 + 0.07206\sigma_z + \sigma_z^2 + \omega_z^2$$

If the following transformation is used for $r = \left(\sigma_z^2 + \omega_z^2\right)^{5/2}$

$$\mathscr{T} : z \mapsto r\frac{w+1}{w-1}$$

and the Routh table is created, then the regions, which are drawn with the help of the inequalities, can be given as in Figure 3.30.
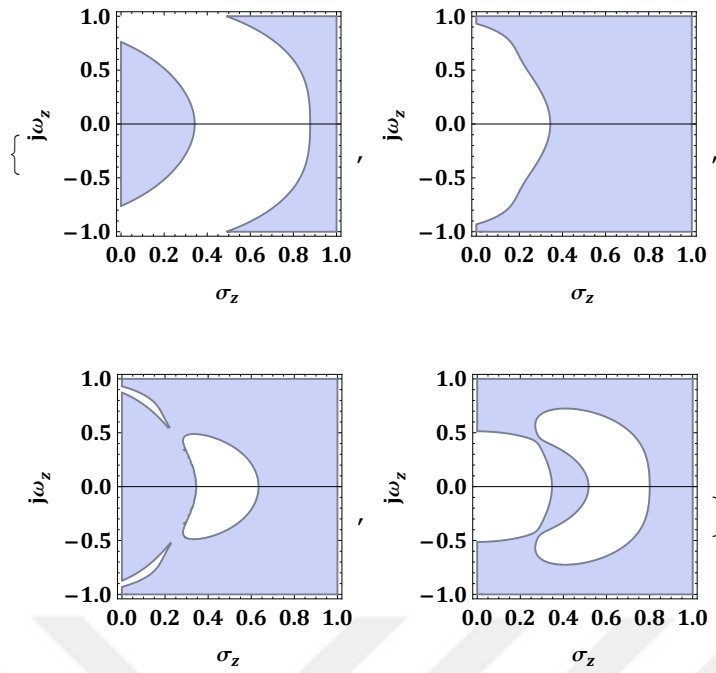
Figure 3.30 : Regions obtained from the first column of Routh table (Example 3.8).

If the intersection of these inequalities are found and the stability region in z-domain

$$\sigma_z^2 + \omega_z^2 < 1$$

is also considered, the region in which the dominant pole pair can be assigned is found as follows.
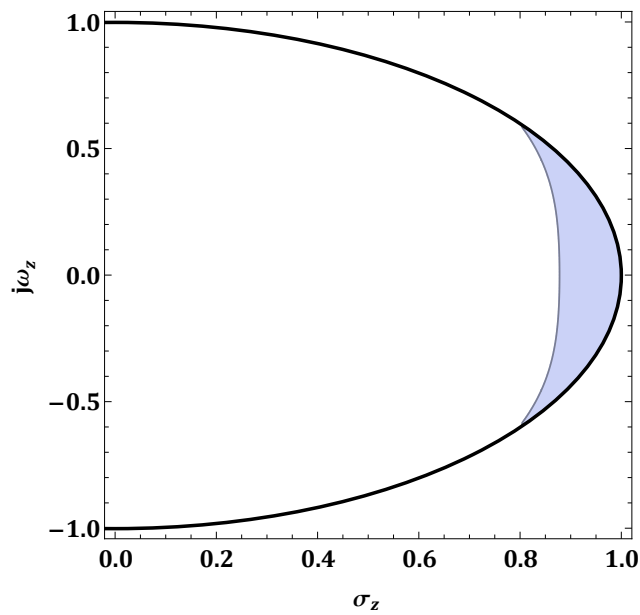
Figure 3.31 : Dominant poles region in z-plane with PI controller (Example 3.8).

As a result, if non-dominant poles are desired to be placed 5 times away from the dominant pole pair with a discrete PI controller, there is a limitation on dominant pole pair selection and this limitation can be seen from the Figure 3.31.

Let dominant poles be chosen as

$$z_{1,2} = 0.88 \pm j0.07$$

from the obtained region in z-plane. In this case, the discrete PI controller can be found as below.

$$G_{PI}(z) = \frac{2.7272z - 2.4835}{z - 1}$$

The closed-loop pole map is given in Figure 3.32 and the closed-loop unit step response is given in Figure 3.33.
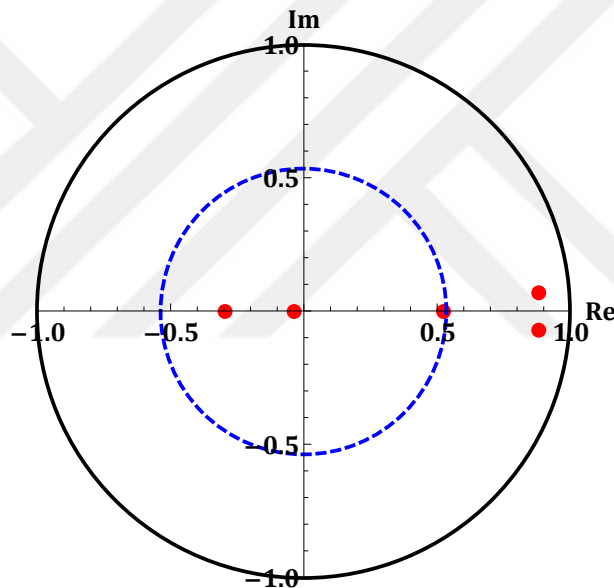
Figure 3.32 : Closed-loop poles with designed PI controller (Example 3.8).

3.5.2 PID controller case

If the limitations on dominant pole pair selection is desired to find for discrete PID controller case, the same procedure can be followed. The polynomial which is constructed by unassigned poles does not only depends the parameters σ_z and ω_z but also the parameter K_p. Therefore, the inequalities written from the first column of the Routh table for the polynomial $P_r(r^m z, \sigma_z, \omega_z, K_p)$ defines a region in 3-dimensional $\sigma_z - \omega_z - K_p$ plane. For a particular K_p value, the solution of the problem is simplified to 2-dimensional region in z-plane as in PI controller case.
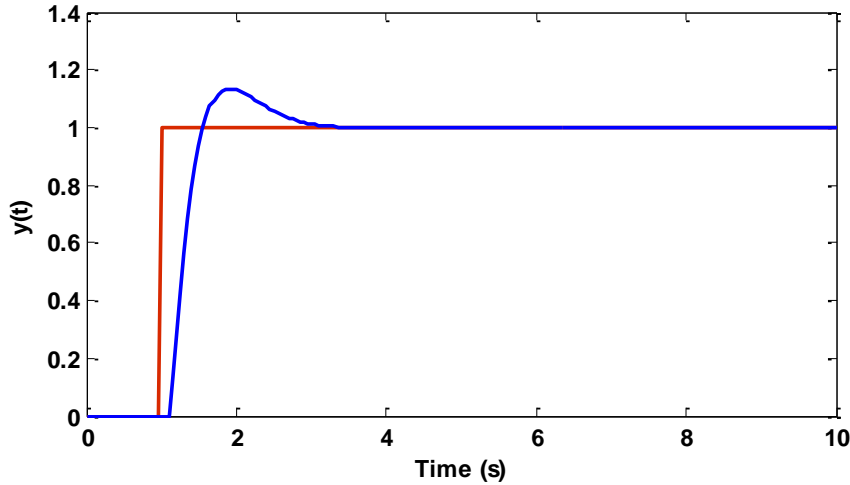
Figure 3.33 : Transient response with designed PI controller in closed-loop (Example 3.8).

Example 3.9:

Let us consider the same system which is used in PI controller case.

$$G(z) = \frac{0.001769 + 0.0491z}{z^3(z - 0.94908)}$$

It is again desired to assign non-dominant poles $m = 5$ times away from the dominant pole pair. The closed-loop performance limitations with discrete PID controller can be found by following the same procedure in previous example.

Let dominant pole pair be $z_{1,2} = \sigma_z + j\omega_z$ and the dominance factor be $m = 5$. The discrete PID controller parameters $(K_i(\sigma_z, \omega_z, K_p), K_d(\sigma_z, \omega_z, K_p))$ can again be obtained in terms of the location of dominant poles via (3.18). However, in discrete PID controller case the inequalities from the first column of the Routh table also depends on the controller parameter K_p as mentioned earlier. Thus, the region is obtained in $(\sigma_z - \omega_z - K_p)$ 3-dimensional space.

After the closed-loop system characteristic polynomial is obtained in terms of the parameters σ_z, ω_z and K_p, the modified polynomial can be obtained for $r = (\sigma_z^2 + \omega_z^2)^{m/2}$. It is then possible to create the Routh table and obtain the inequalities from the first column. If required calculations are done via Mathematica, which allows symbolic calculations, the obtained region is depicted in Figure 3.34.
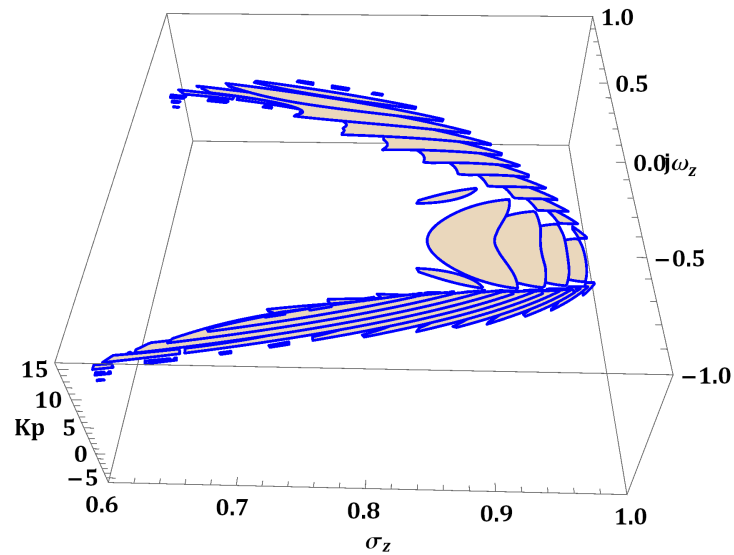
Figure 3.34 : Dominant poles region with PID controller (Example 3.9).

It is possible to see the limitations on dominant pole pair selection from the obtained figure if the dominance factor is desired to be chosen as $m = 5$. For instance, let us obtain the region in z-plane for $K_p = 1$ as in Figure 3.35.
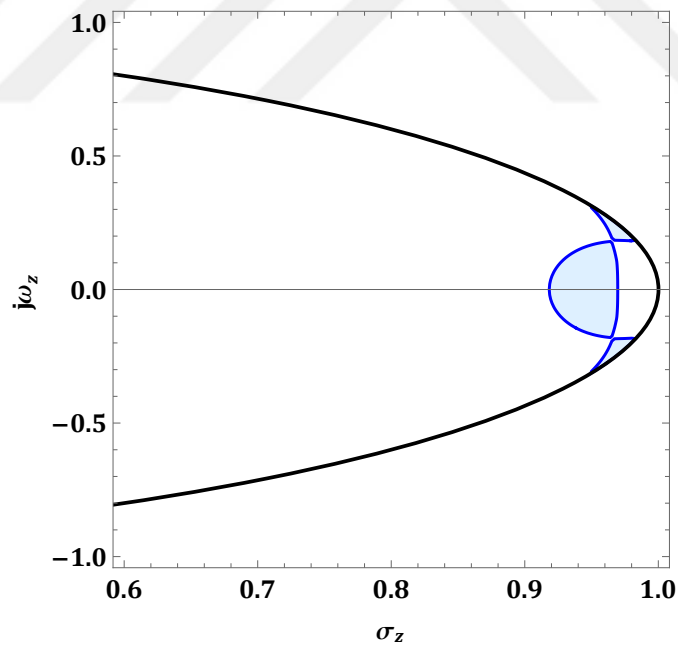
Figure 3.35 : Dominant poles region in z-plane for $K_p = 1$ (Example 3.9).

Let dominant poles be chosen as

$$z_{1,2} = 0.925 \pm j0.05$$

from the obtained region in z-plane for $K_p = 1$. The designed discrete PID controller can be given as follows.

$$G_{PID}(z) = \frac{-2.45885z^2 + 6.10772z - 3.55386}{z(z-1)}$$

Finally, the closed-loop poles are illustrated in Figure 3.36 and the closed-loop transient response is given in Figure 3.37.
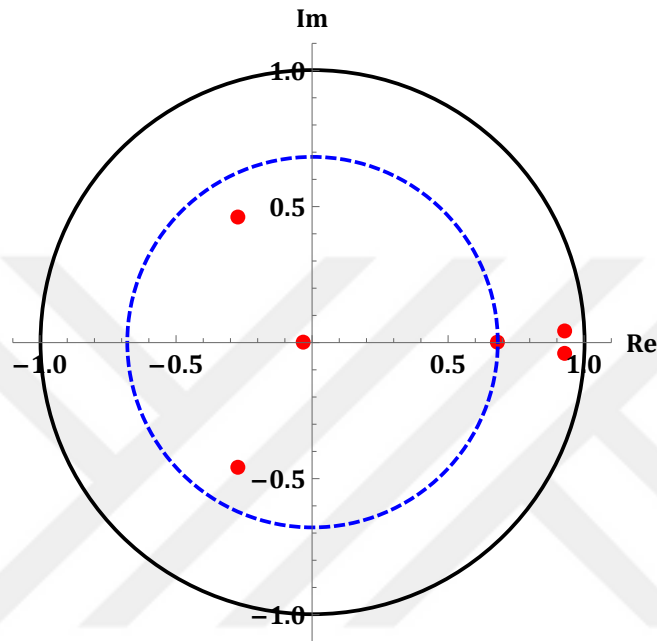
Figure 3.36 : Closed-loop poles with designed PID controller (Example 3.9).
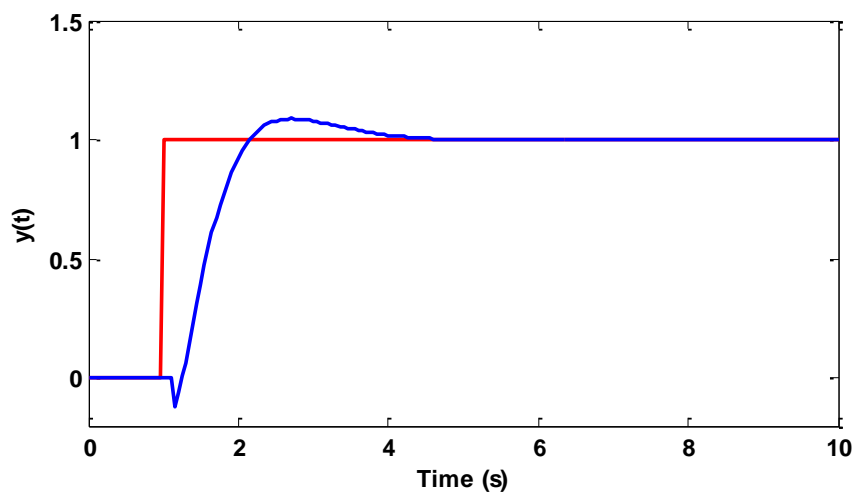
Figure 3.37 : Transient response with designed PID controller in closed-loop (Example 3.9).

Please note that both for discrete PI and PID controller case, limitations are found through closed-loop poles. Thus, the locations of closed-loop zeroes can affect the transient response as can be seen from the examples. Therefore, as proposed earlier, the PI-PD controller structure can be used to eliminate this adverse effect at least for the PID controller case.

3.6 Dominant Pole Region Assignment in Discrete-Time Domain

In this section, it is aimed to perform the dominant pole region assignment (DPRA) with discrete P/PI/PID controllers as performed in continuous-time domain in the previous chapter. The methodology is very similar to the DPRA in continuous-time domain; however, here, it is easier to design such controllers for time-delay systems by taking advantage of discrete-time domain. First of all, the proposed method is explained through P controller and then it is extended to design PI and PID controllers via DPRA.

3.6.1 P controller case

In general, P controller is not useful to control a system due to the fact that it is not always possible to achieve desired performance criteria since there is only one parameter to be tuned. On the other hand, steady state error is observed because there is no integral term. However, the DPRA problem for PI and PID controllers is similar to the method used for the P controller.

In the dominant pole region assignment, it is aimed to assign two of the closed-loop in the desired region whereas the remaining poles are also desired to be located in a region away from the dominant region.

Let (3.64) be the characteristic polynomial of a closed-loop control system with P controller

$$P_c(z) = 1 + K_p \frac{N(z)}{D(z)} = 0 \tag{3.64}$$

and $z = f(\gamma)$ be one of the boundary function of D-region in which dominant poles are desired to be assigned. For the open-loop transfer function $G(z)$, the following can be written,

$$G(f(\gamma)) = \frac{N_{Re} + jN_{Im}}{D_{Re} + jD_{Im}} \tag{3.65}$$

where

$$D_{Im} = Im\left[D(f(\gamma))\right], D_{Re} = Re\left[D(f(\gamma))\right]$$

$$N_{Im} = Im\left[N(f(\gamma))\right], N_{Re} = Re\left[N(f(\gamma))\right]$$

Let us rearrange the expression (3.65) as follows.

$$G(f(\gamma)) = \frac{(N_{Re}D_{Re} + N_{Im}D_{Im}) + j(N_{Im}D_{Re} - N_{Re}D_{Im})}{D_{Re}^2 + D_{Im}^2} \tag{3.66}$$

and by defining

$$X(\gamma) = N_{Re}D_{Re} + N_{Im}D_{Im}$$

$$Y(\gamma) = N_{Im}D_{Re} - N_{Re}D_{Im}$$

$$Z(\gamma) = D_{Re}^2 + D_{Im}^2$$

it is possible to write following equality,

$$G(f(\gamma)) = \frac{X(\gamma)}{Z(\gamma)} + j\frac{Y(\gamma)}{Z(\gamma)} \tag{3.67}$$

Here, the critical frequencies (γ_i^*), which cause roots to cross the boundary $z = f(\gamma)$ in complex z-plane, can be calculated using (3.68).

$$Im\left[G(f(\gamma))\right] = \frac{Y(\gamma)}{Z(\gamma)} = 0 \tag{3.68}$$

After that the intersection points (x_i) of Nyquist curve and real axis can be found with the help of following expression.

$$x_i = Re\left[G(f(\gamma))\right] = \frac{X(\gamma_i^*)}{Z(\gamma_i^*)} \tag{3.69}$$

It is now possible to calculate the gain intervals with the help of Nyquist theorem. The gain intervals can be found by $\mathcal{K}_i \in \left(-\frac{1}{x_i}, -\frac{1}{x_{i+1}}\right)$ such that $x_i < x_{i+1}$ for $i = 1, 2, \ldots$ and the union of these intervals, in which number of the closed-loop system poles (u) located outside of dominant pole region becomes as desired, gives the final interval as follows.

$$\overline{K} \in \bigcup_{j=1}^{n} \mathcal{K}_j \tag{3.70}$$

Please note that this procedure should be repeated for each boundary of the desired D-region in z-plane. As a results, the interval of the controller parameter K_p to provide DPRA is found as follows.

$$K_p \in \bigcap_{j=1}^{m} \overline{K}_j \tag{3.71}$$

110

If the resulting set is found to be an empty set, it means that there is not any P controller which assign the closed-loop poles to the desired regions.

Example 3.10:

The open-loop transfer function of a first order plus dead time (FOPDT) system is given as follows.

$$G(s) = \frac{1}{s+1}e^{-0.4s}$$

The discrete transfer function by taking sampling time as $0.1s$ is found as below.

$$G(z) = \frac{0.09516}{z - 0.904837}z^{-4}$$

In the closed-loop, it is aimed design a P controller such that the dominant poles are assigned in the region between the discs of radius 0.8 and 0.9. Moreover, the non-dominant poles are desired to be located inside the disc of radius 0.6.

The boundaries can be given as follows.

$$f_1(\gamma) = 0.9e^{j\gamma}, f_2(\gamma) = 0.8e^{j\gamma}, f_3(\gamma) = 0.6e^{j\gamma} \mid \gamma \in [0, 2\pi]$$

For the first boundary, the root count outside of the corresponding disc should be 0 whereas for the other boundaries, it should be 2.

If the expressions $G(\gamma)$ are obtained for every desired root boundaries and the proposed method is applied, the critical frequencies are found for the considered boundaries as follows.

Table 3.8 : Critical frequencies calculated for $G_1(\gamma), G_2(\gamma)$ and $G_3(\gamma)$.

$Im[G_1(\gamma)] = 0$	0	0.3457	1.0462	1.7448	2.4432	3.1416
$Im[G_2(\gamma)] = 0$	0	0.2468	1.0229	1.7337	2.4385	3.1416
$Im[G_3(\gamma)] = 0$	0	0.9652	1.7064	2.4267	3.1416	-

It is now possible to find the intersection points of Nyquist plot and real axis. After that the gain intervals and corresponding anti-D-stable root counts can be found as follows.

As a result, the P controller gain should be selected from the interval of

$$K_p \in \bigcap_{j=1}^{3} \overline{K}_j \in (1.008, \ 1.568)$$

111

Table 3.9 : Gain intervals and unstable root counts for $G_1(\gamma)$.

u_i	$\mathscr{K}_i$	u_i	$\mathscr{K}_i$
5	$-11.69 > \mathscr{K}_1 > -\infty$	2	$9.53 > \mathscr{K}_5 > 2.14$
3	$-6.216 > \mathscr{K}_2 > -11.69$	4	$12.443 > \mathscr{K}_6 > 9.53$
1	$0.0334 > \mathscr{K}_3 > -6.216$	5	$\infty > \mathscr{K}_7 > 12.443$
0	$2.14 > \mathscr{K}_4 > 0.0334$		

Table 3.10 : Gain intervals and unstable root counts for $G_2(\gamma)$.

u_i	$\mathscr{K}_i$	u_i	$\mathscr{K}_i$
5	$-6.89 > \mathscr{K}_1 > -\infty$	**2**	$5.601 > \mathscr{K}_5 > 1.008$
3	$-3.613 > \mathscr{K}_2 > -6.89$	4	$7.338 > \mathscr{K}_6 > 5.601$
1	$0.451 > \mathscr{K}_3 > -3.613$	5	$\infty > \mathscr{K}_7 > 7.338$
0	$1.008 > \mathscr{K}_4 > 0.451$		

Table 3.11 : Gain intervals and unstable root counts for $G_3(\gamma)$.

u_i	$\mathscr{K}_i$	u_i	$\mathscr{K}_i$
5	$-1.925 > \mathscr{K}_1 > -\infty$	**2**	$1.568 > \mathscr{K}_4 > 0.415$
3	$-1.02 > \mathscr{K}_2 > -1.925$	4	$2.049 > \mathscr{K}_5 > 1.568$
1	$0.415 > \mathscr{K}_3 > -1.02$	5	$\infty > \mathscr{K}_6 > 2.04$

It means that if the K_p is chosen within the obtained feasible gain interval, the desired closed-loop pole configuration is guaranteed to be satisfied in z-domain. If $K_p = 1.567$ is chosen which is one of the limit values, the closed-loop poles in z-domain calculated as below and are given in Figure 3.38.

$$z_{1,2} = 0.81575 \pm j0.262$$

$$z_{3,4} = -0.08112 \pm j0.5944$$

$$z_5 = -0.56443$$

It can be seen from the figure that the dominant poles are assigned to the desired dominant pole region in z-domain and the remaining poles are located in the desired non-dominant pole region.
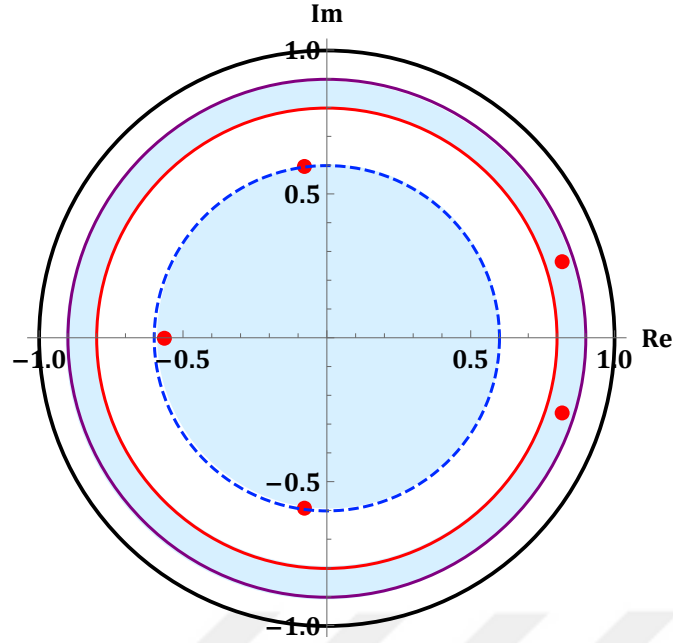
Figure 3.38 : Closed-loop poles with P controller (Example 3.10).

3.6.2 PI and PID controller cases

For the design of discrete PI controller, first of all, the parameters K_p and K_i should be written in terms of the boundary function $(f(\gamma))$ parameter γ for the desired dominant pole region. After that these boundaries should be transferred to the PI controller parameter space one by one. It gives the PI controller parameter set such that the dominant pole pair is assigned into the dominant region. However, the remaining poles should also be located inside the desired non-dominant pole region which is generally given as below.

$$\widetilde{\mathscr{D}} = \left\{z \in \mathbb{C} \mid \ |z| \leq r < 1, \, r \in \mathbb{R}^+\right\} \tag{3.72}$$

If these boundaries are also transferred to the parameter space, then the 2 dimensional $K_p - K_i$ plane is divided into several regions. The region in which the unassigned poles are located inside the desired non-dominant region gives the solution set (unless it is an empty set).

The discrete PID controller design via dominant pole region assignment is almost same as the design of discrete PI controller. However, in this case, the controller parameter $K_p = k_p^*$ is fixed and the boundaries are obtained in 2 dimensional $K_i - K_d$ plane. Finally by gridding the K_p parameter, whole set of PID controllers which perform the DPRA is obtained.

113

Example 3.11:

Consider the open-loop transfer function of a system given below.

$$G(z) = \frac{0.01655 + 0.01746z}{z^2 - 1.7348z + 0.8521} z^{-5}$$

Let dominant poles be inside an elliptic region given by the boundary function,

$$f_1(\gamma) = c + \frac{a+b}{2} e^{j\gamma} + \frac{a-b}{2} e^{-j\gamma}$$

where

$$a = 0.5, \; b = 0.25, \; c = 0.5$$

which actually limits the damping ratio in z-plane and also in the region between the discs whose boundary functions are

$$f_2(\gamma) = 0.95 e^{j\gamma}, \; f_3(\gamma) = 0.85 e^{j\gamma}$$

The remaining poles are also desired to be inside of the disc of radius $r = 0.72$. Figure 3.39 shows the desired dominant and non-dominant poles region in z-plane.
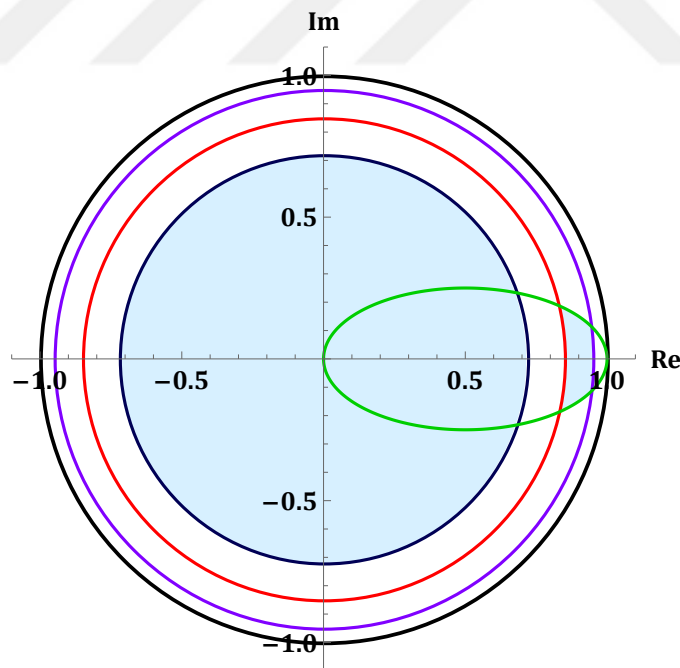
Figure 3.39 : Desired dominant and non-dominant poles region (Example 3.11).

The closed-loop system characteristic polynomial with discrete PID controller can be found as follows.

$$P_c(z) = 0.01655K_d + (-0.015635K_d - 0.01655K_p)z$$
$$+ (-0.01837K_d + 0.01655K_i - 0.00091K_p)z^2$$
$$+ (0.01746K_d + 0.01746K_i + 0.01746K_p)z^3$$
$$- 0.85206z^6 + 2.5869z^7 - 2.7348z^8 + z^9$$

Here, the four edges of the dominant pole region (Figure 3.40) can then be substituted into characteristic polynomial through the boundary functions given above and the parameter K_i and K_d can be obtained in terms of γ for a fixed $K_p = k_p^*$. After that the corresponding boundaries can be found in $K_i - K_d$ plane with the help of frequency sweeping between $\gamma \in [\gamma^-, \gamma^+]$.
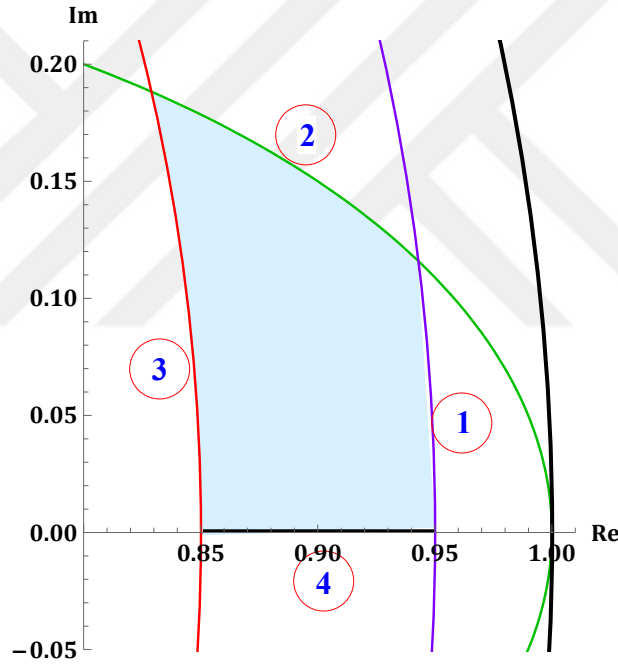
Figure 3.40 : Boundaries of the desired dominant pole region (Example 3.11).

Let us choose the parameter $K_p = -0.82$. In this case, for the first dominant pole region boundary, it is possible to solve the following complex equation and obtain the parameters K_d and K_i in terms of γ.

$$Re\left(P_c\left(0.5 + 0.125e^{-j\gamma} + 0.375e^{j\gamma}\right)\right) = 0$$
$$Im\left(P_c\left(0.5 + 0.125e^{-j\gamma} + 0.375e^{j\gamma}\right)\right) = 0 \implies (K_d(\gamma), K_i(\gamma))$$

After that for $\gamma \in [0.4826, 0.853]$ (which can easily be obtained), it is possible to draw the corresponding boundary in $K_i - K_d$ parameter space. If the explained procedure is

done for all boundaries both for dominant and non-dominant pole regions, the regions in parameter space is obtained as in Figure 3.41.
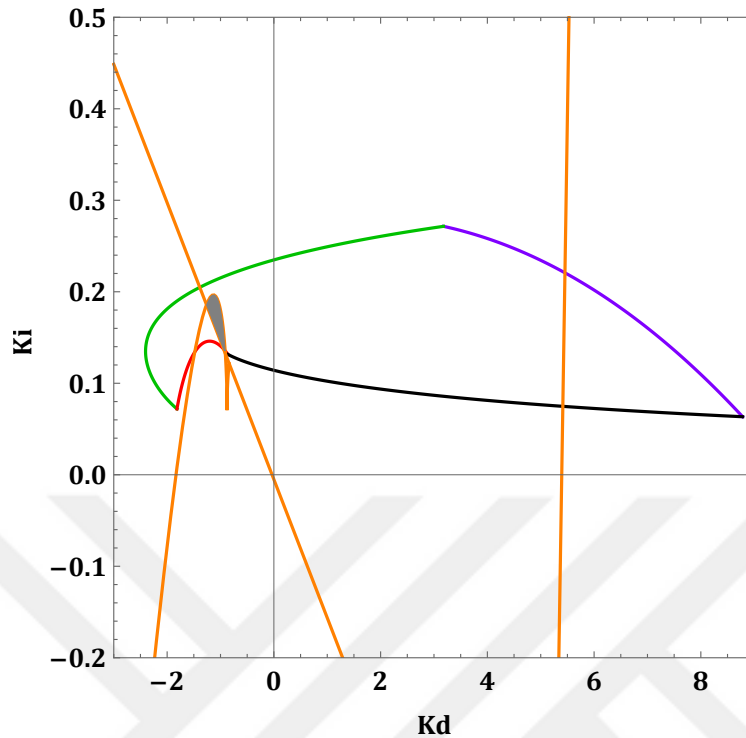
Figure 3.41 : Corresponding sub-regions in parameter space for $K_p = -0.82$ (Example 3.11).

The grey region constitute a solution to the defined problem. In other words, if the PID controller parameters are chosen from the obtained region, two of the closed-loop poles are assigned into the desired dominant region whereas the remaining poles are located inside the disc of radius 0.72.

Let the discrete PID controller parameters be

$$K_p = -0.82, \ \ K_d = -1.1, \ \ K_i = 0.17$$

The closed-loop poles in complex z-plane is then obtained as follows.

Here, it is again possible to use the discrete PI-PD controller structure to avoid the adverse effects of controller zeros as necessary.

Note that similar to the continuous-time domain case, the remaining poles can not always be located away from the dominant pole region especially if the order of considered system is too high. Since PI/PID controllers can assign only limited number of poles in the closed-loop, the resulting solution set in parameter space may be an

116
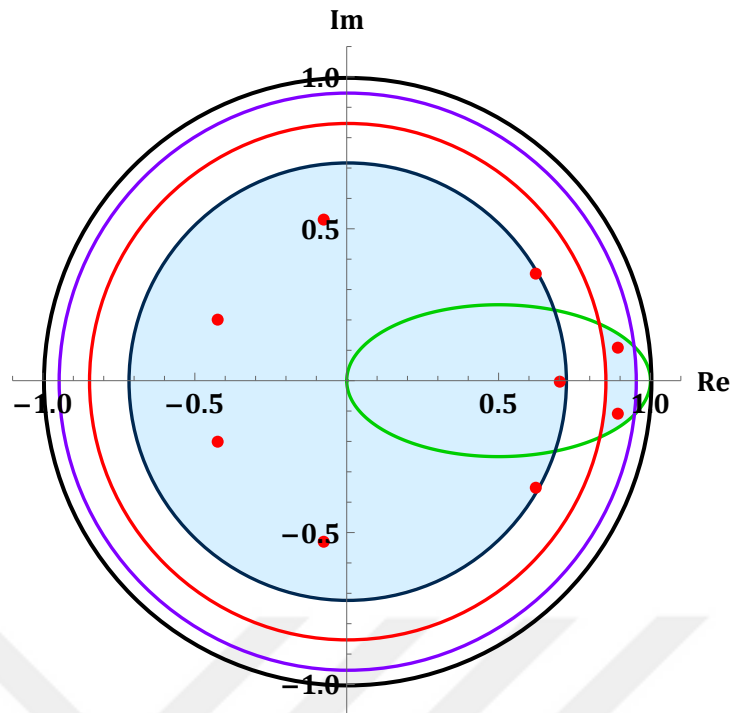
Figure 3.42 : Closed-loop poles in z-domain with discrete PID controller (Example 3.11).

empty set. Therefore, if there is not any sub-region that satisfies the desired pole configuration, the design process should be repeated by changing the performance criteria and/or dominance factor.

4. ROBUST DOMINANT POLE PLACEMENT WITH PID CONTROLLERS FOR PARAMETRIC UNCERTAIN SYSTEMS

For most of the real applications, the linear models of the physical systems can not be obtained precisely due to the fact that inaccurate description of the characteristics of system elements, torn-and-worn effects on the system components, hysteresis and non-linearities, changes in the operation points and other unmodelled/neglected dynamics, thus, the model contains uncertain parameters [50, 51]. If the system parameters are not known exactly but their intervals are known then it is defined as a parametric uncertainty. In order to analyse the stability of systems with parametric uncertainties, there are well-known methods such as the Kharitonov theorem, the edge theorem, the mapping theorem and the Tsypkin-Polyak loci [6, 30, 31].

Design of robust PID type controllers for uncertain parameter systems has an important place. Many researchers have been studied and still continue to study on stabilization of the entire plant using robust PID type controllers via different techniques [34–39]. Although the robust stability of a closed-loop system is the most important criterion, the robust performance is also important. However, in most of the robust PID controller design studies and mentioned references in this paper, only the robust stabilization case is considered. For the robust performance, in some of the studies, the PID controller parameters which satisfy some performance criteria is obtained from the resulting stabilizing set by using an optimization or just trial-error approach. There also exists few studies in which the robust performance is satisfied through the gain and phase margins.

It is clear that a robust PID controller design method, which directly handles the robust performance problem, is required. Here, one of the first approaches that come to mind for the mentioned problem is pole placement approach. It is known that the pole placement approach is one of the most popular technique to design feedback controllers [46]. Here, it is aimed to consider even the higher order system as a second order system by assigning the non-dominant poles away from the dominant pole pair

which directly affects the desired time domain characteristics such as settling time and overshoot. If the robust PID controller design is combined with the dominant pole placement approach, it becomes possible to consider robust performance problem in a systematic way.

In this chapter, a robust PID controller design method is proposed for the parametric uncertain systems via dominant pole placement approach. Here, it is desired two of the closed-loop poles to be assigned in a desired region, whereas, the remaining poles are located away from the dominant pole pair. Thus, it is aimed to achieve the desired closed-loop response under all possible perturbations. The robust PID controller design method is firstly given for the interval type characteristic polynomials with the help of vertex results. After that the proposed method is generalized to cover the affine-linear type characteristic polynomials. The method is based on the well-known robust stability theorems and the generalized Nyquist theorem. The resulting PID controller is then implemented in PI-PD controller structure in order to eliminate the adverse effects of the zeros in the closed-loop. Success of the proposed design methods are demonstrated on example transfer functions through simulation studies. It is shown that the designed robust controllers satisfy the desired pole configuration in the closed-loop and the closed-loop performance criteria are met even in the worst case.

4.1 Preliminaries

4.1.1 Interval polynomials and Kharitonov theorem

Consider a real polynomial family P associated with a linear time-invariant system containing uncertain parameters as below

$$P(s,Q) = \left\{ p(s,\boldsymbol{q}) = \sum_{i=0}^{n} \alpha_i(q)s^i \mid \boldsymbol{q} \in Q \right\}, \ \alpha_n(q) \neq 0, \ \forall \boldsymbol{q} \in Q \qquad (4.1)$$

where

$$\boldsymbol{q} = \begin{bmatrix} q_0 & q_1 & \cdots & q_m \end{bmatrix}^T \qquad (4.2)$$

is the vector of uncertain parameters whose bounds are given as $q_i \in [q_i^-, q_i^+]$. If it is assumed that the coefficients $\alpha_i(q)$ are affine functions of $\boldsymbol{q}$, then it is possible to write

the following.

$$p(s, \boldsymbol{q}) = p_0(s) + \sum_{i=1}^{m} q_i \, p_i(s) \qquad (4.3)$$

For convenience let us denote,

$$\boldsymbol{p} = (p_0(s), p_1(s), \ldots, p_m(s)) \qquad (4.4)$$

Here if $p = (p_0(s), 1, s, \ldots, s^n)$ is considered, in this case a real interval polynomial is obtained. Note that for an interval polynomial, each uncertain coefficient is independent of all other coefficients.

The robust stability of an interval polynomial family can be checked by the Kharitonov theorem, which is given by Kharitonov in 1979 [52].

Theorem (Kharitonov): The interval polynomial family

$$P(s, Q) = \{p(s, \boldsymbol{q}) = q_0 + q_1 s + \cdots + q_n s^n \mid \boldsymbol{q} \in Q\}, \; q_n > 0 \qquad (4.5)$$

is robustly stable if and only if the following polynomials are stable:

$$
\begin{aligned}
p^{+-}(s) &= q_0^+ + q_1^- s + q_2^- s^2 + q_3^+ s^3 + q_4^+ s^4 + \ldots \\
p^{++}(s) &= q_0^+ + q_1^+ s + q_2^- s^2 + q_3^- s^3 + q_4^+ s^4 + \ldots \\
p^{-+}(s) &= q_0^- + q_1^+ s + q_2^+ s^2 + q_3^- s^3 + q_4^- s^4 + \ldots \\
p^{--}(s) &= q_0^- + q_1^- s + q_2^+ s^2 + q_3^+ s^3 + q_4^- s^4 + \ldots
\end{aligned}
\qquad (4.6)
$$

The polynomials given with (4.6) are called as Kharitonov polynomials.

Let the test set be given as follows

$$Q_T = \left\{ \boldsymbol{q}^{+-}, \boldsymbol{q}^{++}, \boldsymbol{q}^{-+}, \boldsymbol{q}^{--} \right\} \qquad (4.7)$$

where

$$
\begin{aligned}
\boldsymbol{q}^{+-} &:= \begin{bmatrix} q_0^+ & q_1^- & q_2^- & q_3^+ & q_4^+ & \ldots \end{bmatrix} \\
\boldsymbol{q}^{++} &:= \begin{bmatrix} q_0^+ & q_1^+ & q_2^- & q_3^- & q_4^+ & \ldots \end{bmatrix} \\
\boldsymbol{q}^{-+} &:= \begin{bmatrix} q_0^- & q_1^+ & q_2^+ & q_3^- & q_4^- & \ldots \end{bmatrix} \\
\boldsymbol{q}^{--} &:= \begin{bmatrix} q_0^- & q_1^- & q_2^+ & q_3^+ & q_4^- & \ldots \end{bmatrix}
\end{aligned}
\qquad (4.8)
$$

If the degree of uncertain polynomial is less than six, it is not required the check all of the Kharitonov polynomials as the following theorem states.

Theorem (Anderson, Jury, Mansour): For an interval polynomial given with (4.5) the testing sets are given as follows.

$$Q_T = \{\boldsymbol{q}^{+-}, \boldsymbol{q}^{++}, \boldsymbol{q}^{-+}, \boldsymbol{q}^{--}\} \quad \text{for } n > 5$$
$$Q_T = \{\boldsymbol{q}^{+-}, \boldsymbol{q}^{++}, \boldsymbol{q}^{-+}\} \quad \text{for } n = 5$$
$$Q_T = \{\boldsymbol{q}^{+-}, \boldsymbol{q}^{++}\} \quad \text{for } n = 4 \tag{4.9}$$
$$Q_T = \{\boldsymbol{q}^{+-}\} \quad \text{for } n = 3$$

For $n = 2$ and $n = 1$ the condition $q_i^- > 0$ is necessary and sufficient. The proof of theorem can be given with the help of the Mikhailov stability conditions.

4.1.2 Affine linear polynomials and edge theorem

Let us consider the following polynomial family with affine coefficients.

$$P(s, Q) = \left\{ p(s, \boldsymbol{q}) = p_0(s) + \sum_{i=1}^{n} q_i \, p_i(s) \mid q_i \in \left[q_i^-, q_i^+ \right] \right\} \tag{4.10}$$

Here, the coefficients depend on the uncertain parameter vector $\boldsymbol{q}$ linearly.

If all parameters q_i take their minimum or maximum value then the corresponding polynomial is named as a vertex polynomial. If only one of the parameters varies between its minimum and maximum value whereas the remaining parameters take their minimum or maximum value, then this polynomial family is called an edge polynomial.

An edge with the end points $p_b(s)$ and $p_c(s)$ can be expressed as follows.

$$P(s, Q) = \{(1 - q)p_b(s) + q \, p_c(s) \mid q \in [0, \ 1]\} \tag{4.11}$$

Stability of the affine linear polynomials is given by edge theorem [53].

Edge Theorem: The polynomial family given by (4.10) is robustly stable if and only if the edge polynomials are stable.

Consider an edge with the end points $p_b(s)$ and $p_c(s)$. In order to check the stability of an edge polynomial, the Bialas theorem can be used. The Bialas theorem states that an edge polynomial given by (4.11) is stable if and only if

- $p_b(s)$ is stable.

- $p_c(0) > 0$

- The matrix $\left(\boldsymbol{H}_{n-1}^b\right)^{-1}\boldsymbol{H}_{n-1}^c$ has no nonpositive real eigenvalues where $\boldsymbol{H}_i$ ($i = 1, 2, \ldots, n-1$) are Hurwitz matrices.

The edge theorem reduces the robustness analysis of an affine linear polynomial family to a finite set of one-dimensional tests. The number of vertices is given as 2^n for n uncertain parameters. From each vertex n edges start; therefore the number of edges is given with $n.2^n$ [6]. The following table gives the number of vertices and edges for different number of uncertain parameters.

Table 4.1 : The number of vertices and edges.

n	Vertices	Edges
1	2	1
2	4	4
3	8	12
4	16	32
5	32	80

It is seen from the table that the number of edges increases drastically as the number of uncertain parameter increases. Moreover, in order to check the stability of the edge polynomials, as mentioned earlier, some matrix operations (inversion, multiplication) should be performed. Due to the fact that the considered problem consists of unknown (controller) parameters, those calculations may be a difficult task to perform. Therefore, another method that is more efficient than Edge theorem may be found for the robust controller design if possible.

4.1.3 D-stability and Kharitonov regions

The robust stability of interval and affine linear polynomials is considered so far. In the stability problem, the open left half plane

$$\mathbb{C}^- = \{s \in \mathbb{C} \mid Re[s] < 0\} \tag{4.12}$$

is considered. If all roots of the polynomial are contained in the above region, the polynomial is said to be stable. However, in the control system design, stability itself

is not sufficient. Roots of the closed-loop system characteristic polynomial are desired to be located in special regions.

In the dominant pole placement, it is required two of the closed-loop poles are desired to be placed in a particular region in complex plane whereas the rest of poles are expected to be placed away from the dominant pole pair. For this reason, the other stability regions should be considered.

D-Stability: For a given polynomial family P and the stability region D in the complex plane, the polynomial family P is said to be D-stable if and only if the roots of every polynomial in P is contained in D.

Consider an uncertain interval polynomial given by (4.5) and a shifted region in s-plane given as follows.

$$\mathscr{D} = \{s \in \mathbb{C} \mid Re[s] < -\sigma, \sigma > 0\} \subset \mathbb{C}^- \tag{4.13}$$

The given problem can be converted to the stability problem through the polynomial $\tilde{p}(s, \boldsymbol{q}) = p(s - \sigma, \boldsymbol{q})$. If this transformation is performed, the resulting polynomial is no longer an interval polynomial but instead an affine linear polynomial. Thus, the edge theorem should be used to check the stability instead of the Kharitonov theorem. However, if the considered D-region in s-plane is a Kharitonov region, the D-stability of the vertex polynomials

$$V_P = \left\{ p(s, \boldsymbol{q}) : \ p(s, \boldsymbol{q}) = p_0(s) + \sum_{i=0}^{n} q_i s^i, \ q_i \in \left\{ q_i^-, \ q_i^+ \right\} \right\} \tag{4.14}$$

implies the D-stability of the whole polynomial family P [54]. Thus, it is possible to use vertex polynomials, which is a lot easier than the edge polynomials, in order to check the D-stability or to find the controller parameter that D-stabilizes the polynomial family.

Decreasing Phase Property: For a stability region $D \subset \mathbb{C}$ and the polynomial vector $\boldsymbol{p}$ in (4.4), $\boldsymbol{p}$ is said to hold the decreasing phase property if for an arbitrary n^{th} order D-stable polynomial $f(s)$ and $1 \leq i \leq m$, $\arg\left(\frac{p_i(s)}{f(s)}\right)$ is monotonously decreasing except at $p_i(s) = 0$ when s traverses on ∂D (i.e. boundary of the D-region) in the counter-clockwise direction [55].

Theorem (Kharitonov Region): The region D is a Kharitonov region with respect to $\boldsymbol{p}$ if $\boldsymbol{p}$ holds the decreasing phase property.

There are several Kharitonov regions in the literature which are presented as below. The details can be found in [55].

Any (rotated) open-half plane,

$$\mathscr{D}_1 = \left\{ s \in \mathbb{C}: \ s = \sigma + j\omega \ \mid \ a + b\sigma + c\omega < 0, \quad a,b,c \in \mathbb{R} \right\} \qquad (4.15)$$

is a Kharitonov region with respect to $\boldsymbol{p}$ in (4.4) for any $p_0(s)$ if $p_i(s)$, $i = 1,\ldots,m$ are anti-D-stable.

Any open circular region,

$$\mathscr{D}_2 = \left\{ s \in \mathbb{C}: \ s = c + \rho e^{j\theta}, \ \ 0 \le \rho < r, \ \ 0 \le \theta \le 2\pi, \ \ c \in \mathbb{C} \right\} \qquad (4.16)$$

is a Kharitonov region with respect to $\boldsymbol{p}$ in (4.4) for any $p_0(s)$ if $p_i(s)$, $i = 1,\ldots,m$ are anti-D-stable.

Any open parabolic region,

$$\mathscr{D}_3 = \left\{ s \in \mathbb{C}: \ s = \sigma + j\omega \ \mid \ (a\sigma)^2 - (b\omega)^2 > 1, \ \ \sigma < 0, \ \ a,b > 0 \right\} \qquad (4.17)$$

is also a Kharitonov region with respect to $\boldsymbol{p} = (p_0(s), 1, s, \ldots, s^n)$ for any $p_0(s)$ of nth order.

Theorem: Suppose that the regions D_1 and D_2 are Kharitonov regions, then $D_1 \cap D_2$ is also a Kharitonov region [54].

The above theorem is very important because the design specifications are generally more than one and this causes the dominant pole region to be intersection of different regions. If these regions satisfy the properties of Kharitonov region then their intersection becomes a Kharitonov region as well.

4.2 Robust Dominant Pole Placement for the Systems with Interval Characteristic Polynomial

For the systems with parametric uncertainty, the closed-loop poles are desired to be in a region instead of a point. Therefore, the selection of robust K_p parameter should be done such that the dominant poles are located in a desired region whereas the remaining poles are also desired to be located away from the dominant pole pair.

Here, it is desired to give the procedure of the robust PID controller design for interval type characteristic polynomials.

4.2.1 Procedures of the design method for interval polynomials

Consider a continuous-time PID controller and an uncertain plant given as follows.

$$G(s, \boldsymbol{q}) = \frac{N_G(s)}{D_G(s, \boldsymbol{q})} \tag{4.18}$$

Note that $D_G(s, \boldsymbol{q})$ is an interval type polynomial. First of all, it is required to determine the closed-loop performance specifications for the nominal system $G_0(s)$. After that the PID controller parameters K_i and K_d should be found in terms of the parameter K_p as proposed earlier via (2.18). Thus, it becomes possible to obtain the closed-loop system characteristic polynomial in terms of the uncertain parameters and the controller parameter K_p as follows.

$$P_c(s, \boldsymbol{q}, K_p) = s^n + f_{n-1}(\boldsymbol{q}, K_p)s^{n-1} + \cdots + f_0(\boldsymbol{q}, K_p) \tag{4.19}$$

The characteristic equation is clearly an interval polynomial due to the considered system class. Therefore, if a Kharitonov region is considered as the dominant pole region, it is possible to use vertex results on controller design.

Let the corresponding vertex polynomials be $P_{V_i}(s, K_p)$ then the following can be written.

$$P_{V_i}(s, K_p) = 1 + K_p \underbrace{\frac{N_i(s)}{D_i(s)}}_{\tilde{G}_i(s)} = 0 \tag{4.20}$$

It is now possible to substitute the boundaries of D-region so that the intersection points of Nyquist curve with real axis are found and the corresponding gain intervals can be calculated.

$$\tilde{G}_i(f(\omega)) = \frac{N_{iRe} + jN_{iIm}}{D_{iRe} + jD_{iIm}} \tag{4.21}$$

where

$$D_{iIm} = Im\left[D_i(f(\omega))\right], D_{iRe} = Re\left[D_i(f(\omega))\right]$$

$$N_{iIm} = Im\left[N_i(f(\omega))\right], N_{iRe} = Re\left[N_i(f(\omega))\right]$$

If (4.21) is rearranged,

$$\tilde{G}_i(f(\omega)) = \frac{(N_{iRe}D_{iRe} + N_{iIm}D_{iIm}) + j(N_{iIm}D_{iRe} - N_{iRe}D_{iIm})}{D_{iRe}^2 + D_{iIm}^2} \tag{4.22}$$

126

and by defining

$$X_i(\omega) = N_{iRe}D_{iRe} + N_{iIm}D_{iIm}$$

$$Y_i(\omega) = N_{iIm}D_{iRe} - N_{iRe}D_{iIm}$$

$$Z_i(\omega) = D_{iRe}^2 + D_{iIm}^2$$

it is possible to write the following equality,

$$\tilde{G}_i(f(\omega)) = \frac{X_i(\omega)}{Z_i(\omega)} + j\frac{Y_i(\omega)}{Z_i(\omega)} \tag{4.23}$$

Here, the critical frequencies for every vertex polynomials (ω_{ij}^*), which cause the roots to cross the boundary (∂D) in s-plane, can be calculating with the help of following equation.

$$\frac{Y_i(\omega)}{Z_i(\omega)} = 0 \tag{4.24}$$

The intersection points (x_{ij}) of Nyquist curve and real axis can then be found with the help of following expression ($\omega^* = 0$ and $\omega^* = \infty$ are also added to the critical frequencies as necessary).

$$x_{ij} = \frac{X_i(\omega_{ij}^*)}{Z_i(\omega_{ij}^*)} \tag{4.25}$$

After that all gain intervals, in which the number of poles (u) outside of the considered D-region is the same, are calculated with the help of generalized Nyquist theorem as follows

$$\mathscr{K}_{ij} \in \left(-\frac{1}{x_{ij}}, -\frac{1}{x_{i(j+1)}} \right), \quad j = 1, 2, \ldots \tag{4.26}$$

such that $x_{ij} < x_{i(j+1)}$. For each vertex polynomials, the final interval for a desired u value is found as follows,

$$\overline{K}_i \in \bigcup \mathscr{K}_{ij} \tag{4.27}$$

The interval of the controller parameter (K_p) is found as the union of all gain intervals calculated for each vertex polynomials.

$$K_p \in \bigcap_{i=1}^{2^m} \overline{K}_i \tag{4.28}$$

where m is the number of uncertain parameters. If there are more than one boundary, then this procedure is repeated for each boundary function $f(\omega)$ and the intersection of the all obtained K_p sets is found. This gives the final feasible interval of the PID controller parameter K_p.

4.2.2 Case studies for interval polynomials

Example 4.1:

Consider an uncertain system given as follows.

$$G(s) = \frac{1}{s^3 + q_2 s^2 + q_1 s + q_0}$$

where $q_0 \in [2,\ 4]$, $q_1 \in [6,\ 8]$ and $q_2 \in [4.6,\ 5.4]$. The open-loop pole spread of the above system in s-plane is illustrated in Figure 4.1.
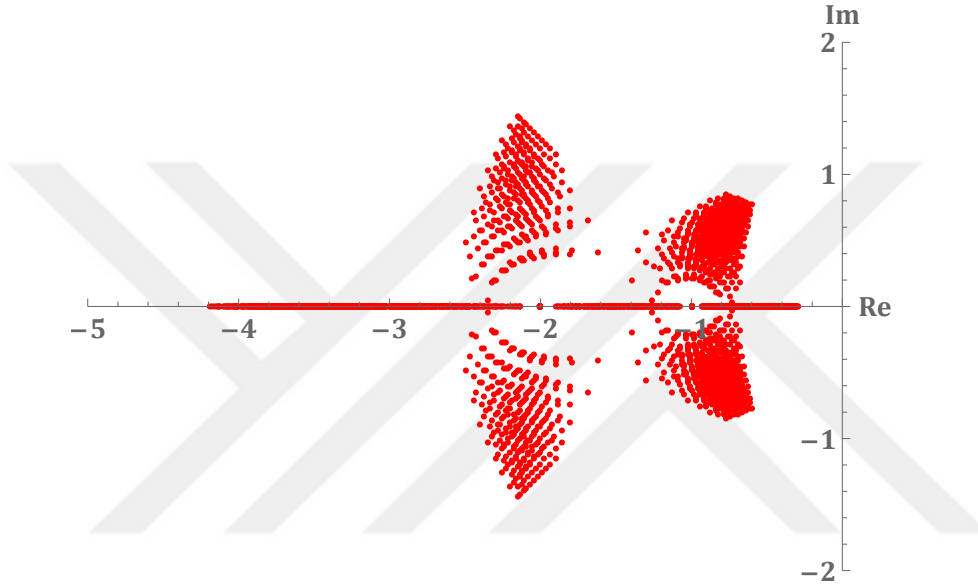
Figure 4.1 : Open-loop pole spread of the uncertain system (Example 4.1).

In the closed-loop, 8 seconds of settling time and 5% overshoot is desired from the nominal system. Furthermore, the closed-loop dominant poles are expected to be in the *D*-region given as follows

$$\mathscr{D}_1 = \{s \in \mathbb{C} \mid Re[s] < -\sigma_1,\quad \sigma_1 > 0\}$$
$$\mathscr{D}_2 = \{s \in \mathbb{C} \mid Re[s] > -\sigma_2,\quad \sigma_2 > 0\}$$
$$\mathscr{D} = \mathscr{D}_1 \cap \mathscr{D}_2$$

where $\sigma_1 = 0.35$, $\sigma_2 = 0.65$ under all possible perturbations. It can be said that the given rectangular region (Figure 4.2) is a Kharitonov region due to the fact that it is the intersection of the Kharitonov regions as given above. The remaining poles are also desired to be 2.5 times away from the dominant pole pair in the worst case.

128
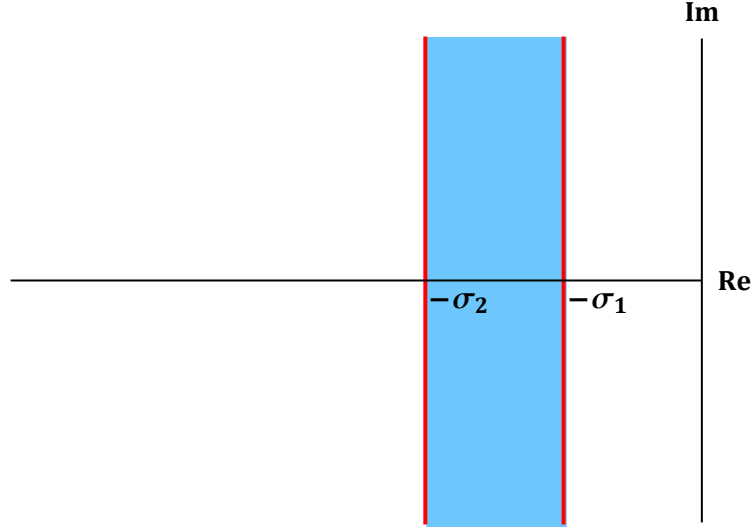
Figure 4.2 : The desired *D*-Region for dominant poles in s-plane (Example 4.1).

The corresponding vertex polynomials are found as below.

$$P_{V_1}(s, K_p) = s^4 + 4.6s^3 + (K_p + 4.425)s^2 + (K_p + 2)s + (0.525K_p + 0.4726)$$

$$P_{V_2}(s, K_p) = s^4 + 4.6s^3 + (K_p + 6.425)s^2 + (K_p + 2)s + (0.525K_p + 0.4726)$$

$$P_{V_3}(s, K_p) = s^4 + 4.6s^3 + (K_p + 4.425)s^2 + (K_p + 4)s + (0.525K_p + 0.4726)$$

$$P_{V_4}(s, K_p) = s^4 + 4.6s^3 + (K_p + 6.425)s^2 + (K_p + 4)s + (0.525K_p + 0.4726)$$

$$P_{V_5}(s, K_p) = s^4 + 5.4s^3 + (K_p + 4.425)s^2 + (K_p + 2)s + (0.525K_p + 0.4726)$$

$$P_{V_6}(s, K_p) = s^4 + 5.4s^3 + (K_p + 6.425)s^2 + (K_p + 2)s + (0.525K_p + 0.4726)$$

$$P_{V_7}(s, K_p) = s^4 + 5.4s^3 + (K_p + 4.425)s^2 + (K_p + 4)s + (0.525K_p + 0.4726)$$

$$P_{V_8}(s, K_p) = s^4 + 5.4s^3 + (K_p + 6.425)s^2 + (K_p + 4)s + (0.525K_p + 0.4726)$$

The critical frequencies (ω_i^*), intersection points (x_i), anti-*D*-stable root counts (u_i) and corresponding gain intervals should be calculated for each vertex polynomial given above with the help of the explained procedure. For instance, Table 4.2, 4.3 and 4.4 show ω_i^*, x_i, u and $\mathcal{K}_i$ of the first vertex polynomial for the boundary of $s = -\sigma_1$, $s = -\sigma_2$ and $s = -\sigma_3$, respectively. The gain intervals are then obtained as below.

$$\overline{K}_1 \in (2.3989, \infty)$$

$$\overline{K}_2 \in (0.143, \infty)$$

$$\overline{K}_3 \in (2.5042, \infty)$$

The final K_p interval for the first vertex polynomial is then found as follows.

$$K_{p1} \in \bigcap_{j=1}^{3} \overline{K}_j \in (2.5042, \infty)$$

129

Table 4.2 : Gain intervals of the first vertex polynomial for $s = -\sigma_1$.

ω_i^*	x_i	u_i	$\mathcal{K}_{1i}$
0	2.2458	1	$-0.5216 > \mathcal{K}_{11} > -\infty$
0.28771	1.9173	3	$-0.4453 > \mathcal{K}_{12} > -0.5216$
0.59713	-0.4169	2	$2.3989 > \mathcal{K}_{13} > -0.4453$
∞	0	**0**	$\infty > \mathcal{K}_{14} > 2.3989$

Table 4.3 : Gain intervals of the first vertex polynomial for $s = -\sigma_2$.

ω_i^*	x_i	u_i	$\mathcal{K}_{1i}$
0	-6.99	3	$0.143 > \mathcal{K}_{11} > -\infty$
∞	0	**2**	$\infty > \mathcal{K}_{12} > 0.143$

Table 4.4 : Gain intervals of the first vertex polynomial for $s = -\sigma_3$.

ω_i^*	x_i	u_i	$\mathcal{K}_{1i}$
0	-0.3993	3	$2.5042 > \mathcal{K}_{11} > -\infty$
∞	0	**2**	$\infty > \mathcal{K}_{12} > 2.5042$

If the same calculations are done for each vertex polynomials, then the resulting K_p interval is found as below.

$$K_p \in \bigcap_{i=1}^{8} K_{pi} \in (11.0857, \infty)$$

If $K_p = 11.5$ is chosen, the PID controller is obtained as follows. The closed-loop pole spread with designed robust PID controller is also given in Figure 4.3.

$$F(s) = \frac{9.925s^2 + 11.5s + 6.509}{s}$$

It is possible to implement the obtained robust PID controller in PI-PD structure to eliminate adverse effects of the controller zeros. For $K_{pi} = 2.5$ the closed-loop zero is located at $s = -2.604$ which is away from the dominant poles region. In this case, designed PI-PD controllers are given as follows.

$$F_{pi}(s) = 2.5 + \frac{6.509}{s}, \quad F_{pd}(s) = 9 + 9.925s$$
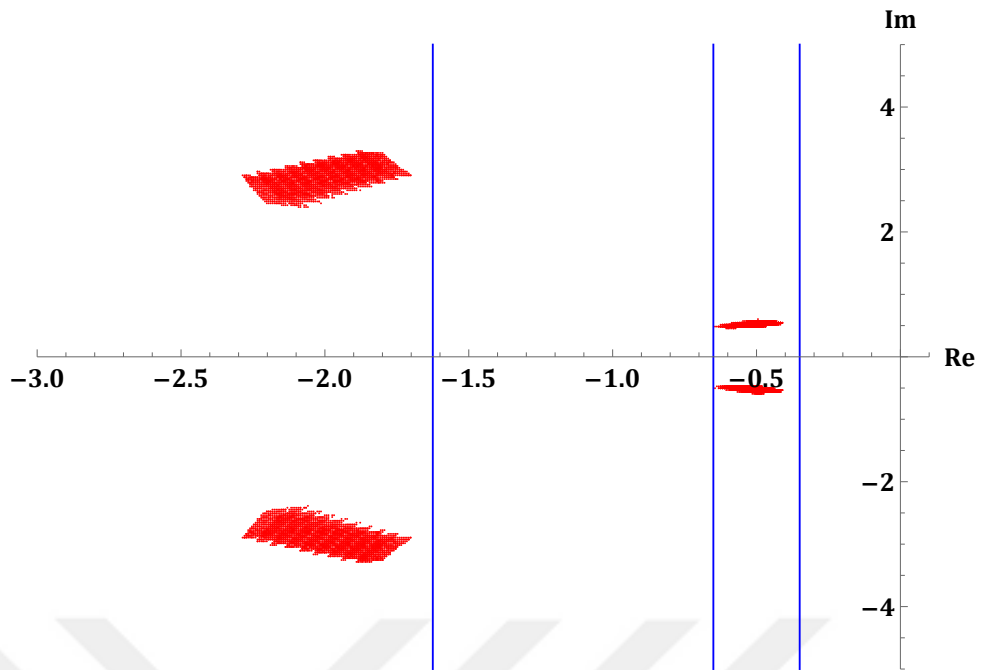
Figure 4.3 : Closed-loop pole spread of the system with robust PID controller (Example 4.1).

The closed-loop transient response with the robust PI-PD controller given above is depicted in Figure 4.4 under all possible perturbations. Disturbance rejection can also be seen from the figure since an input disturbance $D(s) = -\frac{1}{s}$ is applied at $t = 20$ seconds.
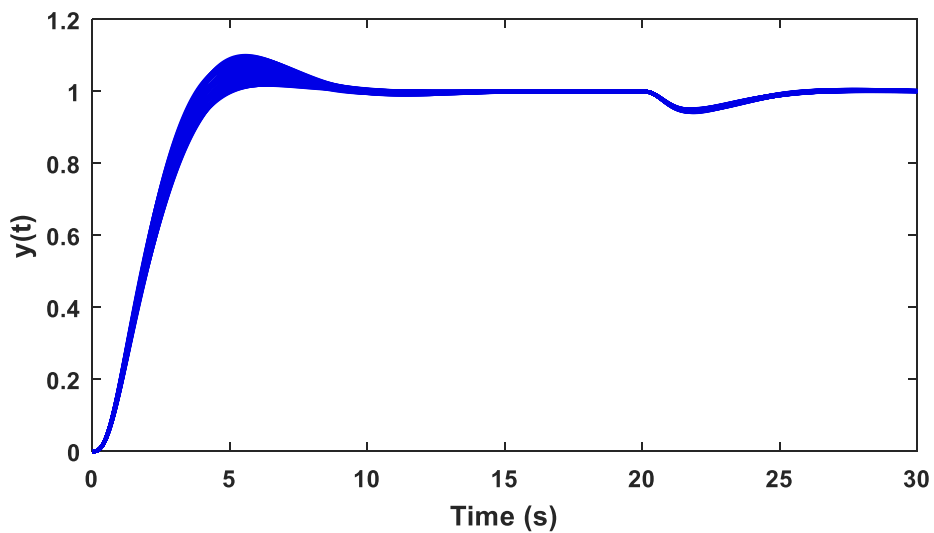
Figure 4.4 : Closed-loop transient response under all possible perturbations (Example 4.1).

For a chosen controller parameter, the perturbation limits of the uncertain parameters can also be found one by one. This is done by choosing the related uncertain parameter as a free parameter and calculating its minimum and maximum limits such that the robustness of the PID controller is not affected with the help of vertex polynomials constructed by the remaining uncertain parameters.

For this particular example and for the designed PID controller, the minimum and maximum limits of the uncertain parameters are found as below.

$$q_0 \in [0.5813,\ 4.1073]$$
$$q_1 \in [5.9025,\ 10.3578]$$
$$q_2 \in [4.438,\ 5.5412]$$

Therefore, as long as only one of the uncertain parameters varies in limits, the robustness of the closed-loop system in terms of the dominant pole placement will not be affected.

Example 4.2:

Consider an uncertain system given with the following transfer function.

$$G(s) = \frac{1}{s^4 + 10s^3 + q_2 s^2 + q_1 s + q_0}$$

where $q_0 \in [38, 42]$, $q_1 \in [54, 58]$ and $q_2 \in [36, 40]$. The open-loop pole spread of the system in s-plane is given in Figure 4.5.

For the nominal system, it is desired that the transient response has 8 seconds of settling time with 5% overshoot in the closed-loop. Furthermore, the complex dominant poles are expected to be in the D-region given below with $\sigma = 0.55$, $\omega = 0.55$ and $r = 0.12$ under all possible perturbations.

$$\mathscr{D}_c = \{ s \in \mathbb{C} : |s - c| < r,\ c = \sigma + j\omega,\ \omega > r,\ \sigma \in \mathbb{R} \}$$

$$\mathscr{D} = \mathscr{D}_c \cup \overline{\mathscr{D}_c}$$

Note that it is possible to show that the defined disc region is a Kharitonov region with the help of following theorem.

Theorem: The disc region given above is a Kharitonov region with respect to

$$\boldsymbol{p} = (p_0(s), 1, s, \dots, s^n)$$

132
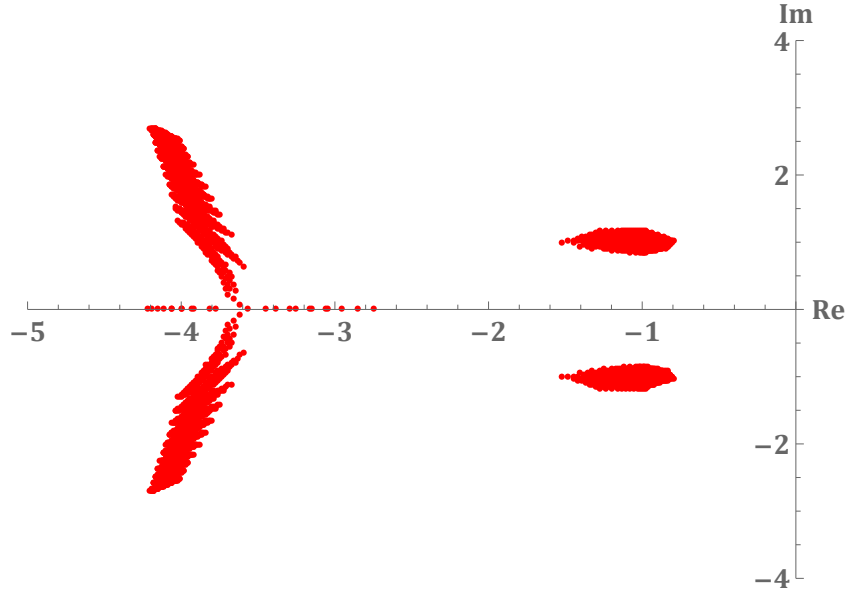
Figure 4.5 : Open-loop pole spread of the uncertain system (Example 4.2).

for any $p_0(s)$ if the condition

$$\frac{r}{2(\omega - r)} + \frac{2r}{r + \sqrt{\sigma^2 + \omega^2}} < \frac{1}{2}$$

holds [56].

Proof: If the aforementioned region is a Kharitonov region, the decreasing phase property should be satisfied. Let $f(s)$ be any n^{th} order D-stable polynomial. From the decreasing phase theorem, it is enough to show that $\arg\left(p_i(s)/f(s)\right)$ for $1 \le i \le m$ is monotonously decreasing when s traverses on ∂D.

Let also $f(s) = (s - s_1)(s - \overline{s_1})$ which is a D-stable polynomial. In order to verify that the $\arg\left(p_i(s)\right) - \arg\left(f(s)\right)$ is monotonously decreasing, it is sufficient to show that the following inequality holds according to Figure 4.6.

$$2 \underbrace{\frac{d\phi_3}{d\theta}}_{\text{max}} < (\underbrace{\frac{d\phi_1}{d\theta} + \frac{d\phi_2}{d\theta}}_{\text{min}})$$

For the ϕ_1 angle, since the derivative is always positive, it is required to find the minimum phase increase. It is also clear from the Figure that the minimum phase increase is found to be on the boundaries of D as below.

$$\min\left(\frac{d\phi_1}{d\theta}\right) = \frac{1}{2}$$

133
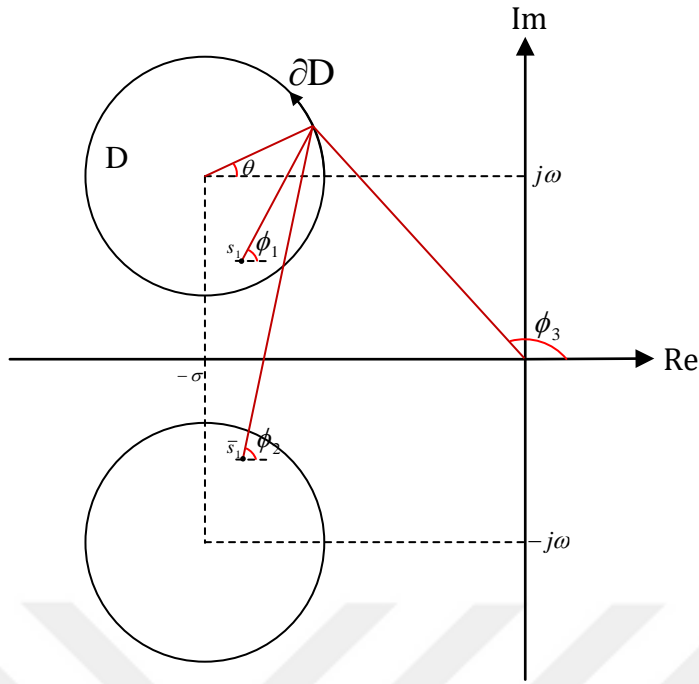
Figure 4.6 : Decreasing phase condition on ∂D (Example 4.2).
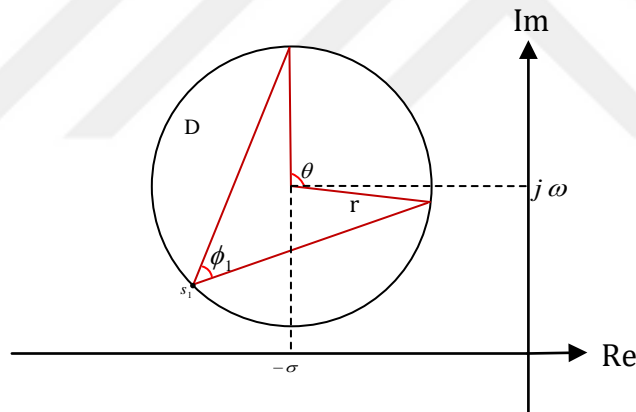
Figure 4.7 : Minimum phase increase of ϕ_1 (Example 4.2).

For the ϕ_2 angle, the derivative can take negative values, thus, the maximum phase decrease should be found. Figure 4.8 shows the point where the maximum phase decrease occurs.

$$-\max\left(\frac{d\phi_2}{d\theta}\right) = \frac{r}{2(\omega - r)}$$

Finally, for the ϕ_3 angle, the maximum of the derivative should be found. It is seen from the Figure 4.9 that the maximum phase increase is calculated as follows.

$$\max\left(\frac{d\phi_3}{d\theta}\right) = \frac{r}{r + |\sigma + j\omega|}$$

134
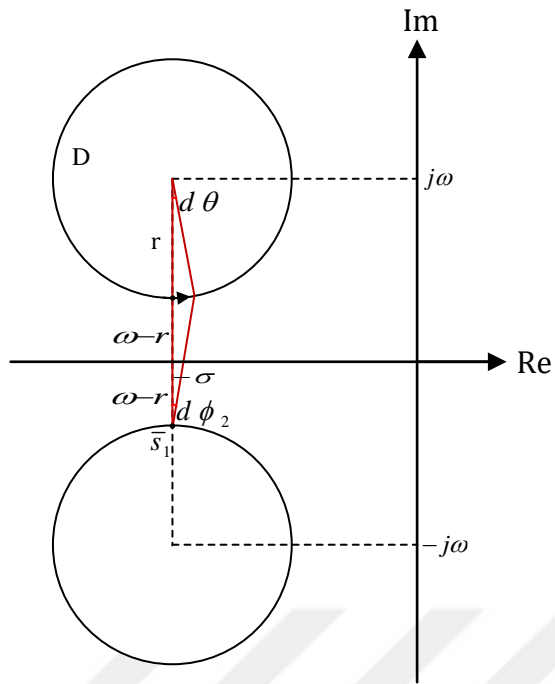
Figure 4.8 : Maximum phase decrease of ϕ_2 (Example 4.2).
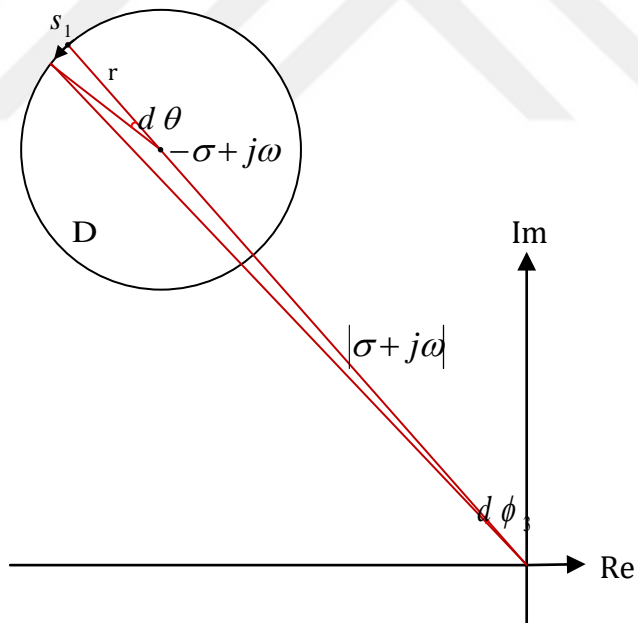
Figure 4.9 : Minimum phase increase of ϕ_3 (Example 4.2).

As a result,

$$2\frac{r}{r+|\sigma+j\omega|} < \frac{1}{2} - \frac{r}{2(\omega-r)}$$

should be satisfied.

135

In the example, the dominant poles should also satisfy less than 8% overshoot even in the worst case. Finally, the remaining (non-dominant) poles are desired to be on the left side of the line $\sigma_0 = -1.5$. The final desired dominant pole region is depicted in Figure 4.10.
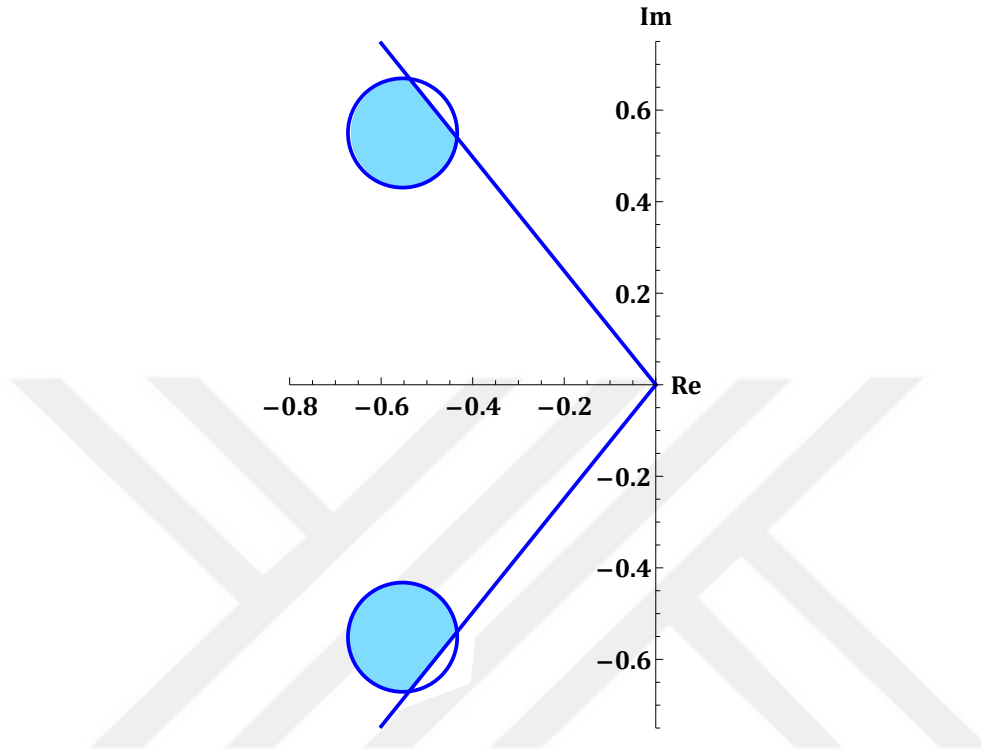
Figure 4.10 : Desired dominant pole region in s-plane (Example 4.2).

The PID controller parameters K_i and K_d can be calculated for the nominal system in terms of the parameter K_p as follows.

$$K_i = 13.15 + 0.525K_p$$

$$K_d = 2.252 + K_p$$

The closed-loop system characteristic polynomial with calculated PID parameters is given as follows.

$$P_c(s, \boldsymbol{q}, K_p) = s^5 + 10s^4 + q_2s^3 + (q_1 + 2.252 + K_p)s^2$$
$$+ (q_0 + K_p)s + (13.15 + 0.525K_p)$$

Here, it is seen that there are three different boundary functions which are given as

$$f_1(\omega) = (-0.55 + 0.55j) + 0.12e^{j\omega}$$

$$f_2(\omega) = -1.5 + j\omega$$

$$f_3(\omega) = \frac{-\omega}{1.2438} + j\omega$$

136

The proposed design procedure should be repeated for each desired boundary functions, respectively.

Let us calculate the vertex polynomials as follows.

$$P_{V_1}(s) = s^5 + 10s^4 + 36s^3 + (56.252 + K_p)s^2 + (38 + K_p)s + (13.15 + 0.525K_p)$$

$$P_{V_2}(s) = s^5 + 10s^4 + 40s^3 + (56.252 + K_p)s^2 + (38 + K_p)s + (13.15 + 0.525K_p)$$

$$P_{V_3}(s) = s^5 + 10s^4 + 36s^3 + (60.252 + K_p)s^2 + (38 + K_p)s + (13.15 + 0.525K_p)$$

$$P_{V_4}(s) = s^5 + 10s^4 + 40s^3 + (60.252 + K_p)s^2 + (38 + K_p)s + (13.15 + 0.525K_p)$$

$$P_{V_5}(s) = s^5 + 10s^4 + 36s^3 + (56.252 + K_p)s^2 + (42 + K_p)s + (13.15 + 0.525K_p)$$

$$P_{V_6}(s) = s^5 + 10s^4 + 40s^3 + (56.252 + K_p)s^2 + (42 + K_p)s + (13.15 + 0.525K_p)$$

$$P_{V_7}(s) = s^5 + 10s^4 + 36s^3 + (60.252 + K_p)s^2 + (42 + K_p)s + (13.15 + 0.525K_p)$$

$$P_{V_8}(s) = s^5 + 10s^4 + 40s^3 + (60.252 + K_p)s^2 + (42 + K_p)s + (13.15 + 0.525K_p)$$

It is now possible to follow the given design procedure in the previous section. If the vertex polynomials are re-written as in (4.20) and the boundary functions are substituted, then the intersection points of Nyquist curve and real axis can be found. By inspecting the obtained gain intervals, it is possible to find the feasible region in which the number of poles (u) outside of the desired region can be calculated. If the required calculations are done, the feasible gain intervals are given as in Table 4.5.

Table 4.5 : Invariant gain intervals and the anti-D-stable root counts.

	Feasible Interval	Anti-D-Stable Roots
$f_1(\omega)$	$\mathscr{K} < -36.977 \cup 19.126 < \mathscr{K}$	$u = 0$
$f_2(\omega)$	$11.962 < \mathscr{K} < 21.798$	$u = 2$
$f_3(\omega)$	$\mathscr{K} < -18.484 \cup 16.686 < \mathscr{K}$	$u = 0$

The final interval is then found as $K_p \in (19.126, 21.798)$ in which all boundary conditions are satisfied. If the K_p parameter is chosen from the obtained feasible interval, the dominant poles are located in the desired D-region, whereas, the remaining poles are located in the non-dominant region under parametric uncertainties. For $K_p = 20$, the PID controller is given as below.

$$F(s) = 20 + \frac{23.65}{s} + 22.25s$$

137

Figure 4.11 shows the closed-loop pole spread with robust PID controller and Figure 4.12 shows a closer look to the dominant pole region.
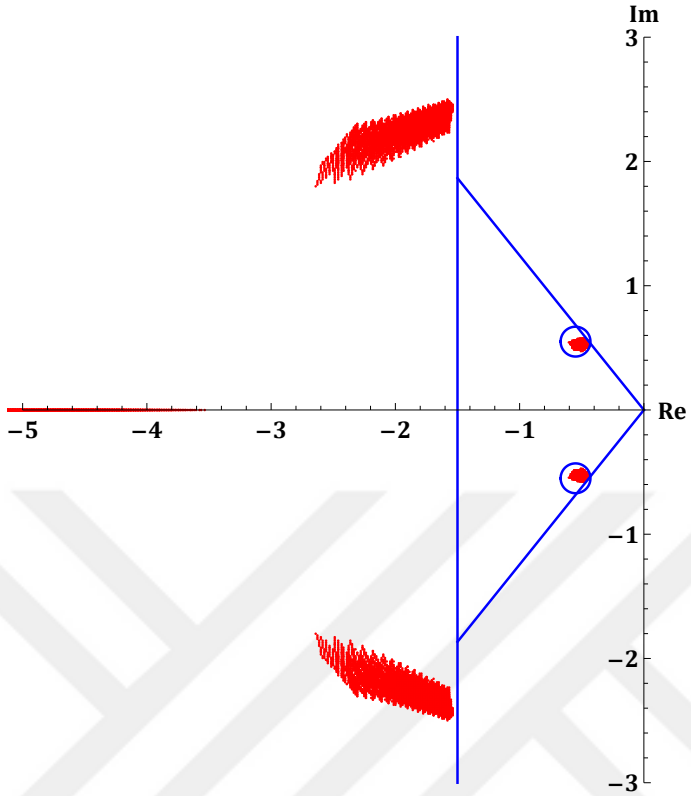
Figure 4.11 : The closed-loop pole spread with designed PID controller (Example 4.2).
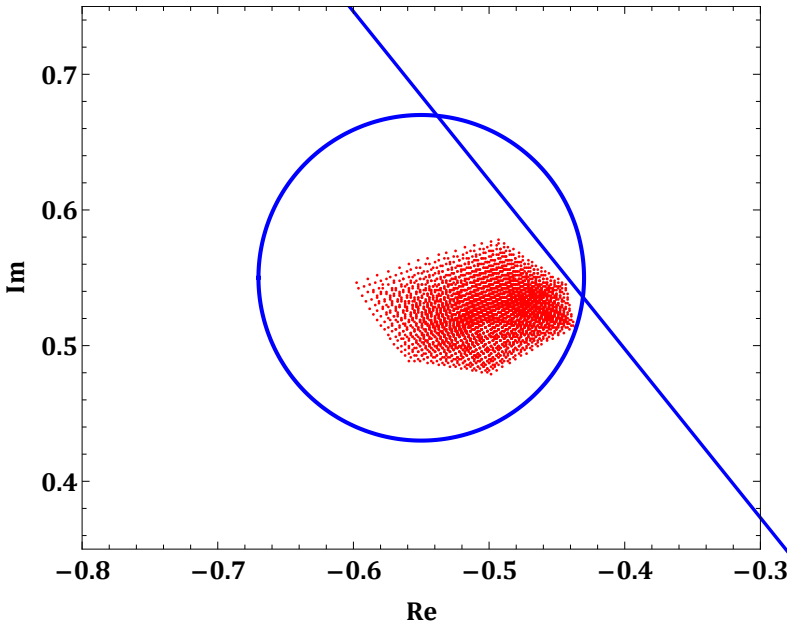
Figure 4.12 : A closer look to the pole spread in dominant region (Example 4.2).

In order to eliminate the adverse effect of the PID controller zeros as mentioned earlier, the PID controller should be implemented in PI-PD structure. Thus, the robust dominant pole placement can be performed successfully. If the PI-PD structure is used, then by choosing the parameter $K_{pi} = 3$, the controller zero is placed to the point of $s = -7.88$ in s-plane. For this case, the PI and PD controllers are given as follows.

$$F_{pi}(s) = 3 + \frac{23.65}{s}, \ F_{pd}(s) = 17 + 22.25s$$

Figure 4.13 shows the step response of the closed-loop system with designed robust PI-PD controller. Disturbance rejection performance is also tested by applying an input disturbance $D(s) = -4/s$ at the time of $t = 25$ during the simulation study.
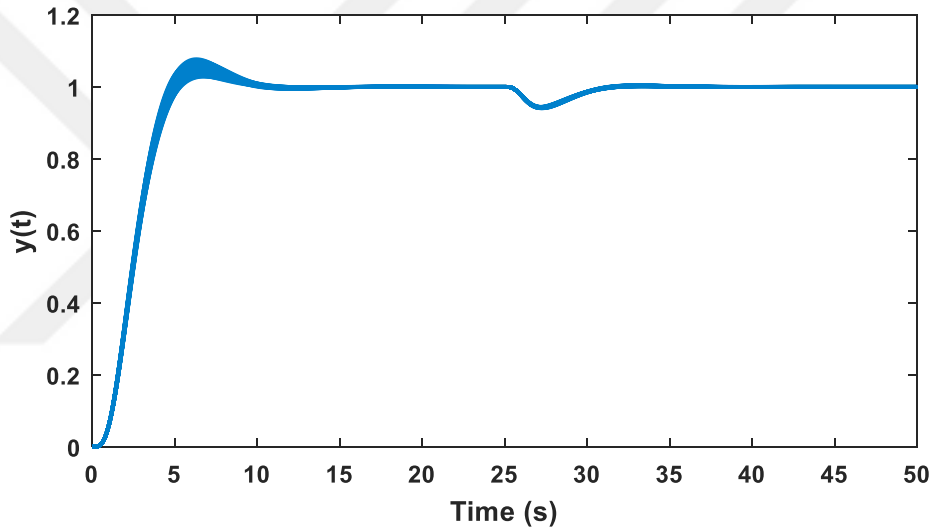
Figure 4.13 : Closed-loop transient response under all possible perturbations (Example 4.2).

It can be concluded that the robust dominant pole placement problem for the systems which have interval type characteristic polynomials with PID controller is solved with the help of proposed method. The given procedure is straightforward and can easily be followed by any software that provides a symbolic algebra environment. It is shown that with the resulting robust controller, the dominant pole pair is assigned to the desired region and the remaining poles are located away from the dominant pole pair under all possible perturbations. Moreover, the desired closed-loop performance specifications are also met as accurate as possible by using the PI-PD structure.

4.3 Robust Dominant Pole Placement for the Systems with Affine-Linear Characteristic Polynomial

The solution of the robust pole placement problem for affine linear characteristic polynomials is similar to the interval case; however, it is required to use the edge polynomials instead of the vertex polynomials. In this case, the characteristic polynomial consists of one more parameter (λ) in addition to the uncertain parameters and the controller parameter K_p.

4.3.1 Procedures of the design method for affine-linear polynomials

Consider a PID controller and an uncertain plant given as follows.

$$G(s,\boldsymbol{q}) = \frac{N_G(s,\boldsymbol{q})}{D_G(s,\boldsymbol{q})} \tag{4.29}$$

Here $N_G(s,\boldsymbol{q})$ and $D_G(s,\boldsymbol{q})$ are interval or affine linear type polynomials. Since the vertex results do not guarantee the robustness of controller due to the considered system class, the edge polynomials should be taken into account. Let the edge polynomials constructed from the closed-loop system characteristic polynomial be expressed as follows.

$$P_{E_i}(s,K_p) = (1-\lambda)P_{V_j}(s,K_p) + \lambda P_{V_k}(s,K_p) \tag{4.30}$$

where $P_{V_j}(s,K_p)$ and $P_{V_k}(s,K_p)$ are two related vertex polynomials. It is required to satisfy the two roots of the characteristic polynomial to be in a specified D-region and the remaining roots to be away from this pole pair under all possible parameter changes.

Let us re-write the edge polynomials as follows.

$$P_{E_i}(s,K_p) = 1 + K_p \underbrace{\frac{N_i(s,\lambda)}{D_i(s,\lambda)}}_{\tilde{G}_i(s,\lambda)} = 0 \tag{4.31}$$

It is again possible to use the generalized Nyquist theorem as given in previous subsection. Thus, the critical frequencies (ω_{ij}^*), which cause the roots to cross the boundary (∂D) in s-plane, are calculated using the same formula proposed earlier.

$$Im\left[\tilde{G}_i(f(\omega),\lambda)\right] = \frac{Y_i(\omega,\lambda)}{Z_i(\omega,\lambda)} = 0 \tag{4.32}$$

The roots of the equation given above should be found such that $\omega_{ij}^*(\lambda) \in \mathbb{R}$ in the interval of $0 \le \lambda_{ij}^- \le \lambda \le \lambda_{ij}^+ \le 1$. The intersection points $(x_{ij}(\lambda))$ of Nyquist curve and real axis is then be found using the following equality ($\omega^* = 0$ and $\omega^* = \infty$ are also added to the critical frequencies as necessary).

$$x_{ij}(\lambda) = Re\left[\tilde{G}_i(f(\omega_{ij}^*), \lambda)\right] = \frac{X_i(\omega_{ij}^*, \lambda)}{Z_i(\omega_{ij}^*, \lambda)} \tag{4.33}$$

After that all gain intervals, in which anti-D-stable root count (u) is the same, are again calculated with the help of the generalized Nyquist theorem.

$$\mathcal{K}_{ij}(\lambda) \in \left(-\frac{1}{x_{ij}(\lambda)}, -\frac{1}{x_{i(j+1)}(\lambda)}\right), \quad j = 1, 2, \ldots \tag{4.34}$$

However, unlike the constant coefficient polynomials, the intersection points $(x_{ij}(\lambda))$ of Nyquist curve and real axis vary with the parameter $\lambda \in [0, 1]$; therefore, the gain intervals $(\mathcal{K}_{ij})$ also vary depending on the parameter λ. In order to guarantee the robust dominant pole placement, it is required to find the *invariant gain intervals* (i.e. the anti-D-stable root count does not change with the parameter λ).

The upper and lower limits of the varying gain intervals for each obtained $\omega_{ij}^*(\lambda)$ are calculated by finding the minimum and maximum of the expression $\frac{-1}{x_{ij}(\lambda)}$ over the parameter λ as follows.

$$\mathcal{K}_{ij_{min}} = \min_{\lambda_{ij}^- \le \lambda \le \lambda_{ij}^+}\left(\frac{-1}{x_{ij}(\lambda)}\right) = \min_{\lambda_{ij}^- \le \lambda \le \lambda_{ij}^+}\left(\frac{-1}{Re\left[\tilde{G}_i(f(\omega_{ij}^*), \lambda)\right]}\right) \tag{4.35}$$

$$\mathcal{K}_{ij_{max}} = \max_{\lambda_{ij}^- \le \lambda \le \lambda_{ij}^+}\left(\frac{-1}{x_{ij}(\lambda)}\right) = \max_{\lambda_{ij}^- \le \lambda \le \lambda_{ij}^+}\left(\frac{-1}{Re\left[\tilde{G}_i(f(\omega_{ij}^*), \lambda)\right]}\right) \tag{4.36}$$

The varying gain intervals for an edge polynomial is then found as the union of the obtained intervals for each $\omega_{ij}^*(\lambda)$. Thus, the invariant gain intervals are then found as follows.

$$\tilde{K}_i \in (-\infty, +\infty) \setminus \left(\bigcup_{j=1}\left(\mathcal{K}_{ij_{min}}, \mathcal{K}_{ij_{max}}\right)\right) \tag{4.37}$$

The next step is to find the feasible interval (i.e. the anti-D-stable root count is found to be as desired) such that $(K_{p_i} \subset \tilde{K}_i)$ by calculating the roots of the considered edge polynomial for each invariant gain interval by taking an arbitrary point.

As a final step, if these calculations are performed for every edge polynomial (total of $m.2^{m-1}$), the interval of parameter K_p is found as below.

$$K_p \in \bigcap_{i=1}^{m.2^{m-1}} K_{pi} \tag{4.38}$$

Note that if there are more than one desired boundary, then this procedure is repeated for each boundary function $f(\omega)$ and the intersection of the all obtained K_p sets is found. It gives the final interval of the PID controller parameter K_p.

4.3.2 Case studies for affine-linear polynomials

Example 4.3:

Firstly, let us start with a simple example (only one uncertain parameter) to demonstrate the proposed method. Consider the closed-loop control system of a railway vehicle given in Figure 4.14.
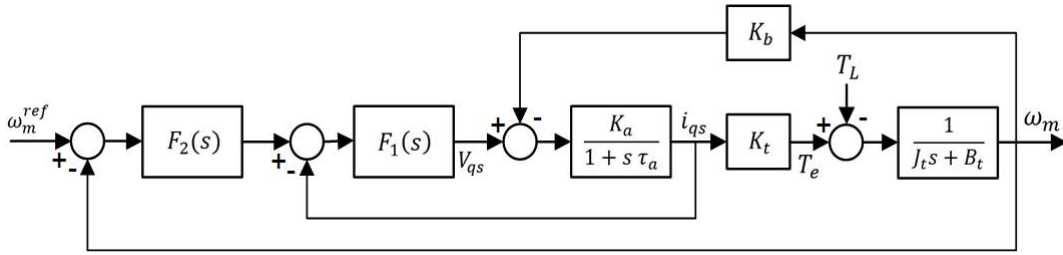
Figure 4.14 : A closed-loop control system (Example 4.3).

In the block diagram, $F_2(s)$ is the PID controller, which is aimed to be designed via robust dominant pole placement. The transfer function of the inner block is given as follows.

$$G(s) = \frac{3914(s+561.4)}{Js^3 + (1457.4J+0.057)s^2 + (778057J+18450)s+44022.5}$$

It is known that the parameter J changes (due to the change of the vehicle mass) in the interval of $[133.6, 204.7]$ with nominal value of 169.15 $kg.m^2$. In the closed-loop loop, it is desired the vehicle speed to have settling time between 13 and 17 seconds (15 seconds nominal) and overshoot at most 2% (1% nominal).

The PID controller parameters (K_d and K_i) which assign the dominant poles to the corresponding locations are found as follows for the nominal system ($G_0(s)$) via

142

dominant pole placement as follows.

$$K_i = 0.0038 + 0.1954K_p$$

$$K_d = -59.863 + 1.875K_p$$

The closed-loop characteristic polynomial with the obtained controller parameters is then found as below.

$$P_c(s, J, K_p) = Js^4 + (7339K_p + 1457.4J - 234311)s^3 + (4123890K_p + 778038J$$
$$- 131519000)s^2 + (2198080K_p + 44036.3)s + 429321K_p + 8357.2$$

It is seen that the given characteristic polynomial is an affine linear polynomial with only one uncertain parameter. Therefore, there is only one edge polynomial, which is given below, to be considered.

$$P_E(s, K_p) = (1 - \lambda)P_{V_1}(s, K_p) + \lambda P_{V_2}(s, K_p)$$

where

$$P_{V_1}(s, K_p) = 133.6s^4 + (7339K_p - 39599.7)s^3 + (4123890K_p - 27572600)s^2$$
$$+ (2198080K_p + 44036.3)s + 429321K_p + 8357.2$$

and

$$P_{V_2}(s, K_p) = 204.7s^4 + (7339K_p + 64023.1)s^3 + (4123890K_p + 27746000)s^2$$
$$+ (2198080K_p + 44036.3)s + 429321K_p + 8357.2$$

It is now possible to construct $\overline{G_i}(f(\omega), \lambda)$ with the help of the boundaries of desired D-region which is illustrated in Figure 4.15.

In this example, 3 boundaries which are $\sigma = -0.235$, $\sigma = -0.308$ and $\sigma = -\omega/0.8031$ should be considered for the dominant pole region. There is one more boundary should be considered such that the remaining poles are located 5 times away from the dominant poles in the worst case (i.e. $\sigma = -1.54$). Therefore, the explained design process should be repeated for all boundaries ($s_1 = j\omega - 0.235$, $s_2 = j\omega - 0.308$, $s_3 = j\omega - \frac{\omega}{0.8031}$ and $s_4 = j\omega - 1.54$) and the intersection of the all obtained K_p intervals should be considered (unless it is an empty set).

If the design process is carried out by a computer software (such as Mathematica) which allows to perform symbolic calculations, the following feasible gain intervals
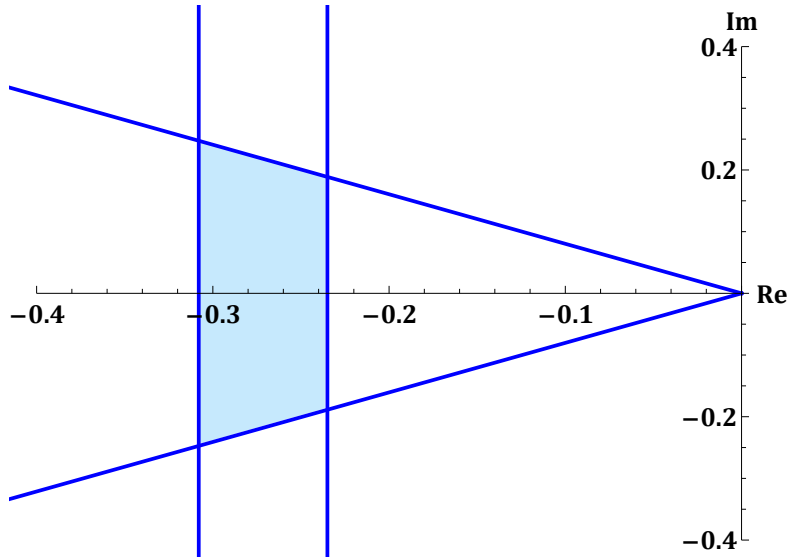
Figure 4.15 : Desired dominant pole region in s-plane (Example 4.3).

are found for the given boundaries, respectively.

$$K_p^1 \in (49.801, \infty)$$

$$K_p^2 \in (50.006, \infty)$$

$$K_p^3 \in (54.779, \infty)$$

$$K_p^4 \in (9.607, \infty)$$

One of the invariant gain intervals and feasible interval which is related to the boundary $\sigma = -0.235$ is depicted in Figure 4.16 as an example.
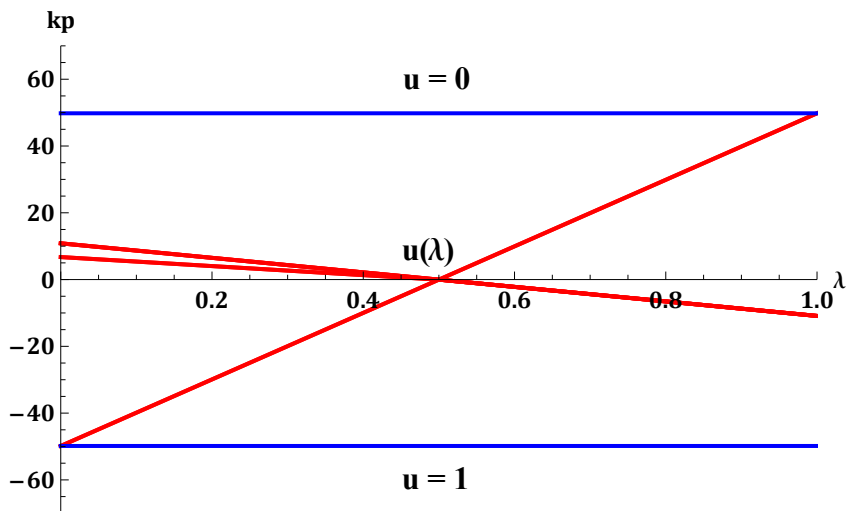
Figure 4.16 : Variation of the gain intervals and invariant regions for $\sigma = -0.235$ (Example 4.3).

144

For the boundaries $\sigma = -0.235$ and $\sigma = -\omega/0.8031$ the anti-D-stable root count should be 0 and for all of the remaining boundaries, the number of anti-D-stable roots should be 2.

Table 4.6 : Gain intervals and anti-D-stable root counts for $\sigma = -0.235$.

Anti-D-Stable Roots	Feasible Interval
1	$-49.838 \geq k_p^1 > -\infty$
0	$\infty > k_p^1 \geq 49.801$

Table 4.7 : Gain intervals and anti-D-stable root counts for $\sigma = -0.308$.

Anti-D-Stable Roots	Feasible Interval
3	$-50.042 \geq k_p^1 > -\infty$
2	$\infty > k_p^1 \geq 50.006$

Table 4.8 : Gain intervals and anti-D-stable root counts for $\sigma = -\omega/0.8031$.

Anti-D-Stable Roots	Feasible Interval
1	$-54.818 \geq k_p^1 > -\infty$
0	$\infty > k_p^1 \geq 54.779$

Table 4.9 : Gain intervals and anti-D-stable root counts for $\sigma = -1.54$.

Anti-D-Stable Roots	Feasible Interval
3	$-9.637 \geq k_p^1 > -\infty$
2	$\infty > k_p^1 \geq 9.607$

As a result, the interval of the K_p parameter is found as follows.

$$K_p \in \bigcap_{j=1}^{4} K_p^j \in (54.779, \infty)$$

As long as the choice of K_p parameter is done in the obtained value range, it is guaranteed that the dominant pole pair is located in the desired region and the

145

non-dominant poles are located on the left side of the line $\sigma = -1.54$ under all possible perturbations.

If the parameter $K_p = 55$ is chosen, the PID controller is given as follows.

$$F_{PID}(s) = 55 + \frac{10.75}{s} + 43.26s$$
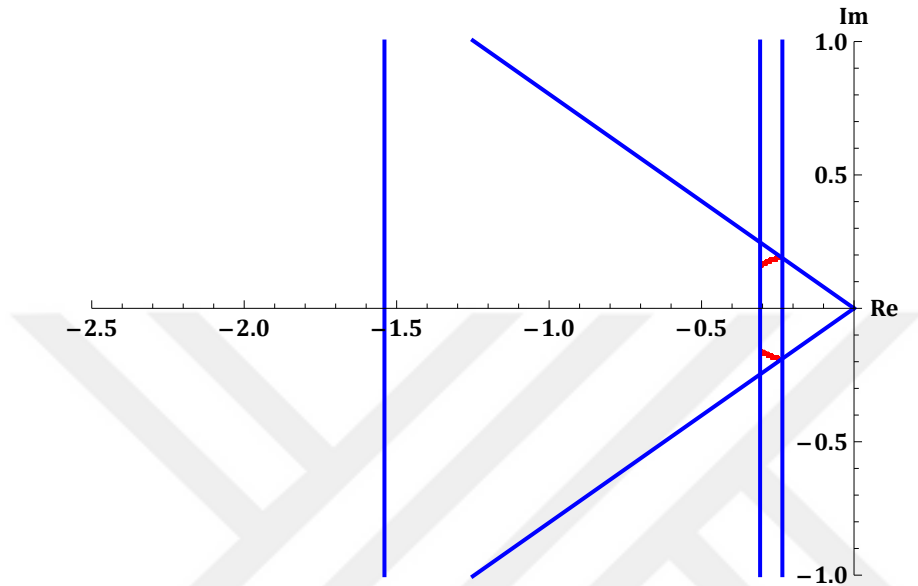
Figure 4.17 : Pole spread of the closed-loop system with PID controller (Example 4.3).
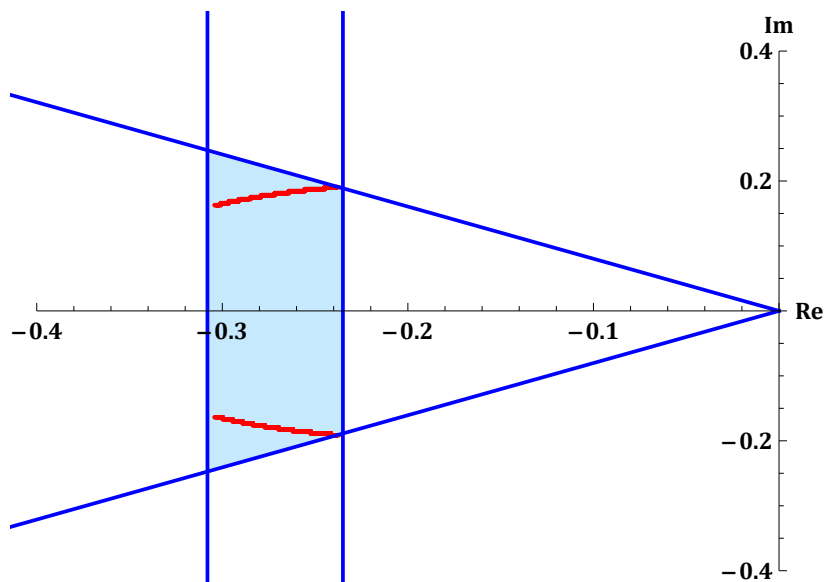
Figure 4.18 : Closed-loop pole spread in the dominant pole region (Example 4.3).

Figure 4.17 and 4.18 show the closed-loop pole spread of the system with proposed robust PID controller. It is seen that the closed-loop poles remain in the desired region

146

under all possible changes of the parameter J and the rest of the poles are already too far away.

In this application, it can be shown that it is not possible to satisfy desired closed-loop performance criteria with designed PID controller. Although the dominant pole placement is performed successfully, the closed-loop controller zeroes are located in the dominant region. In order to eliminate the adverse effect of the controller zeroes, PI-PD structure which is introduced in the previous parts of the thesis can be used to implement the designed PID controller.

$$F_{PI}(s) = 1 + \frac{10.75}{s}$$
$$F_{PD}(s) = 54 + 43.26s$$

The closed-loop step response of the perturbed system with above PI-PD controller is given in Figure 4.19.
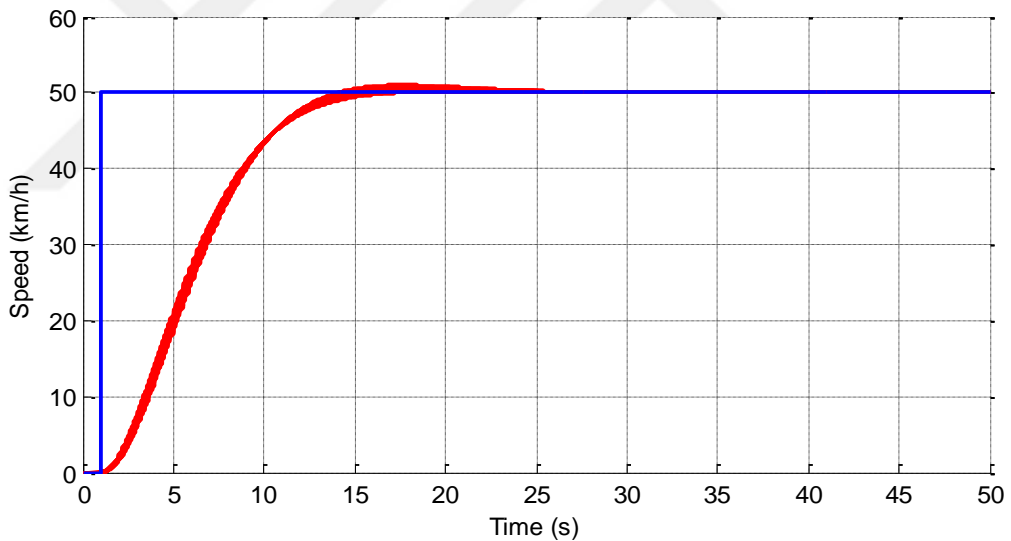
Figure 4.19 : Closed-loop transient response under all possible perturbations (Example 4.3).

In the closed-loop, it can be seen that the vehicle speed satisfies the desired performance specifications under all possible perturbations. Thus, it can be concluded that the proposed robust controller design method works well for the systems have affine-linear type characteristic polynomial. In the next example, a system with more uncertain parameters is considered and also compared with the other methods from the literature to show the success of the proposed method.

147

Example 4.4:

Let us consider a continuous stirred tank reactor with a multiple-model presentation studied by Ge [57], Toscano [58] and Goncalves [59]. If the stable operating range is considered, it is possible to obtain the open-loop transfer function as follows

$$G(s) = \frac{q_2}{s^2 + q_1 s + q_0}$$

where $q_0 \in [5.862, 22.19]$, $q_1 \in [0.01248, 9.251]$ and $q_2 \in [0.03707, 0.04612]$.

In the closed-loop transient response, 1 second of settling time with 0.5% overshoot is desired for the nominal system. Thus, the dominant poles are calculated as $s_{1,2} = -4 \pm 2.3718 j$ and K_i and K_d parameters of the PID controller is obtained in terms of K_p as below.

$$K_i = -493.55 + 2.7032 K_p$$

$$K_d = 58.103 + 0.125 K_p$$

The closed-loop system characteristic polynomial with PID controller is then given as follows.

$$P_c(s, \boldsymbol{q}, K_P) = s^3 + (q_1 + 58.103 q_2 + 0.125 q_2 K_p) s^2$$
$$+ (q_0 + q_2 K_p) s + (2.7032 q_2 K_p - 493.55 q_2)$$

Under all possible perturbations, the dominant poles are desired to be inside the region bounded by the lines $\sigma_1 = -3$ and $\sigma_2 = -6$ which means settling time to be between 0.667 and 1.333 seconds. On the other hand, the maximum allowable overshoot is determined to be 2% in the worst case. The desired dominant pole region in complex s-plane is illustrated in Figure 4.20. Finally the remaining poles are desired to be 3 times away from the dominant pole region in the worst case which means on the left side of the line $\sigma_3 = -18$.

For this problem, it is seen that there are four different boundary functions which are given as $f_1(\omega) = -3 + j\omega$, $f_2(\omega) = -6 + j\omega$, $f_3(\omega) = \frac{-\omega}{0.803} + j\omega$ and $f_4(\omega) = -18 + j\omega$; therefore, the given design procedure should be repeated for all desired boundary functions, respectively.

It is now possible to construct the edge polynomials through the closed-loop system characteristic polynomial. After that for each edge polynomials and the boundary functions, the expressions $\tilde{G}_i(f(\omega), \lambda)$ are obtained, the critical frequencies $(\omega_{ij}^*(\lambda))$

148
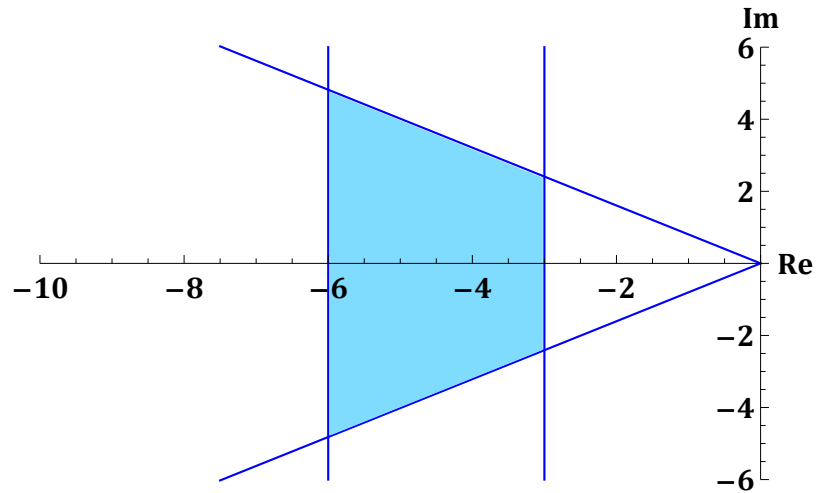
Figure 4.20 : Desired dominant pole region in s-plane (Example 4.4).

are calculated in terms of λ and the intersection points of Nyquist curve and real axis $(x_{ij}(\lambda))$ are obtained, respectively. The next step is to find the upper and lower limits of the varying gain intervals so that the invariant gain intervals can be calculated via (4.37).

For instance, Figure 4.21 shows the varying and invariant gain intervals and the anti-D-stable roots counts for one of the edge polynomial with boundary function of $f_1(\omega)$. Since the first root boundary, the desired anti-D-stable root count is zero $(u = 0)$, the feasible K_p interval can easily be determined.
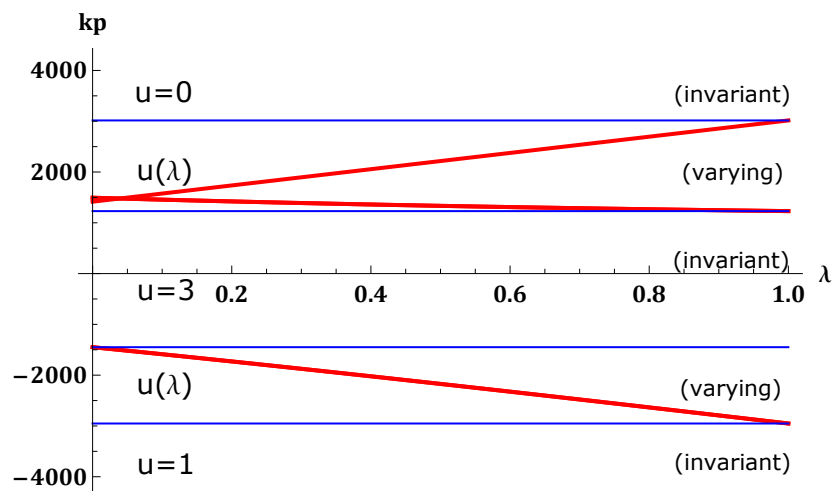
Figure 4.21 : An example of invariant regions and gain intervals (Example 4.4).

149

Details of the calculations are not given in order to improve the readability due to the complex structure of equations. However, the proposed method can be applied step by step in a symbolic algebra environment and the results are obtained.

If the required calculations are completed, the invariant gain intervals and the anti-D-stable root counts for each boundary function is obtained as in Table 4.10. It can be read from the table that since all the roots are desired to be left side of the boundaries $f_1(\omega)$ and $f_4(\omega)$, the feasible intervals are obtained for $u = 0$. However, two of the closed-loop poles (dominant poles) are desired to be left side of the boundaries $f_2(\omega)$ and $f_3(\omega)$; therefore, the feasible intervals are obtained for $u = 2$.

Table 4.10 : Invariant gain intervals and the anti-D-stable root counts for stable range.

	Gain Intervals	Anti-D-Stable Roots
$f_1(\omega)$	$-\infty < \mathcal{K} < -2951.92$	$u = 1$
	$4669.06 < \mathcal{K} < \infty$	$\boldsymbol{u = 0}$
$f_2(\omega)$	$-\infty < \mathcal{K} < -3170.76$	$u = 3$
	$6506.2 < \mathcal{K} < \infty$	$\boldsymbol{u = 2}$
$f_3(\omega)$	$-\infty < \mathcal{K} < -6522.19$	$u = 1$
	$7476.2 < \mathcal{K} < \infty$	$\boldsymbol{u = 0}$
$f_4(\omega)$	$-\infty < \mathcal{K} < 1796.59$	$u = 3$
	$5951.03 < \mathcal{K} < \infty$	$\boldsymbol{u = 2}$

As long as the K_p parameter of PID controller is chosen from the interval of $K_p \in (7476.2, \infty)$, it is guaranteed that the dominant poles are placed in the desired region whereas the remaining poles are located 3 times away from the dominant region under all possible perturbations. It is then possible to obtain the K_i and K_d parameters. The designed PID controller is given as below for $K_p = 7500$.

$$F(s) = 7500 + \frac{19780.2}{s} + 995.6s$$

The closed-loop system pole spread is given in Figure 4.22. It is seen from the figure that the dominant poles are located inside the desired D-region and the remaining poles are located on the left side of $\sigma = -18$ line. It is possible to say that robust PID controller design via the dominant pole placement is performed successfully in

terms of the closed-loop poles. However, note that the closed-loop zeros are found to be located in the dominant region with this PID controller; therefore, the transient response of the system can not satisfy the requirements. In this case, the PI-PD implementation of PID controller should be considered as mentioned earlier.
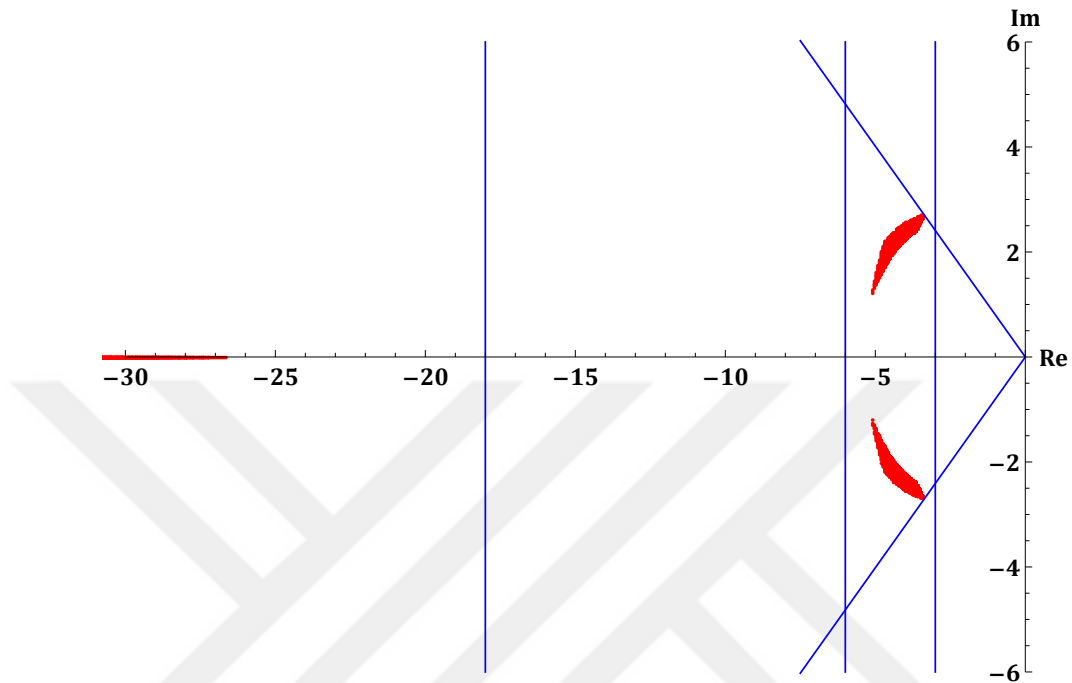
Figure 4.22 : Closed-loop pole spread for stable case in complex s-plane (Example 4.4).

Let us implement the designed robust PID controller as given in Figure 2.9. As long as the equality

$$K_{pi} + K_{pd} = 7500$$

is satisfied, the closed-loop pole spread does not change; however, the number of controller zeros become one (instead of two) and it is possible to locate it in the non-dominant region. The PI and PD controllers are then given as follows for $K_{pi} = 800$ which assigns the closed-loop zero to the point of $s = -24.72$ in s-plane.

$$F_{pi}(s) = 800 + \frac{19780.2}{s}, \ F_{pd}(s) = 6700 + 995.6s$$

In order to demonstrate the success of the proposed method, it is compared with the several PID controllers from the literature which are also designed for the considered system. Table 4.11 shows the parameters of proposed PID controllers in terms of time constants.

Table 4.11 : PID controller parameters for stable range.

Parameters	Ge et al.	Toscano	Goncalves et al.	Proposed
K_p	516.6	698.1	12713.0	7500.0
T_i	0.6749	0.6197	0.4289	0.3792
T_d	0.2784	0.5259	0.1149	0.1327

The closed-loop transient responses with given PID controllers are depicted in Figure 4.23. It can be said that the closed-loop response with proposed controller is smooth, satisfies the desired performance specifications and has an acceptable disturbance rejection under all possible perturbations (see Table 4.12). The transient responses of the controllers proposed by Ge et al. [57] and Toscano [58] change much under parametric uncertainties. Furthermore, these controllers have noticeable overshoot in the closed-loop which is not desired in most of the practical applications. The controller proposed by Goncalves et al. [59] has clearly better and more robust transient response; however, it still has around 15% overshoot in the worst case. On the other hand, the disturbance rejection with PID controllers proposed by Ge et al. and Toscano is not acceptable for most of the practical systems.
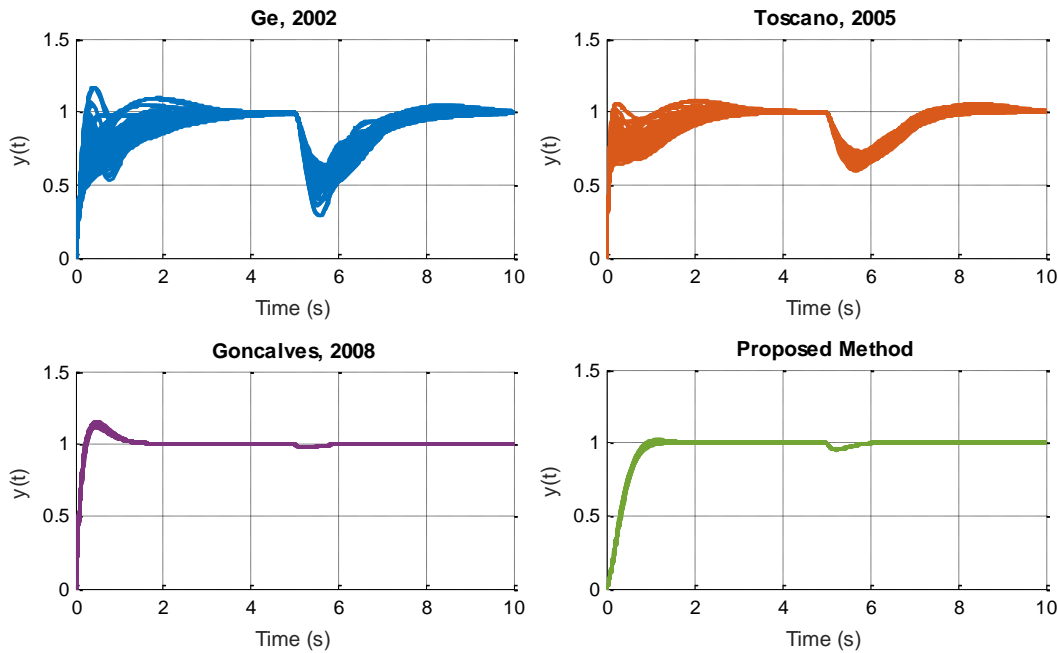
Figure 4.23 : Comparison of the controllers for the stable range (Example 4.4).

Table 4.12 : Performance criteria and control signal norms in the worst case (stable range).

	t_s [s]	os [%]	$\|u\|_2$	$\|u\|_\infty$
Ge et al.	4.655	16.92	2801.0	14897.0
Toscano	3.492	7.706	3737.6	37410.0
Goncalves et al.	1.241	15.29	3204.3	12720.0
Proposed Method	1.247	2.102	2803.2	1183.6

The variation of control signals is given in Figure 4.24 and the signal characteristics are shown in Table 4.12. It is seen that the control signals applied by the other methods have high initial values which is not desired in the industrial applications due to the practical applicability; however, control signal of the proposed controller is low and smooth. It can be concluded that the proposed robust PID controller (implemented in PI-PD structure) has the best response.
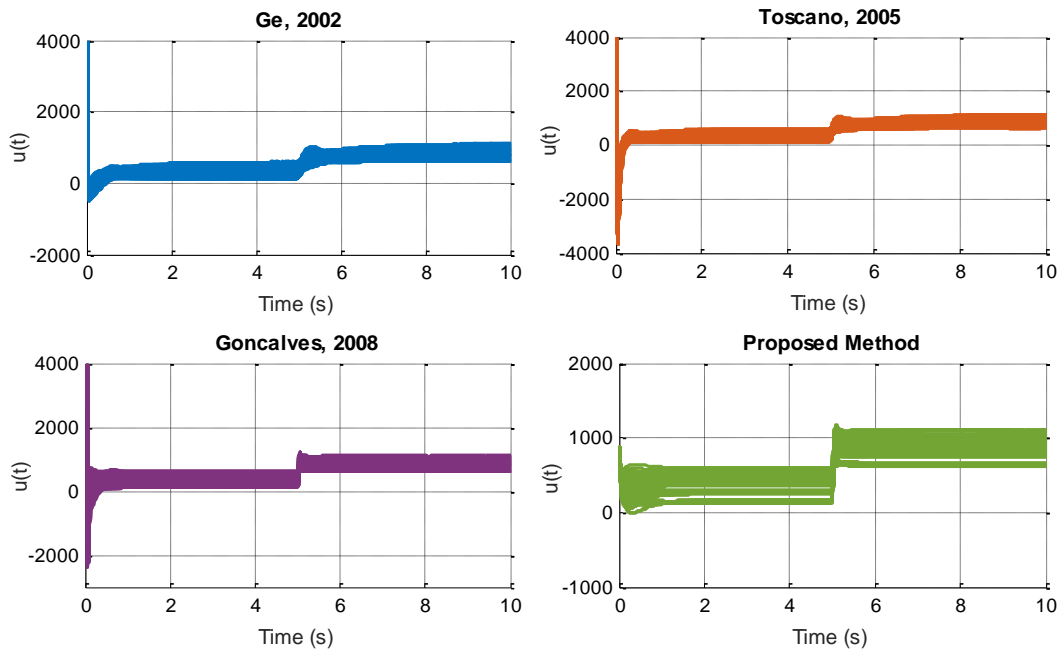
Figure 4.24 : Control signals of the compared controllers for the stable range (Example 4.4).

In the references [57] and [59] the unstable region is also considered. In this case, the uncertain parameters are given as $q_0 \in [-2.252, 4.996]$, $q_1 \in [-2.647, -0.405]$ and $q_2 \in [0.016, 0.036]$. For the same performance specifications (1s settling time with

0.5% overshoot), the PID controller parameters are calculated as follows.

$$K_i = -2105.7 + 2.7032 K_p$$

$$K_d = 269.01 + 0.125 K_p$$

The closed-loop system characteristic polynomial with PID controller is also given as below.

$$P_c(s, \mathbf{q}, K_p) = s^3 + (q_1 + 269.01 q_2 + 0.125 q_2 K_p) s^2$$
$$+ (q_0 + q_2 K_p) s + (2.7032 q_2 K_p - 2105.7 q_2)$$

Let us consider the same dominant pole region in complex s-plane which is illustrated in Figure 4.20. If the proposed method is followed, it is possible to obtain the gain intervals and anti-D-stable root counts for unstable case as in Table 4.13.

Table 4.13 : Invariant gain intervals and the anti-D-stable root counts for unstable range.

	Gain Intervals	Anti-D-Stable Roots
$f_1(\omega)$	$-\infty < \mathcal{K} < -3650.01$	$u = 1$
	$4585.78 < \mathcal{K} < \infty$	$\mathbf{u = 0}$
$f_2(\omega)$	$-\infty < \mathcal{K} < -1287.54$	$u = 3$
	$11583.9 < \mathcal{K} < \infty$	$\mathbf{u = 2}$
$f_3(\omega)$	$-\infty < \mathcal{K} < -6758.49$	$u = 1$
	$1465.52 < \mathcal{K} < 1534.09$	$u = 2$
	$8113.79 < \mathcal{K} < \infty$	$\mathbf{u = 0}$
$f_4(\omega)$	$-\infty < \mathcal{K} < 3152.96$	$u = 3$
	$13437.5 < \mathcal{K} < \infty$	$\mathbf{u = 2}$

Here, if the K_p parameter is chosen from the interval of $K_p \in (13437.5, \infty)$, it is again guaranteed that the dominant pole pair is placed in the desired region whereas the non-dominant poles are located 3 times away from the dominant region. For $K_p = 14000$, the PID controller is given as follows.

$$F(s) = 14000 + \frac{35738.5}{s} + 2019s$$

Figure 4.25 shows the closed-loop pole spread with designed robust controller. It is possible to say that the dominant poles are located inside the desired D-region and
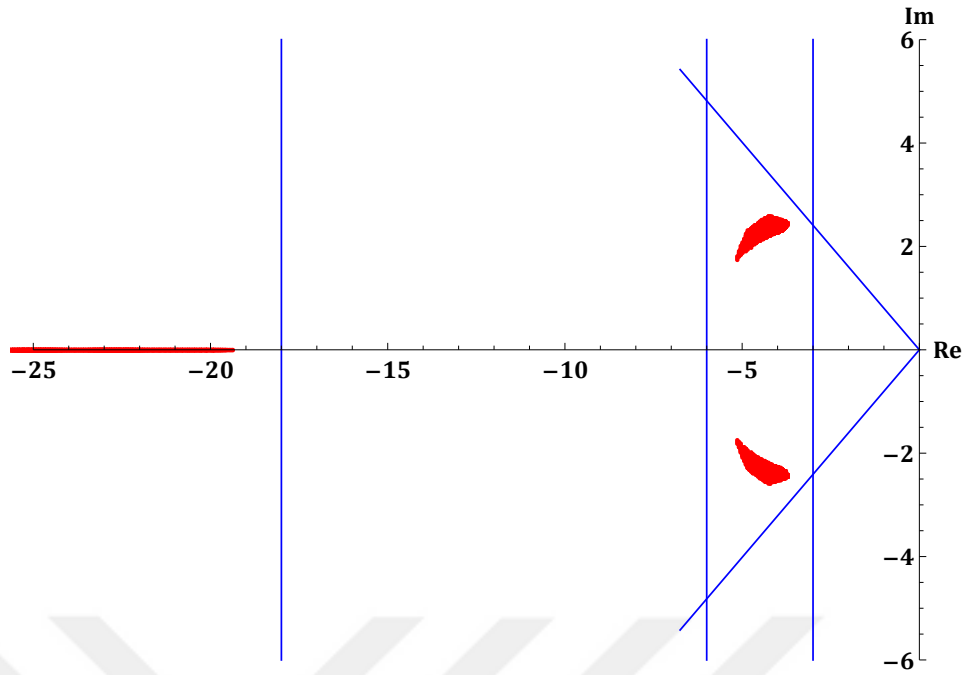
Figure 4.25 : Closed-loop pole spread for unstable case in complex s-plane (Example 4.4).

the non-dominant poles are located on the left side of $\sigma = -18$ line. Thus, in the closed-loop, the desired performance criteria are met under all possible perturbations.

The designed PID controller is then implemented in PI-PD form as follows for $K_{pi} = 1400$ which assigns the closed-loop zero to the point of $s = -25.52$ in s-plane.

$$F_{pi}(s) = 1400 + \frac{35738.5}{s}, \ F_{pd}(s) = 12600 + 2019s$$

In the Table 4.14, the proposed PID controller parameters, which are found for unstable range, are given in terms of time constants.

Table 4.14 : PID controller parameters for unstable range.

Parameters	Ge et al.	Goncalves et al.	Proposed
K_p	804.6	13625.0	14000.0
T_i	1.3249	0.4438	0.3917
T_d	0.393	0.1285	0.1442

The closed-loop transient responses of the controllers are also given in Figure 4.26. The controller proposed by Ge et al. has very large overshoot and unacceptable

disturbance rejection in the closed-loop under parametric uncertainties. Although the PID controller proposed by Goncalves et al. has better alternative to be used, it again has around 18% overshoot in the worst case. However, the transient response with the proposed PID controller has less overshoot, good disturbance rejection and satisfies the desired performance specifications as it is seen from the Table 4.15.
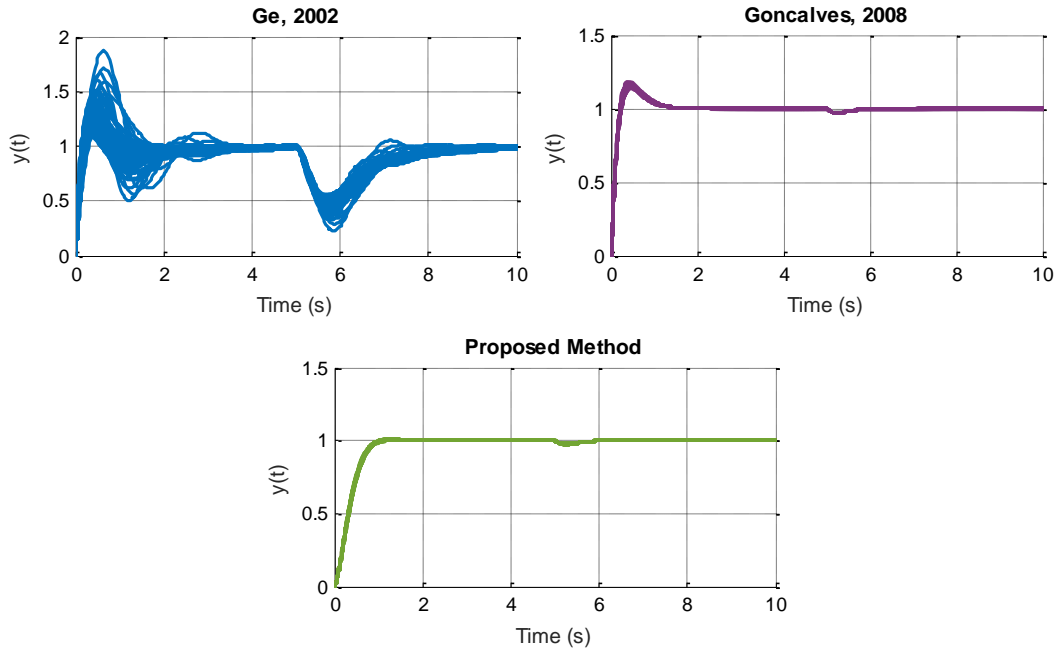
Figure 4.26 : Comparison of the controllers for the unstable range (Example 4.4).

Table 4.15 : Performance criteria and control signal norms in the worst case (unstable range).

	t_s [s]	os [%]	$\|u\|_2$	$\|u\|_\infty$
Ge et al.	5.087	86.92	3011.8	32426.0
Goncalves et al.	1.253	18.18	3029.7	13640.0
Proposed Method	0.969	1.024	1953.5	1563.6

It is also possible to comment on the control signals which is illustrated in Figure 4.27. It is again seen that the control signal of the PID controllers proposed by Ge et al. and Goncalves et al. again have high initial values, whereas control signal with proposed PI-PD controller is smooth and low when compared to the other methods.

In this chapter, a robust PID controller design is given for the systems with parametric uncertainties via dominant pole placement approach. Two of the closed-loop poles are
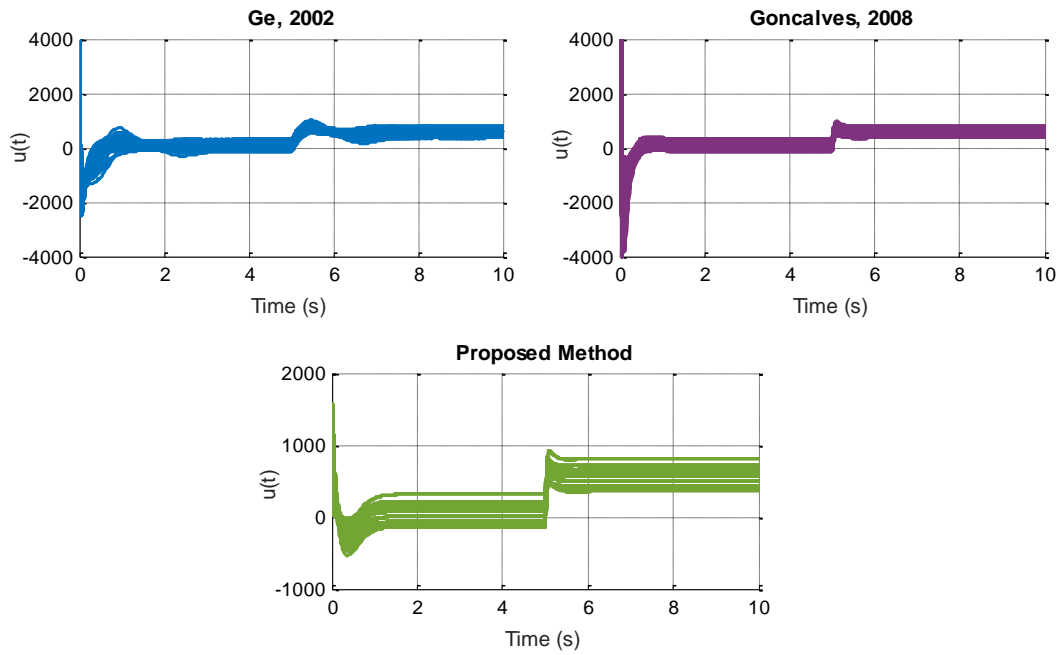
Figure 4.27 : Control signals of the compared controllers for the unstable range (Example 4.4).

assigned in a desired region in complex s-plane and the remaining poles are located away from the dominant pole region. It is shown that with the help of proposed approach, it is possible to handle the design problem for interval and affine-linear characteristic polynomials. Since the obtained robust controller is a set of controllers, it allows designer to consider more criteria such as the specifications on control signal.

It should be noted that the proposed method is based on the dominant pole placement approach. However, satisfying the dominant pole configuration is not always possible for the desired D-region. Therefore, if the resulting controller set is empty, the design procedure should be repeated for the boundary functions both for dominant and non-dominant poles as necessary. This is the only drawback of proposed design method.

5. CONCLUSION

In this thesis, various methods are proposed to design low order controllers via dominant pole placement approach. Parametrization formulations are given for PI and PID controllers which assign the dominant poles in continuous-time domain. In order to assign the remaining poles, three different methods based on root-locus plot, modified Nyquist plot and Routh-Hurwitz stability criterion are presented. Since the PID controller zeros are also affect the transient response, PI-PD structure is proposed to eliminate the adverse effects of the controller zeros. The derivative kick phenomenon in the closed-loop is also solved with the help of this structure. Therefore, in the simulation studies, the results are mostly given for the PI-PD implementation of the resulting PID controller. Maximum achievable dominance factor in continuous-time domain is also calculated with the help of proposed Routh-Hurwitz based approach for the systems with or without open-loop zeros. The similar problem, which is stated as the limitations on the dominant pole pair selection with PI and PID controllers, is also solved via the same approach. Thus, the designer becomes aware of the performance limitations in the closed-loop if the controller is designed via dominant pole placement approach. In the second chapter, the final study consists of the solution to the dominant pole region assignment problem. Here, for a P controller design, generalized Nyquist theorem based approach is proposed and for the PI/PID controllers, a parameter space approach is used to solve the mentioned problem.

It is also desired to solve the problems related with the dominant pole placement with discrete P/PI/PID controllers and the similar steps are followed in the third chapter. Parametrization of the digital PI and PID controllers are given after that the remaining poles are assigned into the disc of desired radius with the help of two different approaches named as modified Nyquist curve and Chebyshev polynomials. As in continuous-time case, the digital PI-PD controller structure is also investigated and advantages are mentioned. The complete digital PI-PD controller design process is

given and the success of proposed method is shown both with simulation studies and a real-time implementation. Calculation of the disc with minimum possible radius (same as the calculation of maximum dominance factor) is also studied with discrete PID controllers. Performance limitations are also obtained similar to the continuous-time case for PI and PID type controllers, respectively. The solution to the dominant pole region assignment problem is given for a P controller via generalized Nyquist theorem based approach and for the PI/PID controllers via parameter space approach. It is shown that it is possible to satisfy desired pole configuration in discrete-time domain with the help of proposed method.

It is worth to note that the proposed design methods rely on the placement of dominant pole pair to the desired points and the remaining poles m times away from the dominant poles. However, it is not always possible to place the unassigned poles as desired for the chosen performance specifications and dominance factor. Therefore, if the resulting controller set is found to be empty then the given design process should be repeated for different m value and/or performance criteria until obtaining a non-empty controller parameter set.

For practical systems, it is not possible to obtain the perfect mathematical model because of the unmodelled dynamics, environmental changes, neglected non-linearities, parameter variations due to torn and worn effects. For this reason, the system may contain uncertain parameters whose intervals are known. In this thesis, interval type and affine-linear type uncertainties are considered and corresponding stability analysis methods are presented. After that since different stability regions are considered, D-stability concept and Kharitonov regions are explained and necessary theorems are given. After the preliminaries part, solution to the robust dominant pole placement problem with continuous PID controller is proposed with the help of vertex polynomials and Kharitonov regions. In case of the parametric uncertainties, it is not possible to place closed-loop system poles to the exact locations, but instead in a defined D-region. It is shown that it is enough to check the D-stability of vertex polynomials via Nyquist stability criterion if the closed-loop system characteristic polynomial with PID controller is an interval type polynomial. The proposed design method is then demonstrated on example uncertain transfer functions for different D-regions. The closed-loop pole spreads and the transient responses are also given

and success of the method is proven. The same procedure is followed for the affine-linear type characteristic polynomials with PID controller. Instead of using the bialas theorem for edge polynomials, a new method is proposed which is a lot easier to check the D-stability of the affine linear characteristic polynomial. The method relies on the Nyquist stability criterion and the calculation of invariant gain intervals concept. Thus, the robust PID controller design for such systems are also completed via robust dominant pole placement. Here, the success of the method is demonstrated via simulation studies and also compared with the other robust PID controller design methods from literature.

Even if it is not considered in the thesis, designing low order controllers for two input–two output (TITO) processes via dominant pole placement is also possible. In order to control a TITO system, a decoupler plus decentralized PID controller is eligible to be considered. As a result, it can be said that the derived results for SISO systems can also be used for most of the TITO systems with the help of decoupling approach.

It is possible to design robust PID controllers for uncertain time-delay systems with the help of discrete-time domain representation. The robust design methods proposed in chapter four can also be used for such systems with the help of bilinear transformation. However, it is also possible to propose similar methods for direct design of robust digital PID controllers as a future work. On the other hand, it might also be possible to extend the dominant pole placement methods to the fractional order systems.

REFERENCES

[1] **Wang, Q.G.**, **Zhang, Z.**, **Astrom, K.J. and Chek, L.S.** (2009). Guaranteed dominant pole placement with PID controllers, *Journal of Process Control*, *19*(2), 349–352.

[2] **Datta, S.**, **Chakraborty, D. and Chaudhuri, B.** (2012). Partial pole placement with controller optimization, *IEEE Transactions on Automatic Control*, *57*(4), 1051–1056.

[3] **Astrom, K.**, **Albertos, P. and Quevedo, J.** (2001). PID Control, *Control Engineering Practice*, *9*(11), 1159–1161.

[4] **Kailath, T.** (1980). *Linear systems*, volume156, Prentice-Hall Englewood Cliffs, NJ.

[5] **Lee, J.** (2005). A new phase-lead design method using the root locus diagrams, *IEEE transactions on automatic control*, *50*(11), 1887–1891.

[6] **Ackermann, J.** (2012). *Robust control: Systems with uncertain physical parameters*, Springer Science & Business Media.

[7] **Persson, P. and Åström, K.J.**, (1993). Dominant pole design-a unified view of PID controller tuning, Adaptive Systems in Control and Signal Processing 1992, Elsevier, pp.377–382.

[8] **Åström, K.J. and Hägglund, T.** (1995). *PID controllers: theory, design, and tuning*, volume 2, Instrument society of America Research Triangle Park, NC.

[9] **Desborough, L. and Miller, R.** (2002). Increasing customer value of industrial control performance monitoring-Honeywell's experience, *AIChE symposium series*, 326, New York; American Institute of Chemical Engineers; 1998, pp.169–189.

[10] **Åström, K.J. and Hägglund, T.** (2006). *Advanced PID control*, ISA-The Instrumentation, Systems and Automation Society.

[11] **Üstoğlu, İ. and Söylemez, M.T.** (2007). Feasibility conditions on PID controller synthesis using dominant pole assignment, *Control Conference (ECC), 2007 European*, IEEE, pp.483–489.

[12] **Cominos, P. and Munro, N.** (2002). PID controllers: recent tuning methods and design to specification, *IEE Proceedings-Control Theory and Applications*, *149*(1), 46–53.

[13] **Hwang, S.H. and Fang, S.M.** (1995). Closed-loop tuning method based on dominant pole placement, *Chemical Engineering Communications*, *136*(1), 45–66.

[14] **Zhang, Y., Wang, Q.G. and Astrom, K.** (2002). Dominant pole placement for multi-loop control systems, *Automatica*, *38*(7), 1213–1220.

[15] **Tang, W., Wang, Q.G., Ye, Z. and Zhang, Z.** (2007). PID tuning for dominant poles and phase margin, *Asian Journal of Control*, *9*(4), 466–469.

[16] **Zítek, P., Fišer, J. and Vyhlídal, T.** (2013). Dominant three pole placement in PID control loop with delay, *Control Conference (ASCC), 2013 9th Asian*, IEEE, pp.1–6.

[17] **Li, Y., Sheng, A. and Qi, Q.** (2011). Further results on guaranteed dominant pole placement with PID controllers, *Control Conference (CCC), 2011 30th Chinese*, IEEE, pp.3756–3760.

[18] **Madady, A. and Reza-Alikhani, H.R.** (2011). First-order controllers design employing dominant pole placement, *Control & Automation (MED), 2011 19th Mediterranean Conference on*, IEEE, pp.1498–1503.

[19] **Dincel, E. and Soylemez, M.T.** (2014). Guaranteed dominant pole placement with discrete-PID controllers: a modified Nyquist plot approach, *IFAC Proceedings Volumes*, *47*(3), 3122–3127.

[20] **Soylemez, M.** (2006). Estimate of the smallest stabilisable left-half-plane for all pole plants, *IEE Proceedings-Control Theory and Applications*, *153*(1), 124–126.

[21] **Dincel, E. and Söylemez, M.T.** (2015). Estimate of the farthest possible non-dominant pole locations with PID controllers, *Control and Automation (MED), 2015 23th Mediterranean Conference on*, IEEE, pp.237–241.

[22] **Dincel, E. and Söylemez, M.T.** (2016). Limitations on dominant pole pair selection with continuous PI and PID controllers, *Control, Decision and Information Technologies (CoDIT), 2016 International Conference on*, IEEE, pp.741–745.

[23] **Lengare, M., Waghmare, L.** *et al.* (2012). Design of decentralized controllers for MIMO processes, *Computers & Electrical Engineering*, *38*(1), 140–147.

[24] **Liu, T., Zhang, W. and Gu, D.** (2005). Analytical multiloop PI/PID controller design for two-by-two processes with time delays, *Industrial & engineering chemistry research*, *44*(6), 1832–1841.

[25] **Liu, T., Zhang, W. and Gu, D.** (2006). Analytical Design of Decoupling Internal Model Control (IMC) Scheme for Two-Input - Two-Output (TITO) Processes with Time Delays, *Industrial & engineering chemistry research*, *45*(9), 3149–3160.

[26] **Huang, H.P. and Lin, F.Y.** (2006). Decoupling multivariable control with two degrees of freedom, *Industrial & engineering chemistry research*, *45*(9), 3161–3173.

[27] **Lee, J.**, **Hyun Kim, D. and Edgar, T.F.** (2005). Static decouplers for control of multivariable processes, *AIChE journal*, *51*(10), 2712–2720.

[28] **Maghade, D. and Patre, B.** (2012). Decentralized PI/PID controllers based on gain and phase margin specifications for TITO processes, *ISA transactions*, *51*(4), 550–558.

[29] **Maghade, D. and Patre, B.** (2014). Pole placement by PID controllers to achieve time domain specifications for TITO systems, *Transactions of the Institute of Measurement and Control*, *36*(4), 506–522.

[30] **Bhattacharyya, S.P. and Keel, L.H.**, (1995). Robust control: the parametric approach, Advances in Control Education 1994, Elsevier, pp.49–52.

[31] **Soylemez, M.T.** (1999). *Pole assignment for uncertain systems*, Research Studies Press Limited.

[32] **Barmish, B.R. and Tempo, R.** (1990). The robust root locus, *Automatica*, *26*(2), 283–292.

[33] **Nesenchuk, A.** (2010). The root-locus method of synthesis of stable polynomials by adjustment of all coefficients, *Automation and Remote Control*, *71*(8), 1515–1525.

[34] **Munro, N. and Soylemez, M.** (2000). Fast calculation of stabilizing PID controllers for uncertain parameter systems, *IFAC Proceedings Volumes*, *33*(14), 549–554.

[35] **Huang, Y.J. and Wang, Y.J.** (2000). Robust PID tuning strategy for uncertain plants based on the Kharitonov theorem, *ISA transactions*, *39*(4), 419–431.

[36] **Matusu, R. and Prokop, R.** (2016). Computation of robustly stabilizing PID controllers for interval systems, *SpringerPlus*, *5*(1), 702.

[37] **Rahimian, M.A. and Tavazoei, M.S.** (2012). Application of stability region centroids in robust PI stabilization of a class of second-order systems, *Transactions of the Institute of Measurement and Control*, *34*(4), 487–498.

[38] **Mihailescu-Stoica, D.**, **Schrödel, F. and Adamy, J.** (2017). All stabilizing PID controllers for interval systems and systems with affine parametric uncertainties, *Control Conference (ASCC), 2017 11th Asian*, IEEE, pp.576–581.

[39] **Ferheen, A. and Chidambaram, M.** (2017). Design of robust PID controller for an interval plant, *Trends in Industrial Measurement and Automation (TIMA), 2017*, IEEE, pp.1–7.

[40] **Dincel, E. and Söylemez, M.T.** (2017). Dominant pole region assignment with continuous PI and PID controllers, *Electrical and Electronics Engineering (ELECO), 2017 10th International Conference on*, IEEE, pp.836–841.

[41] **Kaya, I.** (2003). Obtaining controller parameters for a new PI-PD Smith predictor using autotuning, *Journal of Process Control*, *13*(5), 465–472.

[42] **Zou, H. and Li, H.** (2015). Tuning of PI–PD controller using extended non-minimal state space model predictive control for the stabilized gasoline vapor pressure in a stabilized tower, *Chemometrics and Intelligent Laboratory Systems*, *142*, 1–8.

[43] **Zou, H. and Li, H.** (2017). Improved PI-PD control design using predictive functional optimization for temperature model of a fluidized catalytic cracking unit, *ISA Transactions*, *67*, 215–221.

[44] **Dincel, E. and Söylemez, M.T.** (2018). Digital PI-PD controller design for arbitrary order systems: Dominant pole placement approach, *ISA transactions*, *79*, 189–201.

[45] **Dincel, E.**, **Mutlu, İ.**, **Schrödel, F. and Söylemez, M.T.** (2018). Further Results on Dominant Pole Placement via Stability Mapping Approach, *IFAC-PapersOnLine*, *51*(4), 918–923.

[46] **Aström, K.J. and Murray, R.M.** (2010). *Feedback systems: an introduction for scientists and engineers*, Princeton University Press.

[47] **Keel, L. and Bhattacharyya, S.** (2002). Root counting, phase unwrapping, stability and stabilization of discrete time systems, *Linear Algebra and its Applications*, *351*, 501–518.

[48] **Bayhan, N. and Söylemez, M.T.** (2006). Fast calculation of all stabilizing gains for discrete-time systems, *IU-Journal of Electrical & Electronics Engineering*, *6*(1), 19–26.

[49] **Keel, L. and Bhattacharyya, S.** (2001). Robustness analysis via TChebyshev representations, *Decision and Control, 2001. Proceedings of the 40th IEEE Conference on*, volume 2, IEEE, pp.1557–1561.

[50] **Gu, D.W.**, **Petkov, P. and Konstantinov, M.M.** (2005). *Robust control design with MATLAB®*, Springer Science & Business Media.

[51] **Yedavalli, R.K.** (2016). *Robust control of uncertain dynamic systems*, Springer.

[52] **Kharitonov, V.** (1979). Asymptotic stability of an equilibrium position of a family systems of linear differential equations, *Differential equations*, *14*, 1483–1485.

[53] **Bartlett, A.C.**, **Hollot, C.V. and Lin, H.** (1988). Root locations of an entire polytope of polynomials: It suffices to check the edges, *Mathematics of Control, Signals and Systems*, *1*(1), 61–71.

[54] **Soh, Y. and Foo, Y.** (1991). Kharitonov regions: It suffices to check a subset of vertex polynomials, *IEEE transactions on automatic control*, *36*(9), 1102–1105.

[55] **Fu, M.** (1991). A class of weak Kharitonov regions for robust stability of linear uncertain systems, *IEEE transactions on Automatic control*, *36*(8), 975–978.

[56] **Soh, Y. and Foo, Y.** (1993). Nonconvex Kharitonov regions, *IEEE transactions on automatic control*, *38*(7), 1158–1159.

[57] **Ge, M.**, **Chiu, M.S. and Wang, Q.G.** (2002). Robust PID controller design via LMI approach, *Journal of process control*, *12*(1), 3–13.

[58] **Toscano, R.** (2005). A simple robust PI/PID controller design via numerical optimization approach, *Journal of process control*, *15*(1), 81–88.

[59] **Goncalves, E.N.**, **Palhares, R.M. and Takahashi, R.H.** (2008). A novel approach for H2/Hinf robust PID synthesis for uncertain systems, *Journal of process control*, *18*(1), 19–26.

CURRICULUM VITAE

Name Surname: Emre Dincel

Place and Date of Birth: Istanbul, 14 May 1989

E-Mail: dincele@itu.edu.tr

EDUCATION:

- **B.Sc.:** 2011, Istanbul Technical University, Faculty of Electrical and Electronic Engineering, Control Engineering Department

- **B.Sc. (Double Major Programme):** 2011, Istanbul Technical University, Faculty of Electrical and Electronic Engineering, Electrical Engineering Department

- **M.Sc.:** 2013, Istanbul Technical University, Graduate School of Science Engineering and Technology, Control and Automation Engineering Department

    Thesis Title: Implementation of the Interlocking Systems by Fail-Safe PLC

    Advisor: Prof. Dr. Salman KURTULAN

- **Ph.D.:** 2019, Istanbul Technical University, Graduate School of Science Engineering and Technology, Control and Automation Engineering Department

    Thesis Title: Robust Dominant Pole Placement with Low Order Controllers

    Advisor: Prof. Dr. Mehmet Turan SÖYLEMEZ

PROFESSIONAL EXPERIENCE:

- 2011-2018 : Istanbul Technical University, Control and Automation Engineering Department, Research Assistant.

- 2013-2015 : ABE Technological Engineering Services, Researcher.

INTERNATIONAL JOURNAL PAPERS:

- **Dincel E.**, Söylemez M.T., 2018. Digital PI-PD Controller Design for Arbitrary Order Systems: Dominant Pole Placement Approach, *ISA Transactions*, 79, 189-201.

- Nesimioğlu B.S., Yılmaz S., **Dincel E.**, 2016. Robust Stabilization of a Servomechanism with Respect to Time-Delay, *International Journal of Applied Mathematics, Electronics and Computers*, 4(Special Issue-1), 250-257.

- **Dincel E.**, Eriş O., Kurtulan S., 2013. Automata-Based Railway Signaling and Interlocking System Design, *IEEE Antennas and Propagation Magazine*, 55(4), 308-319.

INTERNATIONAL CONFERENCE PAPERS:

- **Dincel E.**, Nak H., Akkaya Ş., Canevi M., Mutlu İ., Söylemez M.T., 2018. Robust Control of Railway Traction System, *9th IFAC Symposium on Robust Control Design* Florianopolis, BRAZIL, 3-5 September 2018.

- **Dincel E.**, Mutlu İ., Schrödel F., Söylemez M.T., 2018. Further Results on Dominant Pole Placement via Stability Mapping Approach, *3rd IFAC Conference on Advances in Proportional-Integral-Derivative Control*, Ghent, BELGIUM, 9-11 May 2018.

- Mutlu İ., **Dincel E.**, Canevi M., Söylemez M.T., 2018. Robust Control of Railway Traction Electric Drive Systems in Terms of Energy Efficiency, *7th Transport Research Arena*, Vienna, AUSTRIA, 16-19 April 2018.

- **Dincel E.**, Söylemez M.T., 2017. Dominant Pole Region Assignment with Continuous PI and PID Controllers, *10th International Conference on Electrical and Electronics Engineering*, Bursa, TURKEY, 30 November - 2 December 2017.

- **Dincel E.**, Yılmaz S., Nesimioğlu B.S., 2016. Tuning of Discrete PID Controllers Using Dominant Pole Placement Approach for Time-Delay Systems of Any Order, *3rd International Conference on Advanced Technology & Sciences*, Konya, TURKEY, 1-3 September 2016.

- Nesimioğlu B.S., Yılmaz S., **Dincel E.**, 2016. Robust Stabilization of a Servomechanism With Respect to Time-Delay, *3rd International Conference on Advanced Technology & Sciences*, Konya, TURKEY, 1-3 September 2016.

- **Dincel E.**, Söylemez M.T., 2016. Limitations on Dominant Pole Pair Selection with Continuous PI and PID Controllers, *International Conference on Control, Decision and Information Technologies*, Saint Julian's, MALTA, 6-8 April 2016.

- **Dincel E.**, Söylemez M.T., 2015. Estimate of the Farthest Possible Non-Dominant Pole Locations with PID Controllers, *The 23rd Mediterranean Conference on Control and Automation*, Torremolinos, SPAIN, 16-19 June 2015.

- **Dincel E.**, Yalçın Y., Kurtulan S., 2014. A New Approach on Angular Position Control of Fan and Plate System, *International Conference on Control, Decision and Information Technologies*, Metz, FRANCE, 3-5 November 2014.

- **Dincel E.**, Söylemez M.T., 2014. Guaranteed Dominant Pole Placement with Discrete-PID Controllers: A Modified Nyquist Plot Approach, *The 19th IFAC World Congress*, Cape Town, SOUTH AFRICA, 24-29 August 2014.

- **Dincel E.**, Yıldırım U., Söylemez M.T., 2013. Modeling and Control of Under-Damped Second Order Systems with Dead-Time and Inverse Response, *IEEE International Conference on Control System, Computing and Engineering*, Penang, MALAYSIA, 29 November-1 December 2013.

- Yıldırım U., **Dincel E.**, Söylemez M.T., 2013. A Symbolic PI Tuning Method for First Order Systems with Time Delay, *IEEE International Conference on Control System, Computing and Engineering*, Penang, MALAYSIA, 29 November-1 December 2013.

- **Dincel E.**, Genc İ., 2012. A Power System Stabilizer Design by Big Bang-Big Crunch Algorithm, *IEEE International Conference on Control System, Computing and Engineering*, Penang, MALAYSIA, 23-25 November 2012.

- **Dincel E.**, Kurtulan S., 2012. Interlocking and Automatic Operating System Design with Automaton Method, *13th IFAC Symposium on Control in Transportation Systems*, Sofia, BULGARIA, 12-14 September 2012.

NATIONAL CONFERENCE PAPERS:

- **Dincel E.**, Yılmaz S., Nesimioğlu B.S., 2016. Baskın Kutup Yerleştirme Yaklaşımını Temel Alan Bir Dijital PID Kontrolör Tasarımı, *National Conference of Turkish National Committee of Automatic Control*, Eskişehir, TURKEY, 29 September-1 October 2016.

- Nesimioğlu B.S., Yılmaz S., **Dincel E.**, 2016. Uzaktan Kontrollü Bir DC Motorun Kararlılığının Zaman Gecikmesine Göre Dayanıklı Hale Getirilmesi, *National Conference of Turkish National Committee of Automatic Control*, Eskişehir, TURKEY, 29 September-1 October 2016.

- **Dincel E.**, Söylemez M.T., 2015. PI ve PID Kontrolörler İle Baskın Kutup Atamayı Garantileyen Baskın Kutup Bölgesinin Belirlenmesi, *National Conference of Turkish National Committee of Automatic Control*, Denizli, TURKEY, 10-12 September 2015.

- **Dincel E.**, Yıldırım U., Söylemez M.T., 2013. Manyetik Askı (MAGLEV) Sisteminin Kontrolünde PID Tabanlı Yöntemler, *National Conference of Turkish National Committee of Automatic Control*, Malatya, TURKEY, 26-28 September 2013.

- Yıldırım U., **Dincel E.**, Söylemez M.T., 2013. Birinci Dereceden Ölü Zamanlı Sistemler için Optimal PI Kontrolör Tasarımı, *National Conference of Turkish National Committee of Automatic Control*, Malatya, TURKEY, 26-28 September 2013.

- **Dincel E.**, Yalçın Y., Kurtulan S., 2012. Fan ve Levha Sisteminin Açısal Konum Kontrolü, *National Conference of Turkish National Committee of Automatic Control*, Niğde, TURKEY, 11-13 October 2012.

- **Dincel E.**, Genç İ., 2012. Büyük Patlama-Büyük Çöküş Optimizasyon Algoritması Kullanılarak PD Güç Sistemi Kararlı Kılıcısı Tasarımı, *National Conference of Turkish National Committee of Automatic Control*, Niğde, TURKEY, 11-13 October 2012.

INVOLVED PROJECTS:

- *"Robust Control of Railway Traction Electric Drive Systems"*, Istanbul Technical University Control and Automation Department and The Scientific and Technological Research Council of Turkey (Project Number: 115E748), Scholarship Holder (August 2016-August 2018).

- *"Development of a Radio Block Center (RBC) and On-Board Train Unit Simulator"*, The Scientific and Technological Research Council of Turkey, ABE Technological Engineering Services and Yapı Merkezi İDİS (Monitoring Control and Communication Systems) Inc., Researcher (July 2015-December 2015).

- *"İDİS-P Railway Signalization Project"*, ABE Technological Engineering Services and Yapı Merkezi İDİS (Monitoring Control and Communication Systems) Inc., Researcher (July 2013-December 2015).